

FORAMINIFERAL TRACE ELEMENTS:
UPTAKE, DIAGENESIS, AND
100 M.Y. PALEOCHEMICAL HISTORY

by

MARGARET LOIS DELANEY

B.S., Yale University

(1977)

SUBMITTED IN PARTIAL FULFILLMENT
OF THE REQUIREMENTS FOR THE DEGREE OF
DOCTOR OF PHILOSOPHY

at the

MASSACHUSETTS INSTITUTE OF TECHNOLOGY
and the
WOODS HOLE OCEANOGRAPHIC INSTITUTION

SEPTEMBER, 1983

© Massachusetts Institute of Technology 1983

Signature of Author _____

Department of Earth, Atmospheric, and Planetary Sciences,
Massachusetts Institute of Technology and the Joint Program in
Oceanography, Massachusetts Institute of Technology/Woods Hole
Oceanographic Institution, 9 September 1983

Certified by _____

Edward A. Boyle, Thesis Supervisor

Accepted by _____

Cindy Lee, Chairman, Joint Committee for Chemical Oceanography,
Massachusetts Institute of Technology/Woods Hole Oceanographic
Institution

MASSACHUSETTS INSTITUTE OF TECHNOLOGY
WITHDRAWN
NOV 15 1987
FROM Lindgren
LIBRARY

To my friends

and

my parents

FORAMINIFERAL TRACE ELEMENTS:
UPTAKE, DIAGENESIS, AND
100 M.Y. PALEOCHEMICAL HISTORY

by

MARGARET LOIS DELANEY

Submitted to the Joint Committee on Chemical Oceanography of the
Department of Earth, Atmospheric, and Planetary Sciences,
Massachusetts Institute of Technology and the
Joint Program in Oceanography,
Massachusetts Institute of Technology/Woods Hole Oceanographic Institution
on 9 September 1983
in partial fulfillment of the requirements for the degree of
Doctor of Philosophy

ABSTRACT

Crustal generation rates from 80 - 110 m.y.b.p. have been suggested to be a factor of two times those at present from geological and geophysical evidence about eustatic sea levels, sea floor magnetic lineations, and plate configurations. Other geophysical studies have suggested that crustal generation rates in the past have not been more than ~20% larger than those at present. Faster crustal generation should result in increased chemical fluxes to the ocean from hydrothermal circulation. The oceanic balance of Li is dominated by hydrothermal input; oceanic Li concentrations in the past could have been as much as a factor of two higher than those at present. This thesis investigates the history of oceanic Li concentrations over the last 100 m.y. in order to add independent geochemical evidence to the debate about sea floor spreading rate variations.

Li/Ca ratios in the calcite shells of planktonic foraminifera are used in this study to determine oceanic Li/Ca ratios. The elemental uptake from seawater and the diagenetic changes in the sediment of foraminiferal calcite were investigated to assess the utility of these shells as such indicators.

Laboratory culture experiments on planktonic foraminifera showed that Li, Sr, and Mg elemental ratios to Ca in foraminiferal shells are directly proportional to seawater ratios. The mean distribution coefficients determined in this study for foraminiferal calcite are: Li, $(5.2 \pm 0.6) \times 10^{-3}$; Sr, 0.16 ± 0.02 ; and Mg, $(0.89 \pm 0.18) \times 10^{-3}$. For Na, the ratios in foraminiferal shells did not vary in response to changes in seawater solution Na/Ca ratios. In other laboratory culture experiments, Cd and Zn distribution coefficients in foraminiferal calcite were measured by the use of radiotracers. The best estimate from these measurements of the Cd distribution coefficient in foraminiferal calcite is 1.8 ± 0.1 , which compares well with previous estimates from measurements on planktonic and benthic foraminifera from sediment core samples. Planktonic foraminifera were cultured in the laboratory at different temperatures to investigate the effect of temperature on the trace elemental composition of foraminiferal shells. From these experiments, the interspecific

differences in Sr/Ca, Mg/Ca, and Na/Ca ratios of foraminiferal calcite cannot be due solely to differences in calcification temperatures.

Li/Ca, Sr/Ca, Mg/Ca, and Na/Ca ratios were measured in planktonic foraminiferal shells from five DSDP sites; sample ages extended to 100 m.y. The effect of diagenesis on foraminiferal calcite composition was considered from a simple model comparing the composition of the foraminiferal calcite with that of inorganic calcite in equilibrium with the present-day interstitial water. From these comparisons, some foraminiferal calcite appears to be in inorganic equilibrium with the interstitial water. For other samples, the comparison of the various indicators shows that these foraminiferal shells may be substantially unrecrystallized. Quantification of diagenetic changes in foraminiferal calcite chemistry is hampered by the lack of knowledge about inorganic calcite distribution coefficients applicable to sedimentary recrystallization reactions. The open system nature of the chemical balances between sediments and interstitial water must be explicitly included in diagenetic models of changes in the chemical composition of foraminiferal calcite. As an example, the effect of recrystallization on oxygen isotopic records of foraminiferal calcite is determined in a model with typical interstitial water oxygen isotope gradients.

From a Li mass balance model and the paleochemical records, the possible variations in crustal generation rates over the last 100 m.y. are evaluated. Alternate global extrapolations of the importance of hydrothermal circulation to oceanic mass balances, temporal changes in river fluxes of Li, the nature of the processes removing Li from the ocean, and the potential of coupled variations in the cycles of Ca and Li are considered with this model. This study concludes that at no time in the past 100 m.y. have oceanic Li concentrations been significantly greater than those at present. This geochemical evidence suggests that hydrothermal fluxes and sea floor spreading rates from 80 - 110 m.y. were not significantly greater than those at present.

Thesis Supervisor: Dr. Edward A. Boyle
Title: Associate Professor,
Massachusetts Institute of Technology

TABLE OF CONTENTS

ABSTRACT	3
LIST OF FIGURES	8
LIST OF TABLES	9
ACKNOWLEDGEMENTS	11
CHAPTER ONE. INTRODUCTION	13
Elements studied	16
Foraminiferal composition	16
Outline of the thesis	19
References	20
CHAPTER TWO. FORAMINIFERAL CALCITE TRACE ELEMENT DISTRIBUTION COEFFICIENTS	23
Outline of the experiments	24
Laboratory culture procedures	25
Variation of trace elements (Li and Sr) and seawater major elements (Na, Mg, and SO ₄)	29
Experimental design	29
Lithium/calcium	29
Sodium/magnesium	34
Sulfate concentration	43
Natural seawater	43
General discussion	43
Distribution coefficients	43
Ion pairing models of seawater culture solutions	55
Lithium and strontium speciation	56
Chamber amputations vs. the use of whole shells	56
Results and discussion	57
Lithium/calcium	57
Strontium/calcium	60
Magnesium/calcium	60
Sodium/calcium	66
Cadmium and zinc	69
Experimental design	69
Results	75
Cadmium	75
Zinc	81
Discussion	81
Cadmium	81
Zinc	88

Temperature and foraminiferal calcite trace	
element distribution coefficients	89
Outline of the experiments	91
Results and discussion	92
Panama Basin sediment trap samples	92
North Atlantic benthic foraminifera	92
Indian Ocean core top planktonic samples	98
North Atlantic core top planktonic samples	98
Laboratory culture experiments	104
Summary	113
Appendix 2.1 Calculation procedures for relative	
incorporation coefficients	114
References	118

CHAPTER THREE. THE EFFECTS OF DIAGENESIS ON TRACE ELEMENTAL	
RATIOS IN FORAMINIFERAL CALCITE OVER THE LAST 100 M.Y.	121
Sample selection	123
Age assignments on DSDP samples	123
The use of mixed planktonic foraminiferal samples	124
Foraminiferal sample preparation	126
Preliminary cleaning	126
Final cleaning of crushed foraminiferal shells	127
Locations studied	128
Site descriptions	128
Foraminiferal chemistry	128
The effects of diagenesis	128
Partial dissolution	128
Solid diffusion	132
Recrystallization of biogenic calcites	133
Lithium	133
Strontium	135
Magnesium	135
Sodium	135
Modelling of diagenesis	136
Simple model	136
Interstitial water compositions	137
Foraminiferal chemistry and diagenesis	138
Distribution coefficients	138
Magnesium	149
Other elements	151
Diagenetic changes at the sites studied	152
Site 289	152
Site 305	155
Sites 366 and 526	156
Conclusions	156
Inorganic distribution coefficients	156
Diagenetic modelling	157
Appendix 3.1 Foraminiferal calcite composition --	
DSDP samples	160
Appendix 3.2 Interstitial water compositions and	
calculated inorganic calcite compositions	173
References	183

CHAPTER FOUR. OCEANIC PALEOCHEMICAL VARIATIONS OVER THE LAST 100 M.Y.	186
The connection between spreading rates and hydrothermal fluxes	187
Paleochemical records	188
Lithium/calcium	188
Strontium/calcium	191
Magnesium/calcium	191
Sodium/calcium	191
Seawater strontium isotopic ratios	198
Summary	198
Lithium mass-balance model	201
Lithium as an indicator of hydrothermal fluxes	204
Oceanic Li/Ca ratios over the last 100 m.y.	206
Magnitude of hydrothermal fluxes	206
Removal constants	210
River fluxes	212
Calcium and lithium	213
Conclusions	217
Oceanic lithium concentrations	217
Other cycles	217
Seafloor spreading rate changes	218
Appendix 4.1 Li — reservoirs and fluxes	219
References	226
 CHAPTER FIVE. CONCLUSIONS	 230
 APPENDIX 1. ANALYTICAL METHODS FOR TRACE ELEMENTAL RATIOS IN FORAMINIFERAL CALCITE	 233
REFERENCES -- THESIS	244
BIOGRAPHICAL NOTE	253

LIST OF FIGURES

2.1	Li/Ca ratios in foraminiferal calcite and seawater growth solutions	58
2.2	Sr/Ca ratios in foraminiferal calcite and seawater growth solutions	61
2.3	Mg/Ca ratios in foraminiferal calcite and seawater growth solutions	63
2.4	Na/Ca ratios in foraminiferal calcite and seawater growth solutions	67
2.5	Cd distribution coefficients measured on foraminiferal shells grown in radiotracer spiked solutions	79
2.6	Zn distribution coefficients measured on foraminiferal shells grown in radiotracer spiked solutions	86
2.7	Average trace elemental ratios in three species of planktonic foraminifera from Panama Basin sediment traps and benthic foraminifera from a North Atlantic sediment core versus assumed calcification temperatures	96
2.8	Trace elemental ratios in size-fractions of three species of planktonic foraminifera from an Indian Ocean core top (RC14-36) versus $\delta^{18}\text{O}$	101
2.9	Trace elemental ratios in four species of planktonic foraminifera from V25-60 TW core top versus $\delta^{18}\text{O}$	105
2.10	Trace elemental ratios in four species of planktonic foraminifera from V22-26 TW core top versus $\delta^{18}\text{O}$	107
3.1	Map of locations of DSDP sites used in this study	130
3.2	Foraminiferal calcite composition as a function of age for Site 289 (Leg 30)	139
3.3	Foraminiferal calcite composition as a function of age for Site 305 (Leg 32)	141
3.4	Foraminiferal calcite composition as a function of age for Site 366 (Leg 41)	143
3.5	Foraminiferal calcite composition as a function of age for Site 369 (Leg 41)	145
3.6	Foraminiferal calcite composition as a function of age for Site 526 (Leg 74)	147
3.7	Interstitial water elemental ratios as a function of age	181
4.1	Li/Ca ratios in foraminiferal calcite as a function of age	189
4.2	Sr/Ca ratios in foraminiferal calcite as a function of age	192
4.3	Mg/Ca ratios in foraminiferal calcite as a function of age	194
4.4	Na/Ca ratios in foraminiferal calcite as a function of age	196
4.5	Seawater $^{87}\text{Sr}/^{86}\text{Sr}$ ratios as a function of age	199
4.6	Li/Sr ratios in foraminiferal calcite as a function of age	215

LIST OF TABLES

1.1	Elements studied	17
2.1	Li-spiked natural seawater -- <u>G. sacculifer</u> (Barbados)	31
2.2	Li-spiked natural seawater -- <u>O. universa</u> (Barbados)	35
2.3	Li-spiked artificial seawater -- <u>G. sacculifer</u> (Curacao)	37
2.4	Na/Mg variations in artificial seawater -- <u>G. sacculifer</u> (Barbados)	40
2.5	Na/Mg variations in artificial seawater -- <u>G. sacculifer</u> (Curacao)	44
2.6	SO ₄ concentration variations in artificial seawater -- <u>G. sacculifer</u> (Curacao)	47
2.7	30° C natural seawater lab culture and plankton tows -- <u>G. sacculifer</u> and <u>O. universa</u>	50
2.8	Radiotracer information	71
2.9	Cadmium incorporation	76
2.10	Zinc incorporation	82
2.11	Panama Basin sediment trap foraminifera	93
2.12	North Atlantic benthic foraminifera -- Chain 82 Station 31 Core 11PC <u>Uvigerina</u> spp.	95
2.13	Indian Ocean core top planktonic foraminifera	99
2.14	North Atlantic core top planktonic foraminifera	103
2.15	20° C natural seawater lab culture -- <u>G. sacculifer</u> and <u>O. universa</u>	109
2.16	20° C and 30° C natural seawater culture -- <u>G. sacculifer</u> and <u>O. universa</u> means	111
3.1	Time scale	125
3.2	Site information	129
3.3	Distribution coefficients for inorganically precipitated calcites	134
3.4	Inorganic calcite distribution coefficients from "recrystallized" calcite from Sites 289, 366, and 526	153
3.5	Foraminiferal calcite composition at Site 289 (Leg 30)	162
3.6	Foraminiferal calcite composition at Site 305 (Leg 32)	164
3.7	Foraminiferal calcite composition at Site 366 (Leg 41)	168
3.8	Foraminiferal calcite composition at Site 369 (Leg 41)	170
3.9	Foraminiferal calcite composition at Site 526 (Leg 74)	171
3.10	Interstitial water compositions and calculated inorganic calcite compositions at Site 289 (Leg 30)	175
3.11	Interstitial water compositions and calculated inorganic calcite compositions at Site 305 (Leg 32)	177
3.12	Interstitial water compositions and calculated inorganic calcite compositions at Site 366 (Leg 41)	178
3.13	Interstitial water compositions and calculated inorganic calcite compositions at Site 369 (Leg 41)	179
3.14	Interstitial water compositions and calculated inorganic calcite compositions at Site 526 (Leg 74)	180

	10
4.1 Li concentrations and fluxes	202
Al.1 Analytical conditions and furnace programs	235
Al.2 Primary standards	237
Al.3 Mean values for compositions of consistency standards	240
Al.4 Standard deviations (%) of means of multiple determinations of consistency standards within analytical runs	242

ACKNOWLEDGEMENTS

I would especially like to thank my advisor, Ed Boyle, for providing intellectual challenges, encouragement, academic and financial support, and friendship during my graduate student years at M.I.T. His intellect and scientific accomplishments are an inspiration to me. Professor Karl K. Turekian of Yale University first lured me into the field of marine geochemistry when I was a Yale undergraduate desperate for a summer job. His enthusiasm and vitality in pursuit of the truth and his willingness to share his insights were key factors in my choice of studies. A discussion with Karl always leaves me uplifted and eager to return to work, if sometimes a bit rattled. John Edmond played an important role in my graduate studies as well. The global frameworks in which these three scientists think and teach about the earth have stretched my intellectual horizons.

A debt of gratitude is owed as well to the M.I.T./W.H.O.I. Joint Program in Oceanography and the faculty and staff at both places.

This work has benefitted from discussions with many people. I would especially like to thank the members of my thesis committee (Karl Turekian, Yale University; Fred Sayles, W.H.O.I.; and Mike Bender, U.R.I.). Allan Be of L.D.G.O. taught me everything I know about culturing planktonic foraminifera and generously gave me the opportunity to do the experiments reported here. Joris Gieskes of Scripps Institution of Oceanography was generous with his expertise about DSDP sites, carbonate diagenesis, and interstitial water profiles; he gave me access to unpublished interstitial water data and archived interstitial water samples. Karen Von Damm provided data and ideas on hydrothermal systems from her thesis. Jennifer Hess of U.R.I. provided a copy of an enlarged version of the seawater Sr isotopic curve.

Sue Jones, Sally Husted, and Susan Chapnick were responsible for the smooth workings over the years of the laboratory at M.I.T. in which this research was done. Michael Albergo helped with the preparation of the final copy of this document.

I would like to thank the Bellairs Research Institute (St. James, Barbados) and the Curacao Marine Biological Institute (Curacao, Netherland Antilles) where the foraminiferal culture experiments were done. The assistance of Howard Spero, Walter Faber, and Mei Bé and the guidance of Allan Bé in these experiments are gratefully acknowledged. Fred Frey allowed me to use the M.I.T. LEPS γ -counting system and Pilalamarri Ila guided me through its use. The Panama Basin sediment trap samples were supplied courtesy of Sus Honjo (W.H.O.I.). The Chain 82, Station 31, Core 11 PC samples were obtained from the W.H.O.I. core laboratory with the assistance of James Broda. Core collection and curation at W.H.O.I. is supported by U. S. National Science Foundation grant OCE 2025231. W. B. Curry generously supplied the Indian Ocean core top samples and the oxygen and carbon isotopic data. These samples and the North Atlantic core top samples were supplied by the L.D.G.O. core laboratory. Core collection and curation at L.D.G.O. is supported by U. S. National Science Foundation grant OCE 7825448. The Deep Sea Drilling Project samples were supplied through the assistance of the U. S. National Science Foundation.

I would like to thank the curators and staff of DSDP for their assistance.

This research was supported by U. S. National Science Foundation grants OCE 8209362 and OCE 8018665. I would like to thank the Shell Companies Foundation Inc. for the Shell Doctoral Fellow Award which supported me for the academic year 1983-84.

Many people have made the marine geochemistry group at M.I.T. a productive and enjoyable place to work and play. I would like to thank them all for this as well as for the many "starving graduate student subsidies" I have received.

I would like to thank my parents for their support and encouragement in my academic endeavors and for their exorbitant pride in my accomplishments.

Most of all, I would like to thank all those friends who believed in me through thick and thin and have made my life so enjoyable. Their support has meant a great deal to me. I would especially like to thank Susan Chapnick for the hours of painstaking proofreading she did during the preparation of this thesis. Susan Chapnick and Alan Shiller were unfailingly cheerful and optimistic about this thesis, even when the same could not be said of its author. They helped the thesis and the author immeasurably in the final stages of its completion.

CHAPTER ONE:

INTRODUCTION

The temporal variability of seawater composition is a subject of debate. Ridge crest hydrothermal fluxes are calculated to be significant in oceanic mass balances of some elements (e.g., Edmond et al., 1979; 1982). For such elements, changes in the operation of the ridge crest reaction system could have resulted in changes in their oceanic concentrations. Lithium, for example, has a calculated hydrothermal flux to the ocean approximately 10 times the estimated river input (Edmond et al., 1979; 1982).

Several types of evidence have suggested that average crustal generation rates have varied significantly through time. Eustatic sea level variations (Vail et al., 1977) and percentage of continental flooding (Hallam, 1977) were assumed to be due solely to changes in ridge volume (Hays and Pitman, 1973; Turcotte and Burke, 1978). Because of the uniform age-depth and age-heat flow relationships for ocean crust (Parsons and Sclater, 1977), increased ridge volume results in a higher crustal generation rate and higher heat flow at the ridge crest (Turcotte and Burke, 1978; Sprague and Pollack, 1980; Harrison, 1980). The contribution of the ridge crest to global heat flow was calculated to be 28% at present and to have been as high as 50% of the total 80 m.y.b.p. (Turcotte and Burke, 1978).

Ridge volume calculated from magnetic lineations and from an assigned

magnetic reversal time scale indicated a pulse of very rapid spreading from 110-85 m.y.b.p. in the central and South Atlantic and throughout the Pacific (Larson and Pitman, 1972; Hays and Pitman, 1973). Root-mean-square velocities for the lithosphere as a whole were estimated from a plate rotation method to be twice present velocities at 80 m.y.b.p. (Davis and Solomon, 1981).

Crustal generation rate and ridge crest heat flow were estimated to have been larger in the past by as much as a factor of two from these geological and geophysical arguments. However, evidence and techniques used in these calculations have been questioned. Although eustatic sea level was clearly higher than at present in the Late Cretaceous, the absolute sea level difference and the methods used to determine it are debated (e.g., Watts and Steckler, 1979; Watts, 1982). Ridge volume and spreading rate calculated from magnetic lineations of the ocean crust depend on the time scale chosen; results are sensitive to small differences in age assignments (Berggren et al., 1975). Eustatic sea level changes can result from alterations in the area-age distribution of ocean crust or in the total oceanic area as well as from ridge volume changes (Parsons, 1982).

Chemical fluxes due to hydrothermal circulation depend on a number of parameters: flux of water through the ridge crest, depth of penetration of water in the crust, amount of cracking in the rocks, etc. Integrations of observed heat flow anomalies showed that 32% of the total ridge heat flow for a fast-spreading ridge (East Pacific Rise, 3-6 cm/y) and 42% of the total for a composite of slow-spreading ridges (1-2 cm/y) were due to advection of heat by hydrothermal circulation (Wolery and Sleep, 1976). Since the proportion of heat lost by hydrothermal circulation varies by

only 10% in the present day ocean for a factor of two to three difference in spreading rate, the total flux of water through the ridge crest is approximately proportional to the spreading rate. Chemical fluxes from hydrothermal systems with different water fluxes have not yet measured, but increased crustal generation rate and water flux through the ridge crest should result in larger hydrothermal fluxes due to the high-temperature seawater-basalt reactions.

Therefore, the suggested crustal generation rate variations since 80-110 m.y.b.p. would have had profound effects on ocean chemistry. Oceanic Li concentrations could have been as much as a factor of two higher 80-110 m.y.b.p. than at present, with concentrations decreasing over time to the present value.

The purpose of this thesis is to investigate temporal changes in oceanic Li concentrations. The history of this element, whose oceanic cycle is dominated by hydrothermal circulation, is related to the operation of the hydrothermal circulation system through time. This study adds independent geochemical evidence for the resolution of the debate about seafloor spreading rate changes.

The means of determining past seawater chemistry is in the sediments. To deduce solution composition, an indicator phase is required. The relationship of the chemical composition of this phase to that of the seawater in which it formed must be known. The phase must retain its original composition through time; alternatively, a quantitative assessment of any diagenetic changes must be possible for accurate reconstructions.

Calcite shells deposited by foraminifera have been studied as such indicators for the oxygen, carbon, and strontium isotopic compositions of seawater and for the oceanic concentrations of strontium, magnesium,

sodium, and cadmium. This thesis examines foraminiferal calcite as an indicator phase, evaluating its uptake and diagenetic properties.

An introduction to the behavior of lithium, calcium, strontium, magnesium, and sodium in the ocean and in foraminiferal calcite follows.

ELEMENTS STUDIED

River and hydrothermal fluxes as well as oceanic concentrations and residence times for Li, Ca, Sr (including its isotopes), Mg, and Na are given in Table 1.1. Ca, Mg, and Na are major components of seawater salinity and have conservative water column behavior. Li and Sr are present at $\mu\text{mol/l}$ levels in seawater and are also conservative. Li has the shortest calculated residence time of the elements listed, 0.3×10^6 y; Na the longest, 83×10^6 y.

The global hydrothermal fluxes listed are those calculated by Edmond et al. (1979; 1982). A different extrapolation from the measured hydrothermal solution chemistry would affect the description of the elemental cycles to a degree dependent on the importance of hydrothermal fluxes in each cycle. These alternate models and their impact on determining the history of hydrothermal circulation from oceanic Li concentrations are discussed in Chapter 4. For the elements discussed, hydrothermal fluxes are most significant in the mass balances for Li and Mg and for the Sr isotopic balance.

FORAMINIFERAL COMPOSITION

Sr, Mg, and Na compositions of foraminiferal shells have been analyzed by a number of investigators, with different degrees of attention paid to potential contamination in these measurements (e.g., Emiliani,

TABLE 1.1 Elements studied

element	seawater concentration (mmol/l)	river flux (mol/y)	hydrothermal flux (mol/y)	residence time (10 ⁶ y)
Li	0.028	14 × 10 ⁹ ^a	95-160 × 10 ⁹ ^a 115-190 × 10 ⁹ ^b	0.2-0.4 ^a 0.2-0.3
Ca	10.4	12 × 10 ¹² ^a	2.1-4.3 × 10 ¹² ^a 1.8 × 10 ¹² ^b	0.9-1.04 ^a 1.05
Sr	0.087	2.5 × 10 ¹⁰ ^c	no increase at Galapagos ^a ; slight increase at 21°N ^b	4.8
Mg	54.7	5.3 × 10 ¹² ^a	-7.7 × 10 ¹² ^{a,d}	max. 9.6 ^a
Na	470	6.9 × 10 ¹² ^e	hydrothermal end members show increases and decreases from ambient values; no global extrapolation ^{a,b}	83 ^e
⁸⁷ Sr/ ⁸⁶ Sr	0.709 ^f	> 0.712	0.703	

TABLE 1.1 continued

- Notes:
- a. Edmond et al. (1979), Galapagos Spreading Center.
 - b. Edmond et al. (1982) and Von Damm (1983), 21° N, East Pacific Rise.
 - c. Based on river Sr concentration in Brass (1976).
 - d. (-) on the Mg flux indicates that hydrothermal reactions are a sink for oceanic Mg
 - e. Based on river Na concentration in Broecker and Peng (1982); residence time *ibid.*, Table 1.6, pp. 26-27.
 - f. Burke et al. (1982).

Calculations assumed that the river flux of water to the ocean is 3.15×10^{16} l/y and that volume of the ocean is 1.37×10^{21} l.

1955; Thompson and Chow, 1955; Turekian, 1957; Blackmon and Todd, 1959; Krinsley, 1960; Lipps and Ribbe, 1967; Dasch and Biscaye, 1971; Kilbourne and Sen Gupta, 1973; Savin and Douglas, 1973; Bender et al., 1975; Lorens et al., 1977; Graham et al., 1982). There are two reports of Li concentrations in globigerina oozes; the values are high compared to those determined in this study (Horstmann, 1957; Welby, 1958). Paleochemical applications of foraminiferal shell chemistry include studies of Sr/Ca and Na/Ca in the Cenozoic (Graham et al., 1982), studies of cadmium/calcium over the last 200,000 y (Boyle and Keigwin, 1982), and studies of the Sr isotopic composition of foraminiferal calcite to determine seawater $^{87}\text{Sr}/^{86}\text{Sr}$ over geologic time (Dasch and Biscaye, 1971; Brass, 1976; and Burke et al., 1982).

OUTLINE OF THE THESIS

Laboratory experiments culturing planktonic foraminifera to test the response of foraminiferal shell chemistry to solution chemistry are described in Chapter 2. These calibrations are crucial to the use of foraminiferal shells as recorders of oceanic chemistry.

Time studies of foraminiferal shell chemistry over the last 100 m.y. are described in Chapter 3. The effects of diagenetic processes on the original oceanic chemistry signal recorded by the shells are discussed and the extent to which this signal can be deconvolved from these altered records is assessed. The importance of diagenesis and its quantification is emphasized in relation to paleochemical questions.

The time course of oceanic chemistry deciphered in Chapter 3 is related to oceanic mass balances in Chapter 4. Connections to geophysical variations are explored and limits suggested for these variations.

The three lines of research are summarized in Chapter 5.

REFERENCES — CHAPTER ONE

- Bender M. L., R. B. Lorenz, and D. F. Williams (1975) Sodium, magnesium and strontium in the tests of planktonic foraminifera, *Micropal.* 21: 448-459.
- Berggren, W. A., D. P. McKenzie, J. G. Sclater, and J. E. Van Hinte (Discussion) and Larson, R. L. and W. C. Pitman III (Reply) (1975) World-wide correlation of Mesozoic magnetic anomalies and its implications: discussion and reply, *Geol. Soc. Amer. Bull.* 86: 267-272.
- Blackmon, P. D. and R. Todd (1959) Mineralogy of some foraminifera as related to their classification and ecology, *Jour. Paleontol.* 33: 1-15.
- Boyle, E. A. and L. D. Keigwin (1982) Deep circulation of the North Atlantic over the last 200,000 years: geochemical evidence, *Science* 218: 784-787.
- Brass, G. W. (1976) The variation of the marine $^{87}\text{Sr}/^{86}\text{Sr}$ ratio during Phanerozoic time: interpretation using a flux model, *Geochim. Cosmochim. Acta* 40: 721-730.
- Broecker, W. S. and T.-H. Peng (1982) *Tracers in the Sea*, Palisades, N.Y., Lamont-Doherty Geological Observatory Press.
- Burke, W. H., R. E. Denison, E. A. Hetherington, R. B. Koepnick, H. F. Nelson, and J. B. Otto (1982) Variation of seawater $^{87}\text{Sr}/^{86}\text{Sr}$ throughout Phanerozoic time, *Geology* 10: 516-519.
- Dasch, E. J. and P. E. Biscaye (1971) Isotopic composition of strontium in Cretaceous-to-Recent, pelagic foraminifera, *Earth Planet. Sci. Lett.* 11: 201-204.
- Davis, D. M. and S. G. Solomon (1981) Variations in the velocities of the major plates since the Late Cretaceous, *Tectonophys.* 74: 189-208.
- Edmond, J. M., C. Measures, R. E. McDuff, L. H. Chan, R. Collier, B. Grant, L. I. Gordon, and J. B. Corliss (1979) Ridge crest hydrothermal activity and the balances of the major and minor elements in the ocean: the Galapagos data, *Earth and Planet. Sci. Lett.* 46: 1-18.
- Edmond, J. M., K. L. Von Damm, R. E. McDuff, and C. I. Measures (1982) Chemistry of hot springs on the East Pacific Rise and their effluent dispersal, *Nature* 297: 187-191.
- Emiliani, C. (1955) Mineralogical and chemical composition of the tests of certain pelagic foraminifera, *Micropal.* 1: 377-380.
- Graham, D. W., M. L. Bender, D. F. Williams, and L. D. Keigwin, Jr. (1982) Strontium-calcium ratios in Cenozoic planktonic foraminifera, *Geochim. Cosmochim. Acta* 46: 1281-1292.

- Hallam, A. (1977) Secular changes in marine inundation of USSR and North America through the Phanerozoic, *Nature* 269: 769-772.
- Harrison, C. G. A. (1980) Spreading rates and heat flow, *Geophys. Res. Lett.* 7: 1041-1044.
- Hays, J. D. and W. C. Pitman III (1973) Lithospheric plate motion, sea level changes and climatic and ecological consequences, *Nature* 246: 18-22.
- Horstmann, E. L. (1957) The distribution of lithium, rubidium, and caesium in igneous and sedimentary rocks, *Geochim. Cosmochim. Acta* 12: 1-28.
- Kilbourne, R. T. and B. K. Sen Gupta (1973) Elemental composition of planktonic foraminiferal tests in relation to temperature-depth habitats and selective solution, *Geol. Soc. Amer. Abstracts with Programs* 5: 408-409.
- Krinsley, D. (1960) Trace elements in the tests of planktonic foraminifera, *Micropal.* 6: 297-300.
- Larson, R. L. and W. C. Pitman III (1972) World-wide correlation of Mesozoic magnetic anomalies and its implications, *Geol. Soc. Amer. Bull.* 83: 3645-3662.
- Lipps, J. H. and P. H. Ribbe (1967) Electron-probe microanalysis of planktonic foraminifera, *Jour. Paleontol.* 41: 492-496.
- Lorens, R. B., M. L. Bender, and D. F. Williams (1977) The early nonstructural chemical diagenesis of foraminiferal calcite, *Jour. Sed. Petrol.* 47: 1602-1609.
- Parsons, B. (1982) Causes and consequences of the relation between area and age of the ocean floor, *Jour. Geophys. Res.* 87(B1): 289-302.
- Parsons, B. and J. G. Sclater (1977) An analysis of the variation of ocean floor bathymetry and heat flow with age, *Jour. Geophys. Res.* 82: 803-827.
- Savin, S. M. and R. G. Douglas (1973) Stable isotope and magnesium geochemistry of Recent planktonic foraminifera from the South Pacific, *Geol. Soc. Amer. Bull.* 84: 2327-2342.
- Sprague, D. and H. N. Pollack (1980) Heat flow in the Mesozoic and Cenozoic, *Nature* 285: 393-395.
- Thompson, T. G. and T. J. Chow (1955) The strontium-calcium atom ratio in carbonate-secreting marine organisms, *Deep-Sea Res.* 3(Suppl.): 20-39.
- Turcotte, D. L. and K. Burke (1978) Global sea-level changes and the thermal structure of the earth, *Earth Planet. Sci. Lett.* 41: 341-346.

- Turekian, K. K. (1957) The significance of variations in the strontium content of deep sea cores, *Limno. and Ocean.* 2: 309-314.
- Vail, P. R., R. M. Mitchum, Jr., and S. Thompson III (1977) Seismic stratigraphy and global changes of sea level, part 4: global cycles of relative changes of sea level, *Amer. Assoc. Petro. Geol. Mem.* 26: 83-97.
- Von Damm, K. L. (1983) Chemistry of submarine hydrothermal solutions at 21° N, East Pacific Rise and Guaymas Basin, Gulf of California, Ph.D. thesis, M.I.T./W.H.O.I.
- Watts, A. B. (1982) Tectonic subsidence, flexure and global changes of sea level, *Nature* 297: 469-474.
- Watts, A. B. and M. S. Steckler (1979) Subsidence and eustacy at the continental margin of Eastern North America, in Talwani, M., W. Hay, and W. B. F. Ryan, eds., Deep Drilling Results in the Atlantic Ocean: Continental Margins and Paleoenvironment, Maurice Ewing Series, vol. 3, AGU, Washington, D.C., pp. 235-248.
- Welby, C. W. (1958) Occurrence of alkali metals in some Gulf of Mexico sediments, *Jour. Sed. Petrol.* 28: 431-452.
- Wolery, T. J. and N. H. Sleep (1976) Hydrothermal circulation and geochemical flux at mid-ocean ridges, *Jour. Geol.* 84: 249-275.

CHAPTER TWO:

FORAMINIFERAL CALCITE TRACE ELEMENT DISTRIBUTION COEFFICIENTS

The relationship between foraminiferal calcite chemistry and solution chemistry must be known or assumed to use foraminifera as oceanic paleochemistry indicators. The correspondence between solution and foraminiferal calcite compositions can be tested in several ways:

1. Some elements or properties vary in the ocean at present. Foraminiferal calcite from different geographic or hydrographic locations can be compared to the water column properties. For example, cadmium has phosphate-like behavior in the ocean. Cd/Ca ratios in benthic foraminiferal shells from sediment core tops in the Atlantic and Pacific Oceans vary linearly with estimated bottom water Cd concentrations (Hester and Boyle, 1982). Plankton tow foraminiferal oxygen-18 variations correlate with water column temperature profiles (Fairbanks et al., 1980); core top foraminiferal assemblages relate to surface water physical oceanographic parameters (Imbrie and Kipp, 1971).

2. Other elements are conservative; this salinity-like behavior means that there are no significant variations in their elemental ratios to Ca in the present ocean. To test concentration changes in such elements, organisms can be grown in laboratory

culture in artificial or semi-artificial seawater solutions (e.g., studies of coral aragonite (Swart, 1981) and mussel calcite and aragonite (Lorens and Bender, 1980)). The organisms may be subjected to changes exceeding any in their natural lifetimes and perhaps greater than those expected over the geological time range of that species. For paleochemical applications, the response of one or a few modern species studied in culture are generalized to a number of different species over longer time periods.

OUTLINE OF THE EXPERIMENTS

Two series of experiments culturing planktonic foraminifera were done in collaboration with Dr. Allan Bé of Lamont-Doherty Geological Observatory. The first was January - February 1981 at Bellairs Research Institute (St. James, Barbados); the second, March - April 1982 at the Caribbean Marine Biological Institute (Curaçao, Netherland Antilles). Most of the experiments were done with Globigerinoides sacculifer (Brady), a spinose planktonic foraminifera with a distributional range of 40°N - 40°S in all oceans; it is a tropical and subtropical, shallow-water dwelling species (Bé, 1977). Some of the experiments were done with Orbulina universa, a spinose, sub-tropical, intermediate-water dwelling species. The juvenile form of O. universa is a multi-chambered shell; the adult form is a one-chambered spherical shell (Bé, 1977). A few experiments also involved Globigerinoides ruber (pink and white varieties), a spinose, tropical and subtropical, shallow-water dwelling species (Bé, 1977).

The experiments measured the effects of variations in solution Li/Ca, Sr/Ca, Mg/Ca, and Na/Ca ratios and of sulfate concentration changes (Ca

concentration constant) on foraminiferal calcite chemistry. The distribution coefficients of cadmium and zinc were determined using radiotracer techniques. The effects of temperature on biogenic calcite distribution coefficients were also studied. Analyses of foraminiferal shells from sediment trap and sediment core samples were included in the study of temperature effects in addition to the culture experiment results.

Li, Sr, Mg, Na, Ca, and SO_4 are all virtually conservative in the ocean; there are no variations to allow a present-day calibration similar to that done for Cd in benthic foraminifera. Some of the changes made in experimental solution concentrations for these elements are geologically reasonable, while others are larger than expected in oceanic history. These extreme changes serve to delimit the mechanisms of trace element incorporation over the narrower range potentially applicable to oceanic paleochemistry.

LABORATORY CULTURE PROCEDURES

Foraminifera form their calcite shells by the sequential addition of chambers, each representing a significant increment of both shell length and weight. Chambers are formed by secreting calcite layers on either side of a primary organic membrane. These layers are several microns thick, made up of calcite plaques or microgranules ($\sim 0.2 \mu\text{m}$ in diameter). Each layer deposits calcite over previous layers of the new chamber and over previous chambers (Bé, 1980). When foraminifera undergo gametogenesis, up to 20-30% by weight of the calcite shell is deposited over the outer shell layer (Bé, 1980 and Duplessy et al., 1981).

Although foraminiferal gametogenesis has been observed in laboratory culture, successive generations have not been grown from these gametes (Bé et al., 1977). For laboratory studies, foraminifera were captured

individually in glass jars from the upper water column by SCUBA diving, then brought to the laboratory, measured for shell length defined as the largest linear dimension, identified as to species, and placed in culture vessels illuminated by fluorescent lights. Since laboratory culture starts part way through the foraminiferal life cycle, the final calcite shell consists of some calcite secreted in the water column and some calcite secreted in laboratory culture.

In some experiments, foraminifera were individually tended and the chambers known to be formed while in culture were manually separated under a stereomicroscope before chemical analyses. In other experiments, foraminifera were grouped in small populations. The non-linear relationship of shell length and weight (Bé, pers. comm.) and the deposition of calcite on older chambers during chamber formation and gametogenesis (Bé, 1980 and Duplessy et al., 1981) suggest the contribution of initial calcite to the final weight may be as low as 10-20% for appropriate shell length changes. (For example, for an initial length of 350 μm and a final length of 650 μm , the contribution of initial calcite to the final weight on the average is 21%. If the foraminifer underwent gametogenesis with the same total length change, the initial shell constitutes 12% on the average of the total weight.) The use of radiotracers in several experiments insured that the measurements were of calcite deposited while in culture.

The residence time of elements in the protoplasmic pool used in shell formation is unknown. Calcium-45 uptake experiments with foraminifera indicate some delay in radiotracer Ca incorporation in the first chamber formed after transfer to a spiked solution (Anderson and Bé, pers. comm.). Delays due to protoplasmic equilibration affect the results as does the

calcite deposited in the water column before capture. In either case, the proportion of the shell which does not reflect the composition of the laboratory culturing solution increases. Physiological processes may control the composition of the calcifying fluid, discriminating for or against various elements, so that calcite composition is not directly proportional to solution composition (Lorens and Bender, 1977).

Foraminifera were removed from the laboratory culture solutions following gametogenesis or death; some were killed. The shells were rinsed several times with distilled water, air dried, and brought to M.I.T. for chemical analyses. They were cleaned of any remaining protoplasmic organic matter by treatment with hot basic hydrogen peroxide, followed by thorough distilled water and methanol rinses and air drying. The shells were reexamined under a stereomicroscope for cleanliness. Chamber amputations were performed on some samples at this stage.

Because of the graphite furnace atomic absorption spectroscopy (GFAAS) detection limits for Li, the calcite from several foraminifera grown in similar solutions were combined for chemical analyses. Typical sample sizes were 4 - 20 individuals or the separated chambers from that number; samples as small as one shell were also analyzed.

The samples were thoroughly rinsed with distilled water prior to dissolution. The cleaned calcite shell samples were dissolved in purified 0.3N HNO₃, with volumes typically 75 - 100 μ l. Trace elements were determined by GFAAS, Ca by flame atomic absorption spectroscopy. Appendix 1 has a more complete discussion of GFAAS methods and conditions, FAAS methods, and analytical precision.

For experiments changing seawater chemistry (constant temperature, no radiotracer additions), two types of seawater solutions were used: surface

seawater obtained at the foraminiferal collection site, filtered through a 0.45 μm Millipore filter, spiked with additional trace elements; and artificial seawater, 1:1 mixtures of filtered surface seawater and weighed crystalline salts dissolved in distilled water. The major element composition could thus be changed and trace element levels as low as one-half those of normal seawater could be obtained. For solutions in the Barbados experiments, the salts were NaCl, NaHCO₃, Na₂SO₄, MgSO₄, CaCl₂, and K₂SO₄. For the Curacao experiments, the salts were NaCl, Na₂SO₄, MgCl₂, MgSO₄, NaHCO₃, CaCl₂, KCl, and SrCl₂. Li was added as a diluted spike of an atomic absorption primary standard (40.08 $\mu\text{mol/ml}$, Li₂CO₃ in 1% v/v HCl). Compositions of seawater solutions were calculated from the weights of salts or the volumes of solution spikes added and the total volumes of dilutions.

Radioisotope spikes for Cd or Zn and Sr were added to filtered surface seawater for the Cd and Zn incorporation experiments. Culture solutions of filtered surface seawater were used in the temperature variation culture experiments.

In all experiments, foraminifera were fed once daily with one-day old brine shrimp (Artemia) nauplii. They were maintained at 28° - 30°C, with 12 hr alternating light and darkness at a light intensity of 200 - 500 $\mu\text{E/m}^2/\text{sec}$.

To minimize dilution effects, foraminifera grown in solutions other than surface seawater were transferred to the final culture solution through an aliquot of the same solution; the brine shrimp for the daily feedings were also transferred through this aliquot. Culture containers were covered with plexiglass sheets to minimize evaporation.

VARIATION OF TRACE ELEMENTS (Li and Sr) AND
SEAWATER MAJOR ELEMENTS (Na, Mg, and SO₄)

EXPERIMENTAL DESIGN

Lithium/calcium. Li concentrations were varied in two types of solutions. The Li concentration in natural seawater was increased up to twice that of natural seawater by the addition of a Li solution spike. G. sacculifer were grown in a series of these solutions, individually tended with daily measurements of shell length, amount of protoplasm in the shell, rhizopod condition, spine length, and presence and distribution of symbionts in the rhizopodial network. Chamber formation was recognized from substantial length changes and observations of protoplasmic chamber filling. The number of chambers each foraminifer added in culture was thus known. The chambers from 12 - 19 individuals grown in similar seawater solutions were pooled for analyses; the shells remaining after the amputation of the chambers formed in culture were similarly combined. Table 2.1 lists foraminiferal information, seawater compositions, and analytical results.

Juvenile, spiral-stage O. universa were also placed in these Li-spiked natural seawater solutions. Foraminifera which made the transition from this juvenile stage to the adult, spherical-stage while in laboratory culture were analyzed. The weight of calcite associated with the juvenile stage is extremely small compared to that with the adult stage; the juvenile stage shell usually disappears in the transition to adult as well. For O. universa, the contribution of calcite deposited prior to laboratory culture to the final result is minimal. Foraminiferal information, seawater compositions, and analytical results from this

EXPLANATORY NOTES FOR TABLES 2.1.A - 2.7.A, 2.15.A FORAMINIFERAL INFORMATION

of foraminifera was the total number in each sample.

Average weight per shell was calculated from the Ca analyses of the sample solutions, the known dissolution volumes, and the number of foraminifera in each sample. It did not include any calcite lost in sample handling or cleaning; these losses should have been small.

Average initial shell length and average final shell length were the mean shell lengths for each group of foraminifera at the beginning and end of laboratory culture. The population standard deviation for each mean is also reported to give an indication of the range of sizes. For O. universa samples, the initial shell lengths are those of the juvenile spiral-stage foraminifera placed in culture.

Average # of days in culture were the mean survival times in culture for the foraminifera in each sample group.

Average # of days to adult were the mean number of days in culture until the O. universa underwent the transition from the juvenile spiral-stage to the adult spherical-stage.

Culture termination lists codes for the number of foraminifera removed from culture for the following reasons:

G gametogenic
D dead
T terminated

EXPLANATORY NOTES FOR TABLES 2.1.B - 2.7.B, 2.15.B SEAWATER COMPOSITIONS

Seawater compositions were calculated from the weights of salts or volumes of solution spikes added and the total volumes of dilutions, assuming that $S = 36 \text{ ‰}$ for filtered surface seawater culture solutions. The composition of the surface seawater was assumed to be:

concentrations		ratios	
Na	474 mmol/l	Li/Ca	2.55×10^{-3}
Mg	54.5 mmol/l	Sr/Ca	8.68×10^{-3}
Ca	10.6 mmol/l	Mg/Ca	5.14
K	10.4 mmol/l	Na/Ca	44.7
Sr	92 $\mu\text{mol/l}$		
Li	27 $\mu\text{mol/l}$		
SO ₄	29.0 mmol/l		

The ratios listed in the tables are of the total calculated elemental concentrations.

TABLE 2.1 Li-spiked natural seawater -- G. sacculifer (Barbados)

2.1.A FORAMINIFERAL INFORMATION

sample #	# of foraminifera	average weight per shell (µg)	average initial shell length (µm)	average final shell length (µm)	average # of days in culture	total # of chambers separated	culture termination
1	19 (3) ¹	31	343 ± 54	679 ± 139	6	37	8G 6D 5T
2	19 (4) ¹	20	350 ± 67	590 ± 128	4	27	9G 4D 6T
3	15 (1) ¹	30	367 ± 64	695 ± 109	6	32	8G 2D 5T
4	12	25	331 ± 41	650 ± 120	6	26	6G 6T
5	12	36	333 ± 65	660 ± 150	5	28	5G 2D 5T

Notes: 1. Number in parentheses was number of foraminifera which did not form any new chambers after being placed in culture. No chambers were separated from these individuals and they were not included in calculation of average final shell length and average number of days in culture.

2.1.B SEAWATER COMPOSITIONS

sample #	Li/Ca (10 ⁻³)	Sr/Ca (10 ⁻³)	Mg/Ca	Na/Ca	K/Ca	[SO ₄] mmol/l
1	3.00	8.68	5.14	44.7	0.981	29.0
2	3.45	"	"	"	"	"
3	3.91	"	"	"	"	"
4	4.36	"	"	"	"	"
5	4.81	"	"	"	"	"

2.1.C ANALYTICAL RESULTS

sample #	sample designation	weight fraction chambers ¹	Li/Ca (10 ⁻⁶)	Sr/Ca (10 ⁻³)	Mg/Ca (10 ⁻³)	Na/Ca (10 ⁻³)	K/Ca (10 ⁻⁶)
1	chambers	0.56	14.3	1.31	4.84	6.49	258
	bodies		17.4	1.40	5.08	6.88	666
	total ²		15.6	1.35	4.95	6.68	437
2	chambers	0.41	20.2	1.32	3.82	6.43	209
	bodies		20.6	1.39	4.54	6.85	266
	total		20.5	1.36	4.24	6.67	242
3	chambers	0.50	21.0	1.37	4.48	6.10	237
	bodies		20.4	1.41	4.77	7.31	233
	total		20.7	1.39	4.63	6.68	235
4	chambers	0.58	22.4	1.40	4.04	5.43	348
	bodies		27.9	1.41	3.51	6.08	465
	total		24.8	1.40	3.81	5.70	396
5	chambers	0.61	22.0	1.42	5.87	6.06	116
	bodies		23.6	1.42	4.27	6.84	178
	total		22.6	1.42	5.26	6.35	140

- Notes: 1. Weight fraction chambers was proportion of total weight represented by separated chambers calculated from the calcium analyses on each solution and the known sample volumes.
2. Total ratios were calculated from analyses of chambers and bodies recombined in proportion to their weight fractions. The total ratios are the results expected if the foraminifera had been analyzed whole with no chamber amputations.

experiment are listed in Table 2.2.

Li has conservative oceanic behavior; natural seawater Li concentrations less than $\sim 27 \mu\text{mol/l}$ are not found. To test the response of shell chemistry to Li concentrations lower than the present oceanic one, 1:1 mixtures of natural and artificial Li-free seawaters were used. G. sacculifer were grown in seven different 1:1 mixtures with Li concentrations ranging from approximately one-half to twice seawater values. Li concentrations were varied by the volumetric addition of a solution spike. Foraminifera were tended in group populations with several individuals in each culture container. Foraminiferal information, seawater compositions, and analytical results are listed in Table 2.3.

Sodium/magnesium. Na/Ca and Mg/Ca ratios were simultaneously varied to test the response of shell chemistry to changes in these ratios. Two experiments were done, each using a series of 1:1 artificial:natural seawater mixtures similar to those used in the Li experiments.

In the first experiment, Na, Mg, Cl, and SO_4 concentrations all varied. Li and Sr concentrations were one-half those in natural seawater. G. sacculifer were grown in four different solution compositions (Na/Ca, 33.5 - 52.3; Mg/Ca, 7.82 - 2.94; solution with lowest Na/Ca has the highest Mg/Ca), with four individuals in each sample group. Foraminifera were individually tended with daily shell length measurements. Chamber amputation procedures were like those described for the Li-spiked natural seawater G. sacculifer experiment. Foraminiferal information, solution compositions, and analytical results are listed in Table 2.4.

In the second experiment, Na/Ca and Mg/Ca were varied over a wider range (Na/Ca, 22.4 - 52.3; Mg/Ca, 12.5 - 2.58). Ca, SO_4 , Li, and Sr concentrations and ionic strengths of all solutions were equal to those of

TABLE 2.2 Li-spiked natural seawater -- O. universa (Barbados)

2.2.A FORAMINIFERAL INFORMATION

sample #	# of foraminifera	average initial shell length (μm)	average final shell length (μm)	average # of days to adult	average # of days in culture
1	12	604 ± 88	651 ± 95	4	8
2	9	547 ± 87	621 ± 50	2	7
3	16	-	612 ± 68	3	8

2.2.B SEAWATER COMPOSITIONS

sample #	Li/Ca (10^{-3})	Sr/Ca (10^{-3})	Mg/Ca	Na/Ca	K/Ca	[SO ₄] mmol/l
1	3.00	8.68	5.14	44.7	0.981	29.0
2	3.91	"	"	"	"	"
3	4.81	"	"	"	"	"

2.2.C ANALYTICAL RESULTS

sample #	Li/Ca (10^{-6})	Sr/Ca (10^{-3})	Mg/Ca (10^{-3})	Na/Ca (10^{-3})	K/Ca (10^{-6})
1	14.9	1.36	10.3	7.32	399
2	16.9	1.29	9.56	6.11	88
3	27.2	1.27	12.4	6.11	87

TABLE 2.3 Li-spiked artificial seawater -- G. sacculifer (Curacao)

2.3.A FORAMINIFERAL INFORMATION

sample #	# of foraminifera	average weight per shell (μg)	average initial shell length (μm)	average final shell length (μm)	average # of days in culture	culture termination
1	9	23	395 \pm 48	489 \pm 97	5	5G 4D
2	10	22	413 \pm 49	515 \pm 83	5	6G 4D
3	10	22	396 \pm 51	481 \pm 87	4	7G 3D
4	10	22	426 \pm 31	518 \pm 55	4	6G 4D
5	9	23	347 \pm 89	579 \pm 82	7	4G 2D 3T
6	9	27	323 \pm 98	602 \pm 113	6	7G 2D
7	4	19	359 \pm 23	542 \pm 66	5	1G 2D 2T

2.3.B SEAWATER COMPOSITIONS

sample #	Li/Ca (10 ⁻³)	Sr/Ca (10 ⁻³)	Mg/Ca	Na/Ca	K/Ca	[SO ₄] mmol/l
1	1.27	8.58	5.14	44.7	0.981	29.0
2	1.88	"	"	"	"	"
3	2.48	"	"	"	"	"
4	3.08	"	"	"	"	"
5	3.70	"	"	"	"	"
6	4.30	"	"	"	"	"
7	4.91	"	"	"	"	"

2.3.C ANALYTICAL RESULTS

sample #	Li/Ca (10 ⁻⁶)	Sr/Ca (10 ⁻³)	Mg/Ca (10 ⁻³)	Na/Ca (10 ⁻³)
1	12.7	1.49	7.99	6.56
2	14.3	1.55	6.79	6.97
3	15.9	1.53	6.27	7.32
4	17.9	1.56	5.75	6.82
5	17.5	1.51	5.81	5.73
6	20.0	1.60	7.39	5.91
7	22.6	1.05	6.18	5.86

TABLE 2.4 Na/Mg variations in artificial seawater — G. sacculifer (Barbados)

2.4.A FORAMINIFERAL INFORMATION

sample #	# of foraminifera	average weight per shell (μg)	average initial shell length (μm)	average final shell length (μm)	average # of days in culture	total # of chambers separated	culture termination
1	4	38	326 \pm 39	805 \pm 68	9	12	3G 1T
2	4	41	301 \pm 15	670 \pm 49	7	10	4G
3	4 (1) ¹	22	377 \pm 5	669 \pm 49	6	8	3G 1D
4	4	46	373 \pm 101	760 \pm 92	8	7	4G

Notes: 1. Number in parentheses was number of foraminifera which did not form any new chambers after being placed in culture. No chambers were separated from these individuals and they were not included in calculations of average final shell length and average number of days in culture.

2.4.B SEAWATER COMPOSITIONS

sample #	Li/Ca (10^{-3})	Sr/Ca (10^{-3})	Mg/Ca	Na/Ca	K/Ca	[SO ₄] mmol/l
1	1.29	4.38	7.82	33.5	0.981	58.5
2	"	"	7.32	39.1	"	44.6
3	"	"	3.67	50.0	0.971	17.0
4	"	"	2.94	52.3	"	17.0

2.4.C ANALYTICAL RESULTS

sample #	sample designation	weight fraction chambers ¹	Li/Ca (10 ⁻⁶)	Sr/Ca (10 ⁻³)	Mg/Ca (10 ⁻³)	Na/Ca (10 ⁻³)	Na/Mg	K/Ca ² (10 ⁻⁶)
1	chambers	0.62	17.0	0.83	5.27	5.93	1.13	692
	bodies		20.8	1.19	6.91	6.00	0.87	679
	total ³		18.5	0.97	5.88	5.96	1.01	687
2	chambers	0.68	17.5	0.82	6.03	5.84	0.97	432
	bodies		30.4	0.96	6.84	6.52	0.95	1105
	total		21.7	0.87	6.29	6.06	0.96	647
3	chambers	0.70	24.0	0.78	4.54	6.97	1.54	1233
	bodies		38.5	0.97	4.16	8.39	2.02	1201
	total		30.0	0.86	4.39	7.55	1.72	1223
4	chambers	0.61	18.0	0.69	2.55	5.65	2.22	339
	bodies		30.0	0.92	2.99	6.76	2.26	723
	total		22.6	0.78	2.72	6.08	2.24	489

- Notes:
1. Weight fraction chambers was proportion of total weight represented by separated chambers calculated from the calcium analyses on each solution and the known sample volumes.
 2. Potassium numbers are not consistency standard corrected.
 3. Total ratios were calculated from analyses of chambers and bodies recombined in proportion to their weight fractions. The total ratios are the results expected if the foraminifera had been analyzed whole with no chamber amputations.

seawater. G. sacculifer were followed as group populations. Foraminiferal information, solution compositions, and analytical results for this experiment are listed in Table 2.5.

Sulfate concentration. SO_4 concentrations of seawater solutions were varied while the rest of the major element composition was the same as that of natural seawater. The solutions were 1:1 mixtures of artificial and natural seawaters, to give six different SO_4 concentrations (culture solution [SO_4], 14.5 - 59.5 mmol/l; natural seawater [SO_4], 29.0 mmol/l). The ionic strengths in these solutions, unlike those for the other experiments, did vary (culture solution I, 0.69 - 0.74 mol/l; natural seawater I, 0.71 mol/l). G. sacculifer were tended in groups. Foraminiferal information, solution compositions, and analytical results are listed in Table 2.6.

Natural seawater. A few G. sacculifer were grown in unaltered, filtered surface seawater. Table 2.7 lists the foraminiferal information, seawater compositions, and analytical results for the foraminifera cultured in natural seawater and for foraminiferal samples from plankton tows taken at the collection sites.

GENERAL DISCUSSION

Distribution coefficients. A concept relating the trace element composition of a solid to the chemistry of the solution from which it formed is that of a distribution coefficient (or partition coefficient). The distribution coefficient is the proportionality constant between solution and solid ratios of a trace element (here represented as M)

TABLE 2.5 Na/Mg variations in artificial seawater — G. sacculifer (Curacao)

2.5.A FORAMINIFERAL INFORMATION

sample #	# of foraminifera	average weight per shell (μg)	average initial shell length (μm)	average final shell length (μm)	average # of days in culture	culture termination
1	1	2	236	287	4	1D
2	4	3	291 ± 102	337 ± 126	3	4D
3	2	14	265 ± 0	530 ± 57	6	2T
4	4	12	229 ± 36	449 ± 212	5	2D 2T
5	3	16	315 ± 63	490 ± 56	5	1D 2T
6	1	21	428	504	6	1T

2.5.B SEAWATER COMPOSITIONS

sample #	Li/Ca (10 ⁻³)	Sr/Ca (10 ⁻³)	Mg/Ca	Na/Ca	K/Ca	[SO ₄] mmol/l
1	2.55	8.58	12.5	22.4	0.981	29.0
2	"	"	10.6	28.4	"	"
3	"	"	8.57	34.3	"	"
4	"	"	6.58	40.3	"	"
5	"	"	4.58	46.3	"	"
6	"	"	2.58	52.3	"	"

2.5.C ANALYTICAL RESULTS

sample #	Li/Ca (10 ⁻⁶)	Sr/Ca (10 ⁻³)	Mg/Ca (10 ⁻³)	Na/Ca (10 ⁻³)
1	-	1.50	44.64	14.99
2	-	1.35	6.26	6.15
3	-	1.38	7.28	5.11
4	14.3	1.33	5.42	4.08
5	12.1	1.23	4.84	3.62
6	-	1.23	5.27	4.95

TABLE 2.6 SO₄ concentration variations in artificial seawater -- G. sacculifer (Curacao)

2.6.A FORAMINIFERAL INFORMATION

sample #	# of foraminifera	average weight per shell (μg)	average initial shell length (μm)	average final shell length (μm)	average # of days in culture	culture termination
1	4	21	329 ± 91	569 ± 101	6	2D 2T
2	4	30	328 ± 80	663 ± 92	7	1G 3D
3	3	13	347 ± 82	612 ± 72	5	3D
4	4	18	320 ± 81	522 ± 128	6	1G 3D
5	4	14	323 ± 72	489 ± 104	6	1G 3D
6	3	5	353 ± 60	420 ± 113	6	3D

2.6.B SEAWATER COMPOSITIONS

sample #	ionic strength (mol/l)	Li/Ca (10^{-3})	Sr/Ca (10^{-3})	Mg/Ca	Na/Ca	K/Ca	[SO ₄] mmol/l
1	0.69	2.55	8.58	5.14	44.7	0.981	14.5
2	0.70	"	"	"	"	"	22.0
3	0.71	"	"	"	"	"	29.0
4	0.72	"	"	"	"	"	39.5
5	0.73	"	"	"	"	"	49.5
6	0.74	"	"	"	"	"	59.5

2.6.C ANALYTICAL RESULTS

sample #	Li/Ca (10^{-6})	Sr/Ca (10^{-3})	Mg/Ca (10^{-3})	Na/Ca (10^{-3})
1	14.0	1.38	5.84	5.38
2	11.3	1.49	6.71	5.07
3	12.1	1.20	5.70	5.05
4	14.2	1.39	4.82	6.69
5	13.9	1.46	5.48	6.61
6	-	1.42	9.62	6.38

TABLE 2.7 30° C natural seawater lab culture and plankton tows -- G. sacculifer and O. universa

2.7.A FORAMINIFERAL INFORMATION

sample #	sample description	# of foraminifera	average weight per shell (µg)	average initial shell length (µm)	average final shell length (µm)	average # of days in culture	culture termination
<u>G. sacculifer</u>							
1	lab culture	2	12	250 ± 0	385 ± 37	2	2D
2	lab culture	4	14	282 ± 59	460 ± 63	5	4D
3	lab culture ¹	8	44		620 ± 37		
4	lab culture ¹	1	47		590		
5	lab culture ¹	1	77		740		
6	lab culture ¹	1	66		700		
7	lab culture ¹	1	95		700		
8	lab culture ²	9	46		700 ± 47		
9	plankton tow Barbados	37	4		260		
10	plankton tow Curacao	11	21		440 ± 86		

2.7.A continued

sample #	sample description	# of foraminifera	average weight per shell (μg)	average initial shell length (μm)	average final shell length (μm)	average # of days to adult	average # of days in culture
<u>O. universa</u>							
11	lab culture	1	9	340	693	2	4
12	lab culture	2	13		626 \pm 21	5	6
13	lab culture	2	13		716 \pm 23	4	5
14	lab culture	2	13		479 \pm 0	5	5
15	lab culture ¹	8	25		570 \pm 103		

- Notes: 1. These foraminifera were not fed or observed after being placed in culture. Although initial sizes were not recorded, they were generally of large initial size ($> 400 \mu\text{m}$).
2. These foraminifera were placed in culture when the seawater solutions used were contaminated by bacteria. They died shortly after being placed in culture.

2.7.B SEAWATER COMPOSITIONS

sample #	Li/Ca (10 ⁻³)	Sr/Ca (10 ⁻³)	Mg/Ca	Na/Ca	K/Ca	[SO ₄] mmol/l
1-11, 15 (natural seawater)	2.55	8.68	5.14	44.7	0.981	29.0
12-14 (artificial seawater)		8.58	"	"	"	"

2.7.C ANALYTICAL RESULTS

	sample #	Li/Ca (10 ⁻⁶)	Sr/Ca (10 ⁻³)	Mg/Ca (10 ⁻³)	Na/Ca (10 ⁻³)
<u>G. sacculifer</u>	1	(41.4)	0.92	4.43	6.83
	2	20.5	1.35	4.68	7.42
	3	13.7	1.53	4.99	7.04
	4	23.4	1.24	4.21	6.16
	5	12.9	1.13	3.09	5.38
	6	7.66	0.98	2.67	4.39
	7	13.6	0.93	3.02	4.30
	8	15.3	1.47	4.75	7.04
	mean of 1-8	15.3 ¹ ± 5.4	1.19 ± 0.24	3.98 ± 0.91	6.07 ± 1.24
	9	23.4	1.68	7.12	-
	10	15.6	1.35	4.54	3.64
	mean of 9-10	19.5 ± 5.5	1.52 ± 0.23	5.83 ± 1.82	

Notes 1. Mean for Li/Ca did not include sample 1.

2.7.C continued

	sample #	Li/Ca (10 ⁻⁶)	Sr/Ca (10 ⁻³)	Mg/Ca (10 ⁻³)	Na/Ca (10 ⁻³)
<u>O. universa</u>	11	-	1.69	4.68	6.54
	12	-	0.91	10.27	8.51
	13	-	1.03	12.11	8.78
	14	-	0.68	7.20	4.39
	15	11.7	1.32	10.89	5.60
	mean of 11-15		1.13 ± 0.39	9.03 ± 3.03	6.76 ± 1.88

to the major element (Ca) for which it is presumed to be substituting in the solid phase:

$$D = \frac{\{MCO_3\}/\{CaCO_3\}_{\text{solid}}}{\{M^{2+}\}/\{Ca^{2+}\}_{\text{solution}}}$$

For an ideal solid solution, the distribution coefficient is equal to the quotient of the solubility products of the two solids:

$$D = \frac{K_{so}(CaCO_3)}{K_{so}(MCO_3)}$$

The distribution coefficient can be expressed in concentrations in solution and mole fractions in the solids with solid and solution activity coefficients:

$$D = \frac{\gamma_{MCO_3} X_{MCO_3} \gamma_{Ca^{2+}} [Ca^{2+}]}{\gamma_{CaCO_3} X_{CaCO_3} \gamma_{M^{2+}} [M^{2+}]}$$

Foraminiferal calcite distribution coefficients in the following discussion are calculated from solid and solution concentrations.

Ion pairing models of seawater culture solutions. The seawater concentrations listed in Tables 2.1-2.7 are total elemental concentrations calculated from the weights of the crystalline salts, the volume of solution spikes, and the volumes of seawater and distilled water used in preparing each culture solution. In several of the experiments (Na/Mg variations and SO₄ concentration changes), major element compositions were significantly different from seawater. The speciation of the major elements in these solutions was calculated using an ion-pairing model for seawater (Garrels and Thompson, 1962) with a version of MICROEQL running at fixed pH (R. E. McDuff, pers. comm.). Ratios of the major elements to Ca

of the model-derived free ion concentrations are linearly offset from ratios of total concentrations. Free Mg/Ca ratios are lower than total ones; free Na/Ca ratios are greater. The small, nearly linear offsets mean that the relative availability of the free ions did not change significantly with large changes in solution composition.

Lithium and strontium speciation. Li is dominantly present as the free ion in seawater (94%). The two ion-pairs used in this calculation were LiSO_4 , which was 6% of the total Li in seawater, and LiOH , which accounted for less than 1% of the total Li at seawater pH. In all the solutions used in the culture experiments, greater than 90% of the total Li was present as the free ion. The major Sr species in seawater is the free ion.

Chamber amputations vs. the use of whole shells. In two experiments (Li-spiked natural seawater, Table 2.1, and Na/Mg variations with varying SO_4 concentrations, Table 2.4) the chambers formed while the foraminifera were in laboratory culture were separated from the rest of the shells. Both portions were analyzed. The ratios determined for the chambers and the remaining shells of a foraminiferal sample group were mathematically recombined using the relative weight proportions to give the expected results if the samples had been analyzed whole with no separations. The results of the separate analyses of chambers and remaining shells in these two experiments (Tables 2.1 and 2.4) show that the compositions of the separated bodies are often similar to those of the newly formed chambers. This indicates that new chamber formation and/or gametogenic calcification did add layers of new calcite to previously formed chambers, this calcite being a significant proportion of shell weight.

This information led to the easier experimental protocol of

monitoring foraminifera in group populations for some studies. Several foraminifera were placed in each container of culture solution, with only initial and final measurements of shell length taken.

RESULTS AND DISCUSSION

Lithium/calcium. Li/Ca ratios in the calcite of G. sacculifer and O. universa grown in Li-spiked natural seawater and G. sacculifer grown in Li-spiked artificial seawater increase with increases in the growth solution Li/Ca ratio above that of natural seawater (Figure 2.1). The average results of a number of G. sacculifer and O. universa grown in natural seawater agree with the trends defined by the two species grown in Li-spiked natural and artificial seawater. The mean Li distribution coefficient for foraminifera grown in solutions with Li/Ca equal to or greater than that of natural seawater is $4.9 \pm 0.6 \times 10^{-3}$ for four O. universa samples and $5.3 \pm 0.7 \times 10^{-3}$ for eleven G. sacculifer samples. (Unless otherwise specified, quoted errors are 1 σ standard deviations of the data set).

Foraminifera grown in solutions with Li/Ca ratios lower than natural seawater (Tables 2.3 and 2.4) have Li/Ca ratios which are above the trend defined by the mean distribution coefficient of G. sacculifer grown in Li-enriched solutions. This difference is particularly striking for Li/Ca ratios of G. sacculifer grown in solutions with variations in Na/Mg (Barbados experiment only; Table 2.4). The solutions in this experiment had Li/Ca ratios approximately one-half that of seawater, yet the foraminiferal Li/Ca ratios are greater than that of a sample grown in unaltered seawater. The calculated distribution coefficients for these Na/Mg experiment foraminiferal separated chambers range from $(13 - 19) \times 10^{-3}$. One possible

FIGURE 2.1 Li/Ca ratios in foraminiferal calcite and seawater growth solutions. Plot symbols are:

- ☒ G. sacculifer -- Li-spiked natural seawater (Barbados) separated chambers
- ☐ G. sacculifer -- Li-spiked artificial seawater (Curacao)
- × G. sacculifer -- 30° C natural seawater lab culture averages
- △ O. universa -- Li-spiked natural seawater (Barbados)
- + O. universa -- 30° C natural seawater lab culture averages

The line is defined by the mean of the 15 samples with seawater solution Li/Ca ratios greater than or equal to that of natural seawater. The mean distribution coefficient, with the fit forced through zero, is $(5.2 \pm 0.6) \times 10^{-3}$.

Li/Ca ratios in the separated chambers from the Na/Mg G. sacculifer experiment (Table 2.4) are not on this plot.

explanation for this difference is that the SO_4 concentrations in these solutions were not equal to that of seawater (Table 2.4.B). Therefore, in another experiment, major and trace elemental concentrations were kept constant while SO_4 concentrations in the growth solutions were varied (Table 2.6). Li/Ca ratios from foraminifera grown in those solutions do not correlate with solution SO_4 concentrations or solution Li/ SO_4 ratios. There is no obvious explanation for the comparatively high Li/Ca calcite ratios observed in foraminifera grown in this experiment (Table 2.4).

The compositions of the separated chambers and the remaining shells in two experiments are similar (Tables 2.1 and 2.4), so that the contribution of the initial water column calcite to the total shell weight is small.

Strontium/calcium. Mean Sr/Ca ratios in G. sacculifer and O. universa calcite from all experiments are plotted versus the Sr/Ca ratios in the growth solutions (Figure 2.2). The mean Sr distribution coefficient for all 33 G. sacculifer samples is 0.16 ± 0.02 . The mean distribution coefficient for the separated chambers from four G. sacculifer at solution Sr/Ca 4.38×10^{-3} is 0.18 ± 0.01 ; for all G. sacculifer and O. universa at normal seawater Sr/Ca $(8.6 - 8.7) \times 10^{-3}$, the distribution coefficient is 0.16 ± 0.02 (29 samples).

In culturing experiments with the mollusc Mytilus edulis, a Sr distribution coefficient in calcite of 0.13 ± 0.01 was determined (Lorenz and Bender, 1980). Previous measurements on foraminiferal calcite and other biogenic calcites have shown Sr distribution coefficients about 0.16 ± 0.02 (see references in Graham et al., 1982).

Magnesium/calcium. Mg/Ca ratios in foraminiferal calcite increase with increases in the seawater Mg/Ca ratios (Figure 2.3). The

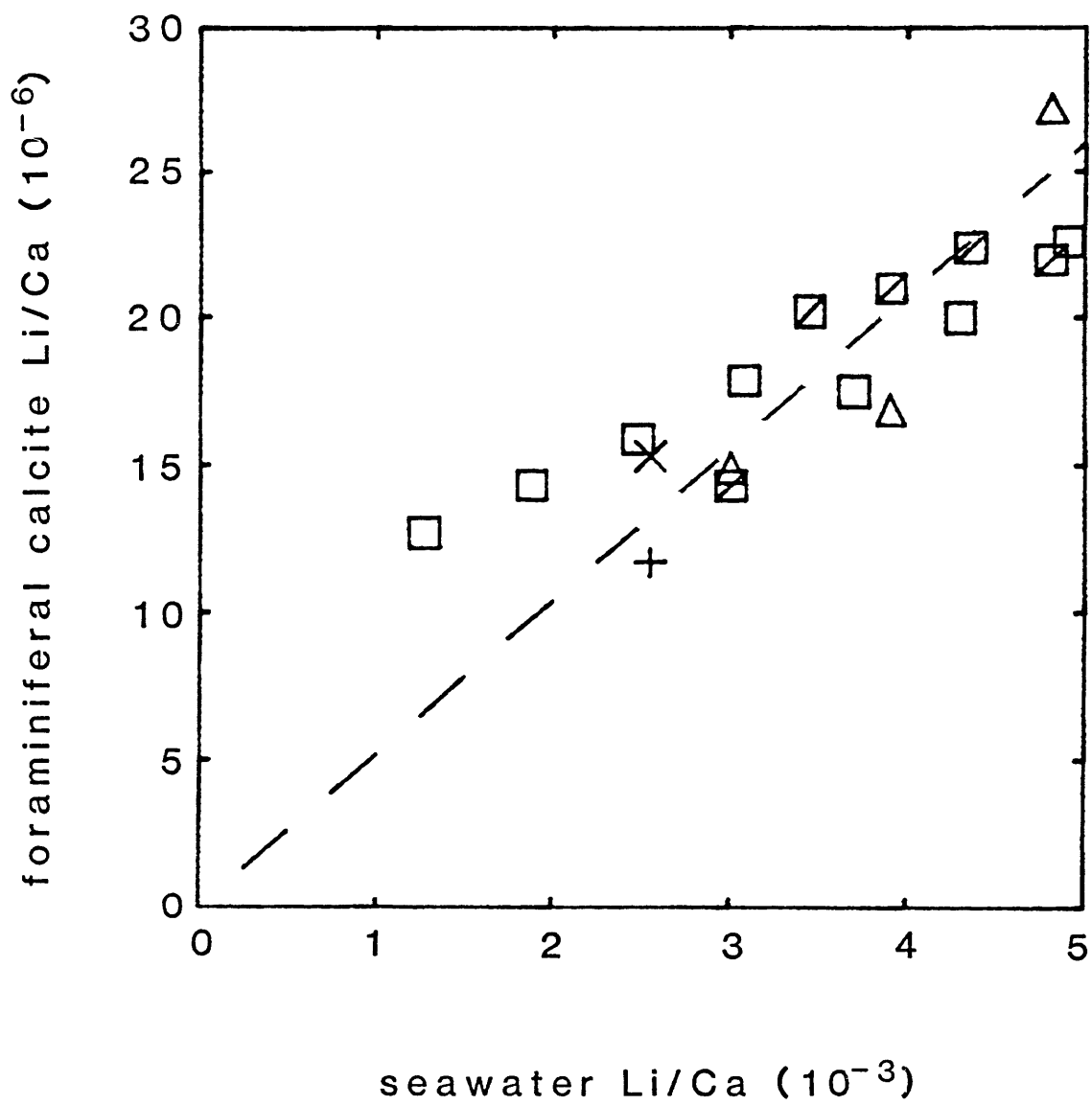


FIGURE 2.2 Sr/Ca ratios in foraminiferal calcite and seawater growth solutions. Mean and standard deviation of the mean are plotted for 2 solution compositions, with 4 samples at the lower solution Sr/Ca and 29 samples at the higher solution Sr/Ca. The line is defined by the mean Sr distribution coefficient for all 33 samples, 0.16 ± 0.02 .

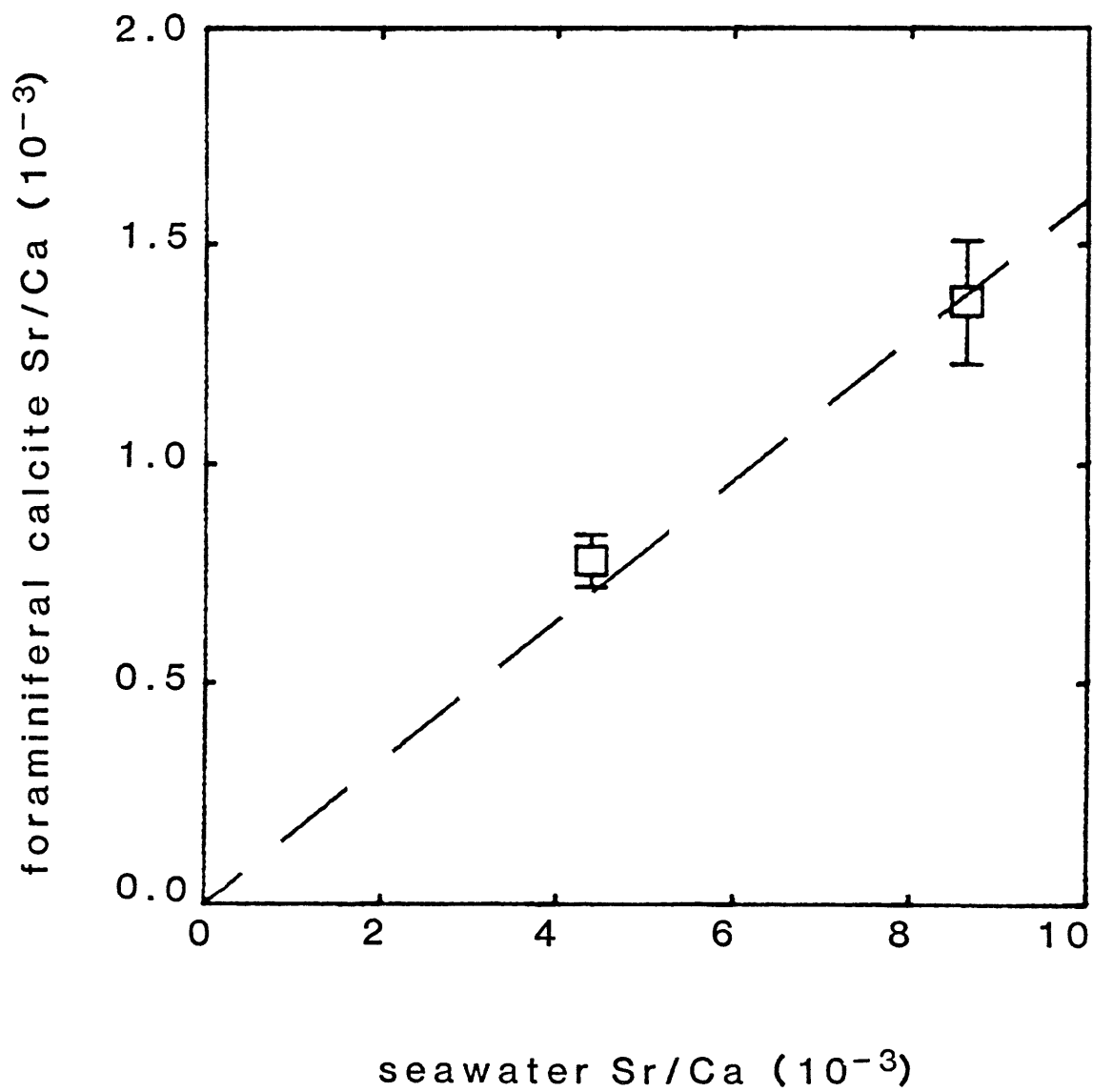


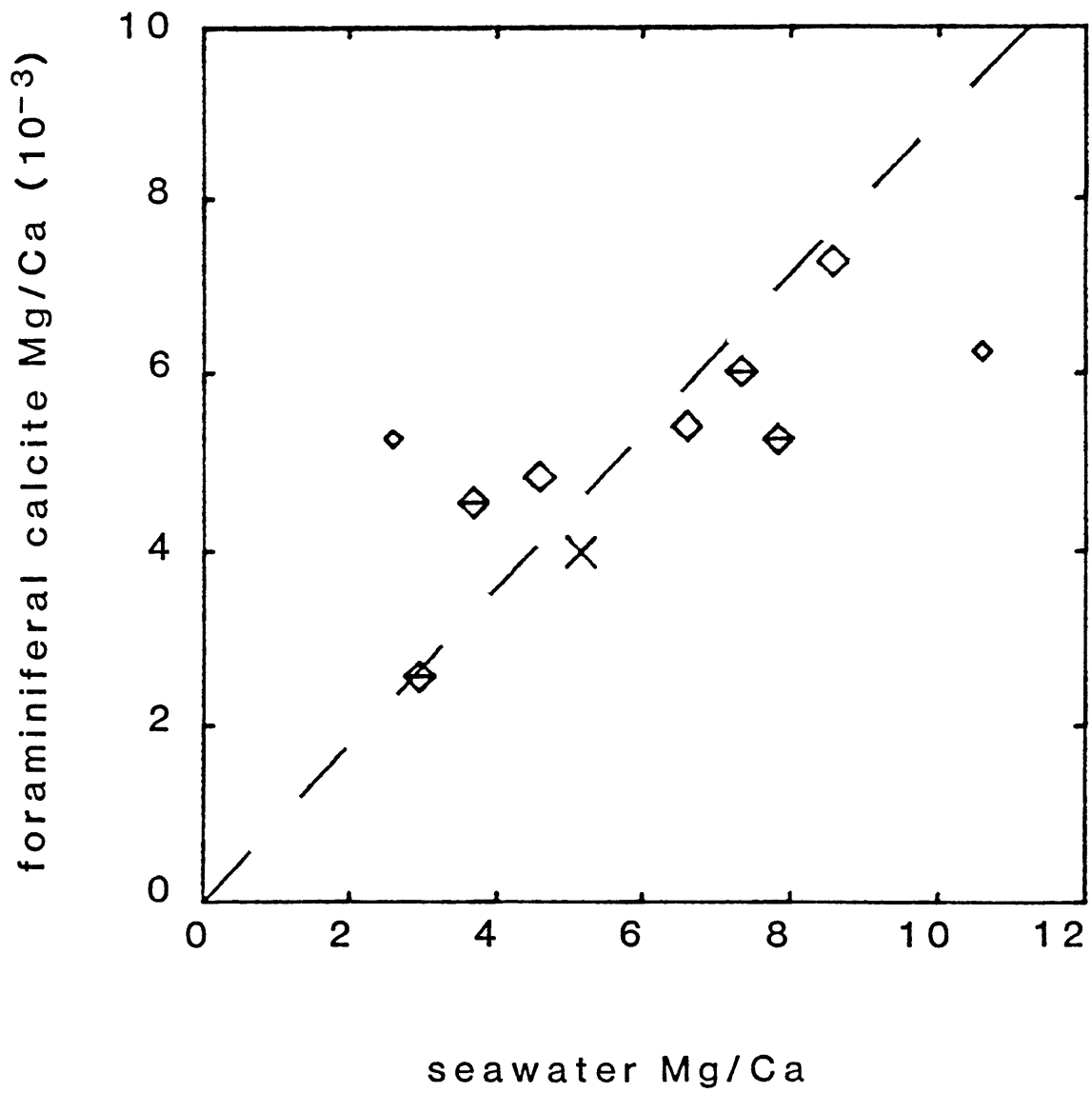
FIGURE 2.3 Mg/Ca ratios in foraminiferal calcite and seawater growth solutions. Plot symbols are:

- ↔ G. sacculifer -- Na/Mg variations in artificial seawater (Barbados) separated chambers
- ◇ G. sacculifer -- Na/Mg variations in artificial seawater (Curacao)
- × G. sacculifer -- 30° C natural seawater lab culture averages

The two samples with smaller plot symbols had relatively small shell length changes while in laboratory culture.

The line is defined by the mean G. sacculifer Mg distribution coefficient, $(0.89 \pm 0.18) \times 10^{-3}$ (not including the samples with smaller plot symbols).

The G. sacculifer sample from the solution with the highest Mg/Ca ratio is not plotted. The solution ratio was 12.5 and the foraminiferal calcite ratio was 45×10^{-3} .



samples with the largest shell length changes (all Barbados samples, 1 - 4; and samples 3 - 5 from the Curacao experiment) and the mean of samples grown in natural seawater demonstrate this trend most clearly. Curacao samples 2 and 6 do not agree with the trend. They had smaller shell length changes than the other samples (Table 2.5.A). Their departure from the trend is in the direction expected from protoplasmic equilibration delays and/or initial water column calcite contributions. Curacao sample 1, at a solution Mg/Ca ratio of 12.5, has an extremely high Mg/Ca foraminiferal calcite ratio (44.6×10^{-3}) and Na/Ca ratio (15.0×10^{-3}) compared to the trends defined by the other samples. It also had a relatively small shell length change in culture.

The mean Mg distribution coefficient for 8 samples, excluding Curacao G. sacculifer samples 1, 2, and 6, is $(0.89 \pm 0.18) \times 10^{-3}$. There is no correlation of foraminiferal Mg/Ca ratios with either solution Mg/SO₄ ratios or solution SO₄ concentrations.

A similar pattern of an approximately linear increase in calcite Mg/Ca ratios with an increase in solution ratios and a large increase at high solution ratios was seen in the calcite deposited by M. edulis in laboratory culture (Lorens and Bender, 1977). The high Mg content of calcite at higher solution ratios was attributed to a breakdown in physiological discrimination. This data set has only one sample with an extreme Mg/Ca ratio, so the process cannot be evaluated here.

The value of the Mg distribution coefficient in inorganically precipitated calcite is a matter of debate (see Chapter 3). Most estimates of the inorganic calcite distribution coefficient are higher than the foraminiferal calcite one determined here. A study of inorganic calcite overgrowths on calcite seed crystals found that the distribution

coefficient for Mg was relatively constant above solution Mg/Ca ratios of 7.5, and exponentially increased at lower solution ratios (Mucci and Morse, 1983). The foraminiferal data, with lower Mg distribution coefficients, do not show any correlation between solution Mg/Ca ratios and the Mg distribution coefficient.

Sodium/calcium. Na/Ca ratios show no correlation between solution and shell chemistries (Figure 2.4). A plot of the compositions of the separated chambers for the Barbados samples does not differ significantly from a plot of the total ratios. The foraminiferal sample from the seawater solution with the lowest Na/Ca ratio (and the highest Mg/Ca ratio) has the highest calcite Na/Ca (15.0×10^{-3}). It also has the highest calcite Mg/Ca ratio (44.6×10^{-3}). There is no correlation between foraminiferal Na/Ca ratios and solution Na/SO₄ or SO₄ concentrations.

Since the Mg/Ca ratios in the same samples as studied for Na/Ca do show a relationship to solution Mg/Ca ratios (Figure 2.3), the lack of correlation between solution and calcite Na/Ca ratios cannot be due to substantial contributions of initial water column calcite to the final sample weights. Protoplasmic equilibration mechanisms would have to be different for Na and Mg to account for the approximately constant Na/Ca calcite ratios while Mg/Ca calcite ratios varied.

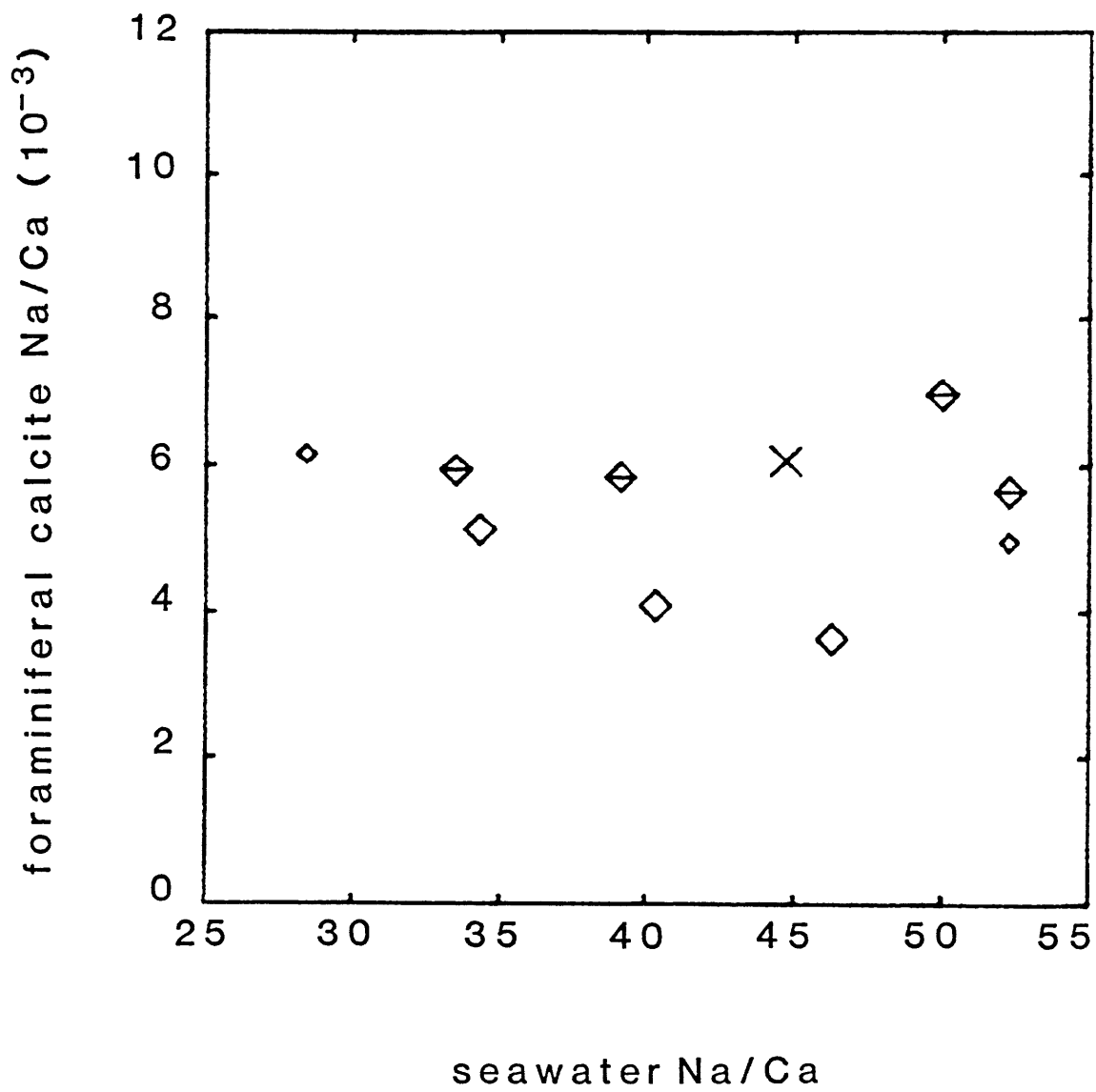
Laboratory culture of M. edulis also showed no variation of calcite Na/Ca ratios with solution Na/Ca ratios, but did show an apparent dependence of increasing calcite Na/Ca ratios on increasing solution Mg/Ca ratios. The foraminiferal data are similar in having the highest Mg/Ca and Na/Ca ratios in the same sample, but do not show the same correlation of calcite Na/Ca ratios with solution Mg/Ca ratios. The high point is only one sample and therefore the possibility of contamination cannot be

FIGURE 2.4 Na/Ca ratios in foraminiferal calcite and seawater growth solutions. Plot symbols are:

- ◊ G. sacculifer — Na/Mg variations in artificial seawater (Barbados) separated chambers
- ◊ G. sacculifer — Na/Mg variations in artificial seawater (Curacao)
- X G. sacculifer — 30° C natural seawater lab culture averages

The two samples with smaller plot symbols had relatively small shell length changes while in laboratory culture.

The G. sacculifer sample from the solution with the lowest Na/Ca ratio is not plotted. The solution ratio was 22.4 and the foraminiferal calcite ratio was 15.0×10^{-3} for that sample.



disregarded in either the Mg/Ca or Na/Ca result.

Three of the elements studied (Li, Sr, and Mg) show an essentially linear relationship between shell chemistry and solution chemistry for certain ranges of solution chemistry. Na does not vary in the calcite shells with variations in solution chemistry. The culture experiment results show that foraminiferal calcite can be used as an indicator of paleochemistry for some elements.

CADMIUM AND ZINC

EXPERIMENTAL DESIGN

The values of the distribution coefficients of Cd and Zn in foraminiferal calcite were determined using radioisotope tracers. Metals such as Cd and Zn may be adsorbed on or incorporated in organic matter associated with calcite shells. To test for organic matter contamination, foraminiferal samples were counted for radioisotope uptake, cleaned of organic matter, and then recounted.

Cd and Zn each have a γ -emitting isotope of easily measured energy and half-life (^{109}Cd and ^{65}Zn). Ca has a β -emitting isotope (^{45}Ca , β^- , 257 keV). Comparing Cd or Zn to Ca requires measuring absolute activities of a γ -emitter and a β -emitter. The determination of absolute activities on both types of detectors is sensitive to sample geometry. Dissolution of the foraminiferal samples would have been necessary to insure reproducible standard and sample geometries, precluding any sample recounts after further cleaning procedures.

Evidence from ion microprobe studies of benthic foraminiferal shells (Lefèvre and Vénec-Peyré, 1977) and from partial dissolution experiments

with G. sacculifer shells (Bender et al., 1975) indicated that Sr is homogeneously distributed in foraminiferal calcite. Culture experiments showed that Sr incorporation in foraminiferal calcite is directly proportional to the solution concentration (Figure 2.2). Sr, unlike Ca, has a γ -emitting isotope of easily measured energy and half-life (^{85}Sr). The procedure of measuring Cd or Zn incorporation relative to Sr incorporation was chosen to satisfy the requirement of cleaning and recounting samples. Ratios of the relative counting rates of the two isotopes in both foraminiferal and seawater samples were measured on the same detector, eliminating absolute activity standardizations.

Table 2.8 lists information on the radioisotope tracers (^{109}Cd , ^{65}Zn , and ^{85}Sr). Two isotopes were used in each experiment: ^{109}Cd and ^{85}Sr or ^{65}Zn and ^{85}Sr . The relative incorporation of the two elements in the foraminiferal calcite deposited while in laboratory culture was measured by the quotient of the count ratio of the radioisotopes in the foraminiferal shell and the count ratio of the radioisotopes in the corresponding seawater solution. This quotient is referred to here as a relative incorporation coefficient since neither element measured is a major component of calcite. Defining this measurement as the relative incorporation coefficient assumes that there are no differences in protoplasmic equilibration times for the elements. For example, if solution Cd equilibrated more rapidly with the elemental pool used for calcification than did Sr, the measured relative incorporation coefficient would be larger than the true value.

Multiplying the relative Cd or Zn incorporation coefficients by the foraminiferal calcite Sr distribution coefficient ($D_{\text{Sr}/\text{Ca}} = 0.16$) converts them to the corresponding distribution coefficients ($D_{\text{Cd}/\text{Ca}}$ or $D_{\text{Zn}/\text{Ca}}$).

TABLE 2.8 Radiotracer information

isotope	half-life (days)	photopeak energy (kev)
Cadmium-109	453	88.03 (^{109}Ag x-ray peak at 22 kev)
Strontium-85	65.2	514.0
Zinc-65	243.8	1115.5

All tracers were obtained from New England Nuclear, Inc. Cadmium-109 and zinc-65 were both carrier-free. All three were initially in 0.5 M HCl in concentrated solution and diluted to give spikes of the appropriate activity. For Sr, the concentrations added to seawater solutions were calculated from the activity and the specific activity. For carrier-free Cd and Zn, the concentrations were calculated from the activities.

This transformation rests on the assumption that there is no discrimination between Ca and Sr in shell calcification.

Radiotracer solution spikes were added to filtered surface seawater and foraminifera were cultured in these solutions. The spikes were sufficient to give detectable levels of the tracers in the foraminiferal samples. The absolute amount of total Sr added ranged from 0.02 - 0.25 $\mu\text{mol/l}$; the Sr spike was not carrier-free, so the added amount of ^{85}Sr was much lower than total Sr added. The added Sr concentration is negligible compared to seawater Sr concentrations of $\sim 90 \mu\text{mol/l}$.

For Cd, radiotracer spikes were equivalent to added concentrations of 0.05 - 0.09 nmol/l for the Barbados experiments and 0.7 nmol/l for the Curacao experiments. An uncontaminated surface seawater sample from the Barbados collection site has a Cd concentration of $\sim 0.05 \text{ nmol/l}$. The Barbados levels added by radiotracer addition are comparable to this; the added levels in Curacao were higher than this. No trace element handling precautions were taken in the foraminiferal culture experiments, so Cd contamination may have been comparable to that added by the radiotracer spikes.

Zn added concentrations were 0.002 - 0.008 nmol/l in the Barbados experiments and 0.074 nmol/l in the Curacao experiments. Uncontaminated open ocean surface seawater values are expected to be no more than a few tenths nmol/l . Because Zn contamination is difficult to avoid, the radiotracer Zn added in each set of experiments is probably a small proportion of the total Zn present in the culturing solutions.

The initial shell length, final shell length, and number of days in culture were recorded for most samples; some foraminifera were measured for shell length only at the end of culture. Temperature, light, and feeding

conditions were the same as the stable element culture experiments. At the end of laboratory culture, the shells were thoroughly rinsed with distilled water. The counting rate ratio of the two isotopes present was determined in the foraminiferal samples and seawater solutions. Some samples were cleaned of organic matter by treatment with hot basic hydrogen peroxide, followed by repeated distilled water and methanol rinses, air dried, and then recounted to test for the presence of these elements in organic matter removed from the shells by this cleaning. In all cleaning steps, ultrasonic agitation of the samples was used. In some cases shells underwent a second hot basic hydrogen peroxide cleaning and a third recount.

Counting of foraminiferal shells and seawater solutions was done using a 1" x 1¹/₂" NaI(Tl) detector (The Nucleus, P2000 detector) and a 256 multi-channel analyzer (The Nucleus, Inc., Model 256 MCA) for pulse height analysis. To reduce high ambient background count rates typical of NaI(Tl) detectors (Friedlander, et al., 1981, p. 263), the detector sample area was surrounded with lead shielding of approximately one inch.

⁸⁵Sr and ⁶⁵Zn were quantified by measurements of their photopeak areas. The direct measurement of the ¹⁰⁹Cd photopeak (88.03 keV) on the NaI(Tl) detector was complicated by a background peak and a peak in the ⁸⁵Sr energy spectrum both close to the photopeak energy. Correcting the ¹⁰⁹Cd photopeak area for these two contributions, each with a counting rate significant relative to sample rates, resulted in large statistical errors on the net rate. The ¹⁰⁹Cd spectrum also has a 22 keV ¹⁰⁹Ag x-ray peak, with the advantages of a lower background rate and no overlapping peaks in the ⁸⁵Sr spectrum, although correction must still be made for the broad ⁸⁵Sr Compton distribution. Additionally it has a higher counting rate than

the corresponding photopeak (factor of ~ 3 on the NaI(Tl) detector). ^{109}Cd was therefore quantified by the ^{109}Ag peak (22 keV) for all of the foraminiferal samples from Curacao.

Since the Barbados foraminiferal shells had low absolute activities, they were counted in groups of single species grown in solutions of the same composition. ^{109}Cd was quantified for these samples by measurement of the ^{109}Cd 88.03 keV photopeak area using the M.I.T. LEPS Ge(Li) γ -system. The separate measurements of Cd and Sr counting rates and conversions to activities means that the results from these Barbados experiments are more uncertain than indicated by the counting statistic errors. These early results were significant because of the lower amounts of Cd added to sample solutions by radiotracer spikes.

Calculation procedures are summarized in Appendix 2.1. Background levels and energy calibrations were monitored to check for contamination problems and for changes in peak locations due to instrumental variations.

Errors reported are 1σ counting statistic \sqrt{N} errors propagated through the calculations. Counting statistic errors reported are a function of both counting rates and times. Many of the peaks measured in the foraminiferal samples had counting rates close to background rates, leading to large statistical errors on the calculated distribution coefficients. There may be systematic errors unaccounted for which would have affected the results with large counting statistic errors to a greater degree than results with smaller errors. Actual errors are probably larger than the quoted counting statistic errors.

In the following discussion, results with a counting statistic error greater than an arbitrary cut-off of 20% will be disregarded.

RESULTS

Cadmium. Foraminiferal information and calculated distribution coefficients for foraminifera grown in solutions spiked with Cd and Sr radiotracers are listed in Table 2.9.

The Barbados results, as discussed earlier, are more uncertain (aside from counting statistic errors) than the Curacao results because of the separate measurements of Cd and Sr. There are no significant differences in the results of the two sets of experiments despite the higher levels of added Cd in the Curacao experiments.

The values for O. universa and G. ruber from the Barbados experiments are similar to the values for G. sacculifer. Within the statistical and experimental errors, the interspecific differences are not significant.

Cleaning procedures to rid the shells of remaining protoplasmic organic matter reduced the measured Cd distribution coefficient for some samples, indicating the presence of Cd in this material (Figure 2.5a). For some samples, the measured distribution coefficients before and after this cleaning did not differ within 1σ counting statistic errors (Figure 2.5b). The weighted mean Cd distribution coefficient and probable error of the mean for all samples after only water-washing is 1.9 ± 0.1 . For samples with counting statistic errors $< 20\%$ after cleaning with hot basic hydrogen peroxide solutions, the mean distribution coefficient is 1.8 ± 0.1 . (This excludes sample numbers 1044, 1100, 1096, and 1041.) If the results from all samples after this cleaning are included, the mean is the same, while the probable error of the mean is smaller. Definitions of the weighted mean and probable error of the weighted mean are given in Appendix 2.1.

The best estimate of the Cd distribution coefficient in foraminiferal calcite from these data is 1.8.

TABLE 2.9 Cadmium incorporation

2.9.A FORAMINIFERAL INFORMATION

	sample #	species	initial shell length (μm)	final shell length (μm)	comments
Curacao experiments	1044	<u>G. sacculifer</u>	590	599	D
	1039	<u>G. sacculifer</u>	495	536	D
	1100	<u>G. sacculifer</u>	~504	523	G
	1096	<u>G. sacculifer</u>	~240	554	G
	1097	<u>G. sacculifer</u>	~240	561	G
	1042	<u>G. sacculifer</u>	524	617	G
	1038	<u>G. sacculifer</u>	495	693	G
	1043	<u>G. sacculifer</u>	590	708	G
	1040	<u>G. sacculifer</u>	495	724	G
	1041	<u>G. sacculifer</u>	524	770	G

2.9.A continued

	sample #	species	initial shell length (μm)	final shell length (μm)	comments
Barbados experiments	72	<u>G. sacculifer</u>	340	504	T
	73		271	630	T
	74		473	724	G
	38	<u>O. universa</u>	juvenile	473	
	39		juvenile	647	
	40		1 juvenile,	605	
	41		2 newly	630	
	42		adult	573	
	44		juvenile	536	
	45		juvenile	693	T
	77	<u>O. universa</u>	juvenile	631	T
	78		juvenile	573	T
	18	<u>G. ruber</u>		473	D
	19			485	D
	20			277	D
	21			498	D

2.9.B DISTRIBUTION COEFFICIENTS

	sample #	species	water rinsed $D_{Cd/Ca}$	cleaned once $D_{Cd/Ca}$	cleaned twice $D_{Cd/Ca}$
Curacao experiments	1044	<u>G. sacculifer</u>	5.3 ± 1.0	3.8 ± 1.7	
	1039	<u>G. sacculifer</u>	4.5 ± 0.5		
	1100	<u>G. sacculifer</u>	6.6 ± 0.5	9 ± 4	5.4 ± 0.8
	1096	<u>G. sacculifer</u>	19 ± 1	11 ± 3	10 ± 1
	1097	<u>G. sacculifer</u>	38 ± 2	14 ± 2	24 ± 6
	1042	<u>G. sacculifer</u>	2.3 ± 0.3	2.6 ± 0.3	
	1038	<u>G. sacculifer</u>	2.0 ± 0.1	2.0 ± 0.1	
	1043	<u>G. sacculifer</u>	1.7 ± 0.1	2.0 ± 0.4	
	1040	<u>G. sacculifer</u>	1.3 ± 0.1	1.3 ± 0.1	
	1041	<u>G. sacculifer</u>	1.9 ± 0.2	2.3 ± 1.1	
Barbados experiments	72-74	<u>G. sacculifer</u>	17 ± 2	4.6 ± 0.6	
	38-42, 44, 45	<u>O. universa</u>	11 ± 1	2.4 ± 0.3	
	77, 78	<u>O. universa</u>	32 ± 3	6.4 ± 0.8	5.8 ± 1.0
	18-21	<u>G. ruber</u>	12 ± 2	$\leq 4 \pm 2$	

FIGURE 2.5 Cd distribution coefficients measured on foraminiferal shells grown in radiotracer spiked solutions.

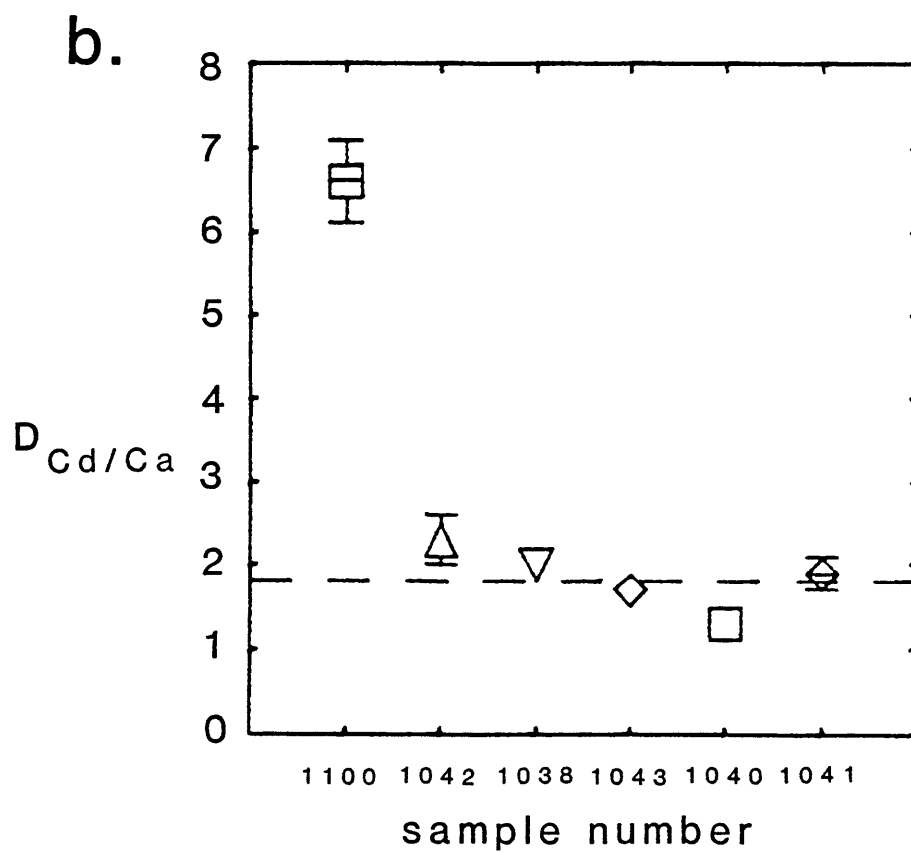
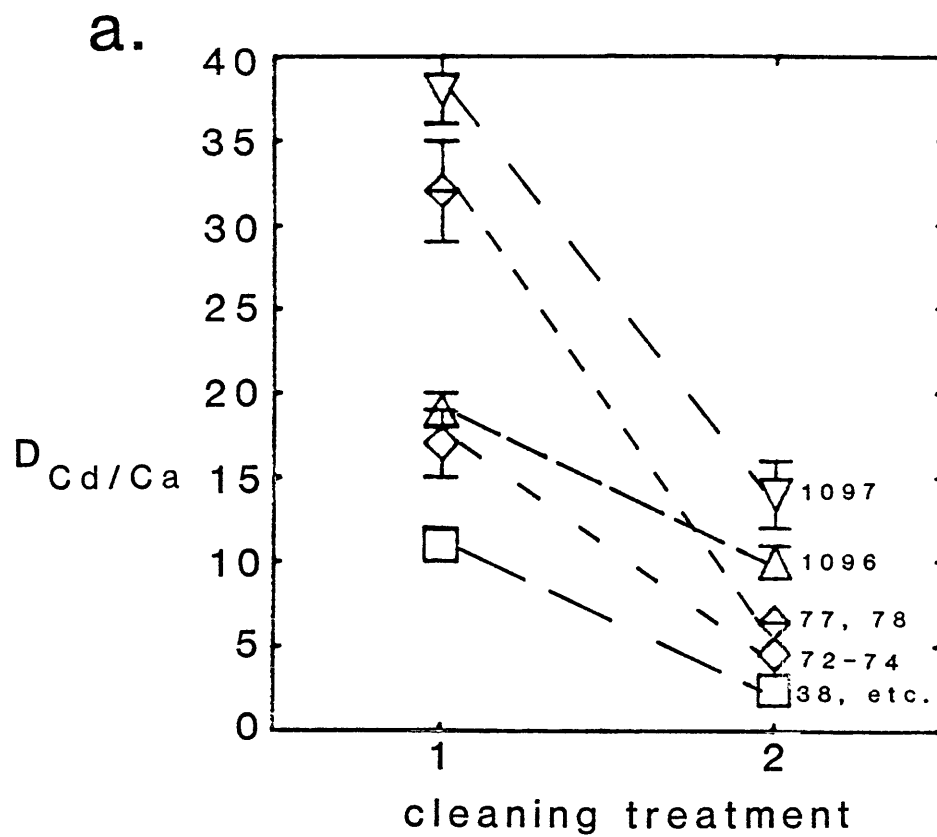
Error bars are $1\sigma \sqrt{N}$ counting statistic errors. Distribution coefficients with errors $> 20\%$ are not plotted.

a. Cd distribution coefficients for those shells whose values changed after organic matter cleaning. The cleaning treatments are indicated as follows:

- 1 rinsed with distilled water
- 2 cleaned of organic matter with hot basic hydrogen peroxide

Foraminiferal sample numbers (Table 2.9) are indicated.

b. Cd distribution coefficients for those shells whose values did not change after organic material cleaning. Dashed line indicates weighted mean value for all samples after organic matter cleaning.



Zinc. Table 2.10 lists foraminiferal information and calculated distribution coefficients for foraminifera grown in seawater spiked with Zn and Sr radiotracers. The results are plotted in Figure 2.6.

For Zn, the distribution coefficients measured on shells which had undergone cleaning to remove organic matter were significantly lower than the values from the water washed shells. Also, some samples which had measurable Zn peaks after water washing had no measurable Zn peaks after the organic matter cleaning step. The estimate of the Zn distribution coefficient from the samples cleaned of organic matter of 0.7 is a maximum value for the actual incorporation of Zn in the calcite shell.

DISCUSSION

Cadmium. The best estimate from these experiments of the Cd distribution coefficient in foraminiferal calcite is 1.8 ± 0.1 (weighted mean and probable error on the weighted mean). Measurements of two species of benthic foraminifera, Uvigerina spp. and Cibicidoides kullenbergei, from a series of core tops showed $D_{Cd/Ca} = 2.0 \pm 0.4$ (mean and standard deviation) (Hester and Boyle, 1982). These two estimates are in excellent agreement. Analyses of Globorotalia truncatulinoides shells from central Atlantic cores had an average of 40×10^{-9} Cd/Ca; from an equatorial Atlantic core, 168×10^{-9} Cd/Ca (E. A. Boyle, pers. comm.). G. truncatulinoides calcifies at $\sigma_t = 26.8$ (Curry and Matthews, 1981a). The depth at $\sigma_t = 26.8$ was used to estimate the water column phosphate concentration. The regression of oceanic Cd and phosphate (Bruland, 1980) was then used to estimate Cd concentrations at the assumed calcification depths. The calculated Cd distribution coefficients for G.

TABLE 2.10 Zinc incorporation

2.10.A FORAMINIFERAL INFORMATION

	sample #	species	initial shell length (μm)	final shell length (μm)	days in culture	comments
Curacao experiments	1107	<u>G. sacculifer</u>	~230	403	average of 4 days	D
	1106	<u>G. sacculifer</u>	~230	466		D
	1109	<u>G. sacculifer</u>	365	536		G
	1108	<u>G. sacculifer</u>	~230	605		G
	1110	<u>G. sacculifer</u>	460	617		G
	1111	<u>G. sacculifer</u>	554	611		D
	1112	<u>G. sacculifer</u>	517	708		D
Barbados experiments	81	<u>G. sacculifer</u>	321	334	5	G
	59	<u>G. sacculifer</u>	~395	447	3	
	28	<u>G. sacculifer</u>		567	8	
	25	<u>G. sacculifer</u>		599	8	
	58	<u>G. sacculifer</u>	~395	678	3	
	80	<u>G. sacculifer</u>	384	678	5	G
	27	<u>G. sacculifer</u>		693	8	

2.10.A continued

	sample #	species	initial shell length (μm)	final shell length (μm)	days in culture	comments
Barbados experiments (continued)	29	<u>G. sacculifer</u>		693	8	
	30	<u>G. sacculifer</u>		693	11	
	82	<u>G. sacculifer</u>	399	708	5	G
	23	<u>G. sacculifer</u>		755	7	
	24	<u>G. sacculifer</u>		755	8	
	22	<u>G. sacculifer</u>		785	5	
	55	<u>O. universa</u>	juvenile	473	9	
	57	<u>O. universa</u>	juvenile	567	7	
	56	<u>O. universa</u>	juvenile	739	7	
	68	<u>G. ruber</u> (pink)	~290	454	4	
	69	<u>G. ruber</u> (pink)	~290	460	7	T

2.10.B DISTRIBUTION COEFFICIENTS

	sample #	species	water rinsed DZn/Ca	cleaned once DZn/Ca
Curacao experiments	1107	<u>G. sacculifer</u>	19 ± 1	ND ¹
	1106	<u>G. sacculifer</u>	28 ± 1	
	1109	<u>G. sacculifer</u>	3.5 ± 0.5	
	1108	<u>G. sacculifer</u>	4.5 ± 0.3	ND
	1110	<u>G. sacculifer</u>	3.6 ± 0.3	0.22 ± 0.08
	1111	<u>G. sacculifer</u>	7.0 ± 0.3	1.5 ± 0.1
	1112	<u>G. sacculifer</u>	10 ± 2	2.2 ± 0.5
Barbados experiments	81	<u>G. sacculifer</u>	37 ± 9	
	59	<u>G. sacculifer</u>	31 ± 5	
	28	<u>G. sacculifer</u>	5.1 ± 0.6	
	25	<u>G. sacculifer</u>	2.4 ± 1.1	ND
	58	<u>G. sacculifer</u>	8.8 ± 1.0	
	80	<u>G. sacculifer</u>	23 ± 2	
	27	<u>G. sacculifer</u>	4.0 ± 0.5	

2.10.B continued

	sample #	species	water rinsed D_{Zn}/Ca	cleaned once D_{Zn}/Ca
Barbados experiments (continued)	29	<u>G. sacculifer</u>	12 ± 1	
	30	<u>G. sacculifer</u>	0.8 ± 0.2	
	82	<u>G. sacculifer</u>	3.7 ± 0.8	
	23	<u>G. sacculifer</u>	5.1 ± 0.5	ND
	24	<u>G. sacculifer</u>	1.8 ± 0.6	
	22	<u>G. sacculifer</u>	2.9 ± 0.6	0.18 ± 0.62
	55	<u>O. universa</u>	31 ± 3	38 ± 4
	57	<u>O. universa</u>	11 ± 1	
	56	<u>O. universa</u>	25 ± 2	23 ± 1
	68	<u>G. ruber</u> (pink)	13 ± 1	
	69	<u>G. ruber</u> (pink)	1.9 ± 0.3	

Notes: 1. ND indicates no detectable zinc activity.

FIGURE 2.6 Zn distribution coefficients measured on foraminiferal shells grown in radiotracer spiked solutions.

Error bars are $1\sigma \sqrt{N}$ counting statistic errors.

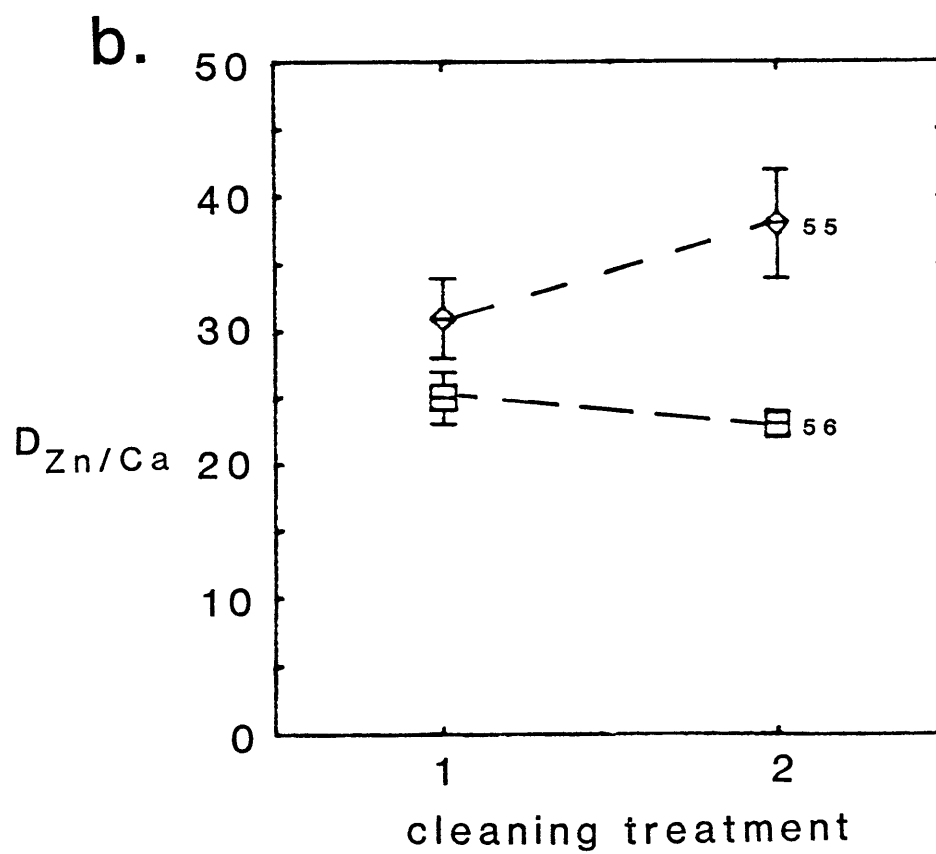
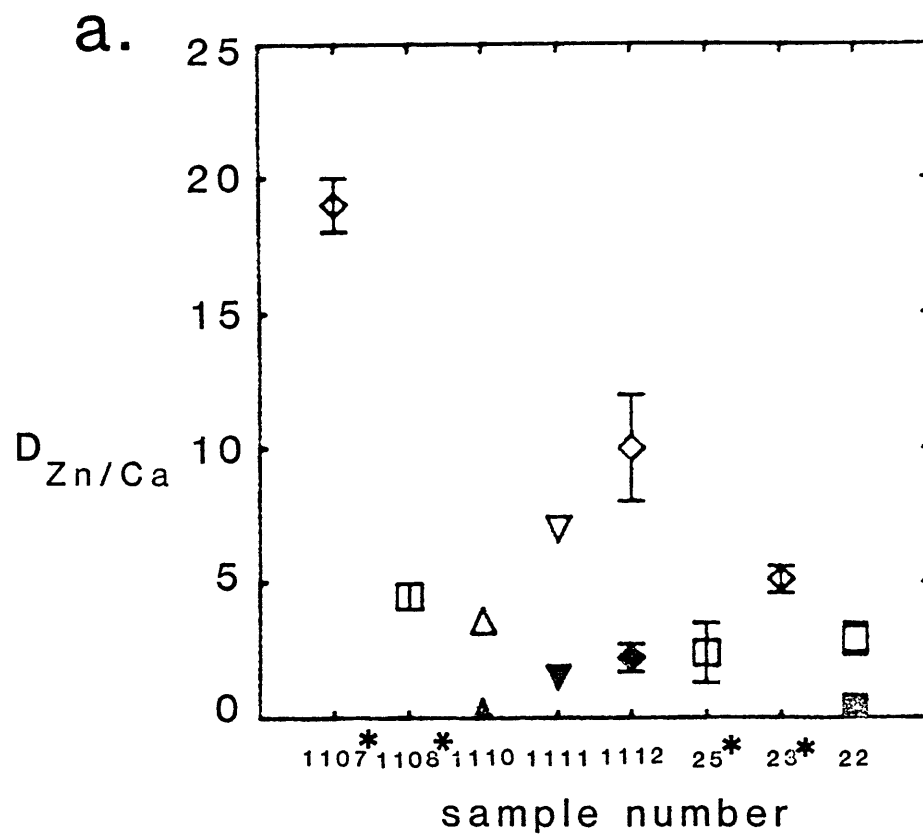
a. G. sacculifer shells -- filled plot symbols indicate distribution coefficients after samples were cleaned of organic matter. Samples whose numbers are marked with an asterisk had no measurable Zn activity after organic matter cleaning.

b. O. universa shells. The cleaning treatments are indicated as follows:

1 rinsed with distilled water

2 cleaned of organic matter with hot basic hydrogen peroxide

Foraminiferal sample numbers (Table 2.10) are indicated.



truncatulinoïdes are 3.4 for shells from the central Atlantic cores and 3.6 for shells from the equatorial Atlantic core. Given the uncertainties in this type of estimation, the three different methods give similar values for the Cd distribution coefficients in foraminiferal calcite over a wide range of calcification temperatures ($\sim 3^{\circ}$ C for the benthic foraminifera to 30° C for the laboratory culture experiments).

Cd distribution coefficients in inorganically precipitated calcite depend on precipitation rates, with $D_{Cd/Ca}$ ranging from ~ 30 at low precipitation rates to ~ 10 at high rates (Lorens, 1978). Up to 20% of the measured distribution coefficient at low precipitation rates may be due to surface adsorption of Cd; the uncertainty in the distribution coefficient due to surface adsorption is smaller at higher precipitation rates (Lorens, 1978). The foraminiferal distribution coefficients are all significantly lower than the inorganic precipitation ones.

Zinc. Based on the culture experiments, the maximum Zn distribution coefficient is 0.7. G. truncatulinoïdes from central Atlantic cores had $(2 \pm 1) \times 10^{-6}$ Zn/Ca, and from an equatorial Atlantic core, 3.3×10^{-6} Zn/Ca; benthic foraminifera from North Atlantic cores had 8.6×10^{-6} Zn/Ca (E. A. Boyle, pers. comm.). Using the $\sigma_t = 26.8$ depth to estimate the water column silicate concentration for the G. truncatulinoïdes samples and estimating bottom water silicate concentrations, the Zn-silicate North Pacific regression (Bruland, 1980) gave Zn concentrations at the assumed calcification depths. The calculated Zn distribution coefficients were 79 and 61 for the central Atlantic and equatorial Atlantic G. truncatulinoïdes samples respectively, and 33 - 158 for the benthic foraminifera. These values are much higher than those measured on samples cleaned of organic matter from the laboratory culture experiments.

The distribution coefficient of Zn in inorganically precipitated calcite ranged from ~60 at high precipitation rates to ~150 at low rates (Lorens, 1978). Surface adsorption corrections are large at low precipitation rates, so those distribution coefficients are more uncertain than those at faster precipitation rates (Lorens, 1978). The foraminiferal estimates from the core sample G. truncatulinoides are in rough agreement with these values; the best estimate from the culture experiments is significantly lower.

TEMPERATURE AND FORAMINIFERAL CALCITE

TRACE ELEMENT DISTRIBUTION COEFFICIENTS

To use foraminiferal shells as paleochemical indicators, effects of temperature as well as solution composition on trace element composition must be evaluated. The paleotemperature history of the ocean shows a general cooling of 10 - 15° C over 70 Ma, with glacial/interglacial cycles for at least the last 13 Ma (Shackleton, 1982). Surface ocean temperature differences from the interglacial present to the last glacial maximum (18 K) average 2.3° C, ranging up to 8 - 10° C in limited areas (CLIMAP, 1976). If biogenic trace element distribution coefficients vary with temperature, oceanic temperature changes could impose variations independent of seawater chemical changes on the trace element composition of foraminiferal calcite. Alternatively, on time scales long relative to an oceanic elemental residence time, a dependence of trace element composition on temperature would allow foraminiferal calcite to be used as an indicator of temperature changes independent of $\delta^{18}\text{O}$.

A simple thermodynamic model for the variation of distribution

coefficients with temperature assumes that since the vibrational energy of the lattice increases with increasing temperature, the lattice's ability to accommodate a foreign ion should also increase. Distribution coefficients should increase with temperature increases by this argument (Krauskopf, 1967).

Ideally, the distribution coefficient is equivalent to the quotient of the solubility products of the two solids. If these vary differently with temperature, their ratio will be a function of temperature. This explanation was invoked for the inverse relationship observed between temperature and the Sr distribution coefficient in aragonite (Kinsman and Holland, 1969). Similarly, if the solution ion activity coefficients for the two ions vary independently with temperature, the distribution coefficient can either increase or decrease with temperature changes (Swart, 1981).

Trace element distribution coefficients for several elements in inorganic calcite were shown to be precipitation rate dependent (Lorens, 1978). For elements with distribution coefficients less than one (Sr), distribution coefficients increased with increasing precipitation rates. For elements with distribution coefficients greater than one (Co, Mn, Cd, and Zn), distribution coefficients decreased with increasing precipitation rates. If temperature directly or indirectly changes the biogenic calcification rate, the value of the distribution coefficient could change.

In considering this last effect on organisms, it is important to distinguish between macroscopic growth observations (e.g. the number of chambers added or the shell length change per days in culture for foraminifera) and the actual rate at which calcite was precipitated in shell formation. Formation of a new, thin-walled chamber for nonspinose

Globorotalia hirsuta or Globorotalia truncatulinoides takes 5-6 hours (Bé et al., 1979).

Interspecific differences in trace elemental ratios in foraminifera have been observed, with temperature often invoked as the controlling mechanism. Average Mg/Ca ratios of six planktonic species increased with increasing $\delta^{18}\text{O}$ calcification temperatures; however, intraspecific Mg/Ca ratios did not correlate with isotopic temperatures (Savin and Douglas, 1973). The down-core Mg/Ca ratios in the G. sacculifer-triloba group were reported to parallel the $\delta^{18}\text{O}$ record in a sediment core (Kilbourne and Sen Gupta, 1973). Interspecific differences in Sr/Ca, Mg/Ca, and Na/Ca ratios, with a general trend of increasing trace elemental ratios with shallower average assigned depth ranking, were found (Bender et al., 1975). However, the trace elemental ratios of the tests of two planktonic species, G. ruber and G. sacculifer, in North Atlantic core top samples did not correlate with surface water temperatures (Bender et al., 1975). Sr/Ca and, less consistently, Mg/Ca ratios in the tests of two planktonic species, Globigerina bulloides and Globorotalia inflata, in two Southern Indian Ocean cores covaried with several paleoclimatic indices over the last 200 - 300 Ka, with lower trace elemental ratios in glacial periods than in interglacials (Cronblad and Malmgren, 1981).

OUTLINE OF THE EXPERIMENTS

Four data sets were examined to evaluate the relationship of trace elemental ratios in foraminiferal calcite and temperature: three species of planktonic foraminifera from Panama Basin sediment trap samples and benthic foraminifera from a North Atlantic sediment core; three species

of planktonic foraminifera in size fractioned samples from an Indian Ocean core top; five species of planktonic foraminifera from two equatorial Atlantic core-tops; and two species of planktonic foraminifera grown at controlled temperatures in laboratory culture experiments.

RESULTS AND DISCUSSION

Panama Basin sediment trap samples. Size-fraction controlled samples for Globoquadrina dutertrei and Globorotalia menardii and population samples for G. sacculifer were analyzed from four sediment trap depths in the Panama Basin (5°21'N 81°53'W, 112 day deployment, August - December 1979). The results are summarized in Table 2.11.

Species abundances and oxygen isotopic data on these species from vertically stratified plankton tows in the Panama Basin and the water-column temperature profile indicated average calcification temperatures of 27° C for G. sacculifer, 20° C for G. dutertrei, and 20° C for G. menardii (Fairbanks et al., 1982). Trace elemental ratios, except for Li/Ca, are higher for G. sacculifer than for the two other species.

North Atlantic benthic foraminifera. Trace elemental ratios were determined on sample solutions of Uvigerina spp. (Chain 82 Station 31 Core 11PC; Boyle and Keigwin, 1982). The results are listed in Table 2.12.

The $\delta^{18}\text{O}$ record in this core reflects mainly ice-volume changes; the bottom water temperatures at this site should be approximately 2° C for all samples. The average trace elemental ratios in these samples are lower than those in the planktonic species analyzed from the Panama Basin sediment trap samples (Figure 2.7). Sr/Ca, Mg/Ca, Na/Ca, and K/Ca ratios increase with increasing assumed calcification temperatures. The Uvigerina

TABLE 2.11 Panama Basin sediment trap foraminifera¹

sample #	species	trap depth (m)	shell length (μm)	average ² weight per shell (μg)	Li/Ca (10 ⁻⁶)	Sr/Ca (10 ⁻³)	Mg/Ca (10 ⁻³)	Na/Ca (10 ⁻³)	K/Ca (10 ⁻⁶)
1	<u>G. sacculifer</u>	667	population	32	23.3	1.46	3.25	7.53	-
2	<u>G. sacculifer</u>	1268	population	36	24.2	1.53	3.56	8.51	178
3	<u>G. sacculifer</u>	2869	population	37	22.0	1.44	3.54	7.35	-
4	<u>G. sacculifer</u>	3791	population	31	22.0	1.47	3.23	7.09	-
average for <u>G. sacculifer</u>					22.9 ±1.1	1.48 ±0.04	3.40 ±0.18	7.62 ±0.62	178
5	<u>G. dutertrei</u>	667	525-675	54	24.0	1.33	2.27	6.59	150
6	<u>G. dutertrei</u>	1268	500-700	39	21.9	1.45	1.90	6.50	133
7	<u>G. dutertrei</u>	2869	450-650	55	22.2	1.37	1.99	5.93	129
8	<u>G. dutertrei</u>	3791	375-600	45	22.8	1.40	-	-	-
average for <u>G. dutertrei</u>					22.7 ±1.0	1.39 ±0.05	2.05 ±0.19	6.34 ±0.36	137 ±11

2.11 continued

sample #	species	trap depth (m)	shell length (μm)	average ² weight per shell (μg)	Li/Ca (10^{-6})	Sr/Ca (10^{-3})	Mg/Ca (10^{-3})	Na/Ca (10^{-3})	K/Ca (10^{-6})
9	<u>G. menardii</u>	667	1000-1230	74	25.0	1.40	-	-	-
10	<u>G. menardii</u>	1268	940-1100	73	26.4	1.32	2.09	5.87	-
11	<u>G. menardii</u>	2869	1150-1300	104	21.0	1.36	2.08	5.38	-
12	<u>G. menardii</u>	3791	1050-1200	89	21.8	1.39	2.16	5.66	-
average for <u>G. menardii</u>					23.6 ± 2.6	1.37 ± 0.04	2.11 ± 0.04	5.64 ± 0.25	-

Notes: 1. Panama Basin sediment trap deployment (Sus Honjo): 5°21'N 81°53'W, 112 day deployment, August-December 1979.

2. Average weight per shell was calculated from total weight and number of foraminifera in each sample.

TABLE 2.12 North Atlantic benthic foraminifera -- Chain 82 Station 31 Core 11PC¹ Uvigerina spp.

sample #	depth in core (cm)	$\delta^{18}O$ ² (‰)	Li/Ca (10^{-6})	Sr/Ca (10^{-3})	Mg/Ca (10^{-3})	Na/Ca (10^{-3})	K/Ca (10^{-6})
1	105-110	4.15	21.4	1.05	1.04	3.82	-
2	110-115	4.09	21.4	1.01	1.01	3.86	-
3	115-120	3.96	25.0	1.07	-	-	-
4	140-145	3.66	27.5	0.99	0.90	3.69	89
5	159-164	3.65	24.2	1.01	0.89	4.01	108
6	205-210	3.62	19.9	0.97	0.84	3.47	-
7	225-230	3.53	34.8	0.97	0.91	3.79	-
8	231-235	3.87	21.4	1.03	0.74	3.63	-
9	318-323	2.92	26.5	0.98	-	-	-
10	403-408	3.68	17.8	1.05	1.01	3.55	-
average of all samples			24.0 ±4.9	1.01 ±0.04	0.92 ±0.10	3.73 ±0.18	97 ±15

Notes: 1. 42°N 32°W; 3209 m water depth; 2.6 cm/1000 yr average sedimentation rate.

2. $\delta^{18}O$ values are of C. wuellerstorfi relative to PDB; data are from Boyle and Keigwin (1982), Table 1, interpolated between depths where necessary.

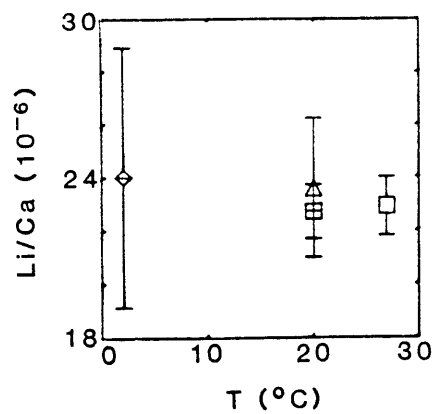
FIGURE 2.7 Average trace elemental ratios in three species of planktonic foraminifera from Panama Basin sediment traps and benthic foraminifera from a North Atlantic sediment core versus assumed calcification temperatures.

- a. Li/Ca
- b. Sr/Ca
- c. Mg/Ca
- d. Na/Ca
- e. K/Ca

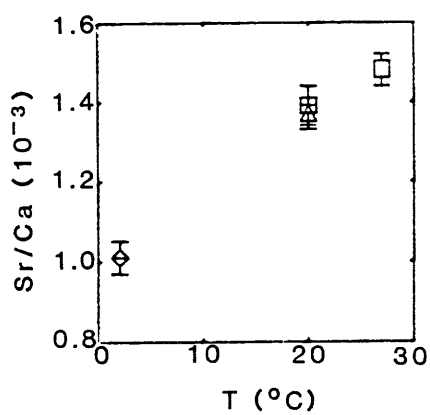
Plot symbols are:

- G. sacculifer -- Panama Basin sediment trap
- △ G. menardii -- Panama Basin sediment trap
- ▢ G. dutertrei -- Panama Basin sediment trap
- ◇ Uvigerina spp. -- North Atlantic sediment core

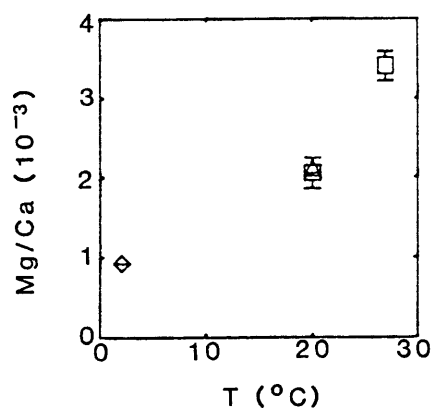
a.



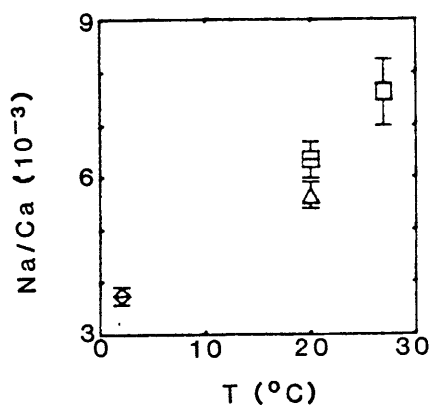
b.



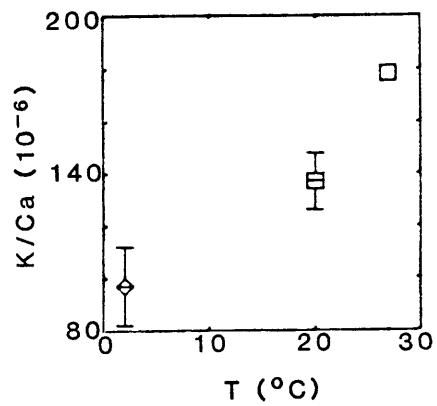
c.



d.



e.



Li/Ca ratio has a wide range; the benthic and planktonic foraminifera data show no systematic trend for Li/Ca ratios with temperature.

Indian Ocean core top planktonic samples. Trace elemental ratios were determined on size-fractionated samples of G. ruber (white), G. sacculifer, and G. menardii from an Indian Ocean core top (RC14-36 00° 27.9'S 89° 59.7'E; 3076 m water depth). The foraminifera used were splits of samples picked by W. B. Curry and analyzed for carbon and oxygen isotopes. The results are summarized in Table 2.13.

The trace elemental ratios are higher in species with lighter $\delta^{18}\text{O}$; the trends within any one species are not as well defined (Figure 2.8).

The $\delta^{18}\text{O}$ of foraminiferal calcite is a function of both the calcification temperature and the $\delta^{18}\text{O}$ of the seawater in which the foraminifera grew. $\delta^{18}\text{O}$ varies with salinity; as depth in the water column increases and salinity decreases, seawater is isotopically lighter. A foraminiferal shell deposited deeper in the water column is isotopically lighter for the same calcification temperature than one secreted at shallower depths because of this water chemistry difference. The temperature decrease with increasing depth in the water column has the opposite effect on the equilibrium calcite $\delta^{18}\text{O}$. For colder temperatures, the calcite is isotopically heavier for the same seawater isotopic composition. Calcite oxygen isotopic values alone do not give independent temperature estimates.

North Atlantic core top planktonic samples. Several species of planktonic foraminifera (G. menardii, G. sacculifer, G. ruber, O. universa, and G. truncatulinoides) were analyzed from two North Atlantic core top trigger weight samples which had been independently sampled and analyzed for oxygen and carbon isotopes (Durazzi, 1981). Table 2.14 summarizes the

TABLE 2.13 Indian Ocean core top planktonic foraminifera

RC14-36 (00°27.9'S 89°59.7'E; 3076 m water depth)

sample #	species	shell length (μm)	average 1 weight per shell (μg)	$\delta^{18}\text{O}$ 2 (‰)	$\delta^{13}\text{C}$ 2 (‰)	Li/Ca (10 ⁻⁶)	Sr/Ca (10 ⁻³)	Mg/Ca (10 ⁻³)	Na/Ca (10 ⁻³)	K/Ca (10 ⁻⁶)
1	<u>G. ruber</u> (white)	212-250	7	-2.30	+0.78	29.1	1.88	4.32	6.61	155
2	<u>G. ruber</u> (white)	250-300	10	-2.18	+0.97	42.3	1.67	4.40	7.00	181
3	<u>G. ruber</u> (white)	300-355	18	-2.36	+1.31	19.4	1.61	4.58	7.01	165
4	<u>G. sacculifer</u>	212-250	7	-2.18	+0.58	14.6	1.10	2.01	3.62	133
5	<u>G. sacculifer</u>	250-300	15	-1.75	+1.08	15.3	1.50	3.88	5.93	127
6	<u>G. sacculifer</u>	300-355	24	-2.03 -2.41	+1.56 +1.24	16.0	1.50	4.05	5.59	116
7	<u>G. sacculifer</u>	355-425	37	-1.91	+1.82	16.1	1.42	4.43	6.18	88
8	<u>G. sacculifer</u>	425-500	67	-2.07	+2.06	16.0	1.43	3.90	5.87	110
9	<u>G. sacculifer</u>	500-600	99	-2.21	+1.89	17.5	1.47	4.39	5.92	103

2.13 continued

sample #	species	shell length (μm)	average 1 weight per shell (μg)	$\delta^{18}O$ 2 (‰)	$\delta^{13}C$ 2 (‰)	Li/Ca (10 ⁻⁶)	Sr/Ca (10 ⁻³)	Mg/Ca (10 ⁻³)	Na/Ca (10 ⁻³)	K/Ca (10 ⁻⁶)
10	<u>G. menardii</u>	250-300	14	-1.76	+1.73	16.6	1.54	2.89	5.58	69
11	<u>G. menardii</u>	300-355	29	-1.75	+1.55	15.7	1.42	3.33	5.42	67
12	<u>G. menardii</u>	355-425	48	-0.65	+1.26	14.2	1.39	2.90	5.07	46
13	<u>G. menardii</u>	425-500	68	-0.57	+1.25	13.8	1.36	2.67	4.82	44
14	<u>G. menardii</u>	500-600	127	-0.97	+1.45	15.3	1.36	2.58	5.10	61
15	<u>G. menardii</u>	>600	203	-0.54	+1.40	14.4	1.42	2.59	4.71	54

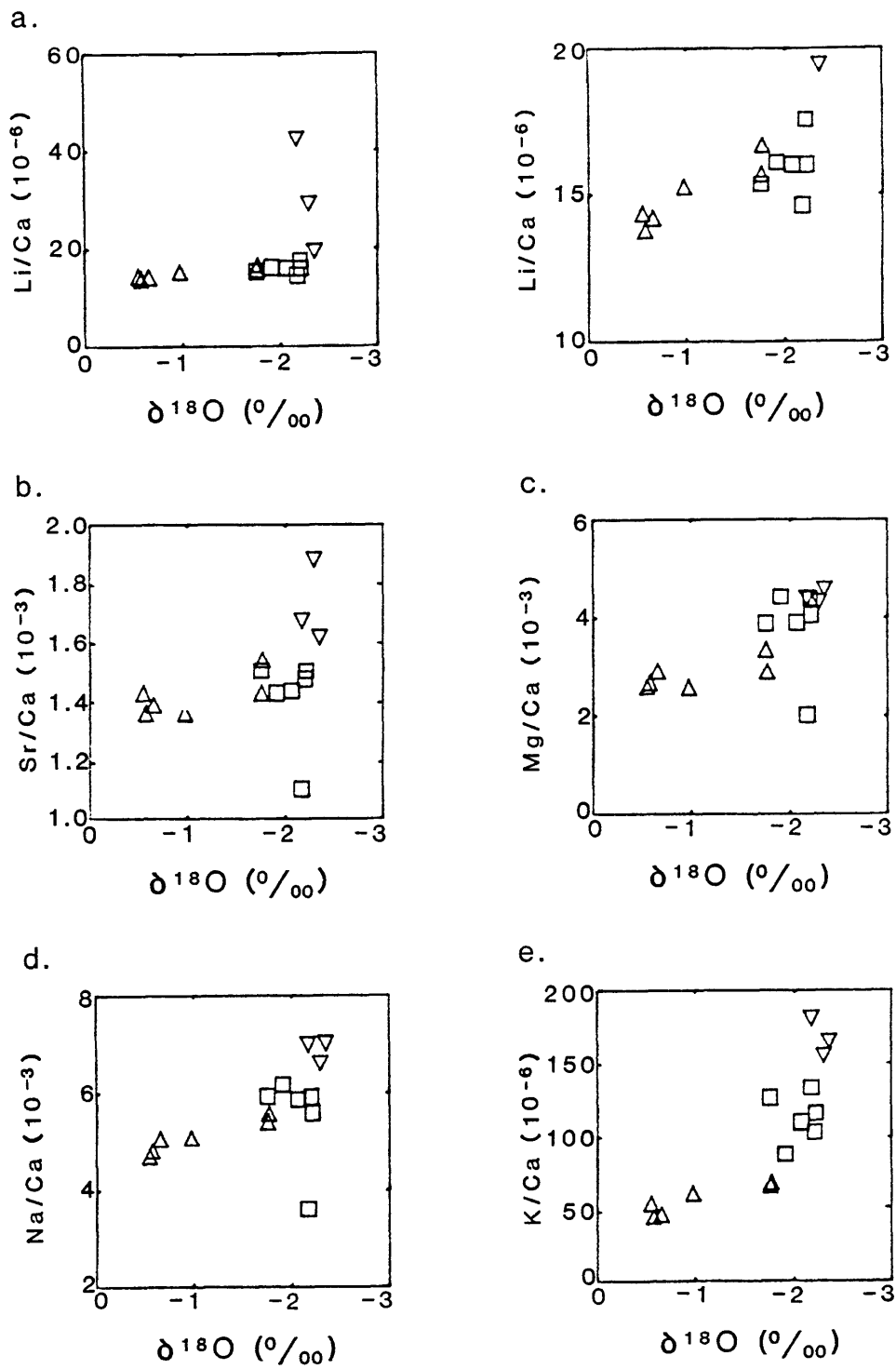
- Notes: 1. Average weight per shell was calculated from total weight and number of foraminifera in each sample.
2. The oxygen and carbon isotopic values are relative to PDB; trace element ratios were determined on splits of the same samples used for isotopic analyses (Curry and Matthews, 1981a and 1981b; W. B. Curry, pers. comm.).

FIGURE 2.8 Trace elemental ratios in size-fractions of three species of planktonic foraminifera from an Indian Ocean core top (RC14-36) versus $\delta^{18}\text{O}$ (‰ relative to PDB).

- a. Li/Ca
- b. Sr/Ca
- c. Mg/Ca
- d. Na/Ca
- e. K/Ca

Plot symbols are:

- ▽ G. ruber
- G. sacculifer
- △ G. menardii



14 North Atlantic core top planktonic foraminifera

species	shell length (μm)	average 1 weight per shell (μg)	$\delta^{18}\text{O}$ 2 ($^{\circ}/\text{‰}$)	$\delta^{13}\text{C}$ 2 ($^{\circ}/\text{‰}$)	Li/Ca (10^{-6})	Sr/Ca (10^{-3})	Mg/Ca (10^{-3})	Na/Ca (10^{-3})
3°17'N ~35°W)								
<u>G. ruber</u> (mixed)	220- 440	7	-1.54	+1.97	20.0	1.74	3.56	6.67
<u>O. universa</u>	260- 590	22	-1.34	+2.72	21.1	1.76	5.00	6.21
<u>G. sacculifer</u>	440- 850	48	-1.09	+2.72	16.9	1.58	3.44	6.66
<u>G. menardii</u>	670-1000	95	-0.11	+1.86	15.3	1.47	1.92	5.18
8°43'N ~42°W)								
<u>G. ruber</u> (mixed)	290- 590	21	-1.27	+1.84	18.8	1.76	4.34	6.80
<u>O. universa</u>	480- 850	70	-1.48	+2.78	15.4	1.64	6.73	6.31
<u>G. sacculifer</u>	550- 925	84	-0.96	+2.84	17.6	1.61	4.50	6.45
<u>G. menardii</u>	960-1300	146	+0.35	+1.82	18.9	1.53	2.58	5.08
<u>G. truncatu-</u> <u>linoides</u>	370- 660	37	+1.57	+0.98	20.9	1.69	2.60	7.05

1. Average weight per shell was calculated from total weight and number of foraminifera in sample.
2. Oxygen and carbon isotopic values, relative to PDB, are from separate samples (Durazzi, 1977). The size fractions used for isotopic analyses were sometimes different than those for trace element analyses. Size ranges reported were those for the trace element samples.

results from V25-60 (3°17'N ~35°W) and V22-26 (8°43'N ~42°W). The trace element foraminiferal ratios are plotted versus $\delta^{18}\text{O}$ in Figures 2.9 and 2.10.

V25-60 shows the same pattern of interspecific differences seen previously: an increase in trace elemental ratios with lighter $\delta^{18}\text{O}$ values. V22-26 shows the inverse trend for Li/Ca and K/Ca ratios and no clear trends for Sr/Ca and Na/Ca ratios.

Laboratory culture experiments. Direct control of temperature was possible in laboratory culture experiments. Foraminiferal samples nominally at 30° C were subjected to temperature variations at ambient laboratory conditions. For the air-conditioned Barbados culturing room, the temperature was $28 \pm 2^\circ \text{C}$. The mean of daily temperature measurements over two weeks in the Curacao culturing lab was $30 \pm 2^\circ \text{C}$. The surface water temperatures at the foraminiferal collection sites were 26 - 29° C. A temperature bath was used to maintain the samples cultured at 20° C, with temperature variations of less than one degree. All other conditions for the two sample groups were identical: light intensity and duration, daily feedings, and daily changes of seawater solutions for the samples in natural seawater. Table 2.15 lists the foraminiferal information and analytical results for two species of planktonic foraminifera (G. sacculifer and O. universa) grown in laboratory culture at 20° C in surface seawater. These results and those of experiments culturing foraminifera at 30° C in a variety of solutions (Tables 2.1 - 2.7) are summarized in Table 2.16.

The means reported for the elemental ratios do not differ more than the standard deviations of the data sets for G. sacculifer and O. universa cultured at 20° C and 30° C. As well, the differences in the means for

FIGURE 2.9 Trace elemental ratios in four species of planktonic foraminifera from V25-60 TW core top versus $\delta^{18}\text{O}$ (‰ relative to PDB).

- a. Li/Ca
- b. Sr/Ca
- c. Mg/Ca
- d. Na/Ca
- e. K/Ca

Plot symbols are:

- ◇ O. *universa*
- ▽ G. *ruber*
- G. *sacculifer*
- △ G. *menardii*

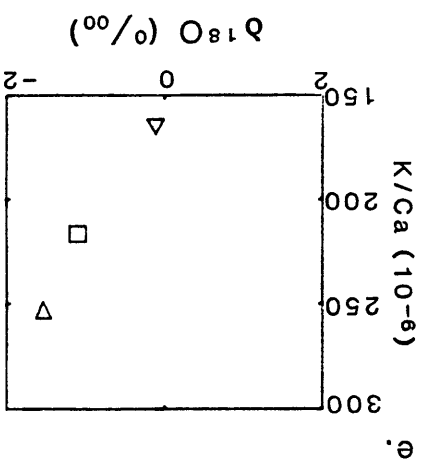
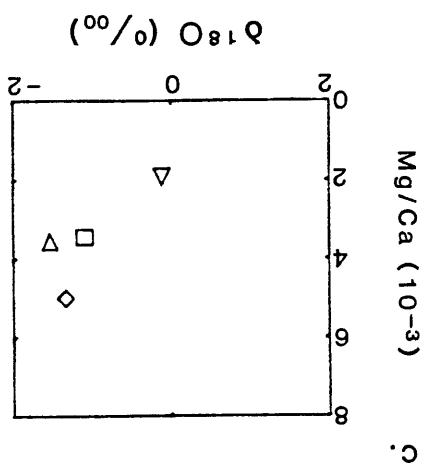
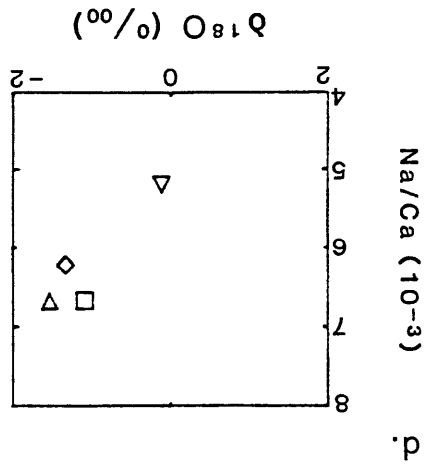
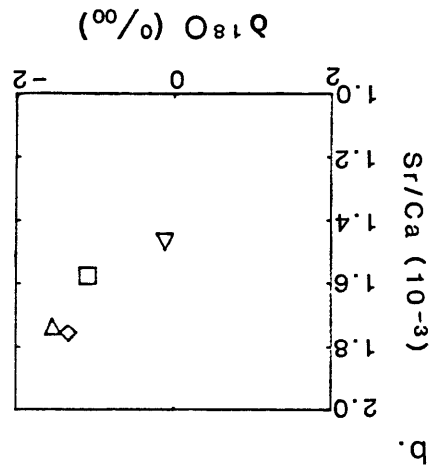
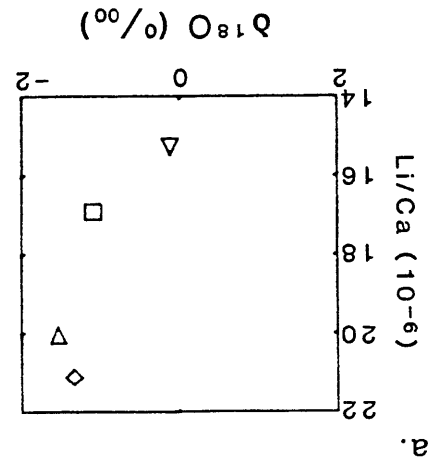


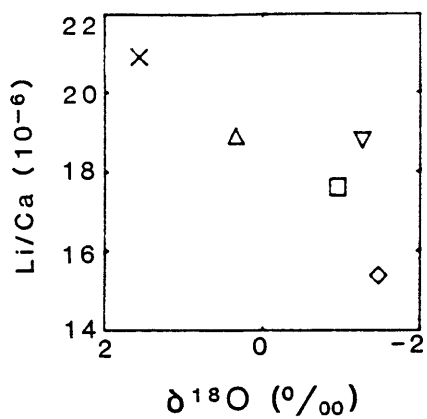
FIGURE 2.10 Trace elemental ratios in five species of planktonic foraminifera from V22-26 TW core top versus $\delta^{18}\text{O}$ (‰ relative to PDB).

- a. Li/Ca
- b. Sr/Ca
- c. Mg/Ca
- d. Na/Ca
- e. K/Ca

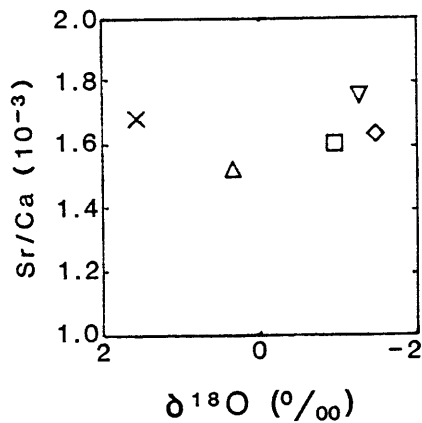
Plot symbols are:

- ◇ O. *universa*
- ▽ G. *ruber*
- G. *sacculifer*
- △ G. *menardii*
- × G. *truncatulinoides*

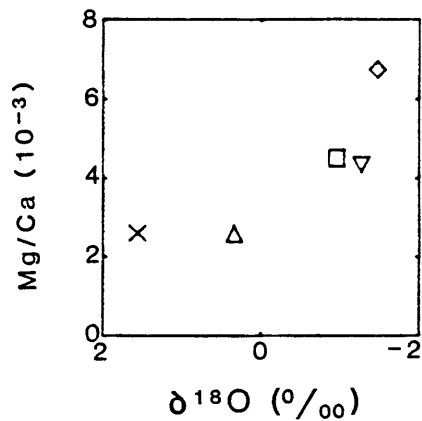
a.



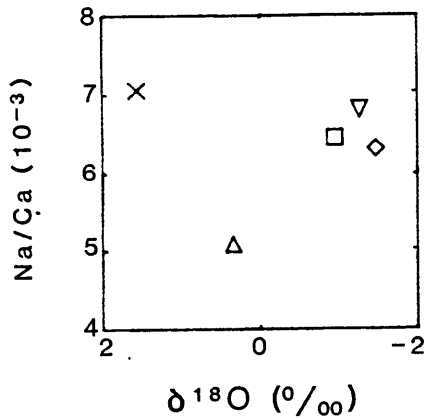
b.



c.



d.



e.

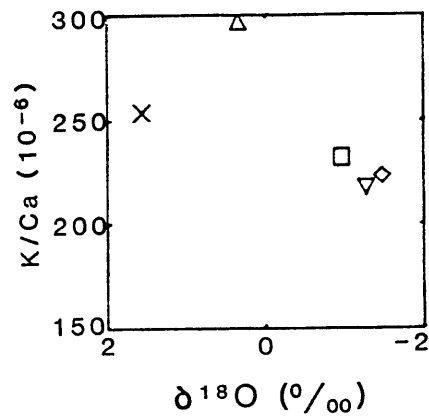


TABLE 2.15 20° C natural seawater lab culture -- G. sacculifer and O. universa

2.15.A FORAMINIFERAL INFORMATION

sample #	sample description	# of foraminifera	average weight per shell (µg)	average initial shell length (µm)	average final shell length (µm)	average # of days in culture	comments
<u>G. sacculifer</u>							
1	lab culture	3	18	296 ± 57	527 ± 47	6	2T 1D
2	lab culture	5	34	341 ± 36	761 ± 71	7	1G 5T
3	lab culture	2	23	315 ± 38	511 ± 32	4	1G 1D
4	lab culture	3	16	355 ± 24	542 ± 9	3	3D
5	lab culture	2	13	442 ± 32	542 ± 13	2	2D
<u>O. universa</u>							
6	lab culture	3	19	327 ± 52	602 ± 90	4/7	1D 2T
7	lab culture	4	12	515 ± 18	527 ± 13	4	

2.15.B FORAMINIFERAL ANALYSES

	sample #	Li/Ca (10 ⁻⁶)	Sr/Ca (10 ⁻³)	Mg/Ca (10 ⁻³)	Na/Ca (10 ⁻³)
<u>G. sacculifer</u>	1	15.8	1.52	3.06	6.99
	2	14.8	1.44	3.51	6.62
	3	-	1.38	5.03	8.18
	4	14.1	1.19	5.54	6.61
	5	-	1.23	4.33	6.36
	mean of 1-5	± 14.9 1.0	± 1.35 0.14	± 4.29 1.03	± 6.95 0.72
<u>O. universa</u>	6	14.4	1.23	6.37	6.50
	7	11.5	1.28	14.0	6.58
	mean of 6-7	± 13.0 2.1	± 1.26 0.04	± 10.2 5.4	± 6.54 0.06

TABLE 2.16 20° C and 30° C natural seawater culture --
G. sacculifer and O. universa means

species	T	data set	Li/Ca (10 ⁻⁶)	Sr/Ca (10 ⁻³)	Mg/Ca (10 ⁻³)	Na/Ca (10 ⁻³)
<u>G. sacculifer</u>	20° C	natural seawater	14.9 ± 0.9	1.35 ± 0.14	4.29 ± 1.03	6.95 ± 0.72
		30° C	natural seawater	15.2 ± 5.2	1.19 ± 0.24	3.98 ± 0.91
		plankton tow	19.5 ± 5.5	1.52 ± 0.23	5.83 ± 1.82	
		Li-spiked natural seawater (Barbados)		1.38 ± 0.03	4.58 ± 0.57	6.42 ± 0.42
		Li-spiked artificial seawater (Curacao)		1.47 ± 0.19	6.60 ± 0.84	6.45 ± 0.62
		Na/Mg (Curacao)	13.2 ± 1.6	1.34 ± 0.10		
		[SO ₄] (Curacao)	13.1 ± 1.3	1.39 ± 0.10	6.36 ± 1.71	5.86 ± 0.78

2.16 continued

species	T	data set	Li/Ca (10^{-6})	Sr/Ca (10^{-3})	Mg/Ca (10^{-3})	Na/Ca (10^{-3})
<u>O. universa</u>	20° C	natural seawater	13.0 ± 2.1	1.26 ± 0.04	10.2 ± 5.4	6.54 ± 0.06
	30° C	natural seawater	11.7	1.13 ± 0.39	9.03 ± 3.03	6.76 ± 1.88
		Li-spiked natural seawater (Barbados)			1.31 ± 0.05	10.8 ± 1.5

Sr/Ca, Mg/Ca, and Na/Ca ratios for G. sacculifer at 20° C and 30° C in natural seawater and for Mg/Ca and Na/Ca ratios for the similar O. universa samples are in the opposite direction than would be expected from the oxygen isotopic correlations previously observed. Cooler temperatures for the foraminifera in natural seawater in laboratory culture resulted in slightly higher trace elemental ratios. These means were determined from a small number of samples. The Sr/Ca and Na/Ca ratios are similar in the foraminifera from other experiments at 30° C to those from foraminifera in natural seawater at 20° C (Table 2.16). The results from the sediment trap and core samples showed increases on the order of 10 - 15% per 10° C temperature for Sr/Ca ratios and much larger percentage increases for Mg/Ca and Na/Ca ratios. No evidence for a systematic increase of trace elemental ratios with increasing temperatures is seen in the results of the culturing experiments.

SUMMARY

Laboratory culture of two species of planktonic foraminifera demonstrated that the observed species differences in trace elemental ratios in foraminiferal calcite versus $\delta^{18}\text{O}$ are not due to a direct dependence of biogenic trace element distribution coefficients on temperature for Sr/Ca, Mg/Ca, and Na/Ca. Foraminifera depositing shells in the water column at different temperatures are subject to different growth conditions -- for example, different light levels and food availability. Some parameter other than direct temperature control results in systematic trace elemental ratio differences among species not observed in the laboratory culture experiments where temperature was the only environmental parameter varied.

APPENDIX 2.1 Calculation procedures for relative incorporation coefficients

The peak regions of the two isotopes were defined as two envelopes of channel numbers at given instrumental settings: for the lower energy isotope, region 1, channels $x_1 - x_2$; and for the higher energy isotope, region 2, channels $y_1 - y_2$. Peaks were defined on each spectrum of isotope standards with statistically significant boundaries. The boundary on either side of the peak was chosen to be the last channel whose counts were greater than those of the next channel away from the peak by an amount equal to or exceeding the counting statistic \sqrt{N} error. In other words, channel i with number of counts z was defined as the boundary when it was the first to the side of the peak to fit the criteria that $z_{i\pm 1} \geq z_i - \sqrt{z_i}$, with $-$ for left boundary, and $+$ for right boundary. Peak boundaries were averaged from several spectra of each isotope and then used consistently on all standard, sample, and background spectra. This procedure ignores any resolution changes due to absolute activity changes.

Spectra of a foraminiferal sample and its seawater solution were measured. A background spectrum (neither isotope present) and a reference spectrum (higher-energy isotope alone) were counted at the same instrumental settings and in the same detector configuration as the sample spectra. For each spectrum, the number of counts in regions 1 and 2 were summed and divided by the counting time for that spectrum to give gross counting rates (cpm) in each peak region: B_1 and B_2 for the background spectrum; R_1 and R_2 for the reference spectrum; S_1 and S_2 for the sample spectrum of either a foraminiferal sample or seawater solution.

The Compton distribution of the higher energy isotope contributes to the counting rate in the photopeak area of the lower energy isotope. The

reference spectrum was used to calculate a factor which normalizes this contribution to the photopeak area of the higher energy isotope. The factor was defined as:

$$F = \frac{R_1 - B_1}{R_2 - B_2}$$

The net corrected counting rates S_1^* and S_2^* , for the sample spectrum were calculated:

$$S_2^* = S_2 - B_2$$

$$S_1^* = S_1 - B_1 - F(S_2^*)$$

Counting times were short relative to the half-lives of the radiotracers so that decay corrections during sample counts were not necessary.

For the foraminifera from the Barbados Cd-Sr experiments, ^{109}Cd was measured on the M.I.T. LEPS Ge(Li) γ -system. Peak locations were determined with statistically significant boundaries. The background in the photopeak area for each sample (due primarily to the Compton distribution of the ^{85}Sr in the sample for this detector) was determined by averaging the counting rates in 8 - 10 channels outside either peak boundary and assuming a linear baseline. ^{85}Sr was determined using the NaI(Tl) detector used for all other experiments. Cd and Sr counting rates were converted to absolute activities by comparison to standards similar to samples in physical size and placement relative to the detector. The calculated activities for these samples were treated equivalently to the net counting rates of the other samples in the rest of the calculations.

Each counting rate was then corrected to a uniform time, t_0 , by:

$$(S_1^*)_0 = S_1^* \exp\{\lambda_1 t\}$$

$$(S_2^*)_0 = S_2^* \exp\{\lambda_2 t\}$$

where: t = number of days from t_0 (the assay date of the radiotracer spikes) to date spectrum was measured

The ratio of the corrected counting rates for the two isotopes was then calculated, either as $(S_1^*)_0 / (S_2^*)_0$ for Cd-Sr or $(S_2^*)_0 / (S_1^*)_0$, for Zn-Sr. For a given sample, the two isotopes were measured in one spectrum or in two sequential spectra at different instrumental settings, but with no change in sample geometry. The relative counting rates of the two isotopes in one sample was related to the relative absolute activities of the two isotopes solely by the efficiency-energy curve of the detector. The counting rate ratio for the foraminiferal sample was divided by the ratio for the corresponding seawater solution to give the relative incorporation coefficient for either Cd or Zn relative to Sr in foraminiferal calcite ($C_{Cd/Sr}$ or $C_{Zn/Sr}$). Since the foraminiferal counting rate ratio for the two isotopes is divided by a similar ratio in the seawater solution, the difference in detector efficiency at the two energies cancels out. The resulting quotient was equivalent to one of absolute activities or concentrations.

To calculate the distribution coefficient for either Cd or Zn in calcite ($D_{Cd/Ca}$ or $D_{Zn/Ca}$), the relative incorporation coefficient was multiplied by the distribution coefficient of Sr in calcite ($D_{Sr/Ca} = 0.16$).

Errors reported were $1\sigma \sqrt{N}$ counting errors, propagated through the calculations.

The weighted mean of the measured distribution coefficients of the samples was calculated as (Perrin, 1970):

$$\bar{X}_W = \frac{\sum w(x_i)x_i}{\sum w(x_i)}$$

where: $w(x_i)$, the weighting factors, are $\{1/(\sigma_{x_i})^2\}$

The probable error of the weighted mean was calculated as:

$$\frac{1}{\sigma_{\bar{x}_w}^2} = \sum \{1/(\sigma_{x_i})^2\}$$

REFERENCES -- CHAPTER TWO

- Bé, A. W. H. (1977) An ecological, zoogeographic and taxonomic review of Recent planktonic foraminifera, in Ramsay, A. T. S., ed., Oceanic Micropaleontology, vol. 1, London, Academic Press, pp. 1-100.
- Bé, A. W. H. (1980) Gametogenic calcification in a spinose planktonic foraminifer, Globigerinoides sacculifer (Brady), Mar. Micropal. 5: 283-310.
- Bé, A. W. H., C. Hemleben, O. R. Anderson, M. Spindler, J. Hacunda, and S. Tuntivate-Choy (1977) Laboratory and field observations of living planktonic foraminifera, Micropal. 23: 155-179.
- Bé, A. W. H., C. Hemleben, O. R. Anderson, and M. Spindler (1979) Chamber formation in planktonic foraminifera, Micropal. 25: 294-307.
- Bender, M. L., R. B. Lorenz, and D. F. Williams (1975) Sodium, magnesium and strontium in the tests of planktonic foraminifera, Micropal. 21: 448-459.
- Boyle, E. A. and L. D. Keigwin (1982) Deep circulation of the North Atlantic over the last 200,000 years: geochemical evidence, Science 218: 784-787.
- Bruland, K. W. (1980) Oceanographic distributions of cadmium, zinc, nickel, and copper in the North Pacific, Earth Planet. Sci. Lett. 47: 176-198.
- CLIMAP Project Members (1976) The surface of the ice-age earth, Science 191: 1131-1137.
- Cronblad, H. G. and B. A. Malmgren (1981) Climatically controlled variation of Sr and Mg in Quaternary planktonic foraminifera, Nature 291: 61-64.
- Curry, W. B. and R. K. Matthews (1981a) Paleo-oceanographic utility of oxygen isotopic measurements on planktic foraminifera: Indian Ocean core-top evidence, Palaeogeogr., Palaeoclimatol., Palaeoecol. 33: 173-191.
- Curry, W. B. and R. K. Matthews (1981b) Equilibrium ^{18}O fractionation in small size fraction planktic foraminifera: evidence from Recent Indian Ocean sediments, Mar. Micropal. 6: 327-337.
- Duplessy, J.-C., P.-L. Blanc, and A. W. H. Bé (1981) Oxygen-18 enrichment of planktonic foraminifera due to gametogenic calcification below the euphotic zone, Science 213: 1247-1250.
- Durazzi, J. T. (1981) Stable-isotope studies of planktonic foraminifera in North Atlantic core tops, Palaeogeogr., Palaeoclimatol., Palaeoecol. 33: 157-172.

- Fairbanks, R. G., M. Sverdrup, R. Free, P. H. Wiebe, and A. W. H. Bé (1982) Vertical distribution and isotopic composition of living planktonic foraminifera from the Panama Basin, Nature 298: 841-844.
- Fairbanks, R. G., P. H. Wiebe, and A. W. H. Bé (1980) Vertical distribution and isotopic composition of living planktonic foraminifera in the western North Atlantic, Science 207: 61-63.
- Friedlander, G., J. W. Kennedy, E. S. Macias, and J. M. Miller (1981) Nuclear and Radiochemistry, third edition, New York, John Wiley & Sons.
- Garrels, R. M. and M. E. Thompson (1962) A chemical model for sea water at 25° C and one atmosphere total pressure, Amer. Jour. Sci. 260: 57-66.
- Hester, K. and E. Boyle (1982) Water chemistry control of cadmium content in Recent benthic foraminifera (1982) Nature 298: 260-262.
- Imbrie, J. and N. G. Kipp (1971) A new micropaleontological method for quantitative paleoclimatology: application to a Late Pleistocene Caribbean core, in Turekian, K. K., ed., Late Cenozoic Glacial Ages, New Haven, Yale University Press, pp. 71-182.
- Kilbourne, R. T. and B. K. Sen Gupta (1973) Elemental composition of planktonic foraminiferal tests in relation to temperature-depth habits and selective solution, Geol. Soc. Amer. Abstracts with Programs 5 (5): 408-409.
- Kinsman, D. J. J. and H. D. Holland (1969) The co-precipitation of cations with CaCO₃ -- IV. The co-precipitation of Sr²⁺ with aragonite between 16° and 96° C, Geochim. Cosmochim. Acta 33: 1-17.
- Krauskopf, K. B. (1967) Introduction to Geochemistry, New York, McGraw-Hill Book Company.
- Lefèvre, R. and M.-T. Vénec-Peyré (1977) Mise en évidence au microanalyseur ionique d'une zonation dans la répartition du sodium, magnésium et strontium dans le test d'un Foraminifère calcaire perforé: Ammonia beccarii (L.), C. R. Acad. Sci. Paris 285 (Série D): 23-26.
- Lorens, R. B. (1978) A study of biological and physical controls on the trace metal content of calcite and aragonite, Ph.D. thesis, University of Rhode Island.
- Lorens, R. B. and M. L. Bender (1977) Physiological exclusion of magnesium from Mytilus edulis calcite, Nature 269: 793-794.
- Lorens, R. B. and M. L. Bender (1980) The impact of solution chemistry on Mytilus edulis calcite and aragonite, Geochim. Cosmochim. Acta 44: 1265-1278.

- Mucci, A. and J. W. Morse (1983) The incorporation of Mg^{2+} and Sr^{2+} into calcite overgrowths: influences of growth rate and solution composition, *Geochim. Cosmochim. Acta* 47: 217-233.
- Perrin, C. L. (1970) Mathematics for Chemists, New York, Wiley-Interscience.
- Savin, S. M. and R. G. Douglas (1973) Stable isotope and magnesium geochemistry of Recent planktonic foraminifera from the South Pacific, *Geol. Soc. Amer. Bull.* 84: 2327-2342.
- Shackleton, N. J. (1982) The deep-sea sediment record of climate variability, *Prog. Oceanog.* 11: 199-218.
- Swart, P. K. (1981) The strontium, magnesium and sodium composition of Recent scleractinian coral skeletons as standards for palaeoenvironmental analysis, *Palaeogeogr., Palaeoclimatol., Palaeoecol.* 34: 115-136.

CHAPTER THREE:

THE EFFECTS OF DIAGENESIS ON TRACE ELEMENTAL RATIOS IN
FORAMINIFERAL CALCITE OVER THE LAST 100 M.Y.

To use foraminiferal calcite chemistry as an indicator of oceanic composition, we must understand:

1. the relationship of biogenic calcite chemistry to that of the seawater in which the foraminifera deposited their shells, and
2. the preservation of this original calcite composition after deposition in the sediments.

Laboratory culture experiments described in Chapter 2 demonstrated that foraminiferal calcite compositions reflect changes in seawater Li/Ca, Sr/Ca, and Mg/Ca ratios. Biogenic calcite chemistry does not change in response to changes in seawater Na/Ca ratios.

Diagenetic processes in biogenic oceanic sediments can have significant effects on the physical properties of the sediments. The evolution of sedimentary texture from ooze to chalk to limestone with increasing sediment depth and age, accompanied by density and seismic velocity increases and porosity decreases, is due to sedimentary recrystallization and compaction processes (e.g., Matter et al., 1975; van der Lingen and Packham, 1975). Diagenetic processes can also change the chemical compositions of bulk sediments, interstitial water, and of individual biogenic components (e.g., Matter et al., 1975; Baker et al.,

1982; Elderfield et al., 1982). A closed-system mass-balance model of interstitial water and calcite compositions has recently been used to consider the effects of recrystallization on foraminiferal oxygen isotopic ratios. The increase of $^{18}\text{O}/^{16}\text{O}$ ratios as sample ages decrease in the Tertiary was suggested from this model to be primarily the result of recrystallization reactions in the sediment column, not of oceanic paleotemperatures during shell formation (Killingley, 1983).

Because of the importance of the trace elemental and isotopic chemistry of foraminiferal shells to deciphering oceanic chemical and thermal histories, an understanding of the processes affecting the composition of their shells after deposition and the ability to model these processes are crucial.

Some models of seafloor spreading and hydrothermal fluxes suggest that oceanic Li concentrations may have been as much as a factor of two higher 80 - 110 m.y.b.p. than at present. The purpose of this thesis is to determine paleoceanic Li concentrations in order to assess the importance of hydrothermal circulation fluxes to oceanic mass-balances through time. For this study, temporal changes in Li/Ca, Sr/Ca, Mg/Ca, and Na/Ca ratios were measured in foraminiferal shells from Deep Sea Drilling Project (DSDP) sediment samples with ages up to 110 m.y.b.p.

The oceanic signal for these conservative elemental ratios should be independent of location. However, diagenetic processes affecting foraminiferal calcite are site-specific, varying, for example, with sedimentary compositions, accumulation rates, thermal profiles, and interstitial water compositions. To constrain both the models of diagenetic processes and the paleochemistry signals, the four elemental ratios were determined in foraminiferal shells from five sites. Diagenetic

effects on foraminiferal calcite composition are discussed in this chapter. The extent to which the original signals of oceanic composition can be qualitatively or quantitatively deciphered from the measured records is assessed. Inferences about oceanic paleochemistry from these measurements and models are discussed in Chapter 4.

SAMPLE SELECTION

Five sample sites were chosen on the basis of core descriptions in DSDP Initial Reports. The goal was to obtain fairly complete records of planktonic foraminiferal chemistry in several sites. Samples were chosen where the qualitative shipboard observations reported in the core logs indicated the highest abundances and best preservation for foraminiferal shells in each age range.

AGE ASSIGNMENTS ON DSDP SAMPLES

The time scale used for age assignments is given in Table 3.1. The divisions between geological time periods were located in the detailed core logs for each site and depths below the seafloor for these transitions were figured as for samples. Sample ages were calculated by linear interpolation between the depths and assigned ages of the transitions (geologic epochs and, where possible, foraminiferal zonations), as follows:

$$\text{sample age (m.y.)} = \frac{A_2 - A_1}{D_2 - D_1} (D - D_1) + A_1$$

where: D_1 and A_1 are the depth (m) and age (m.y.), respectively, of the youngest transition adjacent to the sample

D_2 and A_2 are the depth (m) and age (m.y.), respectively, of the oldest transition adjacent to the sample

D is the sample depth (m)

A change in the time scale (Table 3.1) would stretch and shrink portions of the records versus age in any one site. Since the age assignments for all sites were calculated using the same time scale, the relative age relationships between samples in different sites would not change if the time scale were adjusted.

THE USE OF MIXED PLANKTONIC FORAMINIFERAL SAMPLES

There are interspecific differences in the Li/Ca, Sr/Ca, Mg/Ca, and Na/Ca ratios of modern planktonic foraminifera (see Chapter 2). However, the species differences in Li/Ca and Sr/Ca are small relative to the postulated magnitude of oceanic chemistry changes (factor of two) over the time period surveyed. The primary goal of an age survey is to determine whether a measurable signal exists. If paleochemical Li/Ca variations have occurred, it is unlikely that interspecific differences or changing assemblage compositions could bias the results so it would appear that no change had occurred, particularly when samples from several locations are compared. If a significant Li/Ca change were found, accurate determinations of the absolute magnitude would then require the use of individually calibrated species, as is now done for oxygen isotopic analyses.

TABLE 3.1 Time scale

era	period		epoch	age (m.y.)		
				0		
Cenozoic	Quaternary		Pleistocene	1.8		
				3.0		
	Tertiary	Neogene		Pliocene	5.0	
					11.0	
					14.0	
					22.5	
					30.0	
					37.5	
			Paleocene		Miocene	43.0
					49.0	
					53.5	
					60.0	
					65	
					72	
					80	
					84	
Mesozoic	Cretaceous	Upper		87		
				91		
				100		
				104		
		Lower		109		
				116		

References: Vincent (1974) for Cenozoic; Van Hinte (1972) for Cretaceous.

FORAMINIFERAL SAMPLE PREPARATION

PRELIMINARY CLEANING

Sediment samples were disaggregated on a shaker table. After shaking, samples were wet-sieved through 150 μ m mesh. The coarse fraction was rinsed thoroughly with distilled water and methanol and then air dried. From the coarse fraction, mixed planktonic foraminiferal samples were picked using a stereomicroscope and a camel's hair brush. Only well preserved, whole foraminiferal shells were chosen for analyses.

In initial sample trials, high and erratic losses of samples occurred during cleaning. Visual examination of the shells before cleaning sometimes showed secondary calcite incrustation. To ensure reliable final sample yields and to eliminate as much of this secondary calcite as possible from the samples, a two-stage cleaning process was used: a preliminary cleaning, followed by a more thorough cleaning after samples were weighed. Foraminiferal samples of a few milligrams total weight were cleaned with several ultrasonically agitated methanol rinses, with the supernatant siphoned-off each time. The supernatant in the first rinse was generally cloudy with clay, fine-grained carbonate, and perhaps fragments of weaker shells. Supernatant cloudiness decreased with subsequent rinses; the final rinse was clear. The samples were air-dried in a laminar flow bench and splits weighed for chemical analyses. Wherever there were sufficient number of foraminifera, replicate samples were processed. After weighing, the shells were gently crushed between glass plates to open the chambers and facilitate further cleaning. They were transferred to acid-leached 1.5 ml (in later analyses, 0.5 ml) polypropylene centrifuge tubes for final cleaning.

FINAL CLEANING OF CRUSHED FORAMINIFERAL SHELLS

Cleaning procedures which included reductive cleaning, necessary for the uncontaminated analysis of Cd in foraminiferal shells (Boyle, 1981), were compared to simpler procedures of repeated, ultrasonically agitated, methanol and water rinses. For the elements measured in this study (Li, Sr, Mg, and Na), no significant differences were found between samples reductively cleaned and those which did not undergo this treatment. The simpler cleaning method offered the advantages of smaller sample losses, less possibility of contaminating the samples during sample handling, and faster sample processing. A typical final cleaning of a foraminiferal sample consisted of three distilled water rinses, four methanol rinses, and four additional water rinses. Each rinse included multiple short bursts of ultrasonic agitation and inverting the centrifuge tubes containing the samples. After a brief settling time, supernatants were siphoned off. The samples from one site (holes 369 and 369A, leg 41) were also cleaned with hot basic hydrogen peroxide because of the presence of pyrite and possibly organic matter in some samples.

Samples were briefly air-dried in a laminar flow bench and then dissolved in 0.3 N HNO₃ with ultrasonic agitation of the sample solutions. Solutions were centrifuged for 5 min and transferred to dry, acid-leached centrifuge tubes. Visible solids remained in a few samples at this transfer stage; the solutions were pipetted away from these solids. Analytical methods used to determine trace elemental ratios in sample solutions are discussed in Appendix 1. Results are reported as mole ratios of trace elements to Ca.

LOCATIONS STUDIED

SITE DESCRIPTIONS

Information about the five sites studied is listed in Table 3.2; their locations are depicted in Figure 3.1. Detailed descriptions can be found in the respective site reports (Site 289, Andrews, Packham, et al., 1975; Site 305, Larson, Moberly, et al., 1975; Site 366, Lancelot, Seibold, et al., 1977a; Site 369, Lancelot, Seibold, et al., 1977b; Site 526, Moore, Rabinowitz, et al., in press).

FORAMINIFERAL CHEMISTRY

Sample information and foraminiferal calcite compositions for all five sites are listed in Appendix 3.1, Tables 3.5 - 3.9.

THE EFFECTS OF DIAGENESIS

Foraminiferal calcite compositions may have been altered in the sediments by partial dissolution, solid diffusion of trace elements, or recrystallization of the biogenic calcite to inorganic calcite. The effects of these processes are considered here.

PARTIAL DISSOLUTION

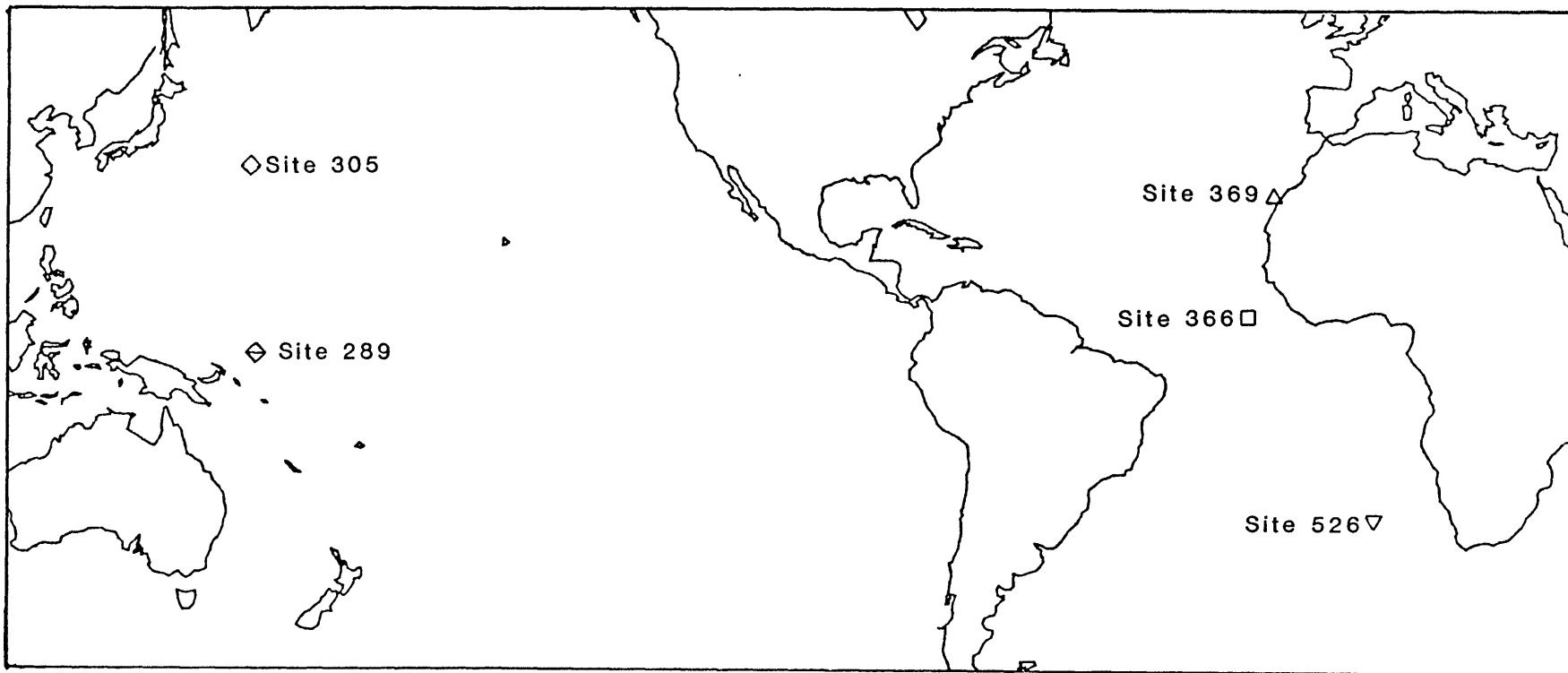
Experiments were performed in which planktonic foraminiferal shells were partially dissolved in dilute acid and the acid analyzed (Bender et al., 1975; Lorens et al., 1977). This procedure was repeated with new aliquots of dilute acid until the shells were completely dissolved. There were no variations in the Sr/Ca, Mg/Ca, or Na/Ca ratios in the successive aliquots of acid (Bender et al., 1975; Lorens et al., 1977). Sr/Ca, Mg/Ca, and Na/Ca ratios were measured also in six species of planktonic foraminifera from core top samples along the East Pacific Rise and central

TABLE 3.2 Site information

site and leg number	location	water depth (m)	oldest sediment drilled	oldest sample in this study
Site 289 Leg 30	Ontong-Java Plateau, Pacific 00° 29.92' S 158° 30.69' E	2224	1262.5 m Aptian 105 m.y.	861.25 m Late Oligocene 29.4 m.y.
Site 305 Leg 32	Shatsky Rise, Pacific 32° 00.13' N 157° 51.00' E	2903	631.0 m Hauterivian 120 m.y.	394.75 m Late Albian 100.9 m.y.
Site 366 Leg 41	Sierra Leone Rise, Atlantic 5° 40.7' N 19° 51.1' W	2853	850.0 m Maestrichtian 70 m.y.	792.89 m Late Paleocene 59.3 m.y.
Site 369 Leg 41	Spanish Sahara continental slope, Atlantic 26° 35.5' N 14° 59.0' W	1770	488.5 m Aptian 106 m.y.	486.36 Late Aptian 106.3 m.y.
Site 526 Leg 74	Walvis Ridge, Atlantic 30° 07.36' S 3° 08.28' E	1054	356.0 m Paleocene 60 m.y.	225.58 m Late Eocene 38.7 m.y.
References:	Site 289	Andrews, Packham, et al. (1975).		
	Site 305	Larson, Moberly, et al. (1975).		
	Site 366	Lancelot, Seibold, et al. (1977a).		
	Site 369	Lancelot, Seibold, et al. (1977b).		
	Site 526	Moore, Rabinowitz, et al. (in press).		

FIGURE 3.1 Map of locations of DSDP sites used in this study. Location symbols are:

- ⚡ Site 289 (Leg 30) Ontong-Java Plateau, Pacific
- ◇ Site 305 (Leg 32) Shatsky Rise, Pacific
- Site 366 (Leg 41) Sierra Leone Rise, Atlantic
- △ Site 369 (Leg 41) Spanish Sahara continental slope, Atlantic
- ▽ Site 526 (Leg 74) Walvis Ridge, Atlantic



Pacific (Lorens et al., 1977). Water depths ranged from 500 to 4700 m and dissolution intensity increased with increasing water depth. Mg/Ca ratios for monospecific samples decreased with increasing water depth, while Na/Ca ratios decreased somewhat less. There was no systematic change in Sr/Ca ratios. The reasons for the different results of laboratory and natural partial dissolutions are not definitively known. Partial dissolution of foraminiferal shells in the sediment may decrease the original Mg/Ca and Na/Ca ratios; it would have no effect on Sr/Ca ratios. Generally, Mg/Ca and Na/Ca ratios in foraminiferal shells correlate with dissolution susceptibility, with more dissolution resistant species having lower Mg/Ca ratios (Bender et al., 1975; Lorens et al., 1977; Chapter 2). The effect of partial dissolution on a mixed planktonic foraminiferal assemblage is to the lower bulk Mg/Ca ratio. Diagenetic models considered in this chapter do not include the effects of partial dissolution on individual species or assemblages.

SOLID DIFFUSION

Solid diffusion is another potential means of altering the composition of foraminiferal calcite. The thickness of a foraminiferal shell is 10 - 100 Å. Using the relationship between the mean squared distance, the diffusion coefficient, and time that ($\overline{x^2} = 2Dt$), the solid diffusion coefficient required for ions to traverse this distance in 20 m.y. is $(8 \times 10^{-20}) - (8 \times 10^{-22})$ cm²/sec. Diffusion coefficients in solids are generally measured at high temperatures (500-1000° C); for temperatures characteristic of sedimentary environments, the experimental data must be extrapolated. The diffusion coefficient at 30° C for Na and Ca in calcite was estimated to be $\sim 10^{-52}$ cm²/sec (Brätter et al., 1972). For comparison, the Na diffusion coefficient at 20° C in NaCl is $\sim 10^{-34}$

cm²/sec (Bénière et al., 1976). Diffusion coefficients are likely to be different in polycrystalline biogenic material from those in the single crystals used in laboratory studies. From these estimates, however, cation diffusion in calcite is not important in diagenetic changes in sediments.

RECRYSTALLIZATION OF BIOGENIC CALCITES

Biogenic calcites are constructed of small, fine-grained calcite particles. A foraminiferal shell has a greater surface area than an equal amount of calcite in larger crystals formed by inorganic processes. The excess surface free energy due to this difference and pressure solution due to non-hydrostatic stress at grain-to-grain contacts are the main driving forces for the recrystallization of biogenic calcites to inorganic ones in the sediment (Baker et al., 1980; Baker et al., 1982).

The distribution coefficients for trace elements in inorganically precipitated calcites are often different than those for biogenic calcites; the mechanistic explanation is not fully known. Because of the differences between distribution coefficients for biogenic and inorganic calcite, the dissolution of foraminiferal calcite and its reprecipitation as inorganic calcite would change the original calcite elemental ratios. Of the processes considered here which could affect calcite composition, recrystallization would cause the largest changes.

For some elements, the values of the inorganic distribution coefficients are subjects of debate, especially those appropriate for sedimentary recrystallization reactions. Inorganic distribution coefficients used in this study are summarized in Table 3.3 and discussed below.

Lithium. There are no reported studies of Li distribution

TABLE 3.3 Distribution coefficients for inorganically precipitated calcites

element	distribution coefficient	comments	calcite composition at seawater element/Ca	reference
Sr	5.29×10^{-2}	value for $[\text{Sr}^{2+}] = 87 \times 10^{-6}$; $T = 30^\circ \text{C}$	0.44×10^{-3}	Baker et al. (1982)
Mg	8.1×10^{-4}	Many higher values have been reported (e.g., Mucci and Morse, 1983).	4.3×10^{-3}	Baker et al. (1982)
Na	1.8×10^{-5}	value for seawater Na/Ca; solid chemistry varies approximately as the cube root of the solution ratio in both studies	0.8×10^{-3}	White (1978)
	9.0×10^{-5}		4.0×10^{-3}	Kitano et al. (1975)

coefficients in inorganic calcites.

Strontium. The Sr distribution coefficient varied with temperature and with Sr concentration in a recent study of aragonite recrystallization to calcite (Baker et al., 1982). A fit to all four data points in this study (two temperatures, two Sr concentrations) gave the relationship:

$$D = 0.0591 - 14.6[\text{Sr}] + (9.0 \times 10^{-5} + 0.1[\text{Sr}])(T - 80)$$

where T is in ° C and Sr concentration is in mol/l. The Sr distribution coefficient is dependent on precipitation rate, with higher distribution coefficients at faster precipitation rates (Lorens, 1978). Sedimentary recrystallization reactions probably take place at very slow rates.

Magnesium. The wide range of values suggested for the Mg distribution coefficient in inorganically precipitated calcite (1.2×10^{-2} to 5.7×10^{-2}) were recently summarized (Mucci and Morse, 1983). The studies to date indicate that the inorganic calcite Mg distribution coefficient is higher than the biogenic calcite one.

Comparison of the bulk carbonate chemistry at DSDP site 305 (Shatsky Rise, Pacific, Leg 32) with interstitial water Sr/Ca and Mg/Ca ratios suggested that the Mg distribution coefficient for inorganic calcite precipitation in sedimentary recrystallization reactions is 8.1×10^{-4} (Baker et al., 1982). No conclusions about the variation of this distribution coefficient with temperature were made. This value, fifteen to seventy times lower than those summarized in Mucci and Morse (1983), is used in this study.

Sodium. In two reported studies of Na coprecipitation in calcite, different values were determined for the distribution coefficient (White, 1978; Kitano et al., 1975). At seawater values of Na/Ca, White (1978)

reported that inorganically precipitated calcite had a Na/Ca mole ratio of 8×10^{-4} , corresponding to a distribution coefficient at that solution ratio of 1.8×10^{-5} . Kitano et al. (1975) measured a calcite Na/Ca ratio of 4×10^{-3} , equivalent to a distribution coefficient of 9.0×10^{-5} at seawater Na/Ca. The two distribution coefficients differ by approximately a factor of five. Distribution coefficients were not constant with changes in solution Na/Ca ratios in either study. The relative insensitivity of calcite composition to solution composition seen in the experimental results is approximated here by relating the solid Na/Ca ratio to the cube root of the solution Na/Ca ratio, with different proportionality constants for the two sets of experimental results (Table 3.3). The effects of temperature on the Na distribution coefficient have not been tested.

MODELLING OF DIAGENESIS

SIMPLE MODEL

The simple model of diagenesis compared to the foraminiferal calcite chemistry in the following discussion is based on the difference between biogenic and inorganic calcite distribution coefficients (Baker et al., 1982). Elemental ratios in 100% recrystallized calcite are computed at each depth in the sediment from the present-day interstitial water chemistry and the inorganic calcite distribution coefficients.

The model relates three values of a calcite trace elemental ratio — the original biogenic calcite ratio reflecting seawater chemistry at the time of deposition, the measured ratio reflecting this original ratio plus any diagenetic effects, and the recrystallized inorganic calcite ratio reflecting 100% equilibrium with the present day interstitial water — to the percentage recrystallization, % R. The equation is:

$$\% R = \frac{(\text{measured} - \text{original})}{(\text{equilibrium} - \text{original})} \times 100$$

The assumptions inherent in this calculation are that: (1) the interstitial water presently in contact with a given sediment layer represents the solution with which the reprecipitated calcite is in equilibrium and (2) the inorganic reprecipitated calcite does not redissolve.

The Sr isotopic composition of the solids and interstitial waters can be compared to the seawater Sr isotopic composition through time. If the calcite has completely recrystallized, its isotopic composition will be equal to that of the interstitial water at the time of recrystallization. For calcite ratios intermediate between those of the contemporaneous seawater curve and of the interstitial water, the percentage recrystallization can thus be calculated in a fashion similar to the elemental ratio approach (Elderfield et al., 1982). However, this analysis requires assumptions about the seawater Sr isotopic curve, for which published versions differ in some age ranges (compare Dasch and Biscaye, 1971 and Burke et al., 1982; Figure 4.5, Chapter 4).

INTERSTITIAL WATER COMPOSITIONS

Interstitial water compositions for the five sites studied and inorganic calcite compositions calculated from the simple model of diagenesis are listed in Appendix 3.2 (Tables 3.10 - 3.14).

Li in interstitial water was not typically analyzed in early DSDP legs. Of the sites studied, Li data was available only for Site 526 (Leg 74). Sealed, acidified interstitial water samples from Sites 366 and 366A (Leg 41) and Sites 369 and 369A (Leg 41) were furnished by J. M. Gieskes.

No samples were available from Site 289 (Leg 30) or Site 305 (Leg 32). Li was analyzed on diluted aliquots of the archived interstitial water samples by GFAAS. Samples were analyzed by one-point standard additions, with ascorbic acid added to give 1% by weight in the final solutions. Duplicate analyses agreed within 10%. An IAPSO standard analyzed as a sample had a calculated concentration of 28.3 $\mu\text{mol/l}$. Li/Ca ratios for Sites 366 and 366A and Sites 369 and 369A were calculated from the corrected Li analyses on the archived samples and the original reported Ca concentrations.

FORAMINIFERAL CHEMISTRY AND DIAGENESIS

Li/Ca, Sr/Ca, Mg/Ca, and Na/Ca ratios in foraminiferal calcite are plotted for the five sites in Figures 3.2 - 3.6. The ratios expected in 100% recrystallized calcite were calculated from the inorganic calcite distribution coefficients given in Table 3.3, assuming equilibrium with the measured composition of the interstitial water. These ratios are plotted as dotted lines as a function of age from comparison with foraminiferal calcite ratios.

Neither the correct model of diagenesis nor the extent of diagenesis is independently known. Accordingly, the data plotted in Figures 3.2 - 3.6 are first used to evaluate the diagenetic model. The extent of diagenetic changes in these samples is then discussed.

DISTRIBUTION COEFFICIENTS

The inorganic calcite Sr distribution coefficient for sedimentary recrystallization reactions is the best known. This distribution coefficient and the diagenetic model have been used to successfully model the distribution of Sr in interstitial water and sediments in a number of DSDP sites (Baker et al., 1982). The following discussion proceeds by

FIGURE 3.2 Foraminiferal calcite composition as a function of age for Site 289 (Leg 30), Ontong-Java Plateau, Pacific.

- a. Li/Ca
- b. Sr/Ca
- c. Mg/Ca
- d. Na/Ca

Foraminiferal data for this site are listed in Table 3.5; interstitial water and inorganic calcite compositions are listed in Table 3.10. Interstitial water Li data were not available for this site.

NOTES FOR FIGURES 3.2 - 3.6, a - d

Foraminiferal calcite mean ratios are plotted as a function of sample age. The smaller symbols represent a single analysis; all other samples, represented by larger symbols, were run at least in duplicate.

a. Li/Ca

Dashed line is inorganic calcite Li/Ca calculated from interstitial water composition and Li distribution coefficient, 7×10^{-4} (Table 3.4). Interstitial water Li data were not available for Sites 289 (Leg 30) and 305 (Leg 32). No inorganic calcite Li/Ca line is plotted for these sites.

b. Sr/Ca

Dashed line is inorganic calcite Sr/Ca calculated from interstitial water composition and Sr distribution coefficient as given in Table 3.3 (Baker et al., 1982).

c. Mg/Ca

Dashed line is inorganic calcite Mg/Ca calculated from interstitial water composition and Mg distribution coefficient, 8.1×10^{-4} , given in Table 3.3 (Baker et al., 1982).

d. Na/Ca

Line (1) is inorganic calcite Na/Ca calculated from distribution coefficient based on data in White (1978) (Table 3.3):

$$(\text{Na/Ca})_{\text{calcite}} = (0.23 \times 10^{-3}) \times [(\text{Na/Ca})_{\text{solution}}]^{1/3}$$

Line (2) is inorganic calcite Na/Ca calculated from distribution coefficient based on data in Kitano et al. (1978) (Table 3.3):

$$(\text{Na/Ca})_{\text{calcite}} = (1.13 \times 10^{-3}) \times [(\text{Na/Ca})_{\text{solution}}]^{1/3}$$

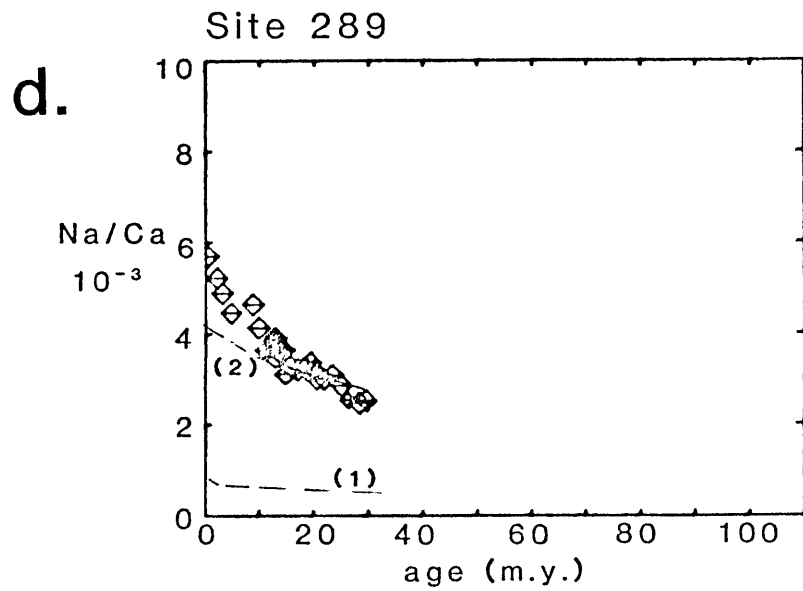
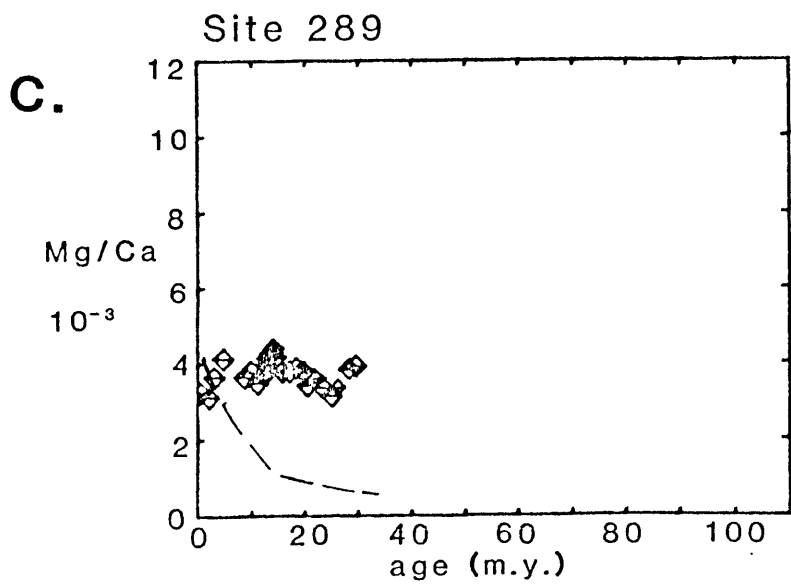
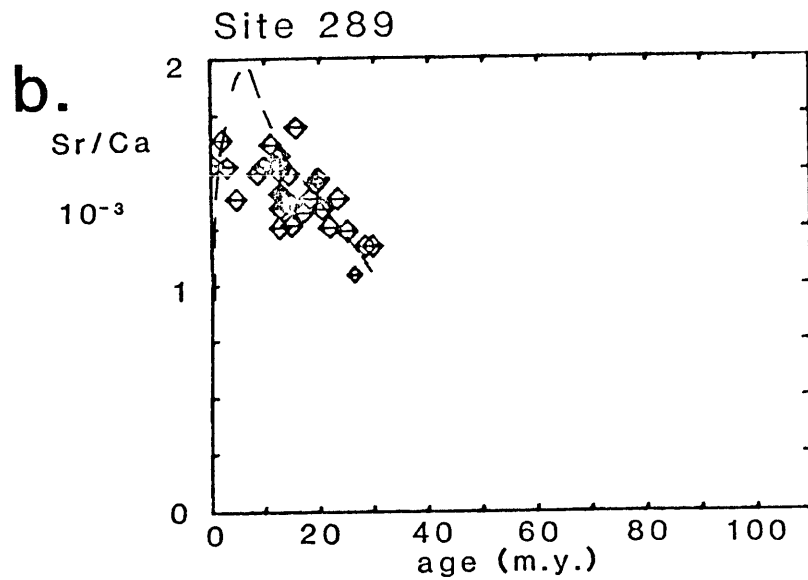
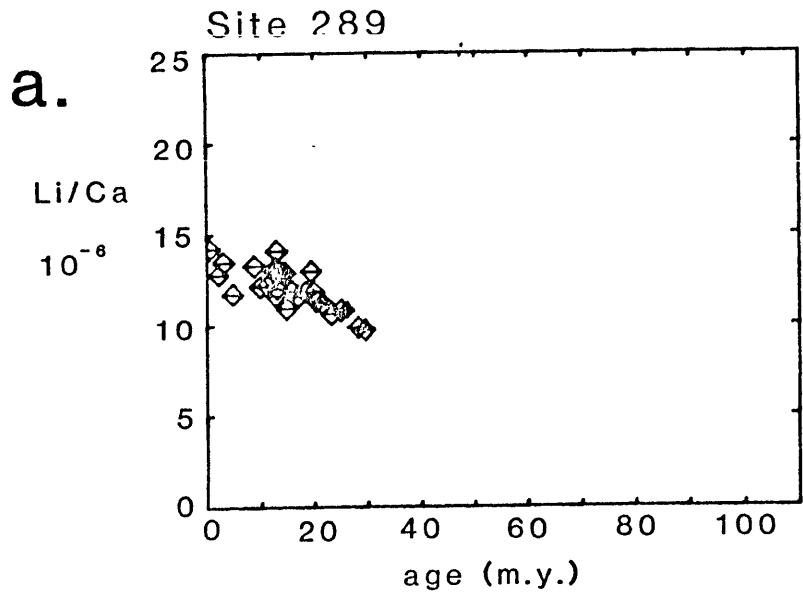


FIGURE 3.3 Foraminiferal calcite composition as a function of age for Site 305 (Leg 32), Shatsky Rise, Pacific.

- a. Li/Ca
- b. Sr/Ca
- c. Mg/Ca
- d. Na/Ca

Foraminiferal data for this site are listed in Table 3.6; interstitial water and inorganic calcite compositions are listed in Table 3.11. Interstitial water Li data were not available for this site.

See explanatory notes in caption of Figure 3.2.

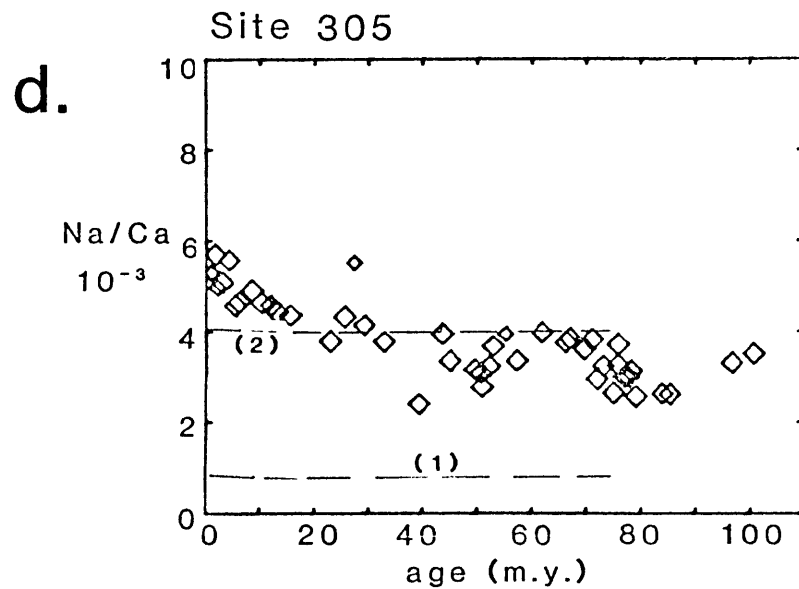
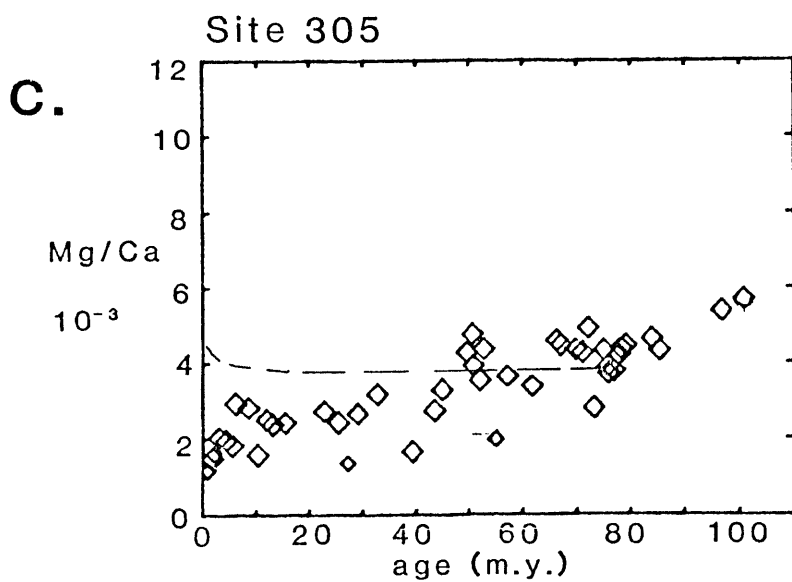
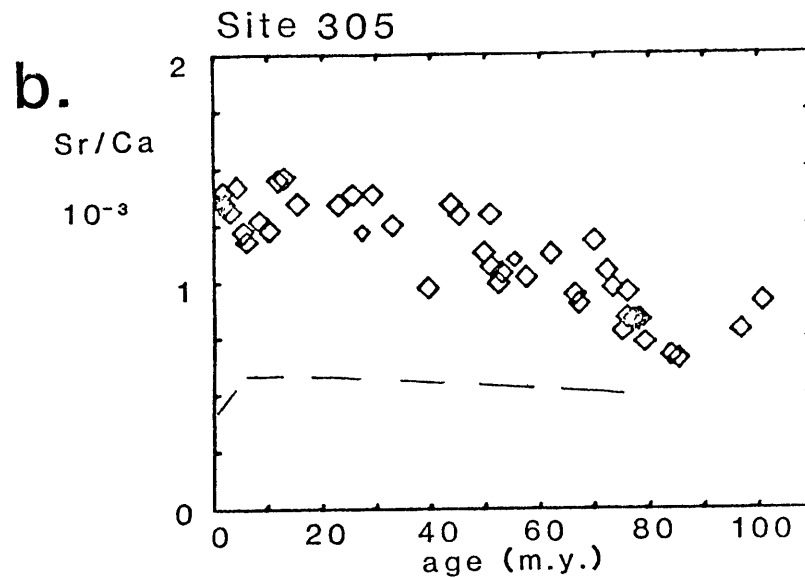
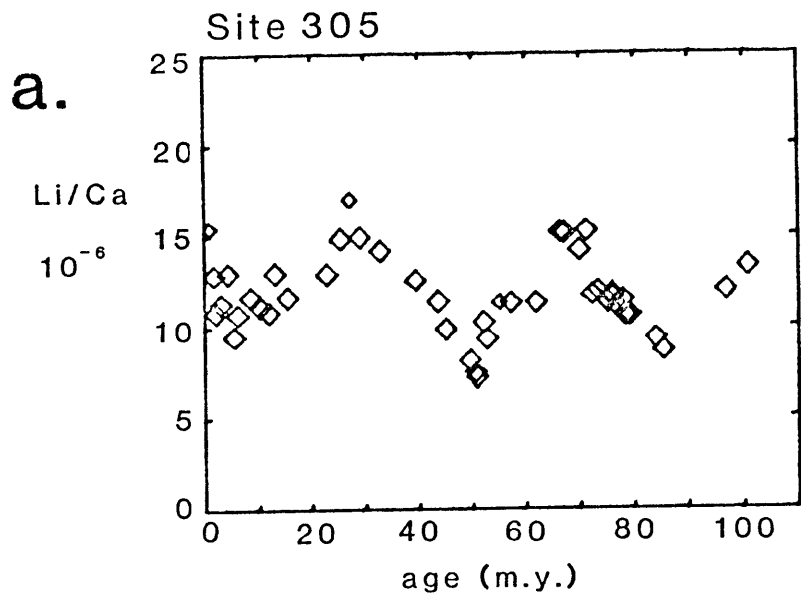


FIGURE 3.4 Foraminiferal calcite composition as a function of age for Site 366 (Leg 41), Sierra Leone Rise, Atlantic.

- a. Li/Ca
- b. Sr/Ca
- c. Mg/Ca
- d. Na/Ca

Foraminiferal data for this site are listed in Table 3.7; interstitial water and inorganic calcite compositions are listed in Table 3.12. The Li distribution coefficient used in calculating the inorganic calcite Li/Ca was determined from the 45 m.y. foraminiferal calcite sample at this site (Table 3.4).

See explanatory notes in caption of Figure 3.2.

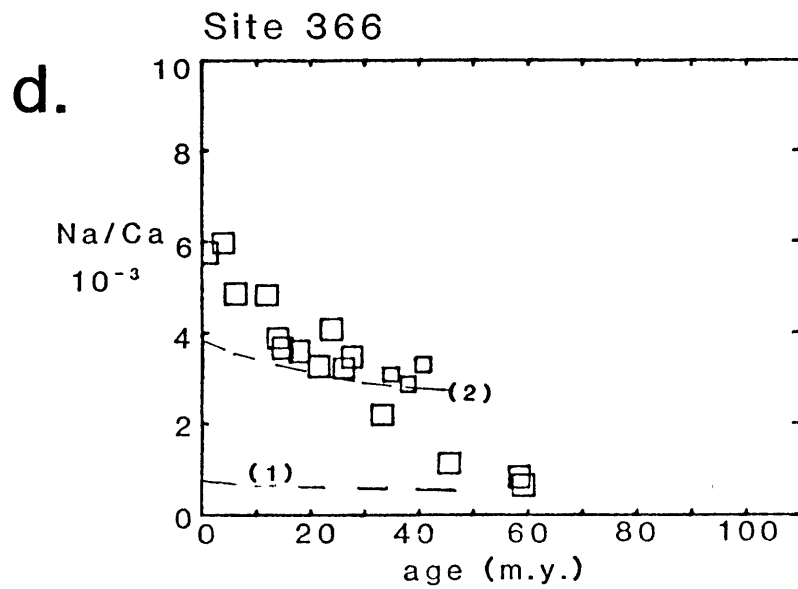
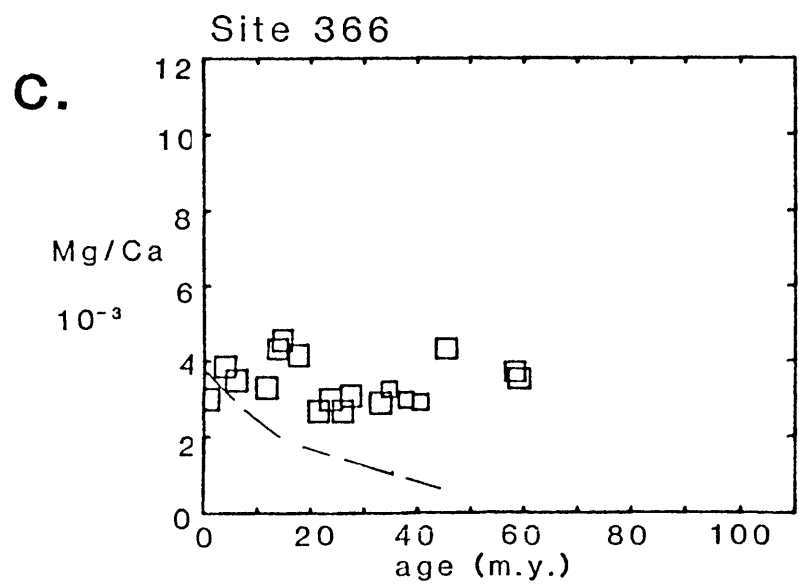
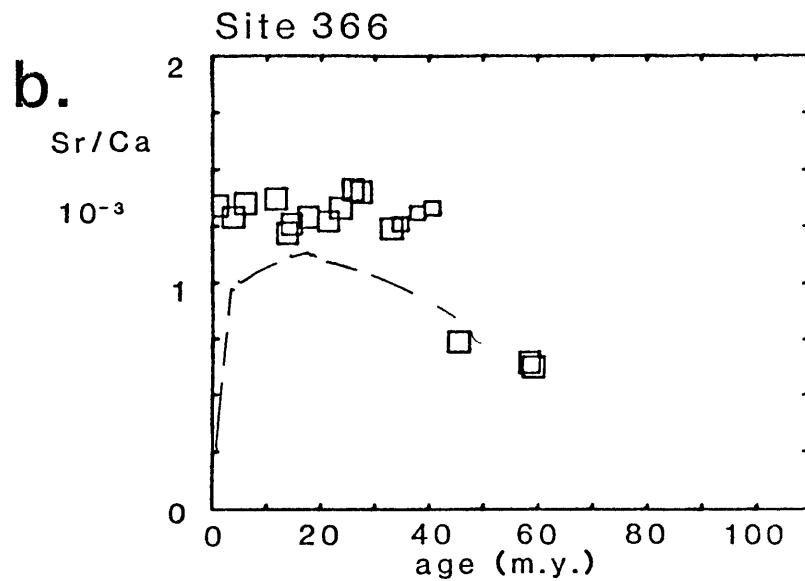
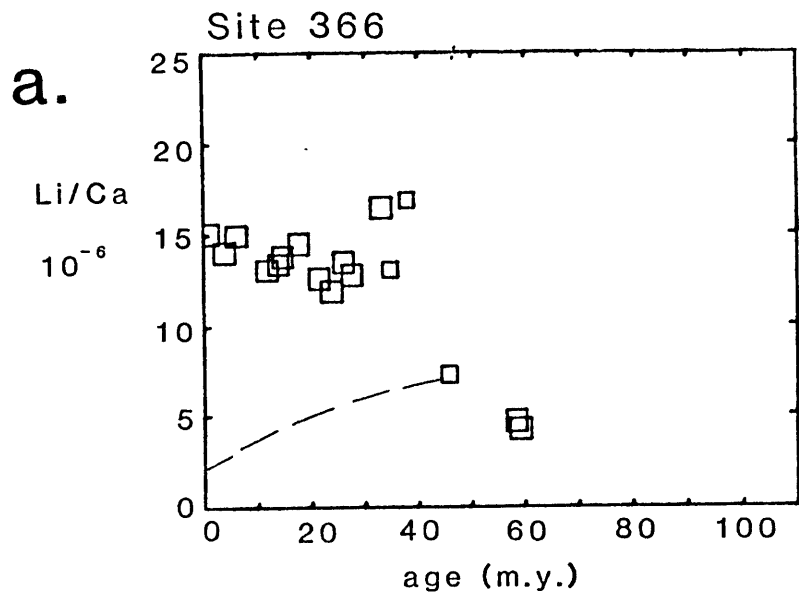


FIGURE 3.5 Foraminiferal calcite composition as a function of age for Site 369 (Leg 41), Spanish Sahara continental slope, Atlantic.

- a. Li/Ca
- b. Sr/Ca
- c. Mg/Ca
- d. Na/Ca

Foraminiferal data for this site are listed in Table 3.8; interstitial water and inorganic calcite compositions are listed in Table 3.13.

See explanatory notes in caption of Figure 3.2.

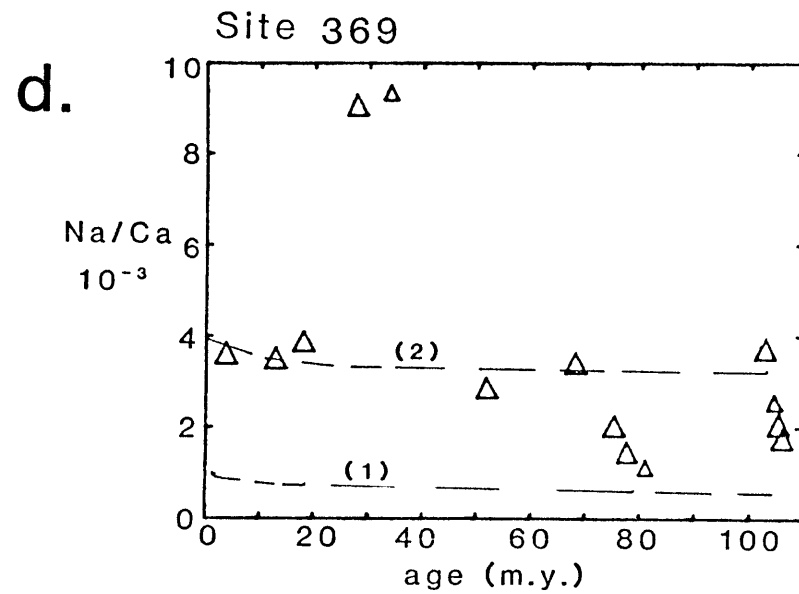
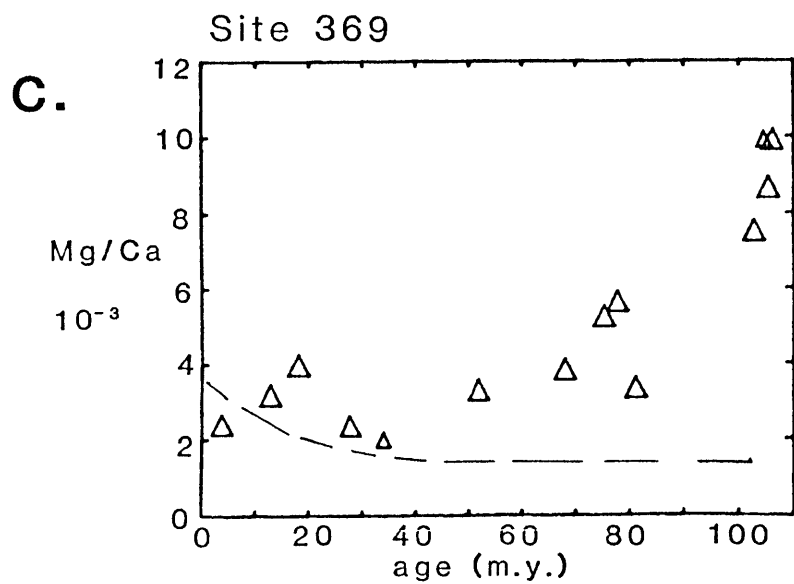
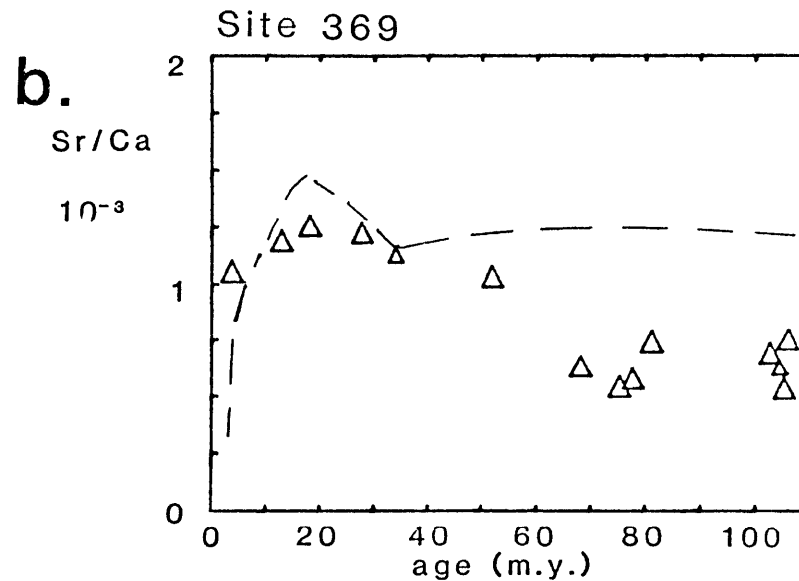
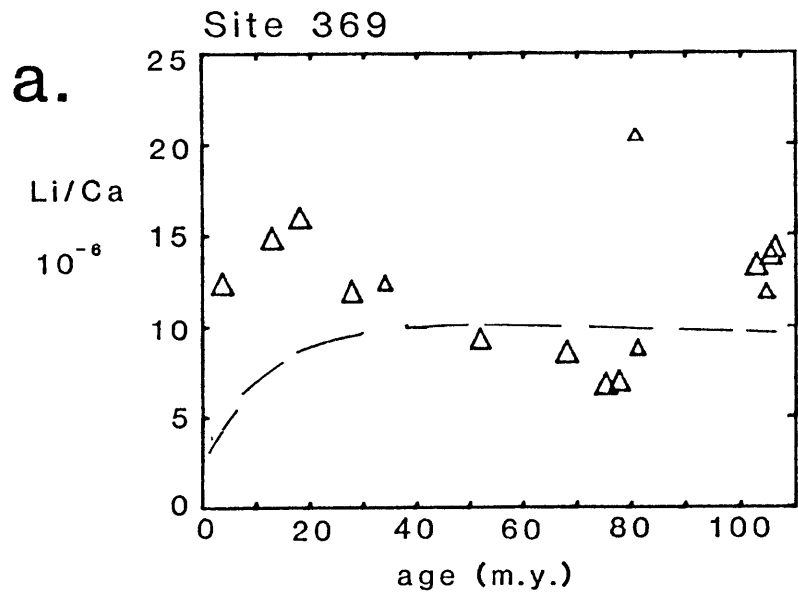
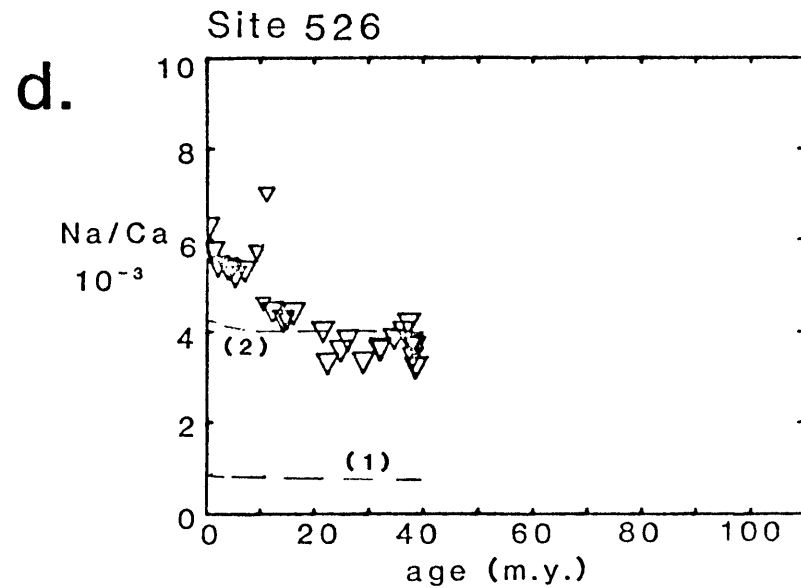
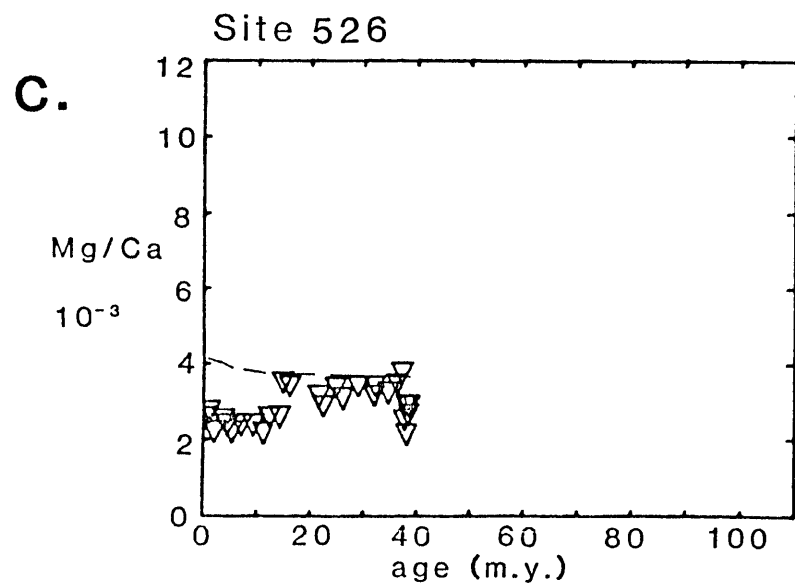
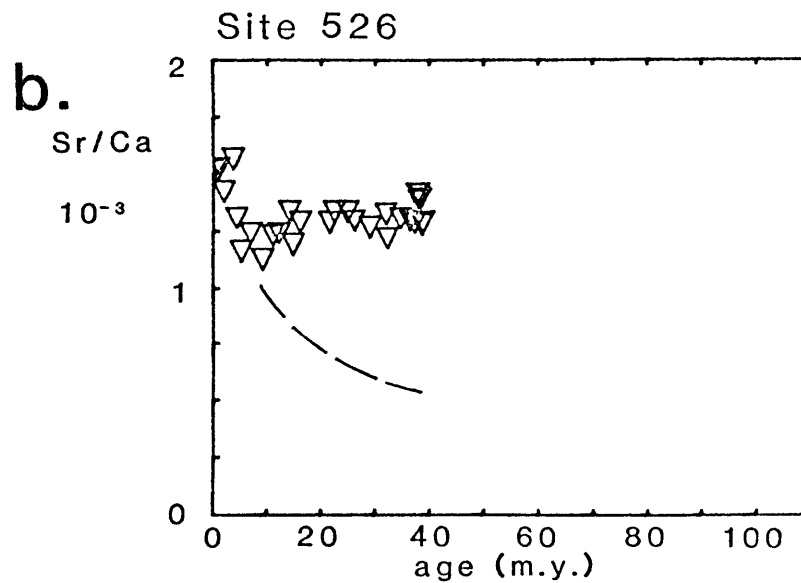
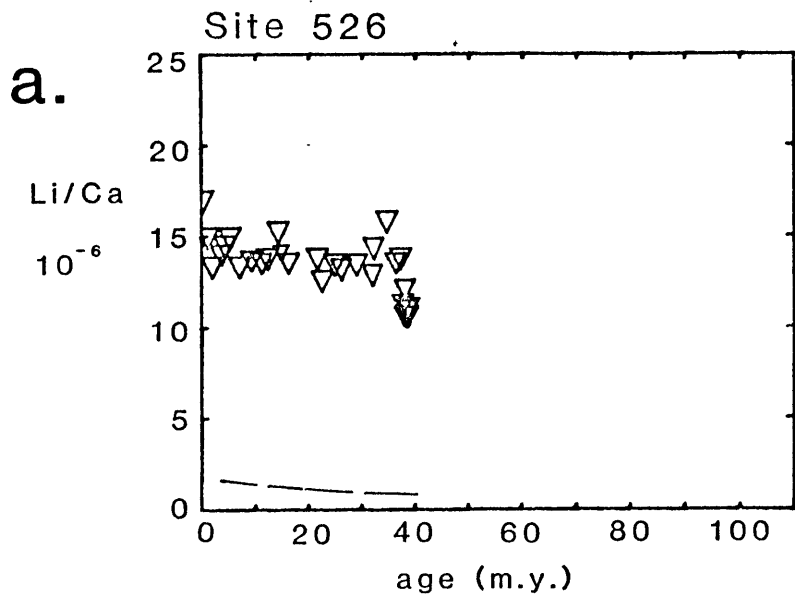


FIGURE 3.6 Foraminiferal calcite composition as a function of age for Site 526 (Leg 74), Walvis Ridge, Atlantic.

- a. Li/Ca
- b. Sr/Ca
- c. Mg/Ca
- d. Na/Ca

Foraminiferal data for this site are listed in Table 3.9; interstitial water and inorganic calcite compositions are listed in Table 3.14.

See explanatory notes in caption of Figure 3.2.



assuming that the prediction of the Sr/Ca inorganic calcite composition is accurate and then evaluates the agreement or discord of the other indicators with Sr/Ca.

Magnesium. For four of the five sites studied (Sites 289, 305, 366, and 369), the calculated inorganic calcite Mg/Ca ratio is \leq the foraminiferal ratio for most ages.

In Site 289, the foraminiferal Sr/Ca ratios at ages greater than ~18 m.y. are equal to the calculated inorganic ratios (Figure 3.2.b). In a previous study of Sr/Ca and Sr isotopes in interstitial water and foraminiferal calcite at Site 289, Elderfield et al. (1982) concluded that all foraminiferal calcite from ages greater than ~18 m.y. were in equilibrium with the interstitial water. Over the same age range where Sr/Ca in foraminiferal and inorganic calcite coincide at Site 289, the inorganic Mg/Ca ratio is decreasing while the foraminiferal calcite ratio remains approximately constant (Figure 3.2.c). If calcite older than 18 m.y. at Site 289 is recrystallized, the Mg distribution coefficient must be a factor of three to five higher than that calculated by Baker et al. (1982). The conclusions about diagenesis in Site 289 are discussed further in a later section.

At Site 305, foraminiferal Sr/Ca ratios generally decrease with increasing age (Figure 3.3.b). The interstitial water elemental ratios at Site 305 are approximately constant with depth; therefore, so is the calculated inorganic calcite composition. The foraminiferal Sr/Ca ratios approach, but do not coincide with, inorganic calcite Sr/Ca ratios (Figure 3.3.b). Mg/Ca foraminiferal calcite ratios at Site 305 increase steadily with increasing age, coinciding with the assumed equilibrium Mg/Ca ratios around 50 m.y. and then exceeding them (Figure 3.3.c). To explain this

trend in foraminiferal Mg/Ca ratios, the inorganic Mg distribution coefficient must be at least 1.5 times higher than that suggested by Baker et al. (1982), who based their value on bulk carbonate chemical data at Site 305.

Further evidence for this conclusion is seen in the foraminiferal calcite chemistry at Site 366 (Figures 3.4, a - d). Sr/Ca and Mg/Ca foraminiferal calcite ratios are approximately constant with increasing age at Site 366, with markedly lower Sr/Ca (and Li/Ca) ratios in the three oldest samples analyzed (Figures 3.4, a, b). Sr/Ca ratios in the three oldest samples (45 - 59 m.y.) coincide with the inorganic calcite ratio. Inorganic calcite Mg/Ca ratios are lower than all the foraminiferal ratios except in the very youngest samples (Figure 3.4.c) and the Mg/Ca ratios in the 45 - 59 m.y. samples with the low Sr/Ca and Li/Ca ratios are, if anything, slightly higher than the Mg/Ca ratios in the younger samples. Using the Mg distribution coefficient from Baker et al. (1982), Sr/Ca and Mg/Ca do not agree as indicators of the percentage recrystallization at Site 366, Site 289, or Site 366. The Mg distribution coefficient indicated by the chemistry at Site 366 must be higher than that determined by Baker et al. (1982) by a factor of eight.

Further support for a higher Mg distribution coefficient is found in the foraminiferal calcite composition at Site 369 (Figures 3.5, a - d). Interstitial water composition at this site is strongly influenced by an underlying brine intrusion (Gieskes, 1981). The interstitial water profiles have almost certainly changed significantly through time at this low-carbonate site; this unknown temporal variation complicates the application of the diagenetic model at this site. In any case, Mg/Ca foraminiferal calcite ratios increase by a factor of five over 110 m.y.

(Figure 3.5.c). Inorganic Mg/Ca ratios based on the distribution coefficient of Baker et al. (1982) decrease with increasing age and are much lower than foraminiferal calcite ratios for all samples older than 40 m.y. The Mg distribution coefficient necessary to explain the observed increase in foraminiferal calcite ratios at Site 369 is a minimum of a factor of seven times higher than the one recently suggested to be applicable to sedimentary recrystallization reactions (Baker et al., 1982).

Foraminiferal calcite Sr/Ca ratios at Site 526 are approximately constant with increasing age and significantly greater than the decreasing inorganic calcite Sr/Ca ratios (Figure 3.6.b). Bulk carbonate analyses of Sr/Ca and Mg/Ca at this site are substantially similar to these foraminiferal analyses (Gieskes et al., preprint) except in the deepest bulk carbonate sample from a chalk layer at 225 m (38 m.y.). The chalk layer sample had a Sr/Ca ratio of 0.34×10^{-3} , lower than those in the younger samples and in good agreement with the calculated equilibrium value of 0.36×10^{-3} . The Mg/Ca ratio of that sample was 12.9×10^{-3} , a factor of 3.5 times the equilibrium ratio calculated from the distribution coefficient of Baker et al. (1982).

The evidence from the comparison of Sr/Ca and Mg/Ca ratios as indicators of recrystallization for the foraminiferal calcite at four sites and for the bulk carbonate at a fifth suggests that the Mg distribution coefficient for sedimentary recrystallization reactions must be a minimum of 1.5 times the value determined by Baker et al. (1982) and up to eight times as large.

Other elements. By comparing Sr/Ca ratios in calcite and interstitial water (along with the Sr distribution coefficient), several samples are observed to be in ~100% inorganic equilibrium: foraminiferal

samples older than ~18 m.y. from Site 289 (Figure 3.2; Elderfield et al., 1982); foraminiferal samples from 45 - 59 m.y. from Site 366 (Figure 3.4); and the bulk carbonate sample from the chalk layer at 38 m.y. from Site 526 (Gieskes et al., 1982). If these samples are in equilibrium, their chemistry and the interstitial water compositions can be used to calculate inorganic distribution coefficients for sedimentary recrystallization reactions.

The results of these calculations are listed in Table 3.4. The results from Site 366 indicate that the inorganic Li distribution coefficient is $\sim 7 \times 10^{-4}$, approximately an order of magnitude lower than the foraminiferal calcite one (5×10^{-3} ; Chapter 2). As discussed, the calculated Mg distribution coefficients are higher than the one suggested by Baker et al. (1982) of 8.1×10^{-4} . Calculation of the Na distribution coefficient is complicated by the nonlinear relationship between solid and solution Na/Ca ratios (Kitano et al., 1975; White, 1978). Assuming a cube-root dependence of solid on solution ratios, the Na distribution coefficients calculated from the samples at Sites 289 and 366 listed in Table 3.4 are equivalent to values at seawater Na/Ca intermediate between those found in the two experimental studies (Table 3.5). The nature of the incorporation of Na and the mechanisms for its behavior in recrystallization may be different than for Li, Sr, and Mg which show linear relationships between solid and solution chemistries for foraminiferal and inorganic calcites.

DIAGENETIC CHANGES AT THE SITES STUDIED

Site 289. Based on a comparison of Sr/Ca ratios and Sr isotopes in foraminiferal calcite and interstitial water at Site 289, it was concluded

TABLE 3.4 Inorganic calcite distribution coefficients from "recrystallized" calcite from Sites 289, 366, and 526 ^a

elemental ratio	location	foraminiferal calcite	interstitial water	distribution coefficient ^b
Mg/Ca	Site 289	3.85×10^{-3}	0.82	4.7×10^{-3}
	Site 366	4.32×10^{-3}	0.65	6.7×10^{-3}
	Site 526	12.9×10^{-3}	4.54	2.8×10^{-3}
Na/Ca	Site 289	2.45×10^{-3}	15.7	16×10^{-5} ^c
	Site 366	1.11×10^{-3}	12.2	9×10^{-5} ^c
Li/Ca	Site 366	7.3×10^{-6} ^d	9.8×10^{-2} ^e	7×10^{-4}

- Notes: a. The samples used in these calculations are ones whose Sr/Ca ratio was equal to the equilibrium calcite ratio based on the interstitial water ratio. The samples used are: Site 289, foraminiferal sample 86/6/25-27, 815.3 m, 28.2 m.y. and interstitial water sample 86/5/144-150, 815.0 m, 28.2 m.y.; Site 366, foraminiferal sample 21/3/80-82, 521.8 m, 45.3 m.y. and interstitial water sample, 20/1/145-150, 510.0 m, 44.8 m.y.; Site 526, bulk carbonate sample and interstitial water sample, A/45/2/143-150 (Gieskes et al., preprint).
- b. Distribution coefficients were calculated as:
- $$D = \frac{(\text{element/Ca})_{\text{calcite}}}{(\text{element/Ca})_{\text{water}}}$$
- c. The relationship between solid and solution Na/Ca ratios is nonlinear. The calculated distribution coefficients are only applicable at the solution ratio at which they were determined. Using the cube-root dependence of solid ratios on solution ratios, these correspond to values intermediate between those of Kitano et al. (1975) and White (1978) at the seawater solution Na/Ca ratio of 44.7.
- d. This sample had a replicate with a high Li/Ca ratio of 38.6×10^{-3} . However, the two oldest samples at this site had low Li/Ca ratios, so the lower of the two replicates is used in this calculation.
- e. Li was not analyzed on this sample, so this ratio is determined from the two adjacent younger interstitial water samples.

that foraminiferal shells from depths greater than 550 m (~18 m.y.) were in equilibrium with the interstitial water chemistry and therefore 100% recrystallized (Elderfield et al., 1982). There are two weaknesses in this argument. The first concerns the original biogenic Sr/Ca ratio. Sr/Ca ratios in the foraminiferal calcite at Site 289 are similar to Sr/Ca ratios of other samples of the same age from different locations (Figure 4.2, Chapter 4; Graham et al., 1982). Since the original Sr/Ca ratio is close to the inorganic recrystallization one, Sr/Ca is an ambiguous and insensitive indicator of percentage recrystallization in this site.

The second objection arises from the comparison of the Sr isotopic compositions of foraminiferal calcite and interstitial waters with the contemporaneous seawater Sr isotopic curve (Elderfield et al., 1982 using data from Dasch and Biscaye, 1971). The Sr isotopic composition of foraminiferal calcite at Site 289 followed the Dasch and Biscaye (1971) contemporaneous seawater curve in the shallowest 550 m, then jumped to an isotopically lighter composition equivalent to that of the interstitial water (Elderfield et al., 1982; their figure 6). Therefore, foraminiferal calcite below 550 m was considered to be substantially recrystallized. If this comparison is made to a different seawater Sr isotopic curve (Burke et al., 1982; summary in Brass, 1976), the Sr isotopic composition of the foraminiferal calcite looks precisely like the contemporaneous seawater curve at all depths. The interstitial water profile still requires a source of isotopically light Sr constituting about 15% of the total Sr concentration in the upper 550 m (Elderfield et al., 1982). The observation that the Sr isotopic compositions of the interstitial water and foraminiferal calcite in the upper 550 m are different and the agreement of the Sr isotopic ratios of the foraminiferal calcite with either

contemporaneous seawater curve implies that foraminiferal shells from 0 - 550 m (0 - 18 m.y.) are not recrystallized. However, the concordance below this depth of the Sr isotopic ratios of foraminiferal calcite and interstitial water does not require recrystallization; both calcite and water Sr isotopic ratios are in accord with Sr isotopic curves in contemporaneous seawater other than that of Dasch and Biscaye (1971). From the Sr isotopic data, the foraminiferal calcite could as easily be interpreted to be completely unrecrystallized in the older age ranges. The Dasch and Biscaye (1971) curve is isotopically heavier than others for ages older than ~10 m.y. (see summary in Brass, 1976). The foraminiferal samples in those age ranges in that study have low Sr/Ca ratios, and may thus be themselves recrystallized.

Based on the Sr, Mg, and Na inorganic distribution coefficients discussed, the older samples at Site 289 could well be in equilibrium with interstitial water. There is no abrupt change in the Li/Ca foraminiferal ratios in the proposed zone of recrystallization. If samples older than 18 m.y. are 100% recrystallized, interstitial Li concentrations in the depth range 550 m - 815 m would have to be 0.42 - 0.44 mmol/l (based on the inorganic Li distribution coefficient estimated from Site 366 data (Table 3.4) and the Li/Ca ratios of the foraminiferal calcite), an approximately constant value fifteen times higher than the seawater Li concentration.

Site 305. For Site 305, if the oldest samples are 100% recrystallized, the inorganic Li distribution coefficient and the foraminiferal Li/Ca ratios would require constant interstitial Li concentrations of 0.21 mmol/l. This is 7.5 times the seawater concentration. In Site 305, the interstitial water composition was fairly constant (Table 3.11), so there is no obvious reaction source for this

elevated Li seen in the other profiles. The minima seen in the foraminiferal Li/Ca ratios are not easily explainable in terms of diagenetic effects evident in the other elemental profiles.

Sites 366 and 526. For most samples at Sites 366 (Figure 3.4) and 526 (Figure 3.6), Li/Ca, Sr/Ca, and Mg/Ca foraminiferal ratios are not in equilibrium with the interstitial water, suggesting that foraminiferal calcite at these sites is substantially unrecrystallized. For Site 526, the interstitial waters have been analyzed for Sr isotopic ratios (J. M. Gieskes and H. Elderfield, pers. comm.). This conclusion could be verified by measuring the Sr isotopic ratios of the bulk carbonates.

CONCLUSIONS

INORGANIC DISTRIBUTION COEFFICIENTS

The simple model of diagenesis as described has been applied to the foraminiferal calcite and interstitial water compositions at five DSDP sites. From the measured calcite chemistry of the oldest foraminiferal samples at Site 366 (Leg 41), the inorganic Li distribution coefficient is estimated to be $\sim 7 \times 10^{-4}$, approximately an order of magnitude lower than one determined for foraminiferal calcite of 5×10^{-3} (Chapter 2). Comparison of the foraminiferal calcite (and bulk carbonate) and interstitial water compositions suggested that the Mg distribution coefficient for sedimentary recrystallization reactions is as much as a factor of eight higher (and at least a factor of 1.5 higher) than the value suggested from a comparison of bulk carbonate Sr/Ca and Mg/Ca ratios at Site 305 (Baker et al., 1982). This value is at least a factor of two (and up to a factor of nine) lower than any of the Mg distribution coefficients determined in laboratory studies (summary in Mucci and Morse, 1983). The

Na/Ca distribution coefficient appears to be intermediate between the values determined in two experimental studies (Kitano et al., 1975; White, 1978). The nonlinear relationship of solid and solution chemistry for Na/Ca ratios makes this analysis less certain for Na than for the other elements.

DIAGENETIC MODELLING

Quantification of diagenetic changes in foraminiferal calcite chemistry is hampered by the lack of knowledge about distribution coefficients applicable to sedimentary recrystallization reactions. The variation of these distribution coefficients with temperature and the temperature profiles themselves in the sediments need to be better known. The most promising indicator of sedimentary recrystallization reactions is the Sr isotopic compositions of foraminiferal calcite and interstitial water. However, the interpretations of Sr isotopic data depend directly on the presumed Sr isotopic history of seawater. Different choices of contemporaneous seawater curves can lead to quite different conclusions, as was discussed for Site 289. Further sophistication in modelling the time course of these diagenetic changes will be required to make the various indicators (elemental ratios, Sr and O isotopes) agree with each other within a site and to have the models successfully applicable to more than one site. There are certainly diagenetic changes which affect the chemical composition of foraminiferal calcite and bulk calcium carbonate in oceanic sediments. An exact deconvolution of these processes is not yet possible.

In the construction and application of diagenetic models, the open-system nature of the interstitial water-sediment system must be explicitly included. For example, Killingley (1983) modelled the effect of

recrystallization on foraminiferal calcite oxygen isotopic records. He concluded that the oxygen isotopic trend observed in the Tertiary of increasing $^{18}\text{O}/^{16}\text{O}$ ratios with decreasing sample age could be due to extensive recrystallization of carbonate (80% at 60 m.y.), not to oceanic paleotemperature changes. This model treated the sediments and their associated interstitial water as a closed system. The $\delta^{18}\text{O}$ changes in the interstitial water in a "typical" sediment column from carbonate recrystallization were calculated to be $< -0.1 \text{ ‰}/100 \text{ m}$, with $\delta^{18}\text{O}$ becoming more negative from 0 - 30 m.y. and more positive from 30 - 60 m.y. However, $\delta^{18}\text{O}$ in interstitial water usually becomes consistently more negative with depth. The average $\delta^{18}\text{O}$ gradient in thirty-six DSDP sites was $-0.72 \pm 0.38 \text{ ‰}/100 \text{ m}$ (Lawrence and Gieskes, 1981). These isotopic decreases correlated with Ca increases. Both gradients are due to reactions primarily with underlying basalts and secondarily with volcanic matter in the sediments (Lawrence and Gieskes, 1981).

The differences between $\delta^{18}\text{O}$ values for 60 m.y.b.p. and present-day produced by recrystallization in Killingley's model for planktonic and benthic foraminifera were -0.5 ‰ and -3.5 ‰ , respectively. To obtain these differences by the mixture of calcite recrystallized in equilibrium with the interstitial water of a typical sediment column and calcite with initial $\delta^{18}\text{O}$ of -1 ‰ (planktonic foraminifera) and $+3.5 \text{ ‰}$ (benthic foraminifera), the percentage recrystallized calcite required is only 9% for the planktonic foraminifera and 36% for the benthic foraminifera. (The typical sediment had the following properties: sedimentation rate, 10 m/m.y.; $\delta^{18}\text{O}$ gradient, $-0.5 \text{ ‰}/100 \text{ m}$; and temperature gradient, $3.5^\circ \text{ C}/100 \text{ m}$ with a 2° C temperature at the sediment-water interface.) The open system model requires that the benthic foraminifera recrystallized to

a greater extent than the planktonic foraminifera if both isotopic signals are due primarily to recrystallization, not oceanic paleotemperature, as was assumed by Killingley. Killingley's model assumed that the recrystallization rates were the same for planktonic and benthic foraminiferal shells.

Although caution should be exercised in interpreting oxygen isotopic records from older samples, Killingley's model was not representative of a typical sedimentary system. In fact, the problem may be potentially greater than was indicated by the closed system calculation. To produce a negative 1‰ shift (equivalent to $\sim 4^\circ\text{C}$ paleotemperature signal) in an oxygen isotopic ratio of a benthic foraminifera by the mixture of recrystallized calcite in equilibrium with the interstitial water and temperature profiles of the typical sediment modelled above, only 10% recrystallized calcite at 60 m.y. is required to change an initial isotopic ratio of $+3.5\text{‰}$.

The similarity of oxygen isotopic records from different locations is encouraging evidence that the measured signal does mainly represent oceanic paleotemperature differences. The measurement of oxygen isotopic records in different sites with different interstitial water profiles and thermal gradients can elucidate which part of the records represent oceanic paleochemistry and paleotemperature. Analyses of trace elemental ratios and Sr isotopic ratios in calcite and interstitial water in the same samples could further clarify this situation.

APPENDIX 3.1 Foraminiferal calcite composition — DSDP samples

Foraminiferal calcite trace elemental ratios for samples from the five sites studied are listed in Tables 3.6 - 3.10. Mixed planktonic foraminiferal samples were analyzed. Each sample is identified in the following tables by a series of numbers: (optional letter designation for additional holes at a site) core/section/interval; CC in place of section/interval indicates a core catcher sample. Depth below the seafloor for each sample was figured to the top of the 2 cm sample interval following standard DSDP assumptions in cases of incomplete recovery. Core catcher samples were assumed to represent the bottom of the cored interval. Depths were figured according to the formula:

$$\begin{array}{l} \text{depth in} \quad \quad \text{depth to} \quad \quad \quad \text{top of} \\ \text{hole below} \quad = \text{top of} \quad + 1.5 \text{ m}(\text{section \#} - 1) + \text{interval in} \\ \text{seafloor (m)} \quad \text{core (m)} \quad \quad \quad \text{section (m)} \end{array}$$

Because of incomplete recoveries, the uncertainty on an assigned depth can be as much as several meters. The resulting age uncertainty depends on the accumulation rate.

Mean Li/Ca, Sr/Ca, Mg/Ca, and Na/Ca ratios, standard deviations, and number of values averaged are listed in the tables. The format used is:

mean
standard deviation
number of values

Reported values have been corrected for variability between analyses at different times (see Appendix 1 for a discussion of analytical precision within and between data sets). Where replicate samples were analyzed in separate analytical runs, individual values were consistency-standard corrected before means were calculated.

Trace elemental ratios marked by parentheses were not included in data plots; the reason for questioning the value is given in a footnote. In some cases, sample replicates disagreed significantly for one or more elemental ratios of a sample with no obvious reason to disregard one of the values. In such cases, both values are listed and plotted.

TABLE 3.5 Foraminiferal calcite composition at Site 289 (Leg 30)

sample	depth (m)	age (m.y.)	Li/Ca (10^{-6})	Sr/Ca (10^{-3})	Mg/Ca (10^{-3})	Na/Ca (10^{-3})
1/6/ 40- 42	7.9	0.6	14.3 1.1 2	1.53 0.01 2	3.21 0.05 2	5.72 0.20 2
5/4/ 48- 50	43.0	2.1	12.8 0.0 2	1.64 0.04 2	3.09 0.16 2	5.22 0.06 2
10/5/ 40- 42	91.9	3.2	13.5 0.8 2	1.52 0.03 2	3.61 0.05 2	4.89 0.32 2
16/6/ 40- 42	150.4	4.7	11.7 0.4 2	1.38 0.10 2	4.12 0.65 2	4.45 0.08 2
22/4/ 40- 42	204.4	8.7	13.3 0.2 2	1.49 0.06 2	3.62 0.12 2	4.64 0.10 2
28/6/ 40- 42	264.4	9.8	12.1 0.3 2	1.52 0.16 2	3.78 0.25 2	4.12 0.12 2
34/6/ 40- 42	321.4	11.0	12.2 0.2 2	1.62 0.13 2	3.46 0.26 2	3.64 0.03 2
39/3/ 76- 78	364.8	12.3	13.0 0.1 2	1.56 0.07 2	3.68 0.09 2	3.80 0.01 2
41/2/ 16- 18	381.7	12.6	13.0 0.8 2	1.50 0.00 2	3.95 0.04 2	3.83 0.22 2
43/6/ 16- 18	406.7	12.7	13.2 0.5 2	1.57 0.01 2	3.74 0.10 2	3.77 0.02 2
44/6/ 16- 18	416.2	12.8	11.6 0.6 2	1.25 0.06 2	4.13 0.96 2	3.83 0.73 2
46/2/ 16- 18	429.2	12.8	12.0 0.5 2	1.34 0.06 2	3.80 0.22 2	3.48 0.01 2
47/6/ 16- 18	444.7	12.9	14.1 1.9 2	1.40 0.01 2	3.92 0.15 2	3.90 0.32 2
49/6/ 16- 18	463.7	13.3	12.9 0.4 2	1.39 0.08 2	4.23 0.13 2	3.69 0.15 2
51/2/ 52- 54	477.0	13.7	12.9 0.2 2	1.38 0.02 2	4.26 0.28 2	3.56 0.14 2

3.5 continued

sample	depth (m)	age (m.y.)	Li/Ca (10^{-6})	Sr/Ca (10^{-3})	Mg/Ca (10^{-3})	Na/Ca (10^{-3})
52/1/103-105	485.5	14.0	12.0 0.1 2	1.36 0.08 2	4.38 0.04 2	3.58 0.06 2
54/2/ 98-100	506.0	14.4	12.9 0.6 2	1.49 0.01 2	4.14 0.12 2	3.63 0.07 2
55/3/ 81- 83	517.8	14.8	10.9 1.6 2	1.26 0.13 2	3.97 0.52 2	3.10 0.39 2
56/4/ 27- 29	527.3	15.8	11.9 0.7 2	1.70 0.05 2	3.77 0.25 2	3.28 0.10 2
57/6/ 12- 14	539.6	17.0	11.6 0.4 2	1.32 0.16 2	3.76 0.57 2	3.20 0.18 2
59/2/ 28- 30	552.8	18.3	11.8 1.1 2	1.38 0.06 2	3.88 0.03 2	3.26 0.08 2
60/6/ 12- 14	568.1	19.3	13.0 0.3 2	1.45 0.08 2	3.79 0.18 2	3.35 0.24 2
62/2/ 12- 14	581.1	19.7	11.8 0.2 2	1.47 0.06 2	3.76 0.06 2	3.19 0.08 2
64/3/ 12- 14	601.6	20.5	11.3 0.2 2	1.33 0.02 2	3.40 0.50 2	2.98 0.05 2
67/6/ 12- 14	634.6	21.8	11.1 0.2 2	1.26 0.01 2	3.57 0.04 2	3.00 0.14 2
71/5/ 12- 14	671.1	23.3	10.6 0.5 2	1.38 0.00 2	3.36 0.00 2	3.08 0.14 2
75/4/ 25- 27	707.8	24.9	10.8 0.3 2	1.24 0.00 2	3.14 0.04 2	2.84 0.12 2
78/2/ 25- 27	733.3	26.0	10.8 0.0 1	1.05 0.00 1	3.36 0.00 1	2.52 0.00 1
86/6/ 25- 27	815.3	28.2	9.8 0.4 2	1.17 0.01 2	3.85 0.28 2	2.45 0.03 2
91/5/ 25- 27	861.3	29.4	9.7 0.0 2	1.17 0.04 2	3.92 0.21 2	2.50 0.12 2

TABLE 3.6 Foraminiferal calcite composition at Site 305 (Leg 32)

sample	depth (m)	age (n.y.)	Li/Ca (10^{-6})	Sr/Ca (10^{-3})	Mg/Ca (10^{-3})	Na/Ca (10^{-3})
1/6/ 25- 27	6.6	1.0	15.5 0.0 1	1.36 0.00 1	1.15 0.00 1	5.31 0.00 1
2/3/ 25- 27	11.3	1.7	12.9 0.6 3	1.40 0.06 3	1.47 0.10 3	5.72 0.30 3
3/3/ 25- 27	20.3	2.1	10.8 0.1 2	1.35 0.01 2	1.50 0.03 1	4.90 0.10 1
4/3/ 25- 27	29.0	3.0	11.3 1.6 3	1.31 0.02 3	2.01 0.10 3	5.10 0.21 3
5/2/ 25- 27	37.3	4.4	13.0 0.9 2	1.42 0.04 2	1.95 0.03 2	5.50 0.07 2
5/5/ 25- 27	41.0	5.5	9.5 2.6 2	1.22 0.11 2	1.00 0.19 2	4.50 0.52 2
5/5/ 98-100	42.6	6.1	10.7 0.7 2	1.18 0.01 2	2.92 0.09 2	4.66 0.06 2
6/1/100-100	46.1	8.6	11.6 0.2 2	1.27 0.01 2	2.01 0.14 2	4.91 0.00 2
6/3/ 47- 49	48.5	10.3	11.1 0.1 3	1.23 0.04 3	1.57 0.07 3	4.65 0.44 3
6/4/ 68- 70	50.2	11.9	10.8 0.2 3	1.45 0.04 3	2.40 0.20 3	4.57 0.23 3
6/5/ 8- 10	51.1	13.1	13.0 1.1 3	1.46 0.05 3	2.36 0.11 3	4.43 0.15 3
6/5/ 95- 97	51.9	15.4	11.7 0.1 3	1.35 0.05 3	2.41 0.01 3	4.36 0.19 3
6/6/ 25- 27	52.0	22.0	12.9 1.0 4	1.34 0.02 4	2.71 0.20 4	3.79 0.22 4
7/3/ 90- 92	58.4	25.4	14.9 0.1 2	1.39 0.01 2	2.42 0.19 2	4.33 0.32 2
7/6/ 25- 27	62.3	27.1	17.0 0.0 1	1.22 0.00 1	1.35 0.00 1	5.52 0.00 1

3.6 continued

sample	depth (m)	age (h.y.)	Li/Ca (10^{-6})	Sr/Ca (10^{-3})	Mg/Ca (10^{-3})	Na/Ca (10^{-3})
8/2/ 90- 92	66.4	29.0	15.0 0.4 3	1.39 0.03 3	2.66 0.11 3	4.13 0.02 3
8/6/ 25- 27	71.8	32.7	14.2 1.2 4	1.25 0.05 4	3.17 0.09 4	3.77 0.29 4
9/6/ 25- 27	80.8	39.2	12.6 0.9 2	0.97 0.12 2	1.66 0.10 2	2.40 0.04 2
10/5/ 25- 27	88.3	43.4	11.4 1.5 3	1.34 0.03 3	2.73 0.31 3	3.95 0.58 3
10/5/112-114	89.1	44.8	9.9 0.8 3	1.30 0.05 3	3.27 0.08 3	3.35 0.15 3
11/2/ 20- 22	93.2	49.4	8.1 0.5 3	1.13 0.04 3	4.26 0.09 3	3.16 0.15 3
11/5/ 22- 24	97.7	50.5	7.5 0.2 3	1.30 0.01 3	4.75 0.17 3	3.08 0.09 3
11/6/ 25- 27	99.3	50.8	7.2 0.5 3	1.06 0.12 3	3.92 0.51 3	2.77 0.70 3
12/3/ 50- 52	104.5	52.1	10.2 2.9 3	0.99 0.07 3	3.53 0.27 3	3.24 0.25 3
12/5/ 25- 27	107.3	52.7	9.3 0.4 3	1.04 0.02 3	4.37 0.27 3	3.67 0.31 3
13/3/ 19- 20	113.7	55.0	11.3 0.0 1	1.09 0.00 1	1.98 0.00 1	3.93 0.00 1
13/6/ 25- 27	118.3	57.2	11.3 0.6 3	1.02 0.02 3	3.64 0.11 3	3.36 0.91 3
14/5/ 25- 27	126.3	61.9	11.3 1.1 2	1.12 0.06 2	3.37 0.26 2	3.97 0.74 2
16/5/ 25- 27	145.3	66.3	15.2 3.1 4	0.94 0.06 4	4.57 0.25 4	3.76 0.95 4
17/6/ 25- 27	156.3	67.1	15.2 0.4 2	0.90 0.06 2	4.45 0.31 2	3.84 0.18 2

3.6 continued

sample	depth (m)	age (m.y.)	Li/Ca (10^{-6})	Sr/Ca (10^{-3})	Mg/Ca (10^{-3})	Na/Ca (10^{-3})	
18/6/ 25- 27	165.8	69.9	14.2 1.7 3	1.18 0.32 3	4.35 0.45 3	3.61 0.94 3	
19/6/ 25- 27	174.8	71.1	15.3 0.7 2	(1.87) 0.12 2	4.27 0.06 2	3.81 0.25 2	possible Sr contamination
20/5/ 25- 27	182.8	72.1	11.7 0.6 3	1.04 0.41 3	4.91 0.39 3	2.95 0.49 3	
21/6/ 25- 27	193.8	73.2	11.9 1.9 2	0.97 0.00 2	2.79 0.04 2	3.22 0.18 2	
23/6/ 25- 27	212.8	75.1	11.3 0.9 3	0.78 0.04 3	4.33 0.08 3	2.64 0.39 3	
24/4/140-142	219.9	75.9	11.7 0.4 3	0.84 0.05 3	3.71 0.08 3	3.71 0.14 3	
24/5/ 25- 27	220.3	75.9	11.6 1.8 2	0.95 0.07 3	3.98 0.28 3	3.25 0.85 3	
25/6/ 25- 27	231.3	77.0	11.0 1.1 3	0.83 0.03 3	3.77 0.31 3	2.98 0.23 3	
26/5/ 25- 27	239.3	77.8	11.4 0.1 2	0.83 0.01 2	4.28 0.28 2	2.98 0.06 2	
27/2/ 25- 27	243.8	78.3	10.6 0.2 3	0.83 0.07 3	4.37 0.39 3	3.12 0.55 3	
28/2/ 26- 28	253.3	79.2	10.6 2.0 3	0.73 0.05 3	4.46 0.37 3	2.56 0.45 3	
31/00	289.5	84.0	9.3 1.1 5	0.67 0.03 5	4.64 0.21 5	2.62 0.42 5	
32/00	298.5	85.3	8.7 1.0 3	0.66 0.05 3	4.33 0.14 3	2.61 0.27 3	
39/00	364.0	96.8	12.0 1.9 3	0.78 0.07 3	5.38 0.26 3	3.31 0.27 3	
42/00	391.5	100.7	(19.3) 2.5 2	(1.04) 0.07 2	(5.53) 0.24 2	(4.26) 0.09 2	solids after dissolution

3.6 continued

sample	depth (m)	age (m.y.)	Li/Ca (10^{-6})	Sr/Ca (10^{-3})	Mg/Ca (10^{-3})	Na/Ca (10^{-3})	
43/1/120-122	392.7	100.8	(20.4) 6.2 2	(1.37) 0.17 2	(5.40) 0.72 2	(5.39) 1.76 2	solids after dissolution
43/3/ 25- 27	394.8	100.9	13.3 0.6 6	0.91 0.22 6	5.69 0.43 6	3.50 0.42 6	

TABLE 3.7 Foraminiferal calcite composition at Site 366 (Leg 41)

sample	depth (m)	age (m.y.)	Li/Ca (10^{-6})	Sr/Ca (10^{-3})	Mg/Ca (10^{-3})	Na/Ca (10^{-3})
2/6/ 20- 22	12.7	0.9	15.1 1.1 2	1.34 0.01 2	2.98 0.48 2	5.76 0.45 2
A/ 9/5/110-112	79.6	4.0	14.1 0.1 2	1.29 0.05 2	3.03 0.30 2	5.97 0.01 2
A/ 12/5/110-112	109.1	6.1	15.0 0.1 2	1.35 0.04 2	3.48 0.09 2	4.87 0.13 2
A/ 14/5/110-112	127.1	11.8	13.1 0.0 2	1.37 0.04 2	3.28 0.06 2	4.81 1.49 2
A/ 16/5/140-150	146.5	13.8	13.4 0.1 2	1.22 0.05 2	4.31 0.45 2	3.87 0.07 2
A/ 17/6/139-141	157.4	14.7	13.8 0.7 2	1.26 0.06 2	4.55 0.38 2	3.66 0.25 2
A/ 21/6/140-142	195.4	17.8	14.5 0.3 2	1.29 0.04 2	4.14 0.16 2	3.57 0.55 2
A/ 26/5/120-122	241.2	21.4	12.6 0.3 2	1.27 0.01 2	2.66 0.02 2	3.25 0.25 2
A/ 30/1/140-142	273.4	23.7	11.9 0.1 2	1.33 0.01 2	2.98 0.30 2	4.06 0.75 2
A/ 33/6/120-122	309.2	26.0	13.5 0.2 2	1.41 0.07 2	2.66 0.05 2	3.21 0.41 2
A/ 36/2/130-132	331.8	27.4	12.8 0.3 2	1.40 0.00 2	3.08 0.04 2	3.45 0.35 2
7/4/110-112	390.6	33.0	16.5 0.9 2	1.24 0.04 2	2.89 0.06 2	2.19 0.18 2
8/4/140-142	400.4	34.6	13.1 0.0 1	1.26 0.00 1	3.24 0.00 1	3.07 0.00 1
10/5/ 94- 96	420.4	37.7	16.9 0.0 1	1.31 0.00 1	2.97 0.00 1	2.85 0.00 1
13/3/ 94- 96	445.9	40.4	32.3 0.0 1	1.33 0.00 1	2.90 0.00 1	3.29 0.00 1

3.7 continued

sample	depth (M)	age (M.y.)	Li/Ca (10^{-6})	Sr/Ca (10^{-3})	Mg/Ca (10^{-3})	Na/Ca (10^{-3})
21-3/ 90- 92	521.8	45.3	[36.8 7.3]	0.74 0.04 2	4.32 0.14 2	1.11 0.00 2
48-6/142-144	793.4	58.4	4.6 0.2 2	0.65 0.02 2	3.70 0.01 2	0.92 0.01 2
49-6/139-141	792.9	59.3	4.2 0.5 2	0.63 0.04 2	3.52 0.00 2	0.64 0.10 2

TABLE 3.8 Foraminiferal calcite composition at Site 369 (Leg 41)

sample	depth (m)	age (m.y.)	Li/Ca (10^{-6})	Sr/Ca (10^{-3})	Mg/Ca (10^{-3})	Na/Ca (10^{-3})	
2/6/106-108	12.6	3.7	12.4 0.5 2	1.05 0.04 2	2.38 0.03 2	3.61 0.13 2	
A/ 6/4/110-112	95.1	12.0	14.9 1.1 2	1.19 0.04 2	3.15 0.10 2	3.51 0.13 2	
A/ 10/6/ 96- 98	136.0	19.1	16.0 0.4 2	1.26 0.02 2	3.96 0.19 2	3.98 0.41 2	
A/ 20/6/100-102 1	231.0	27.7	12.0 0.1 2	1.23 0.02 2	2.34 0.09 2	9.08 2.15 2	
A/ 29/2/100-102	310.5	33.8	12.4 0.0 1	1.13 0.00 1	1.99 0.00 1	9.36 0.00 1	
A/ 35/3/ 40- 42	368.4	51.7	9.3 0.4 2	1.03 0.03 2	3.29 0.14 2	2.95 0.20 2	
A/ 36/5/122-124	381.7	68.1	8.6 0.1 2	0.64 0.00 2	3.83 0.01 2	3.41 0.29 2	
A/ 38/5/149-151	401.0	75.2	6.8 1.2 2	0.55 0.04 2	5.24 0.22 2	2.03 0.14 2	
A/ 39/3/105-107	407.1	77.7	7.0 0.4 2	0.58 0.03 2	5.65 0.37 2	1.46 0.03 2	
A/ 40/2/ 5- 7	414.1	81.1	[20.9 0.0]	0.75 0.16 2	3.35 0.37 2	1.11 0.00 1	
A/ 41/4/121-123	427.7	100.7	(21.9) 0.4 2	(1.02) 0.02 2	(6.29) 0.60 2	(4.00) 0.63 2	brownish foraminifera
A/ 43/4/120-122	446.7	103.0	13.4 1.4 2	0.70 0.12 2	7.53 0.22 2	3.74 2.19 2	
A/ 45/4/ 96- 98	465.5	104.8	11.9 0.0 1	0.63 0.00 1	9.93 0.00 1	2.55 0.00 1	
A/ 46/5/ 26- 28	475.9	105.5	13.9 1.4 2	0.54 0.15 2	8.66 0.35 2	2.07 0.11 2	
A/ 47/5/136-138	486.4	106.3	14.3 0.1 2	0.76 0.12 2	9.91 0.97 2	1.77 0.20 2	

TABLE 3.9 Foraminiferal calcite composition at Site 526 (Leg 74)

sample	depth (m)	age (M.y.)	Li/Ca (10^{-6})	Sr/Ca (10^{-3})	Mg/Ca (10^{-3})	Na/Ca (10^{-3})
1/1/100-102	1.0	0.3	17.0 0.0 2	1.52 0.03 2	2.56 0.05 2	6.27 0.29 2
B/ 1/1/100-102	7.3	1.3	14.9 0.0 2	1.53 0.01 2	2.71 0.56 2	5.73 0.25 2
B/ 3/2/140-142	18.0	2.1	13.3 0.3 2	1.42 0.03 2	2.17 0.26 2	5.43 0.09 2
A/ 1/2/ 90- 92	30.4	3.7	14.0 0.1 2	1.57 0.06 2	2.48 0.44 2	5.37 0.30 2
A/ 3/3/ 90- 92	40.7	4.5	14.4 0.7 2	1.31 0.06 2	2.36 0.09 2	5.34 0.21 2
A/ 5/3/ 89- 91	49.5	5.3	14.9 2.5 2	1.16 0.04 2	2.19 0.09 2	5.20 0.30 2
A/ 7/3/ 90- 92	58.3	7.0	13.3 1.5 2	1.24 0.13 2	2.36 0.22 2	5.31 0.08 2
A/ 10/2/ 90- 92	70.0	9.2	13.7 3.6 2	1.13 0.01 2	2.35 0.68 2	5.72 0.00 1
A/ 12/3/ 70- 72	80.1	11.0	13.5 1.0 2	1.23 0.01 2	2.14 0.26 2	[4.69 7.15]
A/ 16/1/ 90- 92	94.9	12.3	13.0 1.0 2	1.24 0.01 2	2.57 0.09 2	4.42 0.58 2
A/ 20/4/ 32- 34	116.4	14.1	15.2 0.9 2	1.34 0.00 2	2.58 0.07 2	4.22 0.12 2
A/ 21/3/100-102	120.0	14.8	14.1 0.0 1	1.19 0.05 2	3.48 0.22 2	4.21 0.00 1
A/ 23/2/ 90- 92	127.2	16.2	13.5 0.7 2	1.29 0.09 2	3.39 0.34 2	4.37 0.11 2
A/ 29/3/ 90- 92	155.1	21.6	13.0 0.8 2	1.29 0.13 2	3.13 0.19 2	3.98 0.03 2
A/ 30/3/ 70- 72	159.3	22.4	12.5 0.1 2	1.34 0.01 2	2.97 0.03 2	3.27 0.14 2

3.9 continued

sample	depth (m)	age (m.y.)	Li/Ca (10^{-6})	Sr/Ca (10^{-3})	Mg/Ca (10^{-3})	Na/Ca (10^{-3})
A/ 33/3/ 26- 28	172.1	24.8	13.4 0.7 2	1.34 0.04 2	3.37 0.12 2	3.55 0.19 2
A/ 35/1/ 90- 92	178.5	26.0	13.2 0.1 2	1.30 0.02 2	3.06 0.01 2	3.79 0.32 2
A/ 38/2/110-112	193.4	28.8	13.4 0.5 2	1.27 0.13 2	3.39 0.35 2	3.30 0.04 2
A/ 40/2/ 90- 92	202.0	32.1	14.3 0.0 2	1.22 0.03 2	3.39 0.14 2	3.61 0.18 2
C/ 4/6/ 80- 82	202.8	31.9	12.9 0.6 2	1.33 0.06 2	3.15 0.44 2	3.58 0.01 2
A/ 41/1/ 90- 92	204.9	34.5	15.8 2.4 2	1.31 0.01 2	3.23 0.07 2	3.82 0.00 2
A/ 41/3/ 90- 92	207.9	37.1	13.8 0.5 2	1.29 0.06 2	3.74 0.06 2	4.14 0.70 2
C/ 5/5/ 90- 92	210.9	36.1	13.5 0.8 2	1.30 0.02 2	3.45 0.05 2	3.98 0.52 2
C/ 6/1/ 90- 92	214.4	37.6	11.2 0.1 2	1.41 0.04 2	2.51 0.08 2	3.72 0.17 2
A/ 43/2/ 70- 72	215.0	38.0	10.6 1.5 2	1.38 0.02 2	2.13 0.29 2	3.39 0.56 2
C/ 7/1/ 90- 92	218.9	37.9	12.1 1.0 2	1.41 0.03 2	2.91 0.14 2	3.74 0.50 2
A/ 44/2/ 65- 67	219.4	38.2	10.9 0.2 2	1.39 0.04 2	2.63 0.02 2	3.64 0.07 2
A/ 45/3/ 98-100	225.6	38.7	11.0 0.1 2	1.29 0.04 2	2.97 0.00 1	3.20 0.28 2
C/ 8/3/ 10- 14	226.1	38.4	10.6 0.1 2	1.28 0.04 2	2.85 0.20 2	3.17 0.53 2

APPENDIX 3.2 Interstitial water compositions and calculated inorganic calcite compositions

INTERSTITIAL WATER COMPOSITIONS

Interstitial water compositions listed in Tables 3.10 - 3.14 were taken from published and unpublished reports as follows:

Site 289 (Leg 30): Gieskes (unpublished report) and Elderfield et al. (1982).

Site 305 (Leg 32): Matter et al. (1975).

Site 366 (Leg 41)

and

Site 369 (Leg 41): Couture et al. (1977); Li analyzed in this study.

Site 526 (Leg 74): Gieskes et al. (preprint) and J. M. Gieskes and H. Elderfield, Sr isotopic data (pers. comm.).

Na concentrations listed in the following tables were calculated from reported salinities.

Ages for the interstitial water samples were calculated from the sample depths using procedures described in Chapter 3 for foraminiferal samples.

Interstitial water Li/Ca, Sr/Ca, Mg/Ca, and Na/Ca ratios for the five sites are plotted as a function of age in Figure 3.7.

CALCULATED INORGANIC CALCITE COMPOSITIONS

Elemental ratios in calcite from inorganic recrystallization were calculated from interstitial water ratios using the distribution coefficients listed in Table 3.3 (and in Table 3.4 for Li/Ca). The Sr distribution coefficient was calculated as a function of Sr concentration and temperature; no corrections were made for precipitation rate dependence of the distribution coefficient. Temperatures used in calculating the Sr

coefficients were estimated from sample depths, assuming that the temperature at the sediment-water interface was 0° C and that the geothermal gradient was 35° C/km. No temperature dependence was used in calculating inorganic calcite Mg or Na distribution coefficients.

Since the interstitial water elemental ratios for the five sites are different as a function of age (Figure 3.7), computed inorganic calcite ratios are also different for the five sites. For Li/Ca, Mg/Ca, and Na/Ca, the inorganic calcite ratio as a function of age is simply the interstitial water ratio multiplied by a constant distribution coefficient. Sr distribution coefficients depended on Sr concentration and temperature, but the inorganic recrystallization plots are similar to the interstitial water Sr/Ca plots.

NOTES FOR TABLES 3.10 - 3.14

- a. Li/Ca calculated from inorganic calcite Li distribution coefficient, 7×10^{-4} (Table 3.4).
- b. Mg/Ca calculated based on Mg distribution coefficient in Table 3.3 from Baker et al. (1982).
- c. Na/Ca calculated based on proportionality derived from data in White (1978), $(\text{Na/Ca})_{\text{calcite}} = (0.23 \times 10^{-3}) \times [(\text{Na/Ca})_{\text{solution}}]^{1/3}$ (Table 3.3).
- d. Na/Ca calculated based on proportionality constant derived from data in Kitano et al. (1975), $(\text{Na/Ca})_{\text{calcite}} = (1.13 \times 10^{-3}) \times [(\text{Na/Ca})_{\text{solution}}]^{1/3}$ (Table 3.3).

TABLE 3.10 Interstitial water compositions and calculated inorganic calcite compositions at Site 289 (Leg 30)

sample	depth (m)	age (m.y.)	INTERSTITIAL WATER COMPOSITIONS						CALCULATED INORGANIC			CALCITE COMPOSITIONS		
			Ca mM/l	Li uM/l	Sr mM/l	Mg mM/l	S g/kg	Na mM/l	⁸⁷ Sr/ ⁸⁶ Sr	Li/Ca ^a (10 ⁻⁶)	Sr/Ca (10 ⁻⁹)	Mg/Ca ^b (10 ⁻³)	Na/Ca ^c (10 ⁻³)	Na/Ca ^d (10 ⁻³)
1/5/144-150	7.5	0.5	10.0		0.194	52.2	35.2	478	0.70911		0.93	4.23	0.83	4.10
5/5/144-150	49.5	2.3	11.1		0.411	52.3	35.2	478			1.60	3.82	0.81	3.96
10/4/144-150	91.5	3.3	11.7		0.628	47.3	35.2	478	0.70899		2.07	3.27	0.79	3.89
15/3/144-150	137.5	4.9	13.2		0.816	44.8	35.2	478	0.70893		2.14	2.75	0.76	3.74
20/5/144-150	188.0	7.4	15.2		0.902	41.4	35.2	478			1.96	2.21	0.73	3.57
25/3/144-150	232.5	9.2	15.9		0.822	40.9	35.2	478	0.70886		1.81	2.08	0.72	3.51
30/3/ 0- 6	278.5	10.1	17.5		0.834	39.4	35.2	478	0.70882		1.67	1.82	0.69	3.40
35/3/144-150	327.5	11.3	18.2		0.896	38.2	35.5	482			1.68	1.70	0.69	3.37
40/5/144-150	378.0	12.6	19.7		0.896	36.2	35.5	482	0.70873		1.56	1.49	0.67	3.28
45/3/144-150	422.5	12.8	21.3		0.850	35.2	35.8	486	0.70866		1.42	1.34	0.65	3.20
50/5/144-150	473.0	13.6	22.4		0.850	34.2	35.8	486			1.36	1.24	0.64	3.15
55/5/144-150	520.5	15.1	25.8		0.856	30.7	36.0	489	0.70852		1.20	0.96	0.61	3.01
60/5/144-150	568.0	19.3	24.6		1.016	31.9	36.0	489	0.70844		1.37	1.05	0.62	3.06
65/2/144-150	611.0	20.8	24.0		0.873	33.7	35.3	493			1.32	1.14	0.63	3.09

3.10 continued

sample	depth (m)	age (m.y.)	INTERSTITIAL WATER COMPOSITIONS							CALCULATED INORGANIC CALCITE COMPOSITIONS				
			Ca mM/l	Li uM/l	Sr mM/l	Mg mM/l	S g/kg	Na mM/l	⁸⁷ Sr/ ⁸⁶ Sr	Li/Ca ^a (10 ⁻⁶)	Sr/Ca (10 ⁻³)	Mg/Ca ^b (10 ⁻³)	Na/Ca ^c (10 ⁻³)	Na/Ca ^d (10 ⁻³)
70/5/144-150	663.0	22.9	28.2		0.930	29.6	36.3	493	0.70826		1.17	0.85	0.60	2.93
75/3/144-150	707.5	24.9	28.8		0.959	28.7	36.3	493			1.17	0.81	0.59	2.91
80/0/144-150	755.0	26.6	29.7		0.862	27.1	36.3	493	0.70816		1.09	0.74	0.59	2.88
86/5/144-150	815.0	28.2	31.4		0.867	25.6	36.3	493	0.70798		1.04	0.66	0.58	2.83
91/3/144-150	819.5	28.3					36.4	494						
99/4/144-150	937.0	31.8					36.3	493						
99/4/144-150	937.0	31.8					36.6	497						
106/4/144-150	1003.5	42.2					40.2	546						
126/2/144-150	1167.5	67.1					36.6	497						
94/2 †	886.0	30.1	38.1			23.4					0.50			
99/2 †	932.0	31.7	36.1			20.2					0.45			
106/4 †	1002.0	42.1	37.9			27.2					0.50			

† squeezed after prolonged storage of cores

TABLE 3.11 Interstitial water compositions and calculated inorganic calcite compositions at Site 305 (Leg 32)

sample	depth (m)	age (m.y.)	INTERSTITIAL WATER COMPOSITIONS						CALCULATED INORGANIC CALCITE COMPOSITIONS				
			Ca mM/l	Li uM/l	Sr mM/l	Mg mM/l	S g/kg	Na mM/l	⁸⁷ Sr/ ⁸⁶ Sr	Li/Ca ^a (10 ⁻⁶)	Sr/Ca (10 ⁻⁹)	Mg/Ca ^b (10 ⁻³)	Na/Ca ^c (10 ⁻³)
1/5/144-150	7.5	1.2	10.1		0.089	52.4	34.9	474		0.44	4.20	0.83	4.07
3/2/144-150	20.0	2.1	10.1		0.119	53.0	35.2	478		0.58	4.25	0.83	4.09
6/5/144-150	52.5	22.7	11.3		0.131	52.2	35.5	482		0.57	3.74	0.80	3.95
11/5/144-150	99.0	50.8	11.2		0.123	52.2	35.2	478		0.55	3.78	0.80	3.95
16/5/144-150	146.5	66.4	11.3		0.123	52.4	35.8	486		0.54	3.76	0.81	3.96
21/4/144-150	192.0	70.2	11.3		0.117	52.7	35.5	482		0.52	3.78	0.80	3.95
26/4/144-150	239.0	73.7	11.3		0.114	52.4	35.5	482		0.51	3.76	0.80	3.95

TABLE 3.12 Interstitial water compositions and calculated inorganic calcite compositions at Site 366 (Leg 41)

sample	depth (m)	age (m.y.)	INTERSTITIAL WATER COMPOSITIONS							CALCULATED INORGANIC CALCITE COMPOSITIONS				
			Ca mM/l	Li uM/l	Sr mM/l	Mg mM/l	S g/kg	Na mM/l	⁸⁷ Sr/ ⁸⁶ Sr	Li/Ca ^a (10 ⁻³)	Sr/Ca (10 ⁻³)	Mg/Ca ^b (10 ⁻³)	Na/Ca ^c (10 ⁻³)	Na/Ca ^d (10 ⁻³)
1/2/ 0- 6	1.5	0.1	11.6	34.6	0.080	51.8	35.2	478		2.1	0.35	3.62	0.79	3.90
3/5/ 0- 6	131.5	12.2	19.0	116.0	0.510	45.7	35.5	482		4.3	1.11	1.95	0.68	3.32
4/2/144-150	248.5	22.0	23.0	167.0	0.660	43.6	35.8	486		5.1	1.11	1.54	0.64	3.12
5/5/142-150	373.5	30.2	25.6	230.0	0.750	40.4	36.0	489		6.3	1.10	1.28	0.61	3.02
10/4/144-150	419.5	37.6	31.8	305.0	0.950	34.5	35.0	475		6.7	1.00	0.88	0.57	2.78
15/2/ 0- 10	462.5	42.2	32.9	328.0	0.990	34.4	36.3	493		7.0	0.99	0.85	0.57	2.79
20/1/145-150	510.0	44.8	40.2		1.230	26.1	36.0	489			0.87	0.53	0.53	2.60
A/ 1/3/144-150	4.5	0.3	11.3	33.5	0.060	53.1	35.2	478		2.1	0.27	3.81	0.80	3.94
A/ 5/4/144-150	40.5	2.4	13.2	49.9	0.190	51.9	35.8	486		2.6	0.69	3.18	0.77	3.76
A/ 9/5/144-150	80.0	4.0	15.4	73.0	0.320	50.4	35.8	486		3.3	0.94	2.65	0.73	3.57
A/ 14/5/144-150	127.5	11.8	19.3	109.0	0.490	48.0	36.0	489		4.0	1.06	2.01	0.68	3.32
A/ 20/2/144-150	180.0	16.5	22.7	179.0	0.620	45.7	36.0	489		5.5	1.07	1.63	0.64	3.14
A/ 26/3/144-150	238.5	21.2	26.8	204.0	0.740	42.5	36.3	493		5.3	1.02	1.28	0.61	2.98

TABLE 3.13 Interstitial water compositions and calculated inorganic calcite compositions at Site 369 (Leg 41)

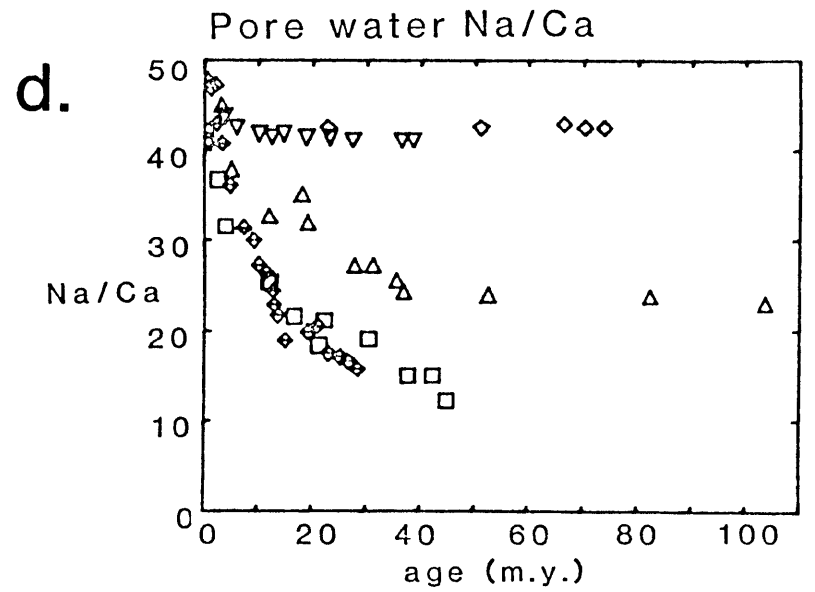
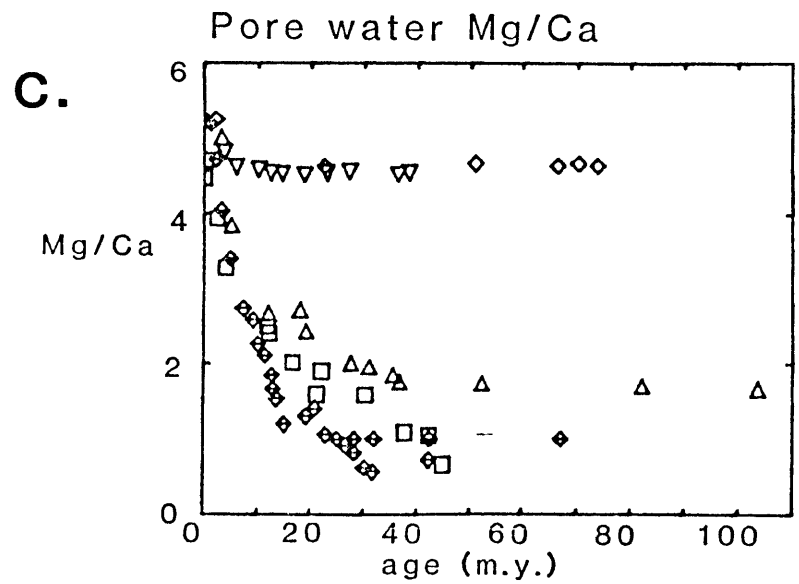
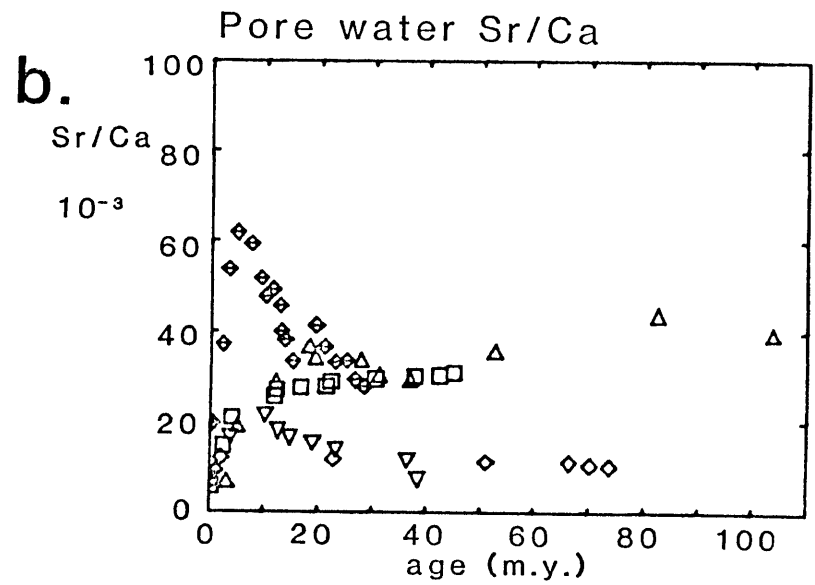
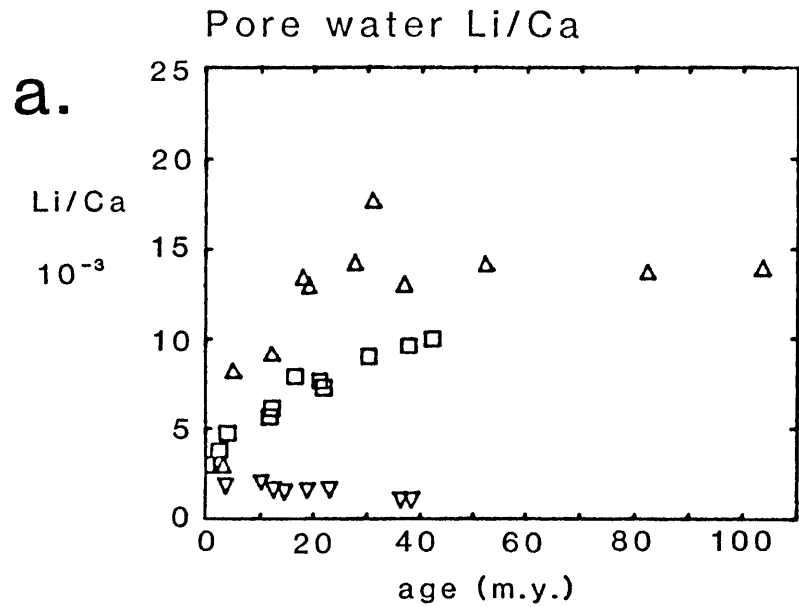
sample	depth (m)	age (m.y.)	INTERSTITIAL WATER COMPOSITIONS						$^{87}\text{Sr}/^{86}\text{Sr}$	CALCULATED INORGANIC CALCITE COMPOSITIONS				
			Ca mM/l	Li uM/l	Sr mM/l	Mg mM/l	S g/kg	Na mM/l		Li/Ca ^a (10^{-6})	Sr/Ca (10^{-9})	Mg/Ca ^b (10^{-9})	Na/Ca ^c (10^{-9})	Na/Ca ^d (10^{-9})
1/2/144-150	3.0	3.2	10.6	31.7	0.070	53.1	35.2	478	2.1	0.33	4.06	0.82	4.02	
5/4/144-150	37.5	5.0	12.7	104.0	0.240	48.9	35.5	482	5.7	0.89	3.12	0.77	3.80	
A/ 5/5/144-150	87.5	12.1	15.0	137.0	0.430	40.0	36.2	491	6.4	1.23	2.16	0.74	3.62	
A/ 10/5/144-15	135.0	18.0	14.2	190.0	0.520	38.5	36.8	499	9.4	1.51	2.20	0.75	3.70	
A/ 14/5/144-150	163.0	19.1	15.8	205.0	0.540	38.4	37.3	506	9.1	1.39	1.97	0.73	3.59	
A/ 20/5/144-150	230.0	27.6	19.4	276.0	0.650	38.8	39.0	529	10.0	1.30	1.62	0.69	3.40	
A/ 25/5/144-150	277.5	31.0	19.9	352.0	0.600	38.8	39.9	542	12.4	1.21	1.58	0.69	3.40	
A/ 30/4/144-150	323.5	35.4	21.6			39.8	40.7	552			1.49	0.68	3.33	
A/ 31/5/144-150	334.5	36.7	22.9	298.0	0.670	40.2	41.2	559	9.1	1.14	1.42	0.67	3.28	
A/ 35/3/144-150	369.5	52.2	24.5	346.0	0.870	42.4	43.4	589	9.9	1.24	1.40	0.66	3.26	
A/ 40/2/144-150	415.5	82.2	26.4	369.0	1.160	45.0	46.2	627	9.8	1.28	1.38	0.66	3.25	
A/ 44/1/144-150	452.0	103.6	27.3	390.0	1.080	45.4	46.3	628	9.7	1.23	1.35	0.65	3.21	

TABLE 3.14 Interstitial water compositions and calculated inorganic calcite compositions at Site 526 (Leg 74)

sample	depth (m)	age (m.y.)	INTERSTITIAL WATER COMPOSITIONS								CALCULATED INORGANIC CALCITE COMPOSITIONS				
			Ca mM/l	Li μM/l	Sr mM/l	Mg mM/l	S g/kg	Na mM/l	⁸⁷ Sr/ ⁸⁶ Sr	Li/Ca ^a (10 ⁻³)	Sr/Ca (10 ⁻³)	Mg/Ca ^b (10 ⁻³)	Na/Ca ^c (10 ⁻³)	Na/Ca ^d (10 ⁻³)	
A/ 1/1/143-150	29.0	3.7	10.9	19.2	0.178	52.5	35.2	478	0.70910	1.23	0.79	3.90	0.81	3.98	
A/ 6/2/143-150	53.0	6.0	11.2			51.7	35.2	478				3.74	0.80	3.95	
A/ 11/2/140-150	75.0	10.1	11.3	22.5	0.240	51.8	34.9	474	0.70899	1.39	1.00	3.71	0.80	3.93	
A/ 16/2/144-150	97.0	12.4	11.4	17.6	0.202	51.7	34.9	474		1.08	0.85	3.67	0.80	3.91	
A/ 21/1/140-150	119.0	14.6	11.4	16.2	0.185	51.6	35.2	478	0.70905	0.99	0.79	3.67	0.80	3.92	
A/ 26/2/140-150	141.0	18.8	11.5	17.6	0.174	51.9	35.2	478		1.07	0.74	3.66	0.80	3.91	
A/ 31/2/140-150	163.0	23.1	11.5	17.8	0.157	52.2	35.2	478	0.70910	1.08	0.67	3.68	0.80	3.91	
A/ 36/2/140-150	185.0	27.2	11.7			53.3	35.5	482	0.70920			3.69	0.79	3.90	
A/ 41/2/143-150	207.0	36.3	11.7	11.4	0.131	52.8	35.5	482		0.68	0.56	3.66	0.79	3.90	
A/ 45/2/143-150	225.0	38.3	11.7	11.7	0.082	53.1	35.5	482	0.70924	0.70	0.36	3.68	0.79	3.90	

FIGURE 3.7 Interstitial water elemental ratios as a function of age. Plot symbols are:

- ↔ Site 289 (Leg 30) Ontong-Java Plateau, Pacific
- ◊ Site 305 (Leg 32) Shatsky Rise, Pacific
- Site 366 (Leg 41) Sierra Leone Rise, Atlantic
- △ Site 369 (Leg 41) Spanish Sahara continental slope, Atlantic
- ▽ Site 526 (Leg 74) Walvis Ridge, Atlantic



REFERENCES -- CHAPTER THREE

- Andrews, J. E., G. Packham et al. (1975) Initial Reports of the Deep Sea Drilling Project, volume 30, Washington, U. S. Government Printing Office, pp. 231-398.
- Baker, P. A., M. Kastner, J. D. Byerlee, and D. A. Lockner (1980) Pressure solution and hydrothermal recrystallization of carbonate sediments -- an experimental study, *Mar. Geol.* 38: 185-203.
- Baker, P. A., J. M. Gieskes, and H. Elderfield (1982) Diagenesis of carbonates in deep-sea sediments--evidence from Sr/Ca ratios and interstitial dissolved Sr²⁺ data, *Jour. Sed. Petrol.* 52: 71-82.
- Bender M. L., R. B. Lorenz, and D. F. Williams (1975) Sodium, magnesium and strontium in the tests of planktonic foraminifera, *Micropal.* 21: 448-459.
- Bénière, M., M. Chemla, and F. Bénière (1976) Vacancy pairs and correlation effects in KCl and NaCl single crystals, *Jour. Phys. Chem. Solids* 37: 525-538.
- Boyle, E. A. (1981) Cadmium, zinc, copper, and barium in foraminifera tests, *Earth and Planet. Sci. Lett.* 53: 11-35.
- Brass, G. W. (1976) The variation of the marine ⁸⁷Sr/⁸⁶Sr ratio during Phanerozoic time: interpretation using a flux model, *Geochim. Cosmochim. Acta* 40: 721-730.
- Brätter, P., P. Möller, and U. Rösick (1972) On the equilibrium of coexisting sedimentary carbonates, *Earth Planet. Sci. Lett.* 14: 50-54.
- Burke, W. H., R. E. Denison, E. A. Hetherington, R. B. Koepnick, H. F. Nelson, and J. B. Otto (1982) Variation of seawater ⁸⁷Sr/⁸⁶Sr throughout Phanerozoic time, *Geology* 10: 516-519.
- Couture, R., R. S. Miller, and J. M. Gieskes (1977) Interstitial water and mineralogical studies, Leg 41, Deep Sea Drilling Project, *in* Lancelot, Y., E. Siebold, et al. (1977) Initial Reports of the Deep Sea Drilling Project, volume 41, U. S. Government Printing Office, pp. 907-914.
- Dasch, E. J. and P. E. Biscaye (1971) Isotopic composition of strontium in Cretaceous-to-Recent, pelagic foraminifera, *Earth Planet. Sci. Lett.* 11: 201-204.
- Elderfield, H., J. M. Gieskes, P. A. Baker, R. K. Oldfield, C. J. Hawkesworth, and R. Miller (1982) ⁸⁷Sr/⁸⁶Sr and ¹⁸O/¹⁶O ratios, interstitial water chemistry and diagenesis in deep-sea carbonate sediments of the Ontong Java Plateau, *Geochim. Cosmochim. Acta* 46: 2259-2268.
- Gieskes, J. M. (unpublished report) Interstitial water studies, Leg 30.

- Gieskes, J. M. (1981) Deep-Sea Drilling interstitial water studies: implications for chemical alteration of the oceanic crust, Layers I and II, SEPM Special Publ. 32: 149-167.
- Gieskes, J. M., K. Johnston, and M. Boehm (preprint) Interstitial water studies, Leg 74, Deep Sea Drilling Project.
- Graham, D. W., M. L. Bender, D. F. Williams, and L. D. Keigwin, Jr. (1982) Strontium-calcium ratios in Cenozoic planktonic foraminifera, *Geochim. Cosmochim. Acta* 46: 1281-1292.
- Killingley, J. S. (1983) Effects of diagenetic recrystallization on $^{18}\text{O}/^{16}\text{O}$ values of deep-sea sediments, *Nature* 301: 594-597.
- Kitano, Y., M. Okumura, and M. Idogaki (1975) Incorporation of sodium, chloride and sulfate with calcium carbonate, *Geochem. Jour.* 9: 75-84.
- Lancelot, Y., E. Siebold, et al. (1977a) Initial Reports of the Deep Sea Drilling Project, volume 41, Washington, U. S. Government Printing Office, pp. 21-162.
- Lancelot, Y., E. Siebold, et al. (1977b) Initial Reports of the Deep Sea Drilling Project, volume 41, Washington, U. S. Government Printing Office, pp. 327-420.
- Larson, R. L., R. Moberly, et al. (1975) Initial Reports of the Deep Sea Drilling Project, volume 32, Washington, U. S. Government Printing Office, pp. 75-158.
- Lawrence, J. R. and J. M. Gieskes (1981) Constraints on water transport and alteration in the oceanic crust from the isotopic composition of pore water, *Jour. Geophys. Res.* 86(B9): 7924-7934.
- Lorens, R. B. (1978) A study of biological and physical controls on the trace metal content of calcite and aragonite, Ph.D. thesis, University of Rhode Island.
- Lorens, R. B., M. L. Bender, and D. F. Williams (1977) The early nonstructural chemical diagenesis of foraminiferal calcite, *Jour. Sed. Petrol.* 47: 1602-1609.
- Matter, A., R. G. Douglas, and K. Perch-Nielson (1975) Fossil preservation, geochemistry, and diagenesis of pelagic carbonates from Shatsky Rise, Northwest Pacific, Leg 32, Deep Sea Drilling Project, in Larson, R. L., R. Moberly, et al. (1975) Initial Reports of the Deep Sea Drilling Project, volume 32, Washington, U. S. Government Printing Office, pp. 891-922.
- Moore, T. C., Jr., P. Rabinowitz, et al. (in press) Initial Reports of the Deep Sea Drilling Project, volume 74, Washington, U.S. Government Printing Office.

- Mucci, A. and J. W. Morse (1983) The incorporation of Mg^{2+} and Sr^{2+} into calcite overgrowths: influences of growth rate and solution composition, *Geochim. Cosmochim. Acta* 47: 217-233.
- van der Lingen, G. J. and G. H. Packham (1975) Relationships between diagenesis and physical properties of biogenic sediments of the Ontong-Java Plateau (Sites 288 and 289, Deep Sea Drilling Project), in Andrews, J. E., G. Packham, et al., Initial Reports of the Deep Sea Drilling Project, volume 30, Washington, U. S. Government Printing Office, pp. 443-481.
- Van Hinte, J. E. (1972) The Cretaceous time-scale and planktonic foraminiferal zones, *Ned. Akad. Wetensch. Proc. Ser. B* 75: 61-68.
- Vincent, E. (1974) Cenozoic planktonic biostratigraphy and paleoceanography of the tropical Western Indian Ocean, Leg 24, Deep Sea Drilling Project, in Fischer, R. L., E. T. Bunce, et al., Initial Reports of the Deep Sea Drilling Project, volume 24, Washington, U. S. Government Printing Office, pp. 1111-1150.
- White, A. (1978) Sodium coprecipitation in calcite and dolomite, *Chem. Geol.* 23: 65-72.

CHAPTER FOUR:

OCEANIC PALEOCHEMICAL VARIATIONS OVER THE LAST 100 M.Y.

Global crustal generation rate and heat flow at the ridge crest 80 - 110 m.y.b.p. were estimated to have been as much as a factor of two higher than at present from several geological and geophysical models (Larson and Pitman, 1973; Turcotte and Burke, 1978; Davis and Solomon, 1981); other investigators have disagreed with these estimates (Berggren et al., 1975; Parsons, 1982). The suggested variations in spreading rate, heat flow, and plate velocity would have resulted in hydrothermal fluxes at 80 - 110 m.y.b.p. double the modern ones with a decline in these fluxes over 80 m.y. to the present-day values.

The oceanic cycle of Li is dominated by input from hydrothermal circulation at the ridge crest (Edmond et al., 1979, 1982). Its oceanic concentration should have been larger if hydrothermal fluxes were greater.

Li/Ca, Sr/Ca, Mg/Ca, and Na/Ca ratios as a function of age were measured in foraminiferal calcite from five DSDP sites. The sites studied, these measurements, and the effects of diagenesis on the original calcite composition are described in Chapter 3. An oceanic mass balance model for Li is used with the oceanic paleochemistry, as determined from foraminiferal calcite chemistry, to evaluate changes in hydrothermal fluxes through time. Alternate models concerning the importance of hydrothermal circulation to oceanic mass balances, variations in removal processes with changing

inputs, and changing continental fluxes as they affect Li and other elements are considered for their impact on the ability to quantify changes in hydrothermal circulation from observations of oceanic Li/Ca ratios.

THE CONNECTION BETWEEN SPREADING RATES AND HYDROTHERMAL FLUXES

As discussed in Chapter 1, the connection between global crustal generation rates and hydrothermal fluxes to the ocean is not necessarily direct. The proportion of the total heat lost by convection is similar on present-day ridge crests with spreading rates differing by factors of two to three (32% - 42% of the total ridge heat flow) (Wolery and Sleep, 1976). The degree of cracking at spreading centers may vary with crustal generation rate; therefore the amount of basalt surface accessible for reactions with seawater may be different. It is the circulation of water through the ridge crest and the concurrent basalt-seawater reactions which generate the chemical fluxes. Therefore, increases in the rate of crustal generation and in the water flux through the ridge crest should increase the associated chemical fluxes. The hydrothermal systems sampled to date (Galapagos, EPR 21° N, Guaymas Basin, EPR 13° N) are from ridges with approximately equal spreading rates. Sampling of hydrothermal solutions from ridge crests with faster or slower spreading rates has yet to be accomplished. For the purposes of the following discussion, doubling the global crustal generation rate is assumed to double the chemical fluxes associated with hydrothermal advection of heat at the ridge crest. The ability to define changes in seafloor spreading rates from oceanic Li concentration depends on this assumption of predicatable geochemical consequences.

PALEOCHEMICAL RECORDS

Li/Ca, Sr/Ca, Mg/Ca, and Na/Ca ratios in foraminiferal calcite were measured in samples from five DSDP sites and are plotted versus sample ages in Figures 4.1 - 4.4. Simple modelling of recrystallization of biogenic to inorganic calcite indicated that many of the foraminiferal samples are substantially unrecrystallized. Samples which were severely affected by diagenesis or which were analytically questionable are not plotted. No other qualitative or quantitative corrections for diagenetic changes are made in these plots. Because the potential for diagenetic changes increases with increasing sample age and because samples from only two sites had ages older than 40 m.y., conclusions about paleochemical variations for times beyond 40 m.y.b.p. are less certain.

LITHIUM/CALCIUM

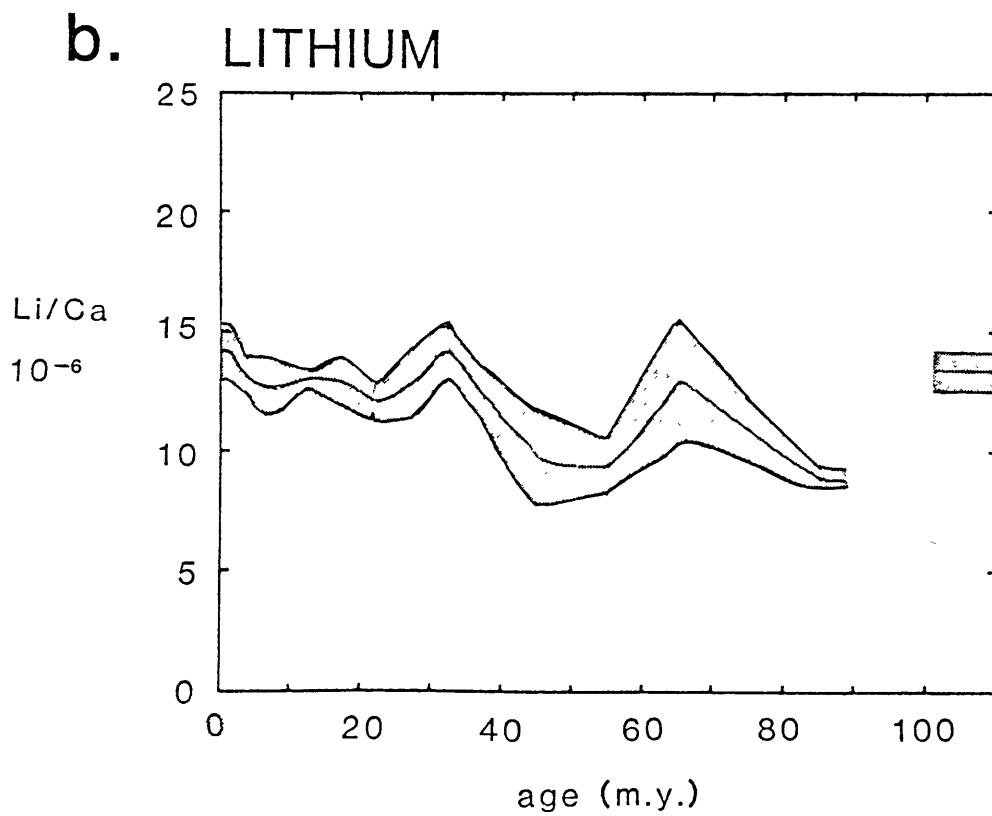
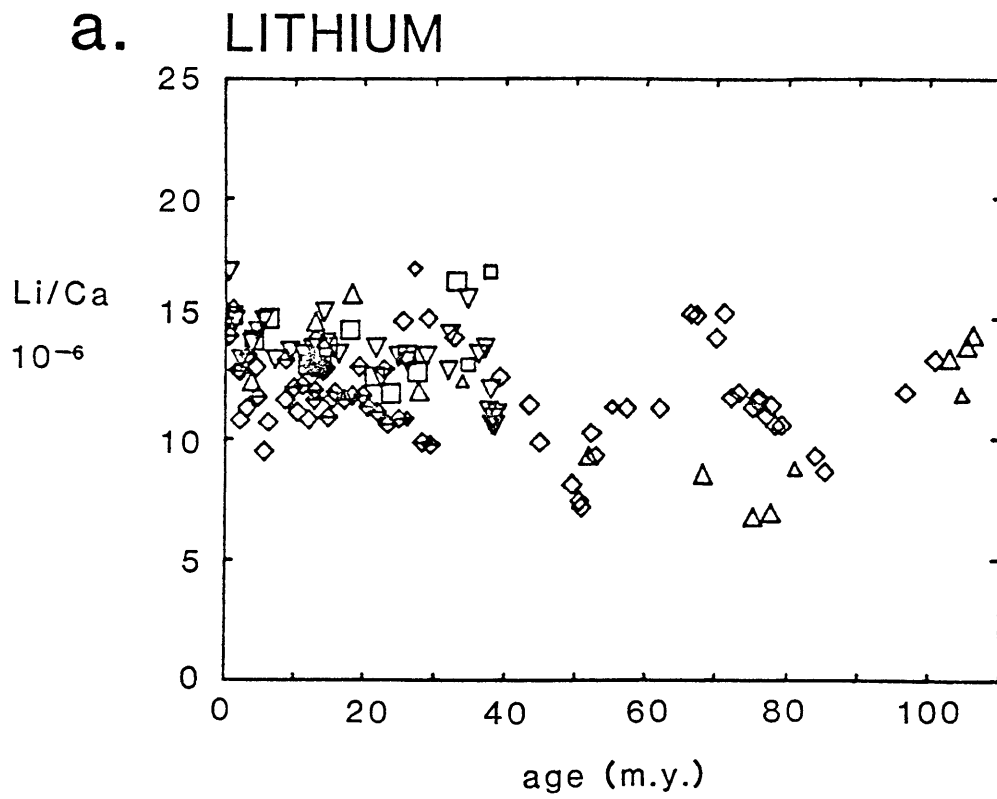
Li/Ca ratios in foraminiferal calcite are plotted versus sample ages in Figures 4.1, a and b. Oceanic Li/Ca ratios have not been a factor of two higher than those at present at any time during the past 100 m.y. The validity of this constant Li/Ca ratio in foraminiferal calcite is strongly supported for the past 40 m.y. by the similarity of the foraminiferal data from three sites (366, 369, and 526) with different interstitial water Li/Ca ratios (Figure 3.7). The calcite ratios would not agree in these three sites if the chemical signals were due to inorganic recrystallization reactions, rather than to oceanic paleochemistry. Mean ratios reach a minimum between 40 and 60 m.y. and possibly another minimum between 70 and 90 m.y. (determined primarily by the samples from Site 305) (Figure 4.1.b). Mean Li/Ca ratios range from 14.1×10^{-6} for 0 - 2.5 m.y. to 8.9×10^{-6} for 80 - 90 m.y., for a maximum decrease of 37% from present-day values. The mean values in each time range are generally within $\pm 20\%$ of the mean Li/Ca ratio of all samples (12.7×10^{-6}).

FIGURE 4.1 Li/Ca ratios in foraminiferal calcite as a function of age.

a. Li/Ca ratios in foraminiferal calcite from all sites. Plot symbols are:

- ↔ Site 289 (Leg 30) Ontong-Java Plateau, Pacific
- ◇ Site 305 (Leg 32) Shatsky Rise, Pacific
- Site 366 (Leg 41) Sierra Leone Rise, Atlantic
- △ Site 369 (Leg 41) Spanish Sahara continental slope, Atlantic
- ▽ Site 526 (Leg 74) Walvis Ridge, Atlantic

b. Li/Ca ratios averaged in 2.5 m.y. intervals for 0 - 10 m.y.; 5 m.y. intervals for 10 - 40 m.y.; and 10 m.y. intervals for 40 - 110 m.y. The shaded area represents $\pm 2\sigma/\sqrt{n}$ of the mean for each age interval.



STRONTIUM/CALCIUM

Sr/Ca ratios in foraminiferal calcite from the five DSDP sites are plotted versus samples ages in Figure 4.2. Mean Sr/Ca ratios are at a minimum from 5 - 6 m.y., approximately 20% lower than the values at present, and show a general decrease with increasing age (Figure 4.2.b). Sr/Ca ratios in samples older than 40 m.y. are similar in two sites (305 and 369) which have different interstitial water compositions (Figure 3.7) and, therefore, different inorganic recrystallization Sr/Ca ratios (Appendix 3.1). Mean Sr/Ca ratios as a function of age agree well for 0-50 m.y. with those determined in another study (Figure 4.2.b); that study found a minimum between 45 and 55 m.y. not clearly defined by these samples (Graham et al., 1982).

MAGNESIUM/CALCIUM

Mg/Ca ratios in foraminiferal calcite from the five DSDP sites are plotted versus samples ages in Figure 4.3. The ratios are approximately constant from 0-40 m.y. In the two sites (Sites 305 and 369) with samples older than 40 m.y., Mg/Ca ratios increase similarly with increasing age despite different interstitial water compositions (Figure 3.7) and, therefore, different recrystallized calcite compositions (Appendix 3.2).

SODIUM/CALCIUM

Na/Ca ratios in foraminiferal calcite from the five DSDP sites are plotted versus sample ages in Figure 4.4. The ratios decrease with increasing sample age, with the sharpest decrease from 0-10 m.y. Similar results were found in another study of foraminiferal calcite composition (Graham et al., 1982). The results of foraminiferal culture experiments (Chapter 2) and inorganic precipitation experiments (Kitano et al., 1975;

FIGURE 4.2 Sr/Ca ratios in foraminiferal calcite as a function of age.

a. Sr/Ca ratios in foraminiferal calcite from all sites. Plot symbols are:

- ◁ Site 289 (Leg 30) Ontong-Java Plateau, Pacific
- ↙ Site 305 (Leg 32) Shatsky Rise, Pacific
- Site 366 (Leg 41) Sierra Leone Rise, Atlantic
- △ Site 369 (Leg 41) Spanish Sahara continental slope, Atlantic
- ▽ Site 526 (Leg 74) Walvis Ridge, Atlantic

b. Sr/Ca ratios averaged in 1.0 m.y. intervals for 0 - 10 m.y.; 5 m.y. intervals for 10 - 40 m.y.; and 10 m.y. intervals for 40 - 110 m.y. The shaded area represents $\pm 2\sigma/\sqrt{n}$ of the mean for each age interval. For comparison, the dotted lines are the mean Sr/Ca ratios and 80% confidence limits determined in another study (Graham et al., 1982).

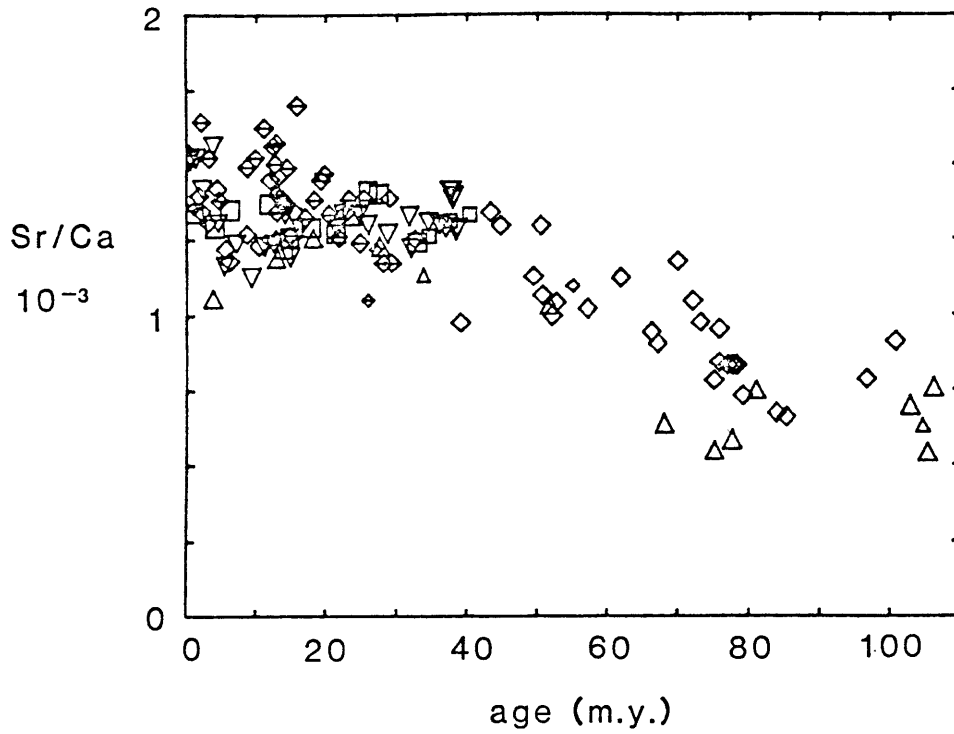
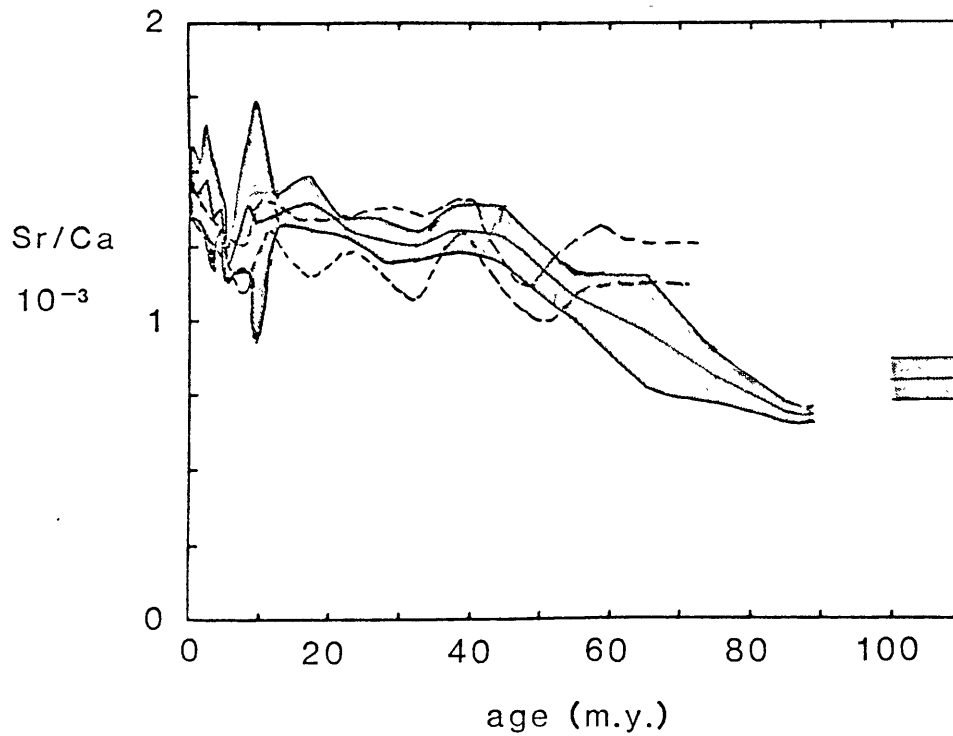
a. STRONTIUM**b. STRONTIUM**

FIGURE 4.3 Mg/Ca ratios in foraminiferal calcite as a function of age for all sites. Plot symbols are:

- ↶ Site 289 (Leg 30) Ontong-Java Plateau, Pacific
- ↷ Site 305 (Leg 32) Shatsky Rise, Pacific
- Site 366 (Leg 41) Sierra Leone Rise, Atlantic
- △ Site 369 (Leg 41) Spanish Sahara continental slope, Atlantic
- ▽ Site 526 (Leg 74) Walvis Ridge, Atlantic

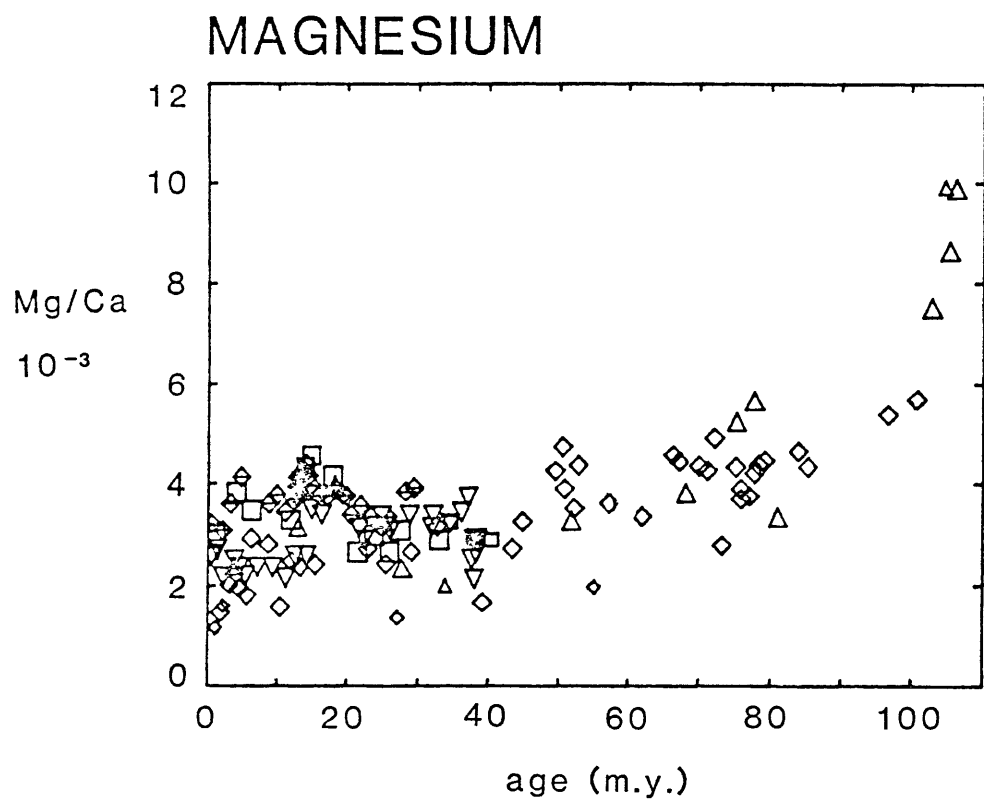
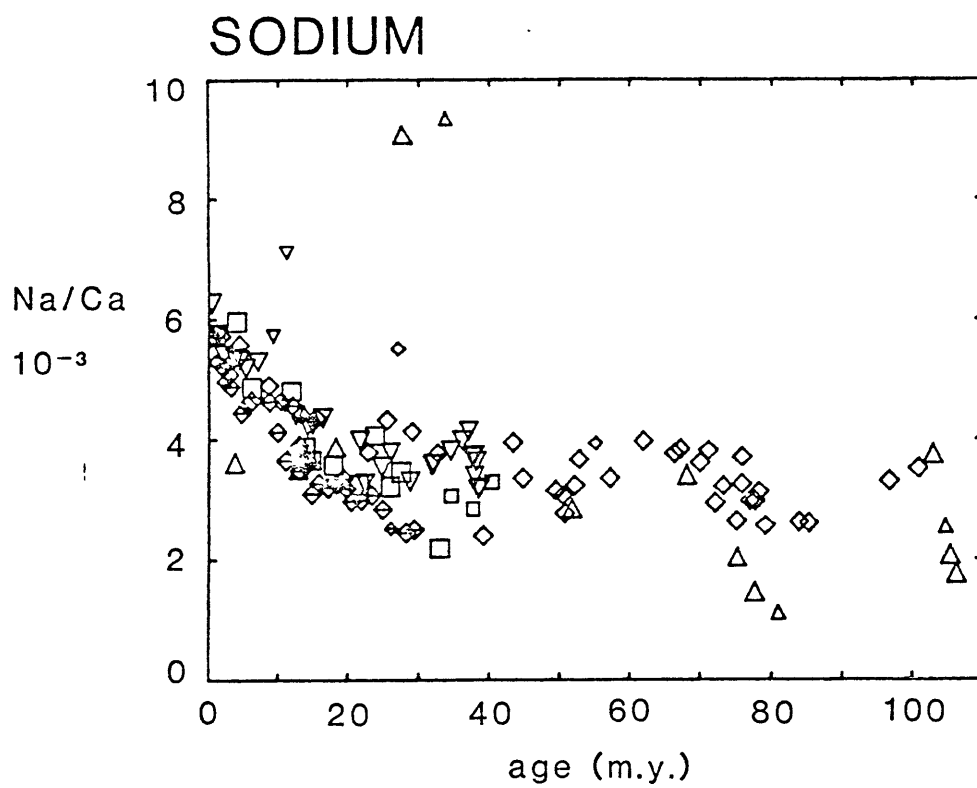


FIGURE 4.4 Na/Ca ratios in foraminiferal calcite as a function of age for all sites. Plot symbols are:

- ↗ Site 289 (Leg 30) Ontong-Java Plateau, Pacific
- ↘ Site 305 (Leg 32) Shatsky Rise, Pacific
- Site 366 (Leg 41) Sierra Leone Rise, Atlantic
- △ Site 369 (Leg 41) Spanish Sahara continental slope, Atlantic
- ▽ Site 526 (Leg 74) Walvis Ridge, Atlantic



White, 1978) showed that Na/Ca ratios in biogenic and inorganic calcites did not respond linearly to solution chemistry changes. Because of this nonlinear relationship between solution and solid chemistry, the interpretation of foraminiferal Na/Ca in terms of oceanic paleochemistry is uncertain.

SEAWATER STRONTIUM ISOTOPIC RATIOS

Seawater $^{87}\text{Sr}/^{86}\text{Sr}$ ratios for 0 - 110 m.y. are plotted in Figure 4.5 (Burke et al., 1982; Brass, 1976; Veizer and Compston, 1974; Dasch and Biscaye, 1971; and Peterman et al., 1970). The $^{87}\text{Sr}/^{86}\text{Sr}$ ratio of seawater has increased from ~ 0.7072 at 110 m.y.b.p. to ~ 0.7091 at present. The rate of increase is greater for the past 40 m.y. (from ~ 0.7077 to ~ 0.7091) than for the earlier time period.

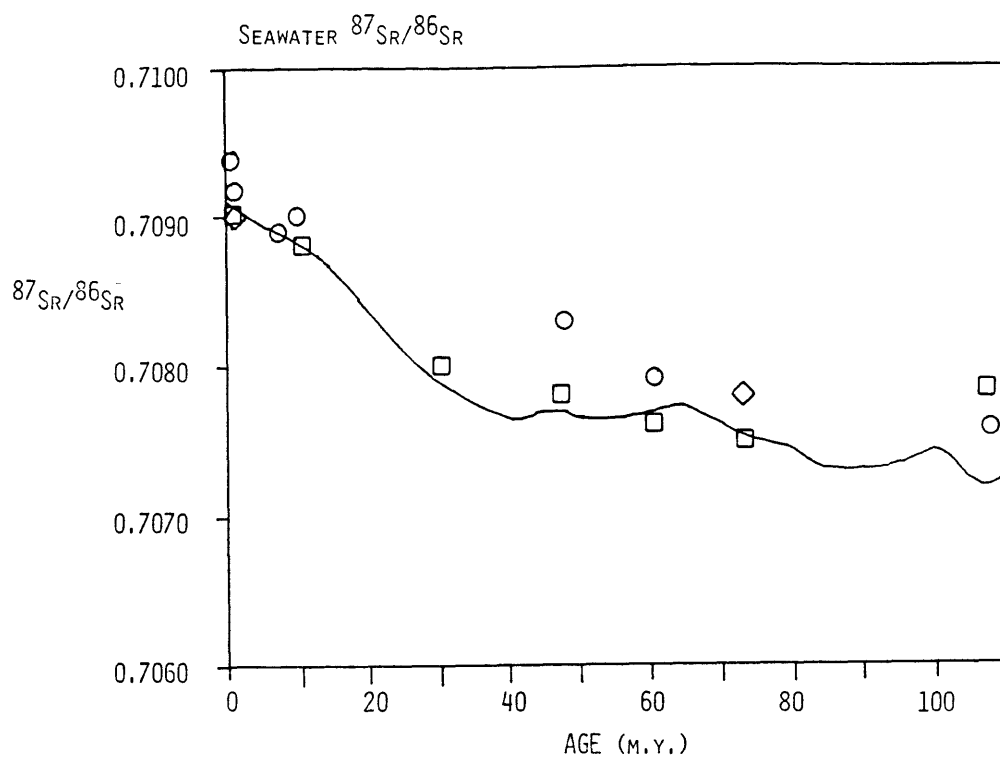
SUMMARY

According to the foraminiferal calcite records, at no time in the past 100 m.y. has the Li/Ca ratio in the ocean been significantly higher than the present-day ratio. Over the past 100 m.y. while Li/Ca ratios appear to have been relatively constant, seawater $^{87}\text{Sr}/^{86}\text{Sr}$ ratios have been increasing to present-day values.

The constancy of the Li/Ca oceanic ratio is discussed primarily in connection with spreading rate and hydrothermal fluxes to help to define the extent of geophysical changes over the past 100 m.y.

FIGURE 4.5 Seawater $^{87}\text{Sr}/^{86}\text{Sr}$ ratios as a function of age. Plot symbols are:

- foraminiferal shells, Dasch and Biscaye (1971)
- fossil shells from shallow marine sediments, Peterman et al. (1970)
- ◇ foraminiferal shells, Brass (1976)
- carbonate, evaporite, and phosphate samples, Burke et al. (1982)



LITHIUM MASS BALANCE MODEL

Li concentrations in various reservoirs and estimated fluxes to and from the ocean are summarized in Table 4.1 and discussed in Appendix 4.1. There are two significant sources of dissolved Li to the ocean -- high-temperature seawater-basalt reactions at the ridge crest and river input. The sinks removing Li from the ocean are the enrichment of Li in marine sediments as compared to their igneous rock precursors and the uptake of Li in low-temperature basalt alteration products. Estimating the global magnitude of the sinks is more difficult than for the sources because of the paucity of adequate geochemical and geological data. Although the Li sinks can be tentatively identified, the mechanisms of the removal are not well-known.

The mass balance for oceanic Li concentration as a function of time can be expressed as:

$$\frac{d[\text{Li}]}{dt} = F_{rc} + F_{ri} - F_s - F_{lt}$$

where: $[\text{Li}]$ = oceanic Li concentration

F_{rc} = rate of Li input from high-temperature
basalt-seawater reactions at the ridge crest

F_{ri} = rate of Li input from rivers

F_s = rate of Li removal in oceanic sediments

F_{lt} = rate of Li removal in basalt alteration products
from low-temperature basalt-seawater reactions

TABLE 4.1 Li concentrations and fluxes¹

reservoir	concentration	estimated flux ² (mol/y)
seawater	28 $\mu\text{mol/l}$	
river water	0.2-0.4 $\mu\text{mol/l}$	(+) 6-14 x 10 ⁹
ridge crest hydrothermal circulation	350° C end member solutions ³	
Galapagos Spreading Center	690-1140 $\mu\text{mol/l}$	(+) 95-160 x 10 ⁹
21° N, EPR (1979)	820 $\mu\text{mol/l}$	(+) 115 x 10 ⁹
21° N, EPR (1981)	890-1320 $\mu\text{mol/kg}$	(+) 125-190 x 10 ⁹
Guaymas Basin, Gulf of California	630-1080 $\mu\text{mol/kg}$	(+) 90-150 x 10 ⁹
suggested average ⁴		(+) 140 x 10 ⁹
oceanic tholeiitic basalts	1.3 \pm 0.9 mmol/kg	
continental material		
granites	7.3 mmol/kg	
basalts	2.7 mmol/kg	
"average" igneous rock	5 mmol/kg	
sedimentary rocks		
shales and clays	10 mmol/kg	
sandstones	4.5 mmol/kg	
carbonates	2.2 mmol/kg	
"average" sedimentary rock	7 mmol/kg	
oceanic sediments	5-16 mmol/kg	(-) 25-65 x 10 ⁹
low-temperature basalt alteration		
celadonite zones, whole rock	0-17 mmol/kg	
saponite zones, whole rock	0-12 mmol/kg	
submarine weathered basalts	1.2-8.7 mmol/kg	
dredged pillow basalts		
altered glass rim	2-10 times fresh basalt	
altered basalt interior	2-4 times fresh basalt	

TABLE 4.1 continued

- Notes:
1. See Appendix 4.1 for a discussion of these values and references.
 2. (+) indicates Li input to the ocean
(-) indicates Li removal from the ocean
 3. The hydrothermal fluxes are those calculated from the hydrothermal solution end member compositions with the assumption that 100% of the ^3He flux and heat flow anomaly are due to hydrothermal circulation associated with chemical fluxes from high-temperature basalt-seawater reactions (Edmond et al., 1979).
 4. From geophysical models of hydrothermal circulation, it has been suggested recently that the global fluxes are one-sixth to one-tenth those calculated with the above assumptions (Sleep et al., in press). Hydrothermal Li fluxes would be on the order of $14 - 24 \times 10^9$ mol/y in this model.

The removal fluxes can be modelled as first-order with respect to Li concentration:

$$F_s = k_s[\text{Li}]$$

$$F_{1t} = k_{1t}[\text{Li}]$$

The sum of the two removal constants is the inverse of the oceanic steady-state residence time; the magnitude of the constants reflects the proportional importance of removal in each sink.

The solution to the mass balance equation is then:

$$[\text{Li}] = [\text{Li}]^\infty - \{[\text{Li}]^\infty - [\text{Li}]^0\} \exp\{-(k_s + k_{1t})t\}$$

$$\text{where: } [\text{Li}]^\infty = \frac{F_{rc} + F_{ri}}{k_s + k_{1t}}, \text{ oceanic steady-state Li concentration}$$

$$[\text{Li}]^0 = \text{oceanic Li concentration at time } t=0$$

LITHIUM AS AN INDICATOR OF HYDROTHERMAL FLUXES

There are two properties of oceanic Li concentration critical to its use as an indicator of changes in hydrothermal circulation fluxes: its temporal responsiveness to changes in sources or sinks and its concentration change, or sensitivity, in response to changes in input fluxes.

A measure of the responsiveness of the Li concentration is the residence time of Li in the ocean. The oceanic residence time with respect to inputs, τ_r , is defined as:

$$\tau_r = \frac{\text{total oceanic inventory}}{\text{total input flux}} = \frac{V_o[\text{Li}]}{F_{rc} + F_{ri}}$$

where: V_o = volume of the ocean, 1.37×10^{21} l
 $[Li]$ = oceanic Li concentration, 28×10^{-6} mol/l
 F_{rc} = rate of Li input from high-temperature
 basalt-seawater reactions at the ridge crest
 F_{ri} = rate of Li input from rivers

The residence time of Li depends on the total hydrothermal and river flux. After an instantaneous change in input fluxes, for each increment of time equal to the residence time, the difference between the oceanic Li concentration and the steady-state concentration decreases by a factor of $1/e$. Changes in input fluxes can thus be discerned on a time scale equal to or greater than the residence time.

The sensitivity of the oceanic Li concentration as an indicator for hydrothermal circulation changes is the second consideration. The steady-state Li concentration for the mass balance model described, with hydrothermal and river sources and sedimentary and basalt alteration sinks, is:

$$[Li]^\infty = \frac{F_{rc} + F_{ri}}{k_s + k_{1t}}$$

Defining today's ocean as state number two and the ocean at some time in the past as state number one, the ratio of the steady-state Li concentrations for the two oceans is:

$$\frac{[Li]^\infty (1)}{[Li]^\infty (2)} = \frac{F_{rc} (1) + F_{ri} (1)}{k_s (1) + k_{1t} (1)} \bigg/ \frac{F_{rc} (2) + F_{ri} (2)}{k_s (2) + k_{1t} (2)}$$

The ratio of the Li concentrations for the two steady-state oceans is directly proportional to the ratio of the total input fluxes and inversely proportional to the ratio of the removal constants.

OCEANIC LI/CA RATIOS OVER THE LAST 100 M.Y.

Oceanic Li concentrations would have been higher than those at present if seafloor spreading rates and hydrothermal fluxes were a factor of two greater 80 - 110 m.y.b.p. The measurement of foraminiferal calcite Li/Ca ratios showed that oceanic Li/Ca ratios have not been greater than those at present at any time in the last 110 m.y. (Figure 4.1). Hypotheses for the lack of any Li/Ca ratios greater than those at present are examined in light of the possible conclusions about oceanic Li concentrations and hydrothermal flux variations. These explanations include:

1. The hydrothermal fluxes are not correct as extrapolated. Hydrothermal fluxes may be of less importance to oceanic mass balances than calculated, so that oceanic Li concentrations might not be responsive to hydrothermal fluxes.
2. The processes removing Li from the ocean vary in concert with the hydrothermal fluxes so that changes in hydrothermal fluxes have no net effect on oceanic Li concentrations.
3. River Li fluxes have changed through time, so that hydrothermal flux variations have been obscured.
4. Oceanic Li concentrations have varied and oceanic Ca concentrations have also changed so that Li/Ca ratios have remained constant.

These hypotheses are evaluated below.

MAGNITUDE OF HYDROTHERMAL FLUXES

The mass balance for Li (Table 4.1 and Appendix 4.1) and the fluxes given for the other elements (Ca, Sr, Mg, Na; Table 1.1) were calculated

with the assumption that the chemical compositions of hydrothermal solutions can be extrapolated to global fluxes by assuming that 100% of the ridge-crest ^3He and ridge crest heat flow anomaly are due to hydrothermal circulation associated with high-temperature basalt-seawater reactions (Edmond et al., 1979). The extrapolations by this method resolve a number of classical geochemical imbalances; the global advective heat flow calculated from the ^3He budget and the observed $^3\text{He}/\text{heat}$ ratio in hydrothermal systems agrees with that determined from geophysical estimates of the convective heat anomaly (Jenkins et al., 1978; Edmond et al., 1979). Despite these successes, the validity of the global fluxes has been questioned from geophysical models of cooling of the magma chamber by hydrothermal circulation (Sleep et al., in press) and from arguments about the size of the crustal reservoir of Rb and Cs available to supply hydrothermal fluxes (Staudigel and Hart, 1983; Hart and Staudigel, 1982). Hydrothermal fluxes have been suggested to be one-sixth to one-tenth as large (Sleep et al., in press) as the previous global estimates (Edmond et al., 1979). The chemical resolution of this problem would be the measurement of an anomaly in the oceanic water-column profile of an element which has conservative behavior in the mixing of hydrothermal solutions with ambient seawater; this anomaly could be compared to the water-column ^3He anomaly to calculate the global fluxes.

The two extrapolations of global hydrothermal fluxes are quantified as follows for this discussion. For the higher estimate, hydrothermal inputs of Li are assigned to be 10 times the river flux (Edmond et al., 1979, 1982; Von Damm, 1983). Models requiring lower hydrothermal fluxes are represented here by assuming that the hydrothermal flux of Li is equal to the river flux.

The impact of lower hydrothermal fluxes on the utility of oceanic Li concentration as an indicator of hydrothermal fluxes must be considered. Lower hydrothermal inputs affect the mass balance of Li in two ways. Smaller input fluxes result in longer oceanic residence times. With a river flux of 14×10^9 mol/y, the Li residence times for the two global extrapolations (hydrothermal flux equals ten times the river flux and hydrothermal flux equals the river flux) are 0.25×10^6 y and 1.4×10^6 y respectively, differing by a factor of approximately six. The residence time with respect to river input alone is 2.7×10^6 y. The postulated variations in spreading rate occurred over tens of millions of years, so that Li is a time responsive indicator for hydrothermal circulation changes even if hydrothermal fluxes are one-tenth those calculated by Edmond et al. (1979).

The second effect of lower hydrothermal fluxes is on the sensitivity of the oceanic Li concentration as an indicator for hydrothermal circulation changes. As discussed with the Li mass balance model, the ratio of the steady-state oceanic Li concentrations in two hypothetical oceans is directly proportional to the total input flux ratio and inversely proportional to the ratio of the sum of the removal constants. If the removal constants do not change with time or with changes in the input fluxes, the ratio of the steady-state Li concentrations is:

$$\frac{[\text{Li}]^\infty (1)}{[\text{Li}]^\infty (2)} = \frac{F_{\text{rc}} (1) + F_{\text{ri}} (1)}{F_{\text{rc}} (2) + F_{\text{ri}} (2)}$$

Another assumption that simplifies this expression is that the river input has not varied between the two oceanic states compared. The

present-day ridge crest flux can be considered as a factor (X) times the river flux. The effect of changing crustal generation rate by a factor (N) is assumed to change the ridge crest flux by the same amount, as discussed earlier. The ratio of the steady-state Li concentrations in the two oceanic states, assuming invariant removal constants and a constant river flux, is:

$$\frac{[\text{Li}]^{\infty} (1)}{[\text{Li}]^{\infty} (2)} = \frac{NX + 1}{X + 1}$$

The two extrapolations of global hydrothermal fluxes are equivalent to setting $X = 10$ for the model based on the fluxes of Edmond et al., 1979, and $X = 1$ for the model of lower global fluxes (Sleep et al., in press). For a doubling of the hydrothermal flux ($N = 2$), the ratio of the steady-state Li concentrations in the two systems is 1.9 for $X = 10$ and 1.5 for $X = 1$. In other words, for a doubling of the hydrothermal flux, the oceanic Li concentration would be 90% or 50% higher than at present for the high and low flux models, respectively. This shows that the relationship between the ratios of the steady-state Li concentrations and the factor (X) of the relative importance of hydrothermal inputs is nonlinear; the ratio of steady-state concentrations increases more rapidly than does the relative importance factor. The calculation demonstrates that an order of magnitude decrease in the relative importance of the hydrothermal flux ($X = 1$ compared to $X = 10$) results in only a difference of 40% in the model steady-state Li concentration for an increased input flux. This is because, even with the lower global fluxes, hydrothermal circulation is still a significant source of Li to the ocean (equal to the river flux).

The steady-state Li concentration ratio for a given relative factor (X) is a linear function of changes in the hydrothermal input (N). For a Li hydrothermal flux 10 times the river flux, the steady-state Li concentration would be 18% greater for a 20% increase in hydrothermal fluxes ($N = 1.2$); for a hydrothermal flux approximately equal to the river flux, a 20% increase in hydrothermal flux result in a 10% increase in the steady-state Li concentration; and for a hydrothermal flux 0.5 times the river flux (i.e., one-twentieth of the flux calculated by Edmond et al., 1979), a 20% increase in hydrothermal flux results in a 7% increase in steady-state oceanic Li concentration. Examination of the Li/Ca foraminiferal calcite record (Figure 4.1), coupled with this analysis of the Li mass balance, indicates that hydrothermal fluxes at any time in the past 100 m.y. could not have exceeded those at present by more than 20%, even for global extrapolations significantly lower than those calculated by Edmond et al. (1979). The assumptions in reaching this conclusion are that: (1) removal constants for Li have not changed with time, (2) river fluxes of Li have not changed with time, and (3) oceanic Li/Ca ratios can be interpreted directly in terms of Li concentrations. These assumptions are examined below.

REMOVAL CONSTANTS

In constructing the mass balance model, Li removal in oceanic sediments and in low-temperature basalt alteration products was assumed to be directly proportional to the oceanic Li concentration. The above calculation of the sensitivity of the oceanic Li concentration to changes in hydrothermal fluxes was done assuming that these first-order time constants were invariant in the systems compared. The possibility of

variations in the removal processes and the effect on oceanic Li concentration are examined here.

The mechanism of the enrichment of Li in oceanic sediments is not known; it is undoubtedly some monotonic function of oceanic Li concentration. If removal is due to a reaction occurring in all detrital igneous sedimentary material, then global increases in sedimentation rates of this material could result in a change in the operation of the sedimentary sink, equivalent to an increase in the removal constant. Removal may be more localized, however, in authigenic phases or in specific geographical locations. Quantifying the changes in the removal constant for this process requires more detailed knowledge of the mechanisms involved.

The second major Li sink is enrichment in low-temperature basalt alteration products. Again, the specific phases accounting for this removal and the conditions governing their formation are not known. It is possible that when crustal generation rates and hydrothermal fluxes increase, the size of the oceanic crustal Li sink could also increase.

If removal constants do increase when hydrothermal fluxes increase, the sensitivity of the oceanic Li concentration as an indicator of hydrothermal fluxes decreases. In the extreme, if both removal processes are directly proportional to hydrothermal fluxes, the steady-state Li concentration is approximately constant for all variations in hydrothermal fluxes.

If the sedimentary sink, the low-temperature basalt alteration sink, and the hydrothermal inputs do covary, this is a powerful feedback loop maintaining constant oceanic Li concentrations. If removal does vary with inputs, it is, however, more likely that only the basalt alteration sink is

proportional to the hydrothermal flux to the ocean. The removal of Li in the oceanic sedimentary sink must consume the river flux and some fraction of the hydrothermal flux; the ocean crust as a whole must represent a net source for Li to the ocean as discussed in Appendix 4.1. For the models requiring lower hydrothermal fluxes, a proportionally smaller quantity of Li is removed in the oceanic crustal sink. The lower the proportion of the total Li input flux due to hydrothermal circulation, the smaller the proportion of removal due to low-temperature basalt alteration. Therefore, the sensitivity of Li as an indicator is less degraded by covariations of the hydrothermal flux and the basalt alteration sink if hydrothermal fluxes are smaller than those calculated by Edmond et al. (1979).

RIVER FLUXES

The assessment of the sensitivity of oceanic Li concentration as an indicator of changing hydrothermal inputs assumed that river fluxes remained constant while hydrothermal inputs varied. Plausible geologic arguments can be constructed for a wide range of assumptions -- faster seafloor spreading rates mean periods of increased orogeny (because of the link between rates of crustal production and consumption) and therefore faster weathering and increased river fluxes or faster seafloor spreading rates mean that a greater percentage of the continental area is covered by water therefore weathering rates and river fluxes are smaller. As well, continental fluxes may vary with the distribution of land masses. River dissolved fluxes and particulate loads may vary independently.

In general, if the river flux increases when the hydrothermal flux does, the ratio of the steady-state Li concentrations is larger for a given increase in hydrothermal flux than if the river flux were constant. If the

river flux decreases when the hydrothermal flux increases, the oceanic Li concentration is not as sensitive an indicator to changes in the hydrothermal flux; the ratio of the steady-state Li concentrations is smaller. The degree of sensitivity enhancement or suppression depends on the proportion of the total Li flux due to river input. The greater the river fraction, the greater the effect of covariations of the river and hydrothermal fluxes.

CALCIUM AND LITHIUM

Another hypothesis to explain the relative constancy of the oceanic Li/Ca ratio over the last 100 m.y. is that oceanic Ca and Li concentrations have both varied. Ca and Li have different oceanic cycles (Table 1.1). Hydrothermal circulation is an important source for Li, approximately ten times the river flux according to the fluxes computed by the assumptions of Edmond et al. (1979). For Ca, the hydrothermal flux is only 15 - 30% of the river flux. While the magnitude of the extrapolated global fluxes may be incorrect (Sleep et al., in press), the relationship between the elemental fluxes must remain the same. If hydrothermal fluxes are one-tenth those calculated by Edmond et al. (1979), the hydrothermal Li flux would be equal to the river flux, while the hydrothermal Ca flux would be 1.5 - 3.0% of the river flux. Thus, even if hydrothermal fluxes are lower than those calculated by Edmond et al. (1979), the oceanic Li concentration should be much more responsive to hydrothermal circulation than the Ca concentration.

The major source of Ca is river input; the major sink at present is removal in biogenic carbonates (Turekian, 1965). For Li, the major source is hydrothermal circulation at the ridge crests; the major sinks are

removal in oceanic sediments and low-temperature basalt alteration products. For Li and Ca oceanic concentrations to vary identically with time, geochemical processes at the ridge crest, in the oceanic crust, and on the continents would have to be closely linked so that two such different geochemical cycles exactly balanced. Additionally, the oceanic residence time of Ca is approximately three to five times the residence time of Li as based on the higher hydrothermal fluxes.

To test the hypothesis that the constancy of the oceanic Li/Ca ratio was due to Ca and Li covariations, Li/Sr ratios were calculated in the foraminiferal samples analyzed. Li/Sr ratios in foraminiferal calcite are plotted as a function of age in Figure 4.6. Within the scatter of the data, Li/Sr ratios are approximately constant from 0 - 70 m.y. except for a minimum around 50 m.y. in the foraminiferal shells from Site 305. This minimum is due to low Li/Ca ratios, not high Sr/Ca ratios, in these samples. Li/Sr ratios may increase somewhat from 70 - 110 m.y.

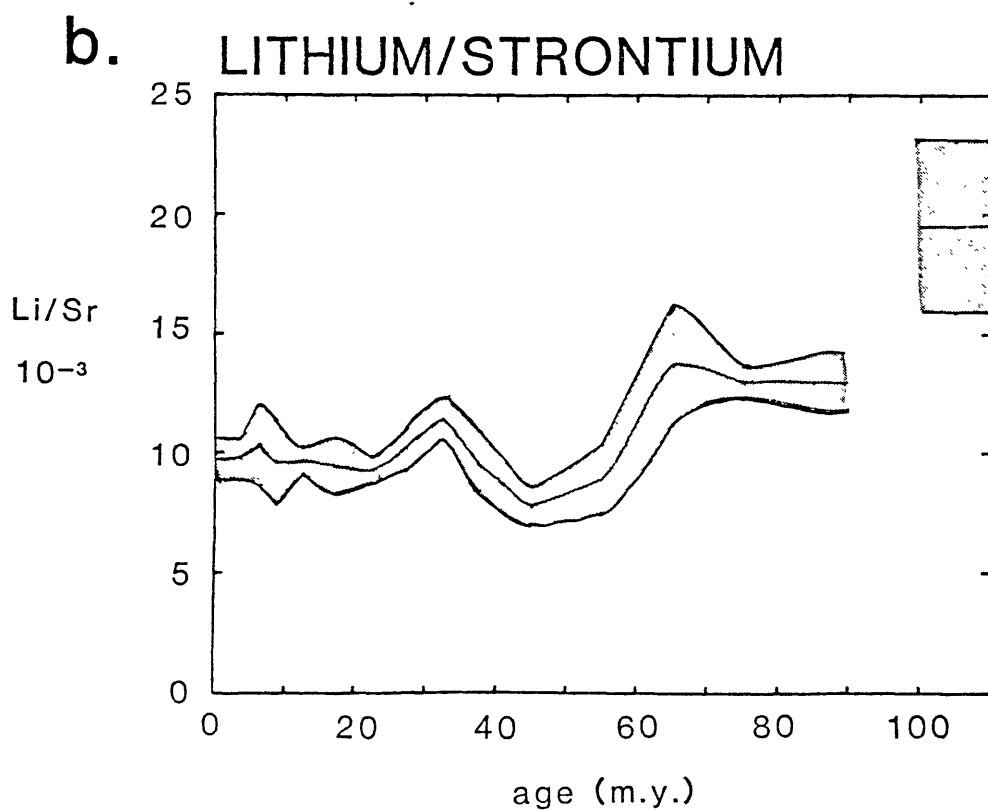
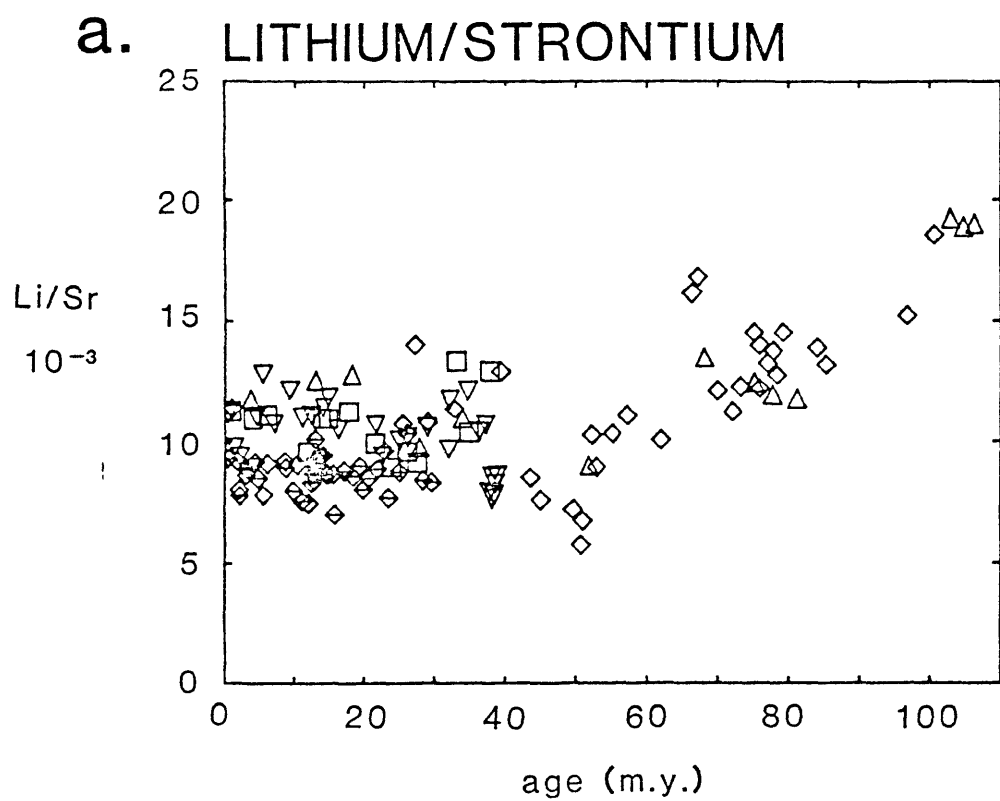
Li and Sr also have very different oceanic cycles. Similarly to Ca, the major source of Sr is river input and the major sink is removal in biogenic calcites (Turekian, 1963). The Sr concentration of hydrothermal solutions does not appear to be changed from that of seawater, although the Sr isotopic ratio of these solutions indicates exchange of seawater Sr isotopes with basaltic Sr isotopes (Table 1.1). The constancy of Li/Sr ratios in the ocean over 70 m.y. also suggests that Li hydrothermal fluxes have not been significantly greater at any time during that period than at present. The higher Li/Sr ratios from 70 -110 m.y. could either be due to higher Li concentrations or lower Sr concentrations. If hydrothermal fluxes had been higher, oceanic Li and Ca concentrations and Li/Ca ratios should have been greater. This is not evident in the foraminiferal calcite

FIGURE 4.6 Li/Sr ratios in foraminiferal calcite as a function of age.

a. Li/Sr ratios in foraminiferal calcite from all sites. Plot symbols are:

- ◇ Site 289 (Leg 30) Ontong-Java Plateau, Pacific
- ◇ Site 305 (Leg 32) Shatsky Rise, Pacific
- Site 366 (Leg 41) Sierra Leone Rise, Atlantic
- △ Site 369 (Leg 41) Spanish Sahara continental slope, Atlantic
- ▽ Site 526 (Leg 74) Walvis Ridge, Atlantic

b. Li/Sr ratios averaged in 2.5 m.y. intervals for 0 - 10 m.y.; 5 m.y. intervals for 10 - 40 m.y.; and 10 m.y. intervals for 40 - 110 m.y. The shaded area represents $\pm 2\sigma/\sqrt{n}$ of the mean for each age interval.



Li/Ca record (Figure 4.1). The general decline in Sr/Ca ratios with increasing age (Figure 4.2) may reflect an increasing proportion of Ca deposition in the past as a calcium carbonate with a higher Sr/Ca ratio, such as in the aragonite deposited by corals. Oceanic Sr concentrations would thus be lower. The conclusion from examining the Li/Sr record remains the same as the one from the Li/Ca record -- oceanic Li concentrations have not been significantly higher than those at present at any time in the last 100 m.y.

CONCLUSIONS

OCEANIC LITHIUM CONCENTRATION

From Li/Ca ratios measured in foraminiferal calcite over the last 100 m.y., including a consideration of the possible coupling of oceanic Li and Ca cycles, the conclusion is that oceanic Li concentration in the past has not exceeded that at present, certainly not by a factor of two.

OTHER CYCLES

Over the time period when oceanic Li/Ca and thus presumably oceanic Li concentration have been constant, seawater Sr isotopic ratios have been increasing (compare Figures 4.1 and 4.5). The Li mass balance model and the foraminiferal calcite records require that hydrothermal fluxes have not been significantly greater at any time in the past 100 m.y. than those at present. The increasing $^{87}\text{Sr}/^{86}\text{Sr}$ contemporaneous seawater ratios toward the present day can not, therefore, be due to a decreasing contribution of basaltic Sr from hydrothermal reactions at the ridge crest.

SEAFLOOR SPREADING RATE CHANGES

If seafloor spreading rates were a factor of two greater 80 - 110 m.y.b.p. (Larson and Pitman, 1973; Turcotte and Burke, 1978; Davis and Solomon, 1981), the oceanic Li concentration could have been as much as a factor of two higher than at present. From an examination of the oceanic mass balance of Li, the effect of changing hydrothermal fluxes, and of other geological variations (sedimentation, low-temperature basalt alteration, continental fluxes), it appears that hydrothermal fluxes in the past have probably not been greater than those at present by more than ~20 - 30%. This conclusion agrees with revised estimates of the magnitude of the sea level change over the past 100 m.y. and of the changes in ridge volume necessary to account for this (Watts and Steckler, 1979; Parsons, 1982). When other factors determining eustatic sea level, such as changes in total oceanic area and changes in the distribution of consumption of oceanic crust with age are considered, only small increases in the crustal generation rate (on the order of ~12%) are necessary to be compatible with the observed sea levels (Parsons, 1982).

The Li/Ca ratios in foraminiferal calcite rule out the possibility that crustal generation rates and hydrothermal fluxes were a factor of two greater 80 - 110 m.y.b.p. Foraminiferal calcite Li/Ca ratios lower than those at present have occurred in the past. Interpretation of these decreases will require more precise analyses and a more exacting screening of samples. Additionally, the Li mass balance model used in reaching this conclusion required a number of assumptions. To evaluate the smaller Li/Ca changes, more careful consideration of the other factors (river fluxes, removal constants, etc.) would be required to make definitive statements about smaller-scale hydrothermal flux variations.

APPENDIX 4.1 Li -- reservoirs and fluxes¹SEAWATER

Reported Li concentrations in seawater are 24 - 28 $\mu\text{mol/l}$ (Chow and Goldberg, 1962; Riley and Tongudai, 1964; Angino and Billings, 1966). Li has conservative water column behavior and is well-mixed in the ocean.

RIVERS

The world average concentration of Li in rivers was estimated to be 0.43 $\mu\text{mol/l}$ (Turekian, 1969). A survey of major rivers confirmed this value (M.I.T. laboratory, as reported in Edmond et al., 1979). In a survey of large North American rivers, the Li concentration range was 0.01 - 5.3 $\mu\text{mol/l}$; the median was 0.16 $\mu\text{mol/l}$ (Duram and Haffty, 1963). A range of 0.01 - 23 $\mu\text{mol/l}$ was found in Russian rivers and a world-wide weighted mean of 0.36 $\mu\text{mol/l}$ suggested (Morozov, 1969).

The estimates for the average Li concentration in rivers range from 0.2 - 0.4 $\mu\text{mol/l}$. Assuming a river flux to the ocean of 3.15×10^{16} l/y, these concentrations are equivalent to a dissolved Li flux of $6 - 14 \times 10^9$ mol/y. The higher estimated river flux is used in the mass balance model in Chapter 4.

RIDGE CREST HYDROTHERMAL CIRCULATION

The 350° C hydrothermal solution end member Li concentrations from the systems sampled to date range from 630 - 1320 $\mu\text{mol/kg}$ (data sources: Galapagos Spreading Center, Edmond et al., 1979; 21° N, East Pacific Rise,

¹For the sake of consistency and geochemical sense, literature values have been converted to mole units in the following discussion: mol/l or mol/kg for water; mol/kg for solids. The atomic weight of Li is 6.939 g/mol. Seawater density is assumed to be 1.026 g/cm³; freshwater density, 1.0 g/cm³.

1979 expedition, Edmond et al., 1982; 21° N, East Pacific Rise, 1981 expedition and Guaymas Basin, Gulf of California, Von Damm, 1983). The resultant estimated global Li fluxes to the ocean range from 90 - 190 x 10⁹ mol/y. An intermediate value of 140 x 10⁹ mol/y is used in the mass balance model in Chapter 4.

Geophysical models of hydrothermal circulation have been recently used to suggest that the hydrothermal fluxes to the ocean are one-sixth to one-tenth those calculated by Edmond et al. (1979) (Sleep et al., in press). A hydrothermal flux of 14 x 10⁹ mol/y of dissolved Li to the ocean, equal to the river flux, is used in the mass balance model in Chapter 4 to represent these extrapolations.

BASALTS

The average Li concentration in oceanic tholeiitic basalts was estimated to be 1.3 ± 0.9 mmol/kg (Engel et al., 1965). The range of Li concentrations in northeast Atlantic tholeiitic basalts found in a literature survey was 0.6 - 1.0 mmol/kg (Bailey and Gwozdz, 1978). Experimental water-rock systems (Ellis and Mahon, 1964; Gieskes et al., 1982), interstitial water and bulk sediment chemistry in the Guaymas Basin (Gieskes et al., 1982), hydrothermally altered oceanic basalts (Humphris, 1977), and evidence from continental thermal springs water samples (Brondi et al., 1973) all demonstrated the mobility of Li in high-temperature water-rock interactions. The water flux through the ridge system is 1.41 x 10¹⁷ g/y, assuming a convective heat flux of 4.9 x 10¹⁹ cal/y, an end-member temperature of 350° C, an ambient water temperature of 2° C, and a specific heat for water of 1.0 cal/g. The reaction of basalt of oceanic tholeiitic composition to produce the estimated hydrothermal flux of

140 x 10⁹ mol/y requires a water/rock ratio of 1.3, assuming complete removal of Li from the rock phase. The depth of reaction required is 12 km assuming that the current production of lithosphere at the ridge crest is 2.94 km²/y (Wolery and Sleep, 1976) and that basalt density is 3.0 g/cm³. The uncertainty in the average oceanic tholeiitic basalt composition is large (60% at least); a larger initial basalt concentration would give a larger water/rock ratio and a shallower depth of reaction. Conversely, incomplete removal of Li from the basalt phase or a lower initial concentration would require a greater reaction depth.

CONTINENTAL MATERIAL

A survey of literature reports of Li measurements in igneous rocks gave the values (Styrt, 1977):

granite	7.3 mmol/kg
basalt	2.7 mmol/kg
"average" igneous rock	5.0 mmol/kg

Morozov (1969) gave the following values (see his Table 2):

igneous rock	4.6 mmol/kg
soils	4.3 mmol/kg
river suspensates	8.5 mmol/kg

In several western American rivers, the mean concentration of suspended load particulates (> 2.5 μm) was 2 mmol/kg; of bottom sediment, 4.4 mmol/kg (Sreekumaran et al., 1968).

OCEANIC SEDIMENTS

Based on a survey of sedimentary rocks, the suggested Li concentration in average sediment is 7.6 mmol/kg (Horstmann, 1957). A

literature survey gave the following values (Styrt, 1977):

shales and clays	10 mmol/kg
sandstones	4.5 mmol/kg
carbonates	2.2 mmol/kg
"average" sedimentary rock	6.7 mmol/kg

Eleven Atlantic clay samples from five cores had a Li concentration range of 8.4 - 16.3 mmol/kg, with a mean of 13.1 mmol/kg (Ohrdorf, 1968). Pacific sediments had a range of 7.1 - 10.1 mmol/kg (Goldberg and Arrhenius, 1958). A study of Gulf of Mexico sediments determined an average Li concentration of 5.0 mmol/kg (Welby, 1958).

These averages show that the average Li content of oceanic sediments is higher than the average content in source rocks (Styrt, 1977); marine shales are enriched in Li (and boron) relative to fresh water shales (Keith and Degens, 1959). A representative concentration range from these measurements for oceanic sediments is 8 - 10 mmol/kg.

Assuming an average river suspended load of 400 mg/l (equivalent to a flux of 1.3×10^{16} g rock/y to the ocean (Turekian, 1969)) with a Li concentration of 5 mmol/kg as the source for oceanic sediments, the enrichment of oceanic sediments to 10 mmol/kg is a Li sink for 65×10^9 mol/y. If a smaller estimate for the amount of igneous rock being weathered is used (0.5×10^{16} g/y; Holland, 1978), oceanic sediments are a Li sink for 25×10^9 mol/y. A smaller enrichment in oceanic sediments would remove proportionally less Li. These removals are two to five times the dissolved river input of 14×10^9 mol/y and 16 - 42% of the estimated total maximum hydrothermal and river flux of 154×10^9 mol/y.

These estimates of the oceanic sediment Li sink are probably order of magnitude approximations. The chemical process by which Li is enriched in average oceanic sediment is not known. This enrichment may be due to the

formation of authigenic phases. The detrital flux of sediments to the ocean and its temporal variability may not be directly related to the size of the sedimentary Li sink.

LOW TEMPERATURE BASALT ALTERATION PRODUCTS

A range of Li concentrations in submarine weathered basalts of 1.2 - 8.7 mmol/kg was measured (Thompson and Melson, 1970), enrichments of 0.9 - 6.7 over the oceanic tholeiitic basalt value of 1.3 mmol/kg. A literature survey of Li concentrations in northeast Atlantic tholeiitic basalts found values ranging from 1.5 - 3 mmol/kg for weathered samples (Bailey and Gwozdz, 1978). A study of dredged pillow basalts (Thompson, 1973) gave a range of enrichment factors of 2 - 10 for altered glass rim/fresh basalt and 2 - 4 for altered basalt interior/fresh basalt.

Secondary phases of diagenetically altered, deep-ocean floor, tholeiitic basalts were analyzed for (Li + B) using charged particle track analysis (McMurtry et al, 1979). The results showed:

celadonite	600-700 ppm Li + B
saponite	30-160 ppm Li + B

Whole-rock analyses of these altered basalts showed:

celadonite zones	40-170 ppm Li + B
saponite zones	40-130 ppm Li + B

B enrichment factors in altered glass zones in dredged pillow basalts were greater than those for Li, approximately 10 (Thompson, 1973). By assuming that 50 ppm of the above whole-rock enrichments are B (5 ppm B in oceanic tholeiites; Fairbridge, 1972), the whole rock analyses represent:

celadonite zones	0-17 mmol/kg Li
saponite zones	0-12 mmol/kg Li

B concentrations are probably overestimated for the less weathered

samples, so the lower limits for Li concentrations are underestimated. The upper Li limits are enrichments of 9 - 13 over fresh basalts.

At DSDP sites 478 and 481 (Leg 64) in the Guaymas Basin, Gulf of California, basaltic sills were present at depth in the sediment. The sills are currently at temperatures of 30 - 35° C, while isotopic evidence indicated that temperatures during intrusion were greater than 167° C (Gieskes et al., 1982). Interstitial water profiles showed reversals in dissolved Li gradients above and below the sills (Gieskes et al., 1982; Site 478, reversal only below the sill). These profiles are evidence for the release of Li to solution in high-temperature water-rock (or water-sediment reactions) and for the uptake of Li in low-temperature water-rock reactions. This behavior was confirmed by sampling of solutions from experimental water-rock reactions which showed increasing solution Li concentrations in reactions at 200° C and 300° C; slight decreases in dissolved Li at 150° C; and no change in dissolved Li after 27 months at 25° C (Gieskes et al., 1982).

The estimated oceanic sedimentary Li sink leaves 58 - 84% of the maximum total Li input to be removed ($90 - 130 \times 10^9$ mol/y). (If the lower hydrothermal fluxes are assumed, the oceanic sedimentary sink can account for removal of the total estimated input.) Low-temperature alteration processes accompanying seawater circulation in the crust occur to at least 500 m and the chemically active phase may terminate within 5 - 10 m.y. after crustal formation (Hart and Staudigel, 1978; Richardson et al., 1980). Circulation and alteration may occur to depths greater than 500 m; depths up to 5 km have been suggested on the basis of heat flow arguments (Anderson et al., 1977). If alteration occurs to 500 m depth, removal of the maximum Li flux remaining would result in an average crustal

composition for this 500 m section of 20 - 30 mmol/kg, enrichments of 15 - 23 times the oceanic tholeiitic basalt concentration of 1.3 mmol/kg. Different secondary alteration products may have different Li concentrations; the effects of reactions on the chemistry of the water and rock reacting may depend on the phases formed as seen for K and Rb (Staudigel et al., 1981; Staudigel and Hart, 1983). Li concentrations typical in alteration products and estimates of the modal abundances of these secondary phases for the entire ocean crust (Staudigel and Hart, 1983) are needed to define the exact size of the oceanic crustal Li sink.

The maximum hydrothermal flux model requires alterations of large amounts of the ocean crust for both inputs and removals of Li. The sizes of the sedimentary and basalt sinks are not adequately constrained from existing data to precisely define the hydrothermal flux. In either model of the extrapolated hydrothermal fluxes, the ocean crust as a whole is a source for Li since some of the hydrothermal flux of Li from high-temperature basalt-seawater reactions is removed by oceanic sediments. This can be contrasted with the behavior of the other alkalis, K, Rb, and Cs, for which the ocean crust, as a whole, was estimated to be a sink (Hart and Staudigel, 1982).

REFERENCES -- CHAPTER 4

- Anderson, R. N., M. G. Langseth, and J. G. Sclater (1977) The mechanisms of heat transfer through the floor of the Indian Ocean, *Jour. Geophys. Res.* 82: 3391-3409.
- Angino, E. E. and G. K. Billings (1966) Lithium content of seawater by atomic absorption spectroscopy, *Geochim. Cosmochim. Acta* 30: 153-158.
- Bailey, J. C. and R. Gwozdz (1978) A low-Li geochemical province in the NE Atlantic, *Lithos* 11: 73-84.
- Berggren, W. A., D. P. McKenzie, J. G. Sclater, and J. E. Van Hinte (Discussion) and Larson, R. L. and W. C. Pitman III (Reply) (1975) World-wide correlation of Mesozoic magnetic anomalies and its implications: discussion and reply, *Geol. Soc. Amer. Bull.* 86: 267-272.
- Brass, G. W. (1976) The variation of the marine $^{87}\text{Sr}/^{86}\text{Sr}$ ratio during Phanerozoic time: interpretation using a flux model, *Geochim. Cosmochim. Acta* 40: 721-730.
- Brondi, M., M. Dall'Aglia, and F. Vitroni (1973) Lithium as a pathfinder element in the large-scale hydrogeochemical exploration for hydrothermal systems, *Geothermics* 2: 142-153.
- Burke, W. H., R. E. Denison, E. A. Hetherington, R. B. Koepnick, H. F. Nelson, and J. B. Otto (1982) Variation of seawater $^{87}\text{Sr}/^{86}\text{Sr}$ throughout Phanerozoic time, *Geology* 10: 516-519.
- Chow, T. J. and E. D. Goldberg (1962) Mass spectrometric determination of lithium in seawater, *Jour. Mar. Res.* 20: 163-167.
- Dasch, E. J. and P. E. Biscaye (1971) Isotopic composition of strontium in Cretaceous-to-Recent, pelagic foraminifera, *Earth Planet. Sci. Lett.* 11: 201-204.
- Davis, D. M. and S. G. Solomon (1981) Variations in the velocities of the major plates since the Late Cretaceous, *Tectonophys.* 74: 189-208.
- Duram, W. H. and J. Haffty (1963) Implications of the minor element content of some major streams of the world, *Geochim. Cosmochim. Acta* 27: 1-11.
- Edmond, J. M., C. Measures, R. E. McDuff, L. H. Chan, R. Collier, B. Grant, L. I. Gordon, and J. B. Corliss (1979) Ridge crest hydrothermal activity and the balances of the major and minor elements in the ocean: the Galapagos data, *Earth and Planet. Sci. Lett.* 46: 1-18.
- Edmond, J. M., K. L. Von Damm, R. E. McDuff, and C. I. Measures (1982) Chemistry of hot springs on the East Pacific Rise and their effluent dispersal, *Nature* 297: 187-191.

- Ellis, A. H. and W. A. J. Mahon (1964) Natural hydrothermal systems and experimental hot-water/rock interactions, *Geochim. Cosmochim. Acta* 28: 1323-1357.
- Engel, A. E. J., C. G. Engel, and R. G. Havens (1965) Chemical characteristics of oceanic basalts and the upper mantle, *Geol. Soc. Amer. Bull.* 76: 719-734.
- Fairbridge, R. W., ed. (1972) The Encyclopedia of Geochemistry and Environmental Sciences, IVA, The Elements, New York, Van Nostrand Reinhold Co.
- Gieskes, J. M., H. Elderfield, J. R. Lawrence, J. Johnson, B. Meyers, and A. Campbell (1982) Geochemistry of interstitial waters and sediments, Leg 64, Gulf of California, in Curray, J. R., D. G. Moore, et al. (1982) Initial Reports of the Deep Sea Drilling Project, volume 64, Washington, U. S. Government Printing Office, pp. 675-694.
- Goldberg, E. D. and G. O. S. Arrhenius (1958) Chemistry of Pacific pelagic sediments, *Geochim. Cosmochim. Acta* 13: 153-212.
- Graham, D. W., M. L. Bender, D. F. Williams, and L. D. Keigwin, Jr. (1982) Strontium-calcium ratios in Cenozoic planktonic foraminifera, *Geochim. Cosmochim. Acta* 46: 1281-1292.
- Hart, S. R. and H. Staudigel (1978) Oceanic crust: age of hydrothermal alteration, *Geophys. Res. Lett.* 5: 1009-1012.
- Hart, S. R. and H. Staudigel (1982) The control of alkalies and uranium in seawater by ocean crust alteration, *Earth and Planet. Sci. Lett.* 58: 202-212.
- Holland, H. D. (1978) The Chemistry of the Atmosphere and Oceans, New York, John Wiley and Sons.
- Horstmann, E. L. (1957) The distribution of lithium, rubidium, and caesium in igneous and sedimentary rocks, *Geochim. Cosmochim. Acta* 12: 1-28.
- Humphris, S. E. (1977) The hydrothermal alteration of oceanic basalts by seawater, Ph.D. thesis, M.I.T./W.H.O.I.
- Jenkins, W. J., J. M. Edmond, and J. B. Corliss (1978) Excess ^3He and ^4He in Galapagos submarine hydrothermal waters, *Nature* 272: 156-158.
- Keith, M. L. and E. T. Degens (1959) Geochemical indicators of marine and fresh-water sediments, in Abelson, P. H., ed., Researches in Geochemistry, vol. 1: 38-61.
- Kitano, Y., M. Okumura, and M. Idogaki (1975) Incorporation of sodium, chloride and sulfate with calcium carbonate, *Geochem. Jour.* 9: 75-84.

- Larson, R. L. and W. C. Pitman III (1972) World-wide correlation of Mesozoic magnetic anomalies and its implications, *Geol. Soc. Amer. Bull.* 83: 3645-3662.
- McMurtry, G. M., A. J. Andrews, and J. D. Macdougall (1978) In situ distribution and abundances of lithium, boron and uranium in secondary minerals of deep-ocean basalts, *Trans. Amer. Geophys. Union* 60: 973.
- Morozov, N. P. (1969) Geochemistry of the alkali metals in rivers, *Geochem. Intern.* 6: 585-594.
- Ohrdorf, R. (1968) Ein Beitrag zur Geochemie des Lithiums in Sedimentgesteinen, *Geochim. Cosmochim. Acta* 32: 191-208.
- Parsons, B. (1982) Causes and consequences of the relation between area and age of the ocean floor, *Jour. Geophys. Res.* 87(B1): 289-302.
- Peterman, Z. E., C. E. Hedge, and H. A. Tourtelot (1970) Isotopic composition of strontium in seawater throughout Phanerozoic time, *Geochim. Cosmochim. Acta* 34: 105-120.
- Richardson, S. H., S. R. Hart, and H. Staudigel (1980) Vein mineral ages of old oceanic crust, *Jour. Geophys. Res.* 85: 7195-7200.
- Riley, J. P. and M. Tongudai (1964) The lithium content of seawater, *Deep-Sea Res.* 11: 563-568.
- Sleep, N. H., J. L. Morton, L. E. Burns, and T. J. Wolery (in press) Geophysical constraints on the volume of hydrothermal flow at the ridge axes.
- Sreekumaran, C., K. C. Pillai, and T. R. Folsom (1968) The concentrations of lithium, potassium, rubidium, and cesium in some western American rivers and marine sediments, *Geochim. Cosmochim. Acta* 32: 1229-1234.
- Staudigel, H., S. R. Hart, and S. H. Richardson (1981) Alteration of the oceanic crust: processes and timing, *Earth Planet. Sci. Lett.* 52: 311-327.
- Staudigel, H. and S. R. Hart (1983) Alteration of basaltic glass: mechanisms and significance for the oceanic crust-seawater budget, *Geochim. Cosmochim. Acta* 47: 337-350.
- Styrt, M. M. (1977) Variations in lithium concentration between igneous and sedimentary rocks, B. S. thesis, Radcliffe College.
- Thompson, G. (1973) Trace-element distribution in fractionated oceanic rocks 2. Gabbros and related rocks, *Chem. Geol.* 12: 99-111.
- Thompson, G. and W. G. Melson (1970) Boron contents of serpentinites and metabasalts in the oceanic crust: implications for the boron cycle in the oceans, *Earth Planet. Sci. Lett.* 8: 61-65.

- Turcotte, D. L. and K. Burke (1978) Global sea-level changes and the thermal structure of the earth, *Earth Planet. Sci. Lett.* 41: 341-346.
- Turekian, K. K. (1963) Rates of calcium carbonate deposition by deep-sea organisms, molluscs, and the coral-algae association, *Nature* 197: 277-278.
- Turekian, K. K. (1965) Some aspects of the geochemistry of marine sediments, *in* Riley, J. P. and G. Skirrow, eds, Chemical Oceanography, vol. 2, chap. 16, pp. 81-126.
- Turekian, K. K. (1969) The oceans, streams, and atmosphere, *in* Wedepohl, K. H., ed., Handbook of Geochemistry, vol. 1, chap. 10.
- Veizer, J. and W. Compston (1974) $^{87}\text{Sr}/^{86}\text{Sr}$ composition of seawater during the Phanerozoic, *Geochim. Cosmochim. Acta* 38: 1461-1484.
- Von Damm, K. L. (1983) Chemistry of submarine hydrothermal solutions at 21° N, East Pacific Rise and Guaymas Basin, Gulf of California, Ph.D. thesis, M.I.T./W.H.O.I.
- Watts, A. B. and M. S. Steckler (1979) Subsidence and eustacy at the continental margin of Eastern North America, *in* Talwani, M., W. Hay, and W. B. F. Ryan, eds., Deep Drilling Results in the Atlantic Ocean: Continental Margins and Paleoenvironment, Maurice Ewing Series, vol. 3, AGU, Washington, D.C., pp. 235-248.
- Welby, C. W. (1958) Occurrence of alkali metals in some Gulf of Mexico sediments, *Jour. Sed. Petrol.* 28: 431-452.
- White, A. (1978) Sodium coprecipitation in calcite and dolomite, *Chem. Geol.* 23: 65-72.
- Wolery, T. J. and N. H. Sleep (1976) Hydrothermal circulation and geochemical flux at mid-ocean ridges, *Jour. Geol.* 84: 249-275.

CHAPTER FIVE:

CONCLUSIONS

This thesis has examined the role of foraminiferal calcite as an indicator primarily of oceanic Li/Ca ratios. The paleochemical history of Li deduced from measurements in foraminiferal calcite from the past 100 m.y. implies that hydrothermal fluxes from high-temperature basalt-seawater reactions at the ridge crest have not significantly exceeded those at present. In turn, given the present understanding of the connection between crustal generation rates and hydrothermal circulation, this suggests that sea floor spreading rates have also remained approximately constant. These conclusions have profound implications about geophysical and geochemical cycles over the last 100 m.y.

As part of this research, laboratory culture experiments on modern planktonic foraminifera tested the relationships between the chemistry of the foraminiferal shells and the seawater from which the shells were deposited. This was the first direct determination of these chemical relationships in foraminifera. Because of the importance of foraminiferal shells for biostratigraphy and for determining oceanic paleotemperatures from their oxygen isotopic ratios, they are potentially exciting tracers of oceanic paleochemistry. Recent work on Cd/Ca ratios in benthic foraminifera in glacial/interglacial cycles over the last 100 m.y. and on Sr/Ca ratios in planktonic foraminifera in the Cenozoic have demonstrated their usefulness in this regard.

This thesis has touched on several questions which need more thorough investigation before the interpretation of the chemical compositions of these shells are truly secure. Vital and species effects on trace elemental ratios must be understood. In particular, there are differences in the trace element compositions of biogenic and inorganic calcites precipitated from seawater. The causes of these differences (e.g., precipitation rate differences as is probably the explanation for Sr, or physiological discrimination) must be related to basic chemical principles. The crystal sites and modes of incorporation of elements (especially ones such as Na) must be determined as part of this understanding. To investigate the biological and chemical processes controlling the trace elemental ratios in foraminiferal shells, the effects of environmental parameters other than temperature must also be studied.

This thesis discussed the effects of diagenesis after deposition in the sediments, particularly recrystallization, on the chemical composition of foraminiferal calcite. There is much to be learned about these processes and the controlling mechanisms that determine how and when changes take place. The knowledge of inorganic calcite distribution coefficients for the incorporation of trace elements is incomplete. A more thorough evaluation of the effect of the chemistry of typical interstitial water and of the chemical and mineralogical composition of the sediments is needed. As with biogenic calcites, the crystal sites and modes of incorporation of trace elements should be determined for inorganic calcites. This may help explain the differences in biogenic and inorganic calcites. Significant progress in understanding carbonate diagenesis should come from the use of Sr isotopic ratios and Sr/Ca ratios in interstitial water and calcite in the sediments, coupled with mass balance

models which include diffusive transport. The understanding of chemical diagenetic effects on biogenic calcite is important in evaluating oceanic paleotemperature history from the oxygen isotopic ratios of foraminiferal shells.

Two as yet unresolved questions about geochemical cycles were discussed in the thesis: (1) the magnitude of global hydrothermal fluxes to the ocean and (2) the role of the oceanic crust as both a source and sink for elemental oceanic cycles. Further determinations of present day mass balances and of oceanic chemical history can help define the answers.

APPENDIX 1 Analytical methods for trace elemental ratios in foraminiferal calcite

Foraminiferal calcite samples were typically 0.5 - 1.0 mg calcite dissolved in 300 μ l 0.3 N HNO_3 , with proportionally smaller dissolution volumes when sample material was limited. Li, Sr, Mg, Na, and K were determined by graphite furnace atomic absorption spectroscopy (GFAAS). Ca was determined by flame atomic absorption spectroscopy (FAAS).

Li was analyzed on undiluted aliquots of the samples. Ca and Sr were analyzed on dilutions of the samples, typically 10 μ l sample solution in 5 ml distilled water. A 250 μ l aliquot was used for Sr GFAAS analyses; La was added to the remainder as an interference suppressant before Ca FAAS analyses. Mg and Na were analyzed on a dilution of the samples, usually 20 μ l sample solution added to 500 μ l 0.3 N HNO_3 . Some K analyses were done on the dilutions used for Mg and Na analyses. Because of contamination problems, K was later analyzed on undiluted samples on a reduced sensitivity line.

A Perkin-Elmer Model 5000 spectrophotometer with a Perkin-Elmer HGA-500 or HGA-400 heated graphite analyzer and a Perkin-Elmer AS-1 Auto-sampling system were used for GFAAS analyses. Background correction with a continuum source was utilized for all GFAAS analyses (deuterium arc for wavelengths < 350 nm; tungsten halide lamp for wavelengths > 350 nm). Ca FAAS analyses were done using a Perkin-Elmer Model 403 spectrophotometer with a triple-slot burner and an air-acetylene flame.

CALCIUM

For the Ca FAAS determinations, La was added to samples and standards to suppress interferences; samples and standards were brought to the same acid concentration (final sample and standard solutions were ~5 mmol La/l in 0.1 N HCl). Standard readings were taken at intervals throughout a sample run. Sample absorbances were corrected for the La blank. Dilution blanks were generally equivalent to the blank due to the La alone.

GFAAS ANALYSES

Analytical conditions and furnace programs are listed in Table A1.1. Ca and acid concentrations interferences were investigated for the various elements and were not found to be significant. Even so, sample and standard Ca and acid concentrations were kept as uniform as possible to minimize the potential for unrecognized interferences.

Secondary standards were diluted for each sample set from primary standards whose compositions are listed in Table A1.2. Working standards from these secondary standards were made up in a Ca-NO₃ matrix diluted to approximately match the samples in Ca concentration. Four point standard curves were run at frequent intervals during the analysis of a sample set, approximately every 6 - 12 sample injection pairs. Standard concentrations and furnace conditions were chosen to give absolute absorbances in the linear range for the highest standard (generally maximum absorbance < 0.15) and to bracket the sample concentrations. Samples and standards were injected in duplicate. When duplicate injections disagreed significantly, the solution was reinjected.

TABLE A1.1 Analytical conditions and furnace programs

ANALYTICAL CONDITIONS

element	wavelength (nm)	slit (nm)	comments	atomization temperature	gas flow during atomization
Li	670.8	1.4 0.4	wider slit in earlier runs	2500° C MPH	30
Sr	460.7	0.4		2500° C MPH	160
Mg	202.6	0.7	secondary line	2200° C MPH	250
Na	330.2 330.3	2.0	secondary line	2100° C MPH	50
K	769.9	1.4	diluted samples secondary line	2400° C 1 sec ramp	30
	404.41 404.72	2.0	undiluted samples secondary line	2400° C MPH	30
Ca	422.7	1.4	PE 403 FAAS air-acetylene flame		

FURNACE PROGRAMSHGA-500 program

step	#	temp (°C)	ramp time (sec)	hold time (sec)	recorder on (sec)	read cycle (sec)	auto- zero (sec)	gas flow (ml/min)
	1	140	1	0				
drying	2	160	15	10				
char	3	1000	15	10	23	19	24	
atomization	4	2500	0	4	0	0		30
cleaning	5	2700	2	2	0			
cool-down	6	20	1	1	0			

HGA-400 program

step	#	temp (°C)	ramp time (sec)	hold time (sec)	recorder on (sec)	read cycle (sec)	auto- zero (sec)	mini flow starts
	1	140	1	0				
drying	2	160	15	10				
char	3	1000	15	7		19		
char	4	1000	1	2	1		2	0
atomization	5	2500	0	4	0	0		0
cleaning	6	2700	2	2	0			
cool-down	7	20	1	1	0			

Comments:

Argon was used as the purge gas throughout. Drying temperatures were adjusted as necessary to ensure smooth, complete drying of the sample aliquots. If drying temperatures were substantially higher than normal, either due to low cooling water temperature or to formation of abnormal resistive coatings on the furnace, char temperatures were raised by an equivalent amount.

For atomizations with 0 sec ramp time (maximum power heating or MPH), the atomization temperature was calibrated with an optical pyrometer. Gas flows on the HGA-500 are entered as numbers in the program and controlled by internal valves. Gas flows on the HGA-400 are turned on and off by the program, but are set manually by a valve with readings on an analog meter. Reduced gas flows take longer to come to equilibrium on the HGA-400 as deduced from visual observations of the gas flow meter. The programs for the HGA-400 thus have a split char step with reduced gas flow in the second part.

Early runs for all elements used graphite tubes which were pyrolytically coated using a mixture of methane and argon with the HGA-500. Later runs for Mg used non-pyrolytically coated graphite tubes. Later runs for the other elements used the new-style pyrolytically coated graphite tubes which were more sensitive and more stable for these elements.

An integration time of 4 seconds for the read cycle of the PE-5000 was used for all elements. The peak appearance times of these elements are all much shorter than this integration time.

TABLE A1.2 Primary standards

element	concentration ($\mu\text{mol/ml}$)	composition
Ca	20.04	CaCO_3 in ~1% v/v HCl
Li	40.08	Li_2CO_3 in 1% v/v HCl
Sr	19.72	$\text{Sr}(\text{NO}_3)_2$ in 1% v/v HNO_3
Mg	39.45	Mg metal in 1% v/v HCl
Na	20.11	NaCl in distilled water
K	19.84	KCl in distilled water

Distilled water and acid blanks were analyzed with each sample set. Occasionally, an empty sample container was processed as a sample in the cleaning, dissolution, and analysis procedures. These sample handling blanks were low, either zero or equivalent to the low blank levels sometimes found in the acid solutions. When necessary, sample absorbances were corrected for these blanks; the blank corrections were usually not significant compared to sample concentrations and were generally zero.

LITHIUM BLANK

Early runs for Li were plagued by a persistent blank present during an analysis cycle of the tube with no sample. Careful investigation showed this to be an artifact of a negative inflection in the AA-only mode tube signal relative to the BG-only mode tube signal, rather than to any Li being atomized. Early attempts to correct this problem used an elliptical template positioned where the light beam reenters the PE-5000 after passing through the furnace. This template improved the correspondance between the AA and BG sources, and lowered the apparent blank. It also lowered sample absorbances ~10%. Later investigations showed that this "tube blank" could be reduced, usually to zero, by careful alignment of the furnace with the primary source light and of the background corrector with the furnace and primary source.

CALCULATIONS

A drift-corrected slope was calculated for each sample from the slopes of the standard curves before and after an interval of samples and from the number of samples in that interval. This drift-corrected slope was used to compute sample concentrations. For sample i in an interval of

n samples bracketed by standard curves with slopes s_1 and s_2 (in units of absorbance/concentration), the concentration was calculated as:

$$\text{conc}_i = \frac{\text{abs}_i - \text{blank abs}}{s_1 + i\{(s_2 - s_1)/(n + 1)\}}$$

Concentrations were corrected for dilutions to give final results in $\mu\text{mol/ml}$ in the undiluted samples. Results were reported as mole ratios of the trace elements to Ca.

CONSISTENCY STANDARDS, INTERRUN COMPARISONS, AND ANALYTICAL PRECISION

Samples comprising a single data set (e.g. those from a foraminiferal culture experiment or from one DSDP site) were generally analyzed in one GFAAS run. With each set of samples, two to four consistency standards were analyzed. The consistency standards were artificial samples made by dissolving reagent grade CaCO_3 in 0.3 N HNO_3 with spikes of standards added to give concentrations similar to those of samples. They were treated as samples in the dilutions, GFAAS analyses, and calculations.

The concentration results for the consistency standards calculated from individual data runs were averaged to give the best estimate of their solution compositions. Table A1.3 lists the mean concentrations of the consistency standards.

The trace elements in the consistency standards have two sources: the added amounts of solution spikes from the primary standards and the amounts associated with the reagent grade calcite. Because of the uncertainties in the amounts contributed by the calcite, accurate calculations of the expected concentrations are not possible. There is semi-quantitative agreement of expected and measured values. Two of the consistency standards (FC3 and FC4) were made by spiking two aliquots of

TABLE A1.3 Mean values for compositions of consistency standards

standard		Ca	Li (10^{-6})	Sr (10^{-3})	Mg (10^{-3})	Na (10^{-3})	K (10^{-3})
FC3	mean	38.47	589	54.7	81.9	130	4.26
	% SD	2.1%	8.6%	8.2%	6.5%	9.6%	53%
	(n)	(22)	(35)	(37)	(29)	(29)	(7)
FC4	mean	38.87	893	80.5	162	209	5.95
	% SD	1.7%	8.7%	7.0%	6.9%	7.4%	37%
	(n)	(21)	(34)	(36)	(31)	(30)	(7)
FC5	mean	19.93	319	17.0	234	55.2	11.6
	% SD	2.0%	13%	10%	5.2%	21%	10%
	(n)	(19)	(27)	(28)	(23)	(22)	(4)
FC6	mean	29.48	986	31.8	309	244	13.3
	% SD	2.0%	6.8%	8.5%	5.3%	6.8%	16%
	(n)	(18)	(27)	(27)	(23)	(22)	(4)
difference of FC4 and FC3:	measured		304	25.8	80	79	1.69
	expected		297	23.8	77	78	1.93

the same original solution. The difference in concentrations for these two standards can be accurately computed. The expected and measured differences are listed in Table A1.3. A comparison of the two shows that the GFAAS methods are accurately measuring relative concentration differences.

The percent standard deviations of the mean concentrations and number of points included in the mean for the consistency standards are also listed in Table A1.3. The analytical variability is highest for the lowest absolute concentration of each element and decreases with increasing concentration. These percent standard deviations represent the uncorrected differences possible between data sets analyzed separately.

The concentrations determined in each individual run for the consistency standards were divided by the calculated mean values. These ratios were used to calculate an average factor to correct each individual data set to the best average results. This correction procedure ideally eliminates the variability between runs indicated by the standard deviations on the mean concentrations.

The analytical precision for an individual data set was checked at various times by multiple consistency standard analyses within an analytical run. Table A1.4 lists the percent standard deviations and the number of points included in the mean for several such tests. The agreement within an analytical run is substantially better than the uncorrected interrune variability. Most data sets were processed in a single analytical run, so these estimates of precision apply to individual data sets. The correction procedure outlined above improves the agreement between separate analytical runs; those standard deviations represent the maximum uncorrected precision between different data sets.

TABLE A1.4 Standard deviations (%) of means of multiple determinations of consistency standards within analytical runs

run number	standard	n	Ca	Li (10 ⁻⁶)	Sr (10 ⁻³)	Mg (10 ⁻³)	Na (10 ⁻³)
26	FC3	2		0.9	1.1	0.8	4.0
	FC4	2		3.9	1.1	0	4.7
	FC5	2		4.3	0.7	2.1	2.7
	FC6	2		3.1	1.7	0	0.5
43	FC3	3	0.62	1.5	3.4	2.8	2.6
	FC4	3	2.02	1.7	1.4	0.4	2.2
	FC5	3	0.67	1.4	4.0	3.6	7.4
	FC6	3	1.12	1.9	5.6	1.2	3.3
46	FC3	4	0.35	6.5	3.9		
	FC4	4	0.40	5.4	2.9		
	FC5	4	0.72	7.3	11		
	FC6	4	0.63	3.1	6.5		
46	FC3	2				1.9	0.5
	FC4	2				0.4	0.3
	FC5	2				0.3	-
	FC6	2				2.7	0.3
48 ¹	FC3	2				7.1	3.5
	FC4	2				4.7	1.6
	FC5	2				5.5	1.7
	FC6	2				2.0	0.6

Notes: 1. The same conditions and standards were used in these determinations, but different graphite tubes.

REAGENTS AND LABWARE

Distilled water and acids twice distilled in Vycor stills were used for all sample handling and analytical procedures. Centrifuge tubes used as sample holders for cleaning, dissolution, and storage and containers used for GFAAS solutions were acid leached in $\sim 1 \text{ N HCl}$ at 60° C for a minimum of 6 hours. Glass vials used for Sr and Ca dilutions were initially acid-leached and later kept filled with distilled water between analytical runs. All equipment was thoroughly rinsed with distilled water after acid leaching and dried in a Class 100 laminar flow hood. All sample transfers and dilutions were done in a laminar flow hood. Transfers and dilutions were done with Eppendorf and Finn pipettes, with the tips having been rinsed in dilute hydrochloric acid and then distilled water immediately prior to use. Pipettes were calibrated for the actual volumes delivered for each analytical run by weighings of distilled water aliquots. These corrected volumes were used in all calculations.

REFERENCES -- THESIS

- Anderson, R. N., M. G. Langseth, and J. G. Sclater (1977) The mechanisms of heat transfer through the floor of the Indian Ocean, *Jour. Geophys. Res.* 82: 3391-3409.
- Andrews, J. E., G. Packham et al. (1975) Initial Reports of the Deep Sea Drilling Project, volume 30, Washington, U. S. Government Printing Office, pp. 231-398.
- Angino, E. E. and G. K. Billings (1966) Lithium content of seawater by atomic absorption spectroscopy, *Geochim. Cosmochim. Acta* 30: 153-158.
- Bailey, J. C. and R. Gwozdz (1978) A low-Li geochemical province in the NE Atlantic, *Lithos* 11: 73-84.
- Baker, P. A., M. Kastner, J. D. Byerlee, and D. A. Lockner (1980) Pressure solution and hydrothermal recrystallization of carbonate sediments -- an experimental study, *Mar. Geol.* 38: 185-203.
- Baker, P. A., J. M. Gieskes, and H. Elderfield (1982) Diagenesis of carbonates in deep-sea sediments--evidence from Sr/Ca ratios and interstitial dissolved Sr²⁺ data, *Jour. Sed. Petrol.* 52: 71-82.
- Bé, A. W. H. (1977) An ecological, zoogeographic and taxonomic review of Recent planktonic foraminifera, in Ramsay, A. T. S., ed., *Oceanic Micropaleontology*, vol. 1, London, Academic Press, pp. 1-100.
- Bé, A. W. H. (1980) Gametogenic calcification in a spinose planktonic foraminifer, *Globigerinoides sacculifer* (Brady), *Mar. Micropal.* 5: 283-310.
- Bé, A. W. H., C. Hemleben, O. R. Anderson, M. Spindler, J. Hacunda, and S. Tuntivate-Choy (1977) Laboratory and field observations of living planktonic foraminifera, *Micropal.* 23: 155-179.
- Bé, A. W. H., C. Hemleben, O. R. Anderson, and M. Spindler (1979) Chamber formation in planktonic foraminifera, *Micropal.* 25: 294-307.
- Bender, M. L., R. B. Lorenz, and D. F. Williams (1975) Sodium, magnesium and strontium in the tests of planktonic foraminifera, *Micropal.* 21: 448-459.
- Bénière, M., M. Chemla, and F. Bénière (1976) Vacancy pairs and correlation effects in KCl and NaCl single crystals, *Jour. Phys. Chem. Solids* 37: 525-538.
- Berggren, W. A., D. P. McKenzie, J. G. Sclater, and J. E. Van Hinte (Discussion) and Larson, R. L. and W. C. Pitman III (Reply) (1975) World-wide correlation of Mesozoic magnetic anomalies and its implications: discussion and reply, *Geol. Soc. Amer. Bull.* 86: 267-272.

- Blackmon, P. D. and R. Todd (1959) Mineralogy of some foraminifera as related to their classification and ecology, *Jour. Paleontol.* 33: 1-15.
- Boyle, E. A. (1981) Cadmium, zinc, copper, and barium in foraminifera tests, *Earth and Planet. Sci. Lett.* 53: 11-35.
- Boyle, E. A. and L. D. Keigwin (1982) Deep circulation of the North Atlantic over the last 200,000 years: geochemical evidence, *Science* 218: 784-787.
- Brass, G. W. (1976) The variation of the marine $^{87}\text{Sr}/^{86}\text{Sr}$ ratio during Phanerozoic time: interpretation using a flux model, *Geochim. Cosmochim. Acta* 40: 721-730.
- Brätter, P., P. Möller, and U. Rösick (1972) On the equilibrium of coexisting sedimentary carbonates, *Earth Planet. Sci. Lett.* 14: 50-54.
- Broecker, W. S. and T.-H. Peng (1982) *Tracers in the Sea*, Palisades, N.Y., Lamont-Doherty Geological Observatory Press.
- Brondi, M., M. Dall'Aglia, and F. Vitroni (1973) Lithium as a pathfinder element in the large-scale hydrogeochemical exploration for hydrothermal systems, *Geothermics* 2: 142-153.
- Bruland, K. W. (1980) Oceanographic distributions of cadmium, zinc, nickel, and copper in the North Pacific, *Earth Planet. Sci. Lett.* 47: 176-198.
- Burke, W. H., R. E. Denison, E. A. Hetherington, R. B. Koepnick, H. F. Nelson, and J. B. Otto (1982) Variation of seawater $^{87}\text{Sr}/^{86}\text{Sr}$ throughout Phanerozoic time, *Geology* 10: 516-519.
- Chow, T. J. and E. D. Goldberg (1962) Mass spectrometric determination of lithium in seawater, *Jour. Mar. Res.* 20: 163-167.
- CLIMAP Project Members (1976) The surface of the ice-age earth, *Science* 191: 1131-1137.
- Couture, R., R. S. Miller, and J. M. Gieskes (1977) Interstitial water and mineralogical studies, Leg 41, Deep Sea Drilling Project, in Lancelot, Y., E. Siebold, et al. (1977) Initial Reports of the Deep Sea Drilling Project, volume 41, U. S. Government Printing Office, pp. 907-914.
- Cronblad, H. G. and B. A. Malmgren (1981) Climatically controlled variation of Sr and Mg in Quaternary planktonic foraminifera, *Nature* 291: 61-64.
- Curry, W. B. and R. K. Matthews (1981a) Paleo-oceanographic utility of oxygen isotopic measurements on planktic foraminifera: Indian Ocean core-top evidence, *Palaeogeogr., Palaeoclimatol., Palaeoecol.* 33: 173-191.

- Curry, W. B. and R. K. Matthews (1981b) Equilibrium ^{18}O fractionation in small size fraction planktic foraminifera: evidence from Recent Indian Ocean sediments, *Mar. Micropal.* 6: 327-337.
- Dasch, E. J. and P. E. Biscaye (1971) Isotopic composition of strontium in Cretaceous-to-Recent, pelagic foraminifera, *Earth Planet. Sci. Lett.* 11: 201-204.
- Davis, D. M. and S. G. Solomon (1981) Variations in the velocities of the major plates since the Late Cretaceous, *Tectonophys.* 74: 189-208.
- Duplessy, J.-C., P.-L. Blanc, and A. W. H. Bé (1981) Oxygen-18 enrichment of planktonic foraminifera due to gametogenic calcification below the euphotic zone, *Science* 213: 1247-1250.
- Duram, W. H. and J. Haffty (1963) Implications of the minor element content of some major streams of the world, *Geochim. Cosmochim. Acta* 27: 1-11.
- Durazzi, J. T. (1981) Stable-isotope studies of planktonic foraminifera in North Atlantic core tops, *Palaeogeogr., Palaeoclimatol., Palaeoecol.* 33: 157-172.
- Edmond, J. M., C. Measures, R. E. McDuff, L. H. Chan, R. Collier, B. Grant, L. I. Gordon, and J. B. Corliss (1979) Ridge crest hydrothermal activity and the balances of the major and minor elements in the ocean: the Galapagos data, *Earth and Planet. Sci. Lett.* 46: 1-18.
- Edmond, J. M., K. L. Von Damm, R. E. McDuff, and C. I. Measures (1982) Chemistry of hot springs on the East Pacific Rise and their effluent dispersal, *Nature* 297: 187-191.
- Elderfield, H., J. M. Gieskes, P. A. Baker, R. K. Oldfield, C. J. Hawkesworth, and R. Miller (1982) $^{87}\text{Sr}/^{86}\text{Sr}$ and $^{18}\text{O}/^{16}\text{O}$ ratios, interstitial water chemistry and diagenesis in deep-sea carbonate sediments of the Ontong Java Plateau, *Geochim. Cosmochim. Acta* 46: 2259-2268.
- Ellis, A. H. and W. A. J. Mahon (1964) Natural hydrothermal systems and experimental hot-water/rock interactions, *Geochim. Cosmochim. Acta* 28: 1323-1357.
- Emiliani, C. (1955) Mineralogical and chemical composition of the tests of certain pelagic foraminifera, *Micropal.* 1: 377-380.
- Engel, A. E. J., C. G. Engel, and R. G. Havens (1965) Chemical characteristics of oceanic basalts and the upper mantle, *Geol. Soc. Amer. Bull.* 76: 719-734.
- Fairbanks, R. G., M. Sverdløve, R. Free, P. H. Wiebe, and A. W. H. Bé (1982) Vertical distribution and isotopic composition of living planktonic foraminifera from the Panama Basin, *Nature* 298: 841-844.

- Fairbanks, R. G., P. H. Wiebe, and A. W. H. Bé (1980) Vertical distribution and isotopic composition of living planktonic foraminifera in the western North Atlantic, *Science* 207: 61-63.
- Fairbridge, R. W., ed. (1972) The Encyclopedia of Geochemistry and Environmental Sciences, IVA, The Elements, New York, Van Nostrand Reinhold Co.
- Friedlander, G., J. W. Kennedy, E. S. Macias, and J. M. Miller (1981) Nuclear and Radiochemistry, third edition, New York, John Wiley & Sons.
- Garrels, R. M. and M. E. Thompson (1962) A chemical model for sea water at 25° C and one atmosphere total pressure, *Amer. Jour. Sci.* 260: 57-66.
- Gieskes, J. M. (unpublished report) Interstitial water studies, Leg 30.
- Gieskes, J. M. (1981) Deep-Sea Drilling interstitial water studies: implications for chemical alteration of the oceanic crust, Layers I and II, *SEPM Special Publ.* 32: 149-167.
- Gieskes, J. M., H. Elderfield, J. R. Lawrence, J. Johnson, B. Meyers, and A. Campbell (1982) Geochemistry of interstitial waters and sediments, Leg 64, Gulf of California, *in* Curray, J. R., D. G. Moore, et al. (1982) Initial Reports of the Deep Sea Drilling Project, volume 64, Washington, U. S. Government Printing Office, pp. 675-694.
- Gieskes, J. M., K. Johnston, and M. Boehm (preprint) Interstitial water studies, Leg 74, Deep Sea Drilling Project.
- Goldberg, E. D. and G. O. S. Arrhenius (1958) Chemistry of Pacific pelagic sediments, *Geochim. Cosmochim. Acta* 13: 153-212.
- Graham, D. W., M. L. Bender, D. F. Williams, and L. D. Keigwin, Jr. (1982) Strontium-calcium ratios in Cenozoic planktonic foraminifera, *Geochim. Cosmochim. Acta* 46: 1281-1292.
- Hallam, A. (1977) Secular changes in marine inundation of USSR and North America through the Phanerozoic, *Nature* 269: 769-772.
- Harrison, C. G. A. (1980) Spreading rates and heat flow, *Geophys. Res. Lett.* 7: 1041-1044.
- Hart, S. R. and H. Staudigel (1978) Oceanic crust: age of hydrothermal alteration, *Geophys. Res. Lett.* 5: 1009-1012.
- Hart, S. R. and H. Staudigel (1982) The control of alkalies and uranium in seawater by ocean crust alteration, *Earth and Planet. Sci. Lett.* 58: 202-212.
- Hays, J. D. and W. C. Pitman III (1973) Lithospheric plate motion, sea level changes and climatic and ecological consequences, *Nature* 246: 18-22.

- Hester, K. and E. Boyle (1982) Water chemistry control of cadmium content in Recent benthic foraminifera (1982) *Nature* 298: 260-262.
- Holland, H. D. (1978) The Chemistry of the Atmosphere and Oceans, New York, John Wiley and Sons.
- Horstmann, E. L. (1957) The distribution of lithium, rubidium, and caesium in igneous and sedimentary rocks, *Geochim. Cosmochim. Acta* 12: 1-28.
- Humphris, S. E. (1977) The hydrothermal alteration of oceanic basalts by seawater, Ph.D. thesis, M.I.T./W.H.O.I.
- Imbrie, J. and N. G. Kipp (1971) A new micropaleontological method for quantitative paleoclimatology: application to a Late Pleistocene Caribbean core, in Turekian, K. K., ed., Late Cenozoic Glacial Ages, New Haven, Yale University Press, pp. 71-182.
- Jenkins, W. J., J. M. Edmond, and J. B. Corliss (1978) Excess ^3He and ^4He in Galapagos submarine hydrothermal waters, *Nature* 272: 156-158.
- Keith, M. L. and E. T. Degens (1959) Geochemical indicators of marine and fresh-water sediments, in Abelson, P. H., ed., Researches in Geochemistry, vol. 1: 38-61.
- Kilbourne, R. T. and B. K. Sen Gupta (1973) Elemental composition of planktonic foraminiferal tests in relation to temperature-depth habits and selective solution, *Geol. Soc. Amer. Abstracts with Programs* 5 (5): 408-409.
- Killingley, J. S. (1983) Effects of diagenetic recrystallization on $^{18}\text{O}/^{16}\text{O}$ values of deep-sea sediments, *Nature* 301: 594-597.
- Kinsman, D. J. J. and H. D. Holland (1969) The co-precipitation of cations with CaCO_3 -- IV. The co-precipitation of Sr^{2+} with aragonite between 16° and 96° C, *Geochim. Cosmochim. Acta* 33: 1-17.
- Kitano, Y., M. Okumura, and M. Idogaki (1975) Incorporation of sodium, chloride and sulfate with calcium carbonate, *Geochem. Jour.* 9: 75-84.
- Krauskopf, K. B. (1967) Introduction to Geochemistry, New York, McGraw-Hill Book Company.
- Krinsley, D. (1960) Trace elements in the tests of planktonic foraminifera, *Micropal.* 6: 297-300.
- Lancelot, Y., E. Siebold, et al. (1977a) Initial Reports of the Deep Sea Drilling Project, volume 41, Washington, U. S. Government Printing Office, pp. 21-162.
- Lancelot, Y., E. Siebold, et al. (1977b) Initial Reports of the Deep Sea Drilling Project, volume 41, Washington, U. S. Government Printing Office, pp. 327-420.

- Larson, R. L. and W. C. Pitman III (1972) World-wide correlation of Mesozoic magnetic anomalies and its implications, Geol. Soc. Amer. Bull. 83: 3645-3662.
- Larson, R. L., R. Moberly, et al. (1975) Initial Reports of the Deep Sea Drilling Project, volume 32, Washington, U. S. Government Printing Office, pp. 75-158.
- Lawrence, J. R. and J. M. Gieskes (1981) Constraints on water transport and alteration in the oceanic crust from the isotopic composition of pore water, Jour. Geophys. Res. 86(B9): 7924-7934.
- Lefèvre, R. and M.-T. Vénec-Peyré (1977) Mise en évidence au microanalyseur ionique d'une zonation dans la répartition du sodium, magnésium et strontium dans le test d'un Foraminifère calcaire perforé: Ammonia beccarii (L.), C. R. Acad. Sci. Paris 285 (Série D): 23-26.
- Lipps, J. H. and P. H. Ribbe (1967) Electron-probe microanalysis of planktonic foraminifera, Jour. Paleontol. 41: 492-496.
- Lorens, R. B. (1978) A study of biological and physical controls on the trace metal content of calcite and aragonite, Ph.D. thesis, University of Rhode Island.
- Lorens, R. B. and M. L. Bender (1977) Physiological exclusion of magnesium from Mytilus edulis calcite, Nature 269: 793-794.
- Lorens, R. B., M. L. Bender, and D. F. Williams (1977) The early nonstructural chemical diagenesis of foraminiferal calcite, Jour. Sed. Petrol. 47: 1602-1609.
- Lorens, R. B. and M. L. Bender (1980) The impact of solution chemistry on Mytilus edulis calcite and aragonite, Geochim. Cosmochim. Acta 44: 1265-1278.
- McMurtry, G. M., A. J. Andrews, and J. D. Macdougall (1978) In situ distribution and abundances of lithium, boron and uranium in secondary minerals of deep-ocean basalts, Trans. Amer. Geophys. Union 60: 973.
- Matter, A., R. G. Douglas, and K. Perch-Nielson (1975) Fossil preservation, geochemistry, and diagenesis of pelagic carbonates from Shatsky Rise, Northwest Pacific, Leg 32, Deep Sea Drilling Project, in Larson, R. L., R. Moberly, et al. (1975) Initial Reports of the Deep Sea Drilling Project, volume 32, Washington, U. S. Government Printing Office, pp. 891-922.
- Moore, T. C., Jr., P. Rabinowitz, et al. (in press) Initial Reports of the Deep Sea Drilling Project, volume 74, Washington, U.S. Government Printing Office.
- Morozov, N. P. (1969) Geochemistry of the alkali metals in rivers, Geochem. Intern. 6: 585-594.

- Mucci, A. and J. W. Morse (1983) The incorporation of Mg^{2+} and Sr^{2+} into calcite overgrowths: influences of growth rate and solution composition, *Geochim. Cosmochim. Acta* 47: 217-233.
- Ohrdorf, R. (1968) Ein Beitrag zur Geochemie des Lithiums in Sedimentgesteinen, *Geochim. Cosmochim. Acta* 32: 191-208.
- Parsons, B. (1982) Causes and consequences of the relation between area and age of the ocean floor, *Jour. Geophys. Res.* 87(B1): 289-302.
- Parsons, B. and J. G. Sclater (1977) An analysis of the variation of ocean floor bathymetry and heat flow with age, *Jour. Geophys. Res.* 82: 803-827.
- Perrin, C. L. (1970) Mathematics for Chemists, New York, Wiley-Interscience.
- Peterman, Z. E., C. E. Hedge, and H. A. Tourtelot (1970) Isotopic composition of strontium in seawater throughout Phanerozoic time, *Geochim. Cosmochim. Acta* 34: 105-120.
- Richardson, S. H., S. R. Hart, and H. Staudigel (1980) Vein mineral ages of old oceanic crust, *Jour. Geophys. Res.* 85: 7195-7200.
- Riley, J. P. and M. Tongudai (1964) The lithium content of seawater, *Deep-Sea Res.* 11: 563-568.
- Savin, S. M. and R. G. Douglas (1973) Stable isotope and magnesium geochemistry of Recent planktonic foraminifera from the South Pacific, *Geol. Soc. Amer. Bull.* 84: 2327-2342.
- Shackleton, N. J. (1982) The deep-sea sediment record of climate variability, *Prog. Oceanog.* 11: 199-218.
- Sleep, N. H., J. L. Morton, L. E. Burns, and T. J. Wolery (in press) Geophysical constraints on the volume of hydrothermal flow at the ridge axes.
- Sprague, D. and H. N. Pollack (1980) Heat flow in the Mesozoic and Cenozoic, *Nature* 285: 393-395.
- Sreekumaran, C., K. C. Pillai, and T. R. Folsom (1968) The concentrations of lithium, potassium, rubidium, and cesium in some western American rivers and marine sediments, *Geochim. Cosmochim. Acta* 32: 1229-1234.
- Staudigel, H., S. R. Hart, and S. H. Richardson (1981) Alteration of the oceanic crust: processes and timing, *Earth Planet. Sci. Lett.* 52: 311-327.
- Staudigel, H. and S. R. Hart (1983) Alteration of basaltic glass: mechanisms and significance for the oceanic crust-seawater budget, *Geochim. Cosmochim. Acta* 47: 337-350.

- Styrt, M. M. (1977) Variations in lithium concentration between igneous and sedimentary rocks, B. S. thesis, Radcliffe College.
- Swart, P. K. (1981) The strontium, magnesium and sodium composition of Recent scleractinian coral skeletons as standards for palaeoenvironmental analysis, *Palaeogeogr., Palaeoclimatol., Palaeoecol.* 34: 115-136.
- Thompson, G. (1973) Trace-element distribution in fractionated oceanic rocks 2. Gabbros and related rocks, *Chem. Geol.* 12: 99-111.
- Thompson, G. and W. G. Melson (1970) Boron contents of serpentinites and metabasalts in the oceanic crust: implications for the boron cycle in the oceans, *Earth Planet. Sci. Lett.* 8: 61-65.
- Thompson, T. G. and T. J. Chow (1955) The strontium-calcium atom ratio in carbonate-secreting marine organisms, *Deep-Sea Res.* 3(Suppl.): 20-39.
- Turcotte, D. L. and K. Burke (1978) Global sea-level changes and the thermal structure of the earth, *Earth Planet. Sci. Lett.* 41: 341-346.
- Turekian, K. K. (1957) The significance of variations in the strontium content of deep sea cores, *Limno. and Ocean.* 2: 309-314.
- Turekian, K. K. (1963) Rates of calcium carbonate deposition by deep-sea organisms, molluscs, and the coral-algae association, *Nature* 197: 277-278.
- Turekian, K. K. (1965) Some aspects of the geochemistry of marine sediments, in Riley, J. P. and G. Skirrow, eds, Chemical Oceanography, vol. 2, chap. 16, pp. 81-126.
- Turekian, K. K. (1969) The oceans, streams, and atmosphere, in Wedepohl, K. H., ed., Handbook of Geochemistry, vol. 1, chap. 10.
- Vail, P. R., R. M. Mitchum, Jr., and S. Thompson III (1977) Seismic stratigraphy and global changes of sea level, part 4: global cycles of relative changes of sea level, *Amer. Assoc. Petro. Geol. Mem.* 26: 83-97.
- van der Lingen, G. J. and G. H. Packham (1975) Relationships between diagenesis and physical properties of biogenic sediments of the Ontong-Java Plateau (Sites 288 and 289, Deep Sea Drilling Project), in Andrews, J. E., G. Packham, et al., Initial Reports of the Deep Sea Drilling Project, volume 30, Washington, U. S. Government Printing Office, pp. 443-481.
- Van Hinte, J. E. (1972) The Cretaceous time-scale and planktonic foraminiferal zones, *Ned. Akad. Wetensch. Proc. Ser. B* 75: 61-68.
- Veizer, J. and W. Compston (1974) $^{87}\text{Sr}/^{86}\text{Sr}$ composition of seawater during the Phanerozoic, *Geochim. Cosmochim. Acta* 38: 1461-1484.

- Vincent, E. (1974) Cenozoic planktonic biostratigraphy and paleoceanography of the tropical Western Indian Ocean, Leg 24, Deep Sea Drilling Project, in Fischer, R. L., E. T. Bunce, et al., Initial Reports of the Deep Sea Drilling Project, volume 24, Washington, U. S. Government Printing Office, pp. 1111-1150.
- Von Damm, K. L. (1983) Chemistry of submarine hydrothermal solutions at 21° N, East Pacific Rise and Guaymas Basin, Gulf of California, Ph.D. thesis, M.I.T./W.H.O.I.
- Watts, A. B. (1982) Tectonic subsidence, flexure and global changes of sea level, Nature 297: 469-474.
- Watts, A. B. and M. S. Steckler (1979) Subsidence and eustacy at the continental margin of Eastern North America, in Talwani, M., W. Hay, and W. B. F. Ryan, eds., Deep Drilling Results in the Atlantic Ocean: Continental Margins and Paleoenvironment, Maurice Ewing Series, vol. 3, AGU, Washington, D.C., pp. 235-248.
- Welby, C. W. (1958) Occurrence of alkali metals in some Gulf of Mexico sediments, Jour. Sed. Petrol. 28: 431-452.
- White, A. (1978) Sodium coprecipitation in calcite and dolomite, Chem. Geol. 23: 65-72.
- Wolery, T. J. and N. H. Sleep (1976) Hydrothermal circulation and geochemical flux at mid-ocean ridges, Jour. Geol. 84: 249-275.

BIOGRAPHICAL NOTE

The author was born in Buffalo, N.Y. July 7, 1955. She resided with her family in Kenmore, N. Y. and attended public schools there. She graduated from Yale in the spring of 1977 with a B.S. summa cum laude with distinction in the chemistry major. While an undergraduate, she was employed for two years as a laboratory assistant in research for Professor Karl K. Turekian. The author entered the M.I.T./W.H.O.I. Joint Program in Oceanography in September, 1978 as a candidate for the degree of Doctor of Philosophy. She was the recipient of a Shell Doctoral Fellow award for the academic year 1982-1983.